À ma famille,

À mes amis,

À Zoé et Sandra

Remerciements

Je tiens tout d'abord à remercier les Professeurs Freddy Coignoul et Daniel Desmecht pour m'avoir accueilli au sein du laboratoire de Pathologie de la Faculté de Médecine Vétérinaire.

Pour son implication dans son travail, sa confiance et ses efforts constants dans l'écriture de projets et le développement de l'activité du laboratoire, je tiens encore à remercier le Professeur Daniel Desmecht.

Pour leur aide précieuse, pour tout ce qu'ils ont appris au vétérinaire que je suis à son arrivée dans le monde de la biologie moléculaire, de la virologie et de la recherche en général, un merci tout particulier à Etienne Baise, Anne Cornet, François Cornet, Annabelle Decreux, Thomas Fett, Bénédicte Lambrecht, Mickaël Leroy, Mélanie Palm, Grégory Pire et Monique Spronken.

Pour sa disponibilité et la qualité constante de son travail, je remercie Michaël Sarlet.

Un très grand merci à Carine Garot, Nathalie Guillaume et Christophe Reuchert pour la gestion des commandes et des (trop nombreux) petits problèmes administratifs.

Pour les discussions constructives et les collaborations que nous avons eues, merci à Aurore Broers, Karine Cloquette, Martin Dermine, Amélie Halleux, Déborah Kleijnen, Laurence Pesesse, Jean-François Pirlot et Els Van de Paar.

Merci aux autres membres, passés et présents, du service de Pathologie de la Faculté de Médecine Vétérinaire pour les bons moments passés ensemble : Adélite, Anne (Thomas), Benoît, Calixte, Christine, Dao, Dominique, Etienne, Hoang, Hussein, Jérôme, Laurent, Lucian, Michel, Nicolas, Patrick, Philippe, Raphaël, Sandra, Sandy, Sébastien, Soumya, Stéphanie, Tam, Thierry, Vanessa.

Pour sa présence constante à mes côtés, je remercie mon épouse, Sandra.

Liste des abréviations

aa : acide aminé / *amino acid*
ADN / DNA : acide désoxyribonucléique / *deoxyribonucleic acid*
ADNc / cDNA : ADN complémentaire / *complementary DNA*
AEC : *aminoethylcarbazole*
AP-1 : *activator protein 1*
ARDS: *acute respiratory distress syndrome*
ARN / RNA : acide ribonucléique / *ribonucleic acid*
ARNc / cRNA : ARN complémentaire / *complementary RNA*
ARNm / mRNA : ARN messager / *messenger RNA*
ATP : *adenosine triphosphate*
BAC : *bacterial artificial chromosome*
BSA : *bovine serum albumin*
BT : *bovine turbinate*
CCID50 : *50% cell culture infective dose*
CCT : *chaperonin containing TCP-1*
CID : *central interactive domain*
COPI : *coat protein type I*
CPSF : *cleavage and polyadenylation specificity factor*
DED : *death effector domain*
DMEM : *Dulbecco's minimal essential medium*
dpi : *day post infection*
dsRNA : *double-stranded RNA*
eGFP : *enhanced green fluorescent protein*
eIF4GI : *eukaryotic initiation factor 4GI*
ELISA : *enzyme-linked immunosorbent assay*
EMCV : *encephalomyocarditis virus*
FACS : *fluorescence activated cell sorting*
FADD : *Fas-associated protein with a death domain*
FCS : *fetal calf serum*
GAPDH : *glyceraldehyde 3-phosphate dehydrogenase*
GDP : *guanosine diphosphate*
GED : *GTPase effector domain*

GTP : *guanosine triphosphate*

GTPase : *guanosine triphosphate hydrolase*

HA : hémagglutinine / *hemagglutinin*

HAT : *human airway trypsin-like protease*

HBS : *Hepes buffered saline*

hCRM1 : *chromosome region maintenance 1 protein*

HE : *hematoxylin and eosin*

HEF : *hemagglutinin-esterase-fusion protein*

HEPA : *high efficiency particulate air filter*

HPAI/LPAI : *highly/low pathogenic avian influenza*

HRP : *horseradish peroxidase*

Hsc70 : *heat shock cognate 70*

Hsp : *heat shock protein*

HSV : *Herpes simplex virus*

HTLV-1 : *human T-cell leukaemia virus type 1*

IFN : interféron / *interferon*

IFNAR : *interferon-alpha/beta receptor*

IFNLR : *interferon-lambda receptor*

IL6 : *interleukin 6*

IPS-1 : *interferon β promoter stimulator 1*

IRF3 : *interferon regulatory factor 3*

IVPI : *intravenous pathogenicity index*

JAK : *Janus kinase*

mAb : *monoclonal antibody*

MAVS : *mitochondrial antiviral signaling protein*

MD : *middle domain*

MDBK : *Madin-Darby bovine kidney*

MDCK : *Madin-Darby canine kidney*

MEF : *mouse embryonic fibroblasts*

MLD50 : *50% mouse lethal dose*

MOI : *multiplicity of infection*

MTS : signal de localisation mitochondriale / *mitochondrial targeting signal*

NA : neuraminidase

NAI : *neuraminidase inhibitor*

NEP : *nuclear export protein*

NES : *nuclear export signal*

Neu5Ac : *N-acetylneuraminic acid*

Neu5Gc : *N-glycolylneuraminic acid*

NF-κB : *nuclear factor-kappa b*

NLS : signal de localisation nucléaire / *nuclear localization signal*

NP : nucléoprotéine / *nucleoprotein*

NS1 : *non structural protein 1*

NS1-BP : *NS1-binding protein*

NS1-I : *NS1-interactor*

OD : *optic density*

OIE : Office International des Epizooties

ORF : *open reading frame*

PA : *polymerase acidic protein*

PABII : *poly(A)-binding protein II*

PABP1 : *poly(A)-binding protein 1*

PAGE : *polyacrylamide gel electrophoresis*

PAP : *poly(A) polymerase*

PAS : *periodic acid schiff*

PB1 : *polymerase basic protein 1*

PB2 : *polymerase basic protein 2*

PBM : *PDZ binding motif*

PBS : *phosphate buffered saline*

pdb : *protein data bank*

PFU : *plaque forming unit*

pI : *isoelectric point*

PI3K : *phosphatidylinositol 3-kinase*

PKC : *protein kinase C*

PKI : *protein kinase inhibitor*

PKR : *protein kinase R*

PRD : *proline/arginine-rich domain*

PVP : *polyvinylpyrrolidone*

RACK-1 : *receptor of the activated C kinase*

RAF : *RNA polymerase activating factor*

RanBP5 : *Ran binding protein 5*

RBS : *receptor binding site*

RNAse : *ribonuclease*

RNP1 : *ribonucleoprotein 1 motif*

RT-PCR : *reverse transcription – polymerase chain reaction*

SA : *sialic acid*

SAS : *self assembly sequence*

SD : *standard deviation*

SH3 : *SRC homology 3*

SNP : *single nucleotide polymorphism*

STAT : *signal transducer and activator of transcription*

SV40 : *simian virus 40*

TCID50 : *50% tissue culture infective dose*

TMB : *tetramethylbenzidine*

TMD : *transmembrane domain*

TNFα : *tumor necrosis factor* α

TPCK : *tosyl phenylalanyl chloromethyl ketone*

TTSP : *type II transmembrane serine protease*

UTP : *uridine triphosphate*

UTR : *untranslated region*

VMD : *visual molecular dynamics*

vRNA : *viral RNA*

vRNP : *viral ribonucleoprotein*

VSV : virus de la stomatite vésiculeuse / *vesicular stomatitis virus*

Table des matières

Résumé

Les protéines Mx, découvertes au début des années 1960 chez la souris, sont des GTPases de haut poids moléculaire de la famille des dynamines. Elles dépendent pour leur expression des interférons de types I et III et comptent parmi les effecteurs de la réponse innée dotés de la plus grande activité antivirale. La puissance de cette activité et le spectre antiviral varient selon la protéine. Ainsi, la protéine Mx1 bovine apparaît-elle comme la plus efficace à ce jour en termes d'inhibition du virus influenza de type A. Bien que des hypothèses existent à ce sujet, le mécanisme d'action des protéines Mx reste à ce jour largement méconnu. Une complexation de la nucléoprotéine virale par la protéine MxA humaine, basée sur l'observation d'une co-immunoprécipitation faible des deux protéines, a été proposée. Néanmoins, le spectre antiviral très large de cette protéine MxA fait que l'existence d'une interaction spécifique entre la Mx et une protéine de chacun de ces virus très différents paraît hautement improbable. Il semble beaucoup plus plausible que les Mx inhibent une fonction cellulaire communément utilisée par tous ces virus lors de leur cycle réplicatif.

Pour apporter de nouveaux éléments de réponse, après avoir créé les outils nécessaires et étudié en détail l'activité anti-influenza de la protéine Mx1 bovine *in vitro* et *in vivo*, nous avons entrepris l'isolement de souches virales résistantes à l'effet Mx. En principe, l'identification de mutations liées à l'acquisition d'une résistance devrait permettre de mettre le doigt sur la cible virale directe ou indirecte des Mx. Une telle stratégie a déjà fait ses preuves, ayant historiquement permis la compréhension du mode d'action de la drogue antivirale amantadine. Après plusieurs tentatives infructueuses, l'isolement de souches résistantes à la protéine Mx1 bovine fut possible. La caractérisation phénotypique a confirmé l'acquisition d'une résistance, totale, à l'effet *in vitro* de la protéine Mx1 bovine, mais aussi à l'activité antivirale d'autres Mx, cytoplasmiques et nucléaires. Quatre mutations candidates ont été identifiées et la substitution I100T dans la nucléoprotéine virale s'est avérée suffisante pour conférer le phénotype de Mx-résistance par des expériences de complémentation et de *reverse genetics*. Ce résultat concorde avec les données récentes de la littérature puisque la nucléoprotéine semble impliquée dans les différences de sensibilité entre souches de virus influenza A à l'effet Mx. Le résidu 100 de la nucléoprotéine est fortement exposé en surface de la protéine tant sous sa forme monomérique qu'oligomérique, ce qui le rend fortement susceptible d'être impliqué dans une interaction avec d'autres protéines. Notre hypothèse est que la

protéine Mx1 bovine entre en compétition avec la nucléoprotéine virale pour la liaison avec un facteur cellulaire et que la substitution I100T permette d'augmenter l'affinité de la nucléoprotéine pour ce facteur et donc de déplacer la Mx, ou rende possible l'utilisation par la nucléoprotéine d'une voie alternative via liaison à un autre facteur. L'étude détaillée du rôle joué par le résidu 100 de la nucléoprotéine et la comparaison des interactomes des Mx et de la nucléoprotéine permettront sans nul doute de préciser ce point.

Summary

Mx proteins are high molecular weight GTPases of the dynamin superfamily discovered in the early sixties in mice. Their expression depends on type I and type III interferons. They constitute one of the most powerful antiviral effectors of the innate immune response. The antiviral efficiency and spectrum vary depending on the Mx protein. Bovine Mx1 protein appears to be the most potent anti-influenza Mx described so far. In spite of the existence of several hypotheses, the mechanism underlying the antiviral activity of Mx proteins is still poorly understood. Based on a weak interaction discovered in a co-immunoprecipitation study, the complexation of influenza nucleoprotein by human MxA has been proposed. But the antiviral spectrum of human MxA is extremely wide, making the existence of such a virus-specific complexation model very unlikely given the diversity of all these viruses. An inhibition by Mx proteins of a cellular function commonly used by these viruses is much more probable.

To enlighten this point, after a complete description of the *in vitro* and *in vivo* anti-influenza activity of bovine Mx1 (boMx1), we decided to isolate Mx-resistant influenza A strains. The identification of mutations associated with resistance would allow a better understanding of the mechanism underlying the inhibition. Years ago, such an approach permitted to understand the mode of action of the antiviral drug amantadine. After several attempts, boMx1-resistant strains were obtained. These strains were confirmed as completely resistant to boMx1 but also to other tested cytoplasmic and nuclear Mx proteins. Four mutations were identified, and complementation and reverse genetics studies demonstrated that mutation I100T in the viral nucleoprotein was sufficient to confer resistance. This is in agreement with recent data from the literature pointing out the role of NP in the variation of susceptibility of influenza strains to the inhibitory activity of Mx proteins. Residue 100 is highly exposed on the 3D structure of monomeric and oligomeric nucleoprotein and is thus very likely to be involved in protein-protein interactions. Our hypothesis is that Mx and NP compete for the interaction with a common cellular factor, the NP I100T mutation either increasing the affinity of NP for its ligand, or allowing the NP to bind another factor and to use an alternative route. Further studies on the role played by residue 100 of NP and comparison of the NP and Mx interactomes will shed new light on this point.

Introduction

Position de la question

Le virus influenza de type A est un pathogène majeur, tant en médecine humaine qu'en médecine vétérinaire. Responsable du décès d'environ 500.000 personnes par an dans le monde, il fut par ailleurs à l'origine de plusieurs pandémies, dont l'épisode de la « grippe espagnole » de 1918, auquel ont été attribués entre 20 et 40 millions de décès.

Les oiseaux aquatiques sauvages sont considérés comme le réservoir épidémiologique des différents sous-types du virus influenza A. Ces sous-types sont déterminés par les caractéristiques antigéniques de leur hémagglutinine et de leur neuraminidase. Seize sous-types d'hémagglutinine et neuf sous-types de neuraminidase ont ainsi été décrits à ce jour. Parmi les 144 combinaisons possibles d'hémagglutinine et de neuraminidase, seule une fraction est rencontrée en pratique, une compatibilité fonctionnelle entre les deux protéines étant nécessaire. Des sous-types spécifiques se rencontrent par ailleurs chez certaines espèces de mammifères, dont l'homme, le porc, le cheval et plusieurs espèces de mammifères marins. Récemment, des souches canines ont aussi été identifiées et l'infection du chat apparaît également de moins en moins rare. Cet élargissement progressif du panel des espèces susceptibles pose de nouvelles questions sur les risques de réassortiment génétique du virus au sein de ces espèces, elles-mêmes en contact étroit avec l'homme. En effet, le virus influenza A possédant huit segments génomiques, un réassortiment de ces segments est possible en cas de co-infection d'un même hôte par deux souches virales différentes. Ce type d'événement fut à l'origine de plusieurs pandémies, et le porc fut, et est toujours, considéré comme un hôte de choix pour le réassortiment entre souches virales aviaires et humaines, notamment parce que son arbre respiratoire présente des caractéristiques intermédiaires quant aux types de récepteurs (acides sialiques) entre ce qui est observé chez l'homme et chez les oiseaux aquatiques. D'autres espèces pourraient néanmoins jouer le même rôle.

Sur le plan clinique, une infection se traduit chez les mammifères par de la fièvre et des troubles respiratoires caractéristiques d'une atteinte respiratoire supérieure. Dans certains cas, un syndrome de détresse respiratoire aiguë (souches virales à tropisme pulmonaire) ou une pneumonie bactérienne secondaire peuvent compliquer le tableau clinique. Une tempête cytokinique caractérise l'infection par certaines souches hautement pathogènes. Enfin, certaines souches peuvent également infecter le système nerveux central, voire, notamment pour les souches de virus H5N1 hautement pathogènes, se répandre de façon systémique (foie, rein, système nerveux, tube digestif,

rate, pancréas, etc.).

Il existe des traitements antiviraux efficaces, notamment les inhibiteurs de la neuraminidase et les inhibiteurs de la protéine M2, mais de plus en plus de souches virales y sont largement résistantes. De plus, le traitement est souvent administré trop tard dans le cours de la maladie. Enfin, ces inhibiteurs du cycle viral ne modifient pas la réponse immunitaire de l'hôte, qui semble jouer un rôle essentiel en termes de pronostic vital. Les infections humaines par le virus H5N1 hautement pathogène sont, toujours actuellement, associées à un taux de mortalité élevé, supérieur à 50%, en dépit des traitements disponibles. De même, pour le virus H1N1 pandémique de 2009, les cas les plus sévères qui ont été traités avec succès ont nécessité le recours à l'oxygénation par membrane extra-corporelle, technique extrêmement lourde, difficilement applicable dans les pays en voie de développement et irréalisable à large échelle. La vaccination se révèle efficace mais, d'une part, un délai de plusieurs mois est nécessaire entre l'apparition d'une nouvelle souche virale et la disponibilité des premières doses vaccinales et, d'autre part, les capacités de production seraient très largement dépassées par rapport aux besoins en cas de pandémie sévère.

Il y a donc un besoin pressant de nouveaux traitements, plus efficaces, induisant moins de résistances, administrables à grande échelle et si possible pour un coût raisonnable.

Parmi les défenses innées opposées par l'hôte au virus influenza, le système Mx, un des effecteurs de la cascade interféron, apparaît comme extrêmement puissant. Ainsi, la protéine Mx1 murine, découverte il y a près de 50 ans, confère aux souris porteuses une protection clinique très importante contre de nombreuses souches de virus influenza hautement pathogènes. D'autres protéines Mx ont depuis été associées à un effet anti-influenza plus ou moins marqué, en ce compris la protéine MxA humaine, la protéine Mx1 porcine et, plus récemment décrite, la protéine Mx1 bovine. Cette dernière semble, de loin, la plus efficace parmi les protéines Mx testées contre une infection par le virus influenza A, tant *in vitro* qu'*in vivo*. Nos travaux ont pu montrer une protection clinique complète associée à l'expression de cette protéine chez la souris après infection par des souches de virus influenza hautement pathogènes, pourtant extrêmement virulentes (dose létale 50 de moins de 10 particules virales par souris Mx-négative) et ce, quelle que soit la dose virale employée. Ces résultats très prometteurs renforcent encore la nécessité d'identifier précisément les modalités d'action de l'effet antiviral de ces protéines, toujours largement méconnues à ce jour. Il n'est toujours pas clairement établi

à l'heure actuelle si les protéines Mx agissent via un mode direct, spécifique du virus (complexation d'une protéine virale par exemple) ou de façon indirecte en agissant sur l'environnement cellulaire, même si plusieurs hypothèses circulent à ce sujet. Pourtant, au vu de l'efficacité anti-influenza de la protéine Mx1 bovine, la mise en évidence de son mode d'action permettrait assurément de mettre à jour de nouvelles cibles thérapeutiques. Face à cette nécessité, nous avons opté pour une méthodologie expérimentale qui a déjà fait ses preuves puisqu'elle a permis la compréhension du mode d'action de la drogue antivirale amantadine (inhibiteur de la protéine M2). Elle consiste à isoler des variants viraux résistants à l'effecteur antiviral, à déterminer quelles sont les mutations responsables de cette résistance et, ainsi, à identifier la cible virale de cet agent antiviral. Grâce aux données accumulées à ce jour dans la littérature sur les fonctions des différentes protéines du virus influenza et de leurs domaines voire résidus spécifiques au cours du cycle de réplication, il devrait être possible de préciser le mode d'action de la protéine Mx1 bovine.

Objectifs de la thèse

Lorsque j'ai débuté mes travaux, le laboratoire de pathologie avait développé une lignée clonale de cellules Vero conditionnellement capables d'exprimer la protéine Mx1 bovine (boMx1). Cette préparation biologique avait servi jusque-là à mesurer l'activité antivirale de boMx1 vis à vis de plusieurs virus appartenant aux familles des *Paramyxoviridae* et des *Rhabdoviridae*.

Ma première campagne expérimentale, de nature strictement descriptive, a consisté à utiliser cette lignée de cellules Vero pour examiner son éventuelle activité anti-influenza. Comme l'intensité de l'activité anti-influenza s'est avérée remarquablement élevée par rapport aux données disponibles dans la littérature, je me suis donné pour second objectif d'agréger les ressources biologiques nécessaires pour confirmer mes résultats *in vivo*. D'abord, un jeu de souris transgéniques capables d'exprimer boMx1 sous la dépendance de son promoteur naturel a été généré et le patron d'expression des différentes lignées a été établi. Ensuite, deux souches sauvages, l'une d'origine aviaire (H5N1) et l'autre d'origine porcine (H1N1), ont été rendues hyperpathogènes pour la souris par évolution contrainte en souris progressivement moins sensibles. Ces deux

virus murinisés sont à la base du développement et de la caractérisation de deux modèles distincts de pneumonie virale fatale pour la souris. Ces modèles m'ont ensuite permis d'étendre mes conclusions obtenues *in vitro* à l'animal entier et de confirmer la fonction anti-influenza exacerbée de boMx1.

Pour identifier le mécanisme moléculaire sous-jacent, j'ai ensuite entrepris de contraindre une souche quelconque à évoluer en présence de la protéine boMx1 et ce, dans le but d'isoler une ou des souches capables d'esquiver la fonction anti-influenza précitée. Après quoi, une série de travaux ont été entrepris pour caractériser la stabilité génétique, la biofitness et les mutations caractéristiques des variants Mx-résistants. L'étape suivante a consisté à réaliser des expériences de complémentation et de mutagenèse dirigée visant à identifier la (les) mutation(s) nécessaire(s) et suffisante(s) pour la fonction d'évasion.

Toujours pour tendre vers l'identification du mécanisme moléculaire sous-jacent, j'ai également entrepris de tester la fonction anti-influenza de protéines Mx artificielles constituées de différents segments de protéines Mx naturelles plus ou moins capables d'inhiber le cycle biologique des virus influenza A.

Les objectifs ponctuels successifs de mon travail peuvent s'énoncer comme suit :

- Création de lignées de souris capables d'exprimer la protéine boMx1 ;
- Etablissement de modèles d'infection de la souris par deux virus influenza A ;
- Etude de la fonction anti-influenza de boMx1 *in vitro* et *in vivo* ;
- Isolement et caractérisation de souches Mx-résistantes ;
- Identification de la mutation sous-jacente à la « Mx-résistance » ;
- Testage du statut « nécessaire et suffisant » du domaine GED C-terminal des protéines Mx.

Partie I : Données de la littérature

1. Les GTPases « Mx » des vertébrés

1.1. Structure et fonctions

Les protéines Mx sont des GTPases de haut poids moléculaire de la famille des dynamines, protéines notamment impliquées dans les phénomènes d'endocytose/exocytose et de division cellulaire (Horisberger *et al.*, 1990 ; Nakayama *et al.*, 1991). Elles doivent leur nom à leurs propriétés antivirales, identifiées pour la première fois en 1962 sur le virus influenza A, virus de la famille des *Orthomyxoviridae*, d'où la dénomination « *myxovirus resistance* », en abrégé, « Mx ».
Des protéines Mx ont été identifiées chez de nombreuses espèces de vertébrés et des gènes similaires sont présents chez la levure et des invertébrés comme le gastéropode *Haloitis discus* (Rothman *et al.*, 1990 ; Haller *et al.*, 1998 ; De Zoysa *et al.*, 2007). Deux à trois isoformes de cette protéine existent selon l'espèce, associées ou non à des propriétés antivirales. On distingue plusieurs sous-groupes de protéines Mx, en fonction de l'homologie de leur séquence primaire. La classification actuellement admise comprend les sous-groupes des protéines Mx de poissons, d'oiseaux, de rongeurs, ainsi que les MxA-like et les MxB-like (Haller *et al.*, 2010 ; Figure 1).

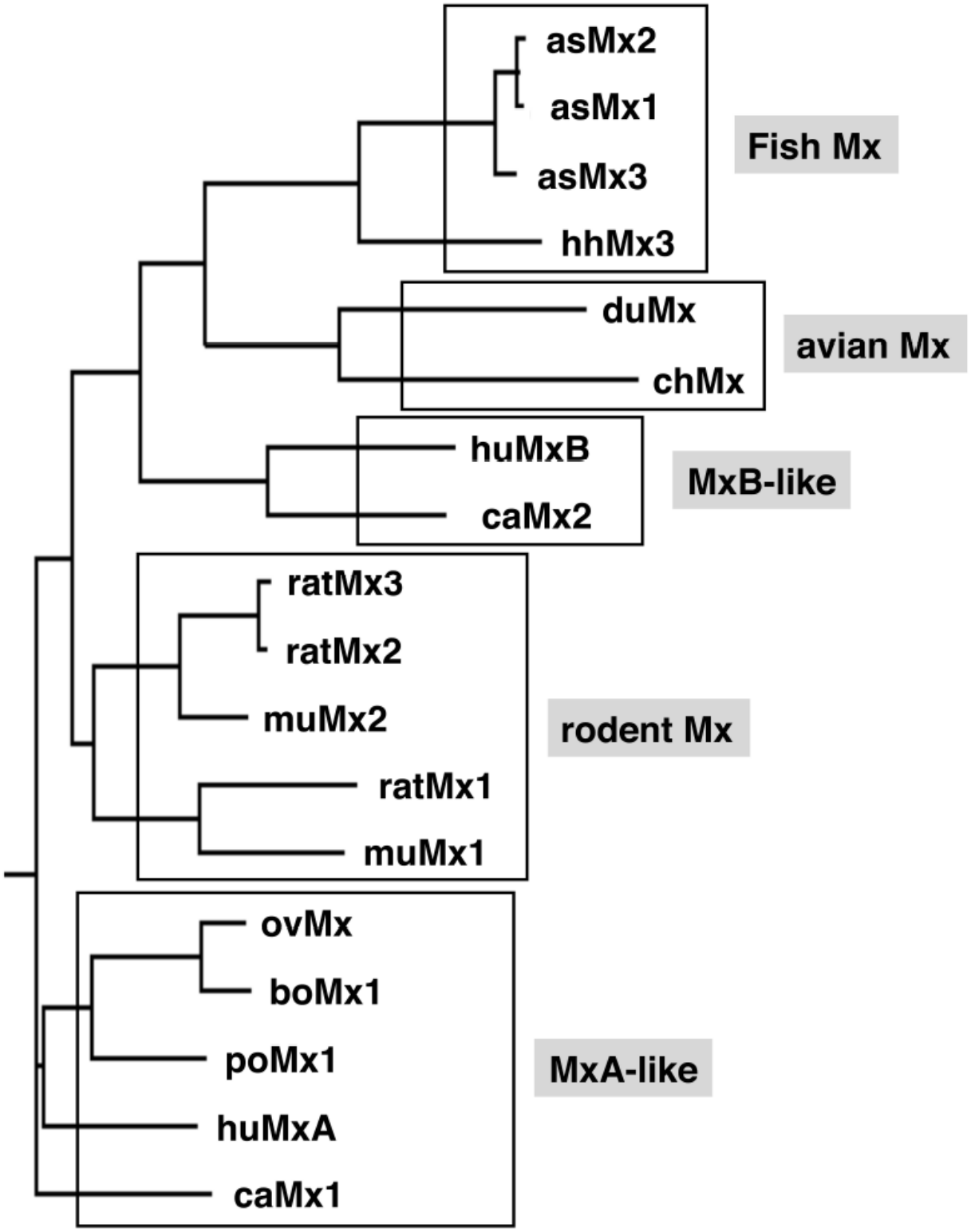

Figure 1 : Arbre phylogénétique des protéines Mx selon Haller *et al.* (2010).

L'expression de ces protéines dépend, de façon très spécifique, des interférons de type I (α et/ou β) et de type III (λ), sans effet des interférons de type II (γ), bien que certaines, comme la protéine MxB humaine, soient produites de façon constitutive (Staeheli *et al.*, 1984 et 1986 ; Aebi *et al.*, 1989 ; Goetschy *et al.* 1989 ; King *et al.*, 2004 ; Holzinger *et al.*, 2007). Si la plupart des protéines Mx n'ont, à l'heure actuelle, aucune fonction physiologique connue en dehors de leur activité antivirale, la protéine MxB humaine, dépourvue d'activité antivirale, semble réguler le processus d'import nucléaire ainsi que le cycle cellulaire (King *et al.*, 2004). L'expression de la protéine MxA humaine a été associée à une sensibilité cellulaire accrue à l'apoptose, ainsi qu'à une réduction de l'invasivité de cellules tumorales, mais aucun lien avec des fonctions cellulaires précises n'a été établi (Mibayashi *et al.*, 2002 ; Mushinski *et al.*, 2009).

La stimulation de cellules au moyen d'IFN de type I induit une production rapide et importante d'ARN messagers Mx, qui représentent alors jusqu'à 0,1% des ARN messagers totaux pendant les huit heures suivant l'induction. Cette stimulation est transitoire et les ARNm Mx disparaissent dans les 48 heures (Staeheli *et al.*, 1986). La concentration maximale en protéines Mx est obtenue entre 24 et 48 heures après stimulation, lesquelles protéines persistent pendant plusieurs jours (demi-vie d'environ 55 heures pour la MxA humaine) au sein de la cellule (Goetschy *et al.*, 1989 ; Ronni *et al.*, 1993 et 1995). L'expression, tant par les interférons de type I que par ceux de type III, se fait via la voie JAK/STAT (*Janus-activated kinase*, *signal transducer and activator of transcription*), après activation de récepteurs spécifiques (IFNAR ou IFNLR) (Haller et Kochs, 2011).

Les protéines Mx sont, pour la plupart d'entre elles, cytoplasmiques, la protéine Mx1 des rongeurs étant nucléaire (Horisberger et Hochkeppel, 1985 ; Horisberger et Gunst, 1991).

Structurellement, les protéines Mx sont caractérisées par un domaine GTPase N-terminal, un domaine interactif central (« CID ») ou « *middle domain* », impliqué dans l'oligomérisation, et un domaine effecteur GTPase C-terminal (« GED »), qui semble essentiel à l'activité antivirale et qui participe également à l'auto-assemblage (Haller et Kochs, 2002 ; Figure 2). Le domaine N-terminal contient un domaine consensus tripartite de liaison au GTP (guanosine-5'-triphosphate) (GDXXXXGKS/T, DXXG et TINKXD), une séquence d'auto-association (appelée « *self-assembly sequence* » ou « *SAS* »), ainsi que la signature des dynamines « LPRGSGIVTR » (Haller et Kochs, 2002). Pour les protéines Mx nucléaires, le signal de localisation

nucléaire est contenu dans la partie C-terminale de la protéine (Haller et Kochs, 2002).

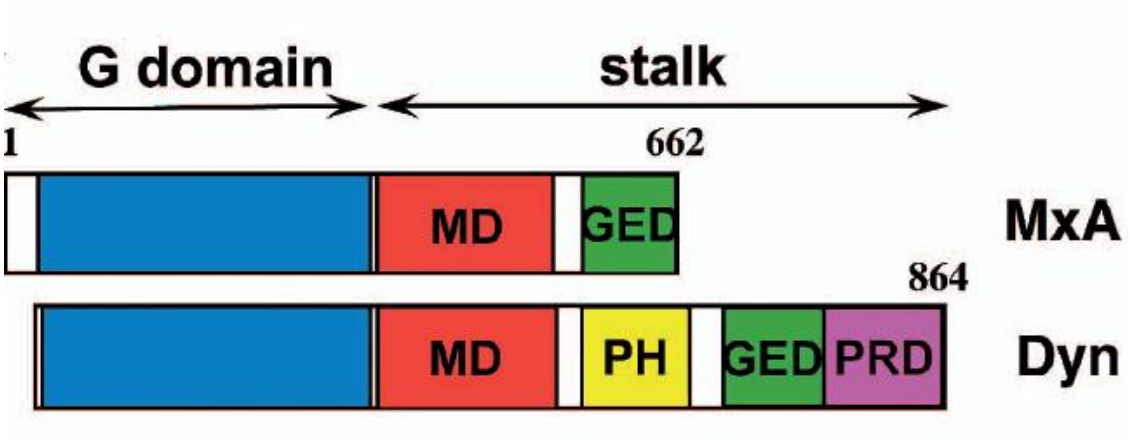

Figure 2 : Structure des protéines Mx en comparaison avec celle des dynamines. La structure générale des protéines Mx est constituée d'un domaine N-terminal GTPase (G domain) et d'un « tronc », lui-même constitué d'un domaine central ou « *middle domain* » et d'un domaine GTPase effecteur (« GED »). Les dynamines comportent en plus un domaine d'homologie de type pleckstrine et un domaine riche en proline et arginine (« PRD »). Selon Haller *et al.* (2010).

Par comparaison avec les autres dynamines, les protéines Mx sont dépourvues de deux motifs : un domaine d'homologie de type pleckstrine, impliqué dans la liaison aux membranes, et un domaine riche en acides aminés proline et arginine, contenant plusieurs domaines de liaison à SH3 (Haller *et al.*, 2010 ; Figure 2). En dépit de l'absence de domaine d'homologie de type pleckstrine (et de tout domaine de liaison aux lipides), la protéine MxA humaine est capable de se lier à des lipides et d'induire la formation de tubules lipidiques *in vitro*, comme les dynamines classiques (Accola *et al.*, 2002 ; Figure 3). La protéine MxA humaine est capable de former des oligomères de grande taille, du même type que ceux formés par d'autres dynamines (Kochs *et al.*, 2002 ; Haller et Kochs, 2002). Ces données tendent à confirmer les résultats antérieurs montrant l'aspect granuleux pris par les cellules stimulées aux IFNs de type I lorsqu'elles sont marquées avec des anticorps anti-Mx (Dreiding *et al.*, 1985 ; Melen *et al.*, 1992 ; Schwemmle *et al.*, 1995). Ainsi, la protéine Mx1 murine forme des granules nucléaires en contact étroit avec le PML-NBs (*promyelocytic leukemia nuclear bodies*), la protéine MxA s'organisant quant à elle en granules qui colocalisent partiellement avec les complexes COPI (*coat proteins type I*) du compartiment intermédiaire de l'appareil

de Golgi (Haller *et al.*, 2010).

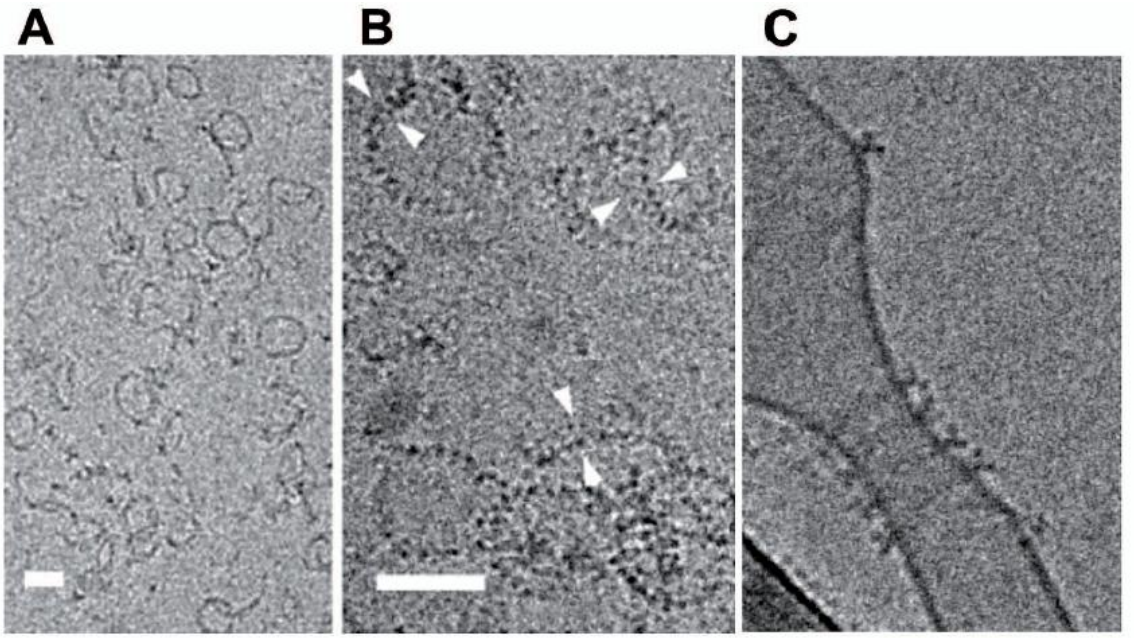

Figure 3 : Structures oligomériques formées par la protéine MxA humaine avec liaison aux liposomes, au microscope électronique à transmission (Haller *et al.*, 2010). A : Anneaux de protéines MxA humaine. B : Grossissement plus important des structures observées en A, montrant un double alignement circulaire de domaines globulaires. C : En présence de GTP et après incubation avec des liposomes, la protéine MxA humaine induit une tubulation des liposomes en formant des structures circulaires entourant ces liposomes. Barre = 50nm. Haller *et al.* (2010).

L'oligomérisation de la protéine MxA humaine implique le domaine central (CID ou *middle domain*) et le GED. Ces domaines prennent une forme tridimensionnelle allongée principalement constituée d'hélices alpha et de boucles, appelée « tronc » (Gao *et al.*, 2010 ; Figure 4). Le domaine GTPase N-terminal est fixé d'un côté du « tronc », alors que deux boucles désorganisées (L2 et L4) sont présentes de l'autre côté de ce « tronc ». L'entrecroisement du « tronc » de plusieurs protéines MxA donne un oligomère de forme circulaire, en anneau, avec le domaine GTPase N-terminal de chaque protéine exposé à l'extérieur et les boucles L2 et L4 exposées vers l'intérieur (Gao *et al.*, 2010 ; Figure 5). L'introduction de mutations au sein des zones d'interface entre protéines dans le « tronc » de la protéine MxA humaine résulte en une perte des capacités d'oligomérisation et de l'activité antivirale (Gao *et al.*, 2010). Les boucles (L2 et L4) sont supposées servir de site de liaison entre la protéine et ses ligands, ce qui

suggère que les oligomères de protéines MxA entourent leur ligand (Haller et Kochs, 2011). D'abord supposées servir de forme de stockage des monomères de protéine Mx, ces structures oligomériques semblent en fait jouer un rôle essentiel dans l'activité antivirale (Haller *et al.*, 2010).

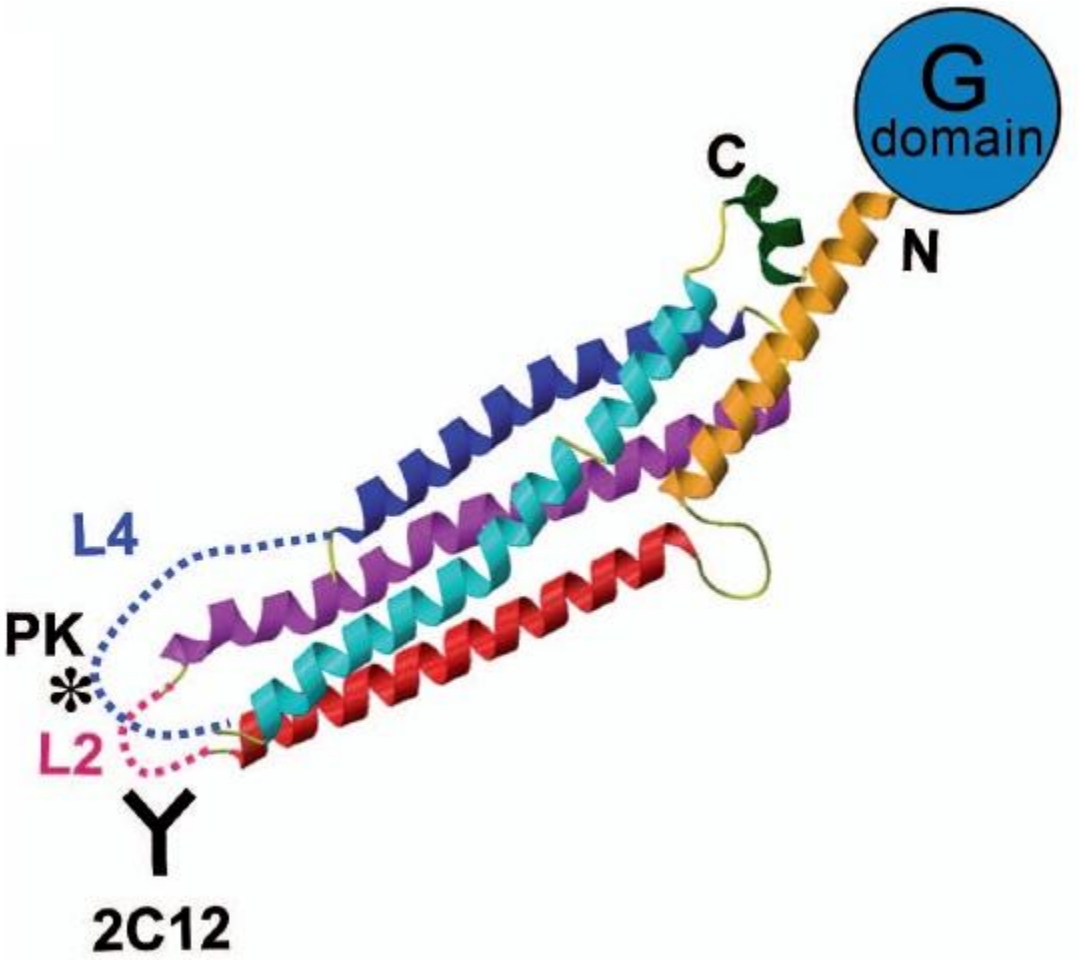

Figure 4 : Structure générale de la protéine MxA humaine, la structure tridimensionnelle du « tronc » (résidus 366 à 633) est détaillée, alors que le domaine globulaire N-terminal, dont la structure n'est pas connue de façon précise pour les protéines Mx, est représenté schématiquement (Haller *et al.*, 2010). La position des deux boucles désorganisées L2 et L4 est indiquée, ainsi que le site de fixation de l'anticorps monoclonal 2C12 et le site de clivage par la protéinase K (résidu 564).

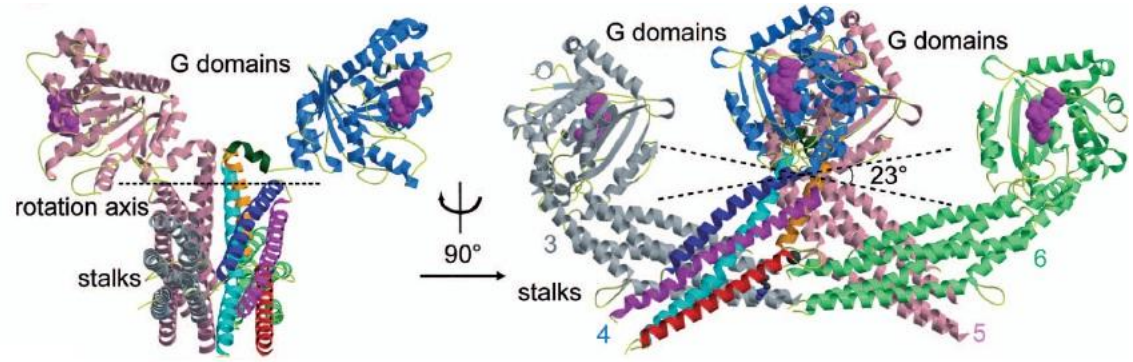

Figure 5 : Modèle de la structure oligomérique de la protéine MxA humaine, basé sur la structure du domaine globulaire de la dynamine et du « tronc » de la protéine MxA humaine (Gao *et al.*, 2010 ; Haller *et al.*, 2010).

L'activité GTPase n'a été étudiée que pour les protéines MxA humaine et Mx1 murine (Nakayama *et al.*, 1991 et 1992 ; Horisberger, 1992 ; Melen *et al.*, 1994 ; Richter *et al.*, 1995). Ces deux protéines sont capables de fixer et d'hydrolyser le GTP mais pas le GDP, l'ATP ou l'UTP (Horisberger, 1992 ; Melen *et al.*, 1994 ; Richter *et al.*, 1995). Cette activité GTPase est abolie lorsque des mutations dirigées du domaine de liaison au GTP sont introduites, ou lorsqu'un analogue non hydrolysable du GTP, tel que le GDPγS, est utilisé (Pitossi *et al.*, 1993 ; Melen et Julkunen, 1994). L'efficacité antivirale de la protéine MxA humaine est conservée en présence de GTPγS ou lorsqu'une Mx mutante, capable de lier le GTP mais plus de l'hydrolyser, est utilisée (Schwemmle *et al.*, 1995 ; Janzen *et al.*, 2000). Il ressort de ces différentes expériences que la liaison du GTP, et non son hydrolyse, est nécessaire à l'activité antivirale de la protéine MxA humaine. De même, en présence de GTPγS, la structure oligomérique de la protéine MxA humaine change, passant d'une structure circulaire à des structures en spirale ou en empilement d'anneaux, confirmant des résultats antérieurs obtenus pour la protéine Mx1 murine ou la dynamine (Nakayama *et al.*, 1993 ; Carr et Hinshaw, 1997 ; Accola *et al.*, 2002).

Des expériences de mutations et de délétions dirigées ont montré que le domaine effecteur C-terminal des protéines Mx est un déterminant important pour l'activité antivirale (Zurcher *et al.*, 1992 ; Johannes *et al.*, 1997 ; Kochs *et al.*, 2002). La fixation d'un anticorps monoclonal spécifique 2C12 sur la région centrale (CID ou MD) des protéines MxA humaine et Mx1 murine inhibe leur activité GTPase (Flohr *et al.*, 1999 ; Kochs et Haller, 1999). Cet anticorps se fixerait sur la boucle L2 et inhiberait ainsi

l'interaction entre cette boucle et son ligand potentiel (Haller *et al.*, 2010 ; Figure 4). La boucle L4, quant à elle, correspondrait au domaine d'homologie de type pleckstrine des autres dynamines et serait, comme celui-ci, responsable de l'interaction de la protéine avec les lipides (Haller *et al.*, 2010).

1.2. Les protéines Mx bovines

Le premier transcrit Mx bovin, de 2.280 paires de bases, a été identifié et décrit en 1998 (Ellinwood *et al.*, 1998). Le locus Mx1 se trouve sur le chromosome 1 de *Bos taurus* (Ellinwood *et al.*, 1998 et 1999). Le gène Mx1 est constitué de 15 exons et un ISRE (*interferon-sensitive responsive element*) est présent dans la région -118 à -107 du début du transcrit (Gérardin *et al.*, 2004). Un motif NF-κB, deux sites de liaison à l'interleukine-6, deux sites Sp1 et cinq motifs riches en GC sont aussi présents (Gérardin *et al.*, 2004). Le premier cDNA boMx1 fut cloné à partir d'une vache croisée Aberdeen-Gelbvieh (Ellinwood *et al.*, 1998). Un total de 11 génotypes sont décrits au sein de l'espèce *Bos taurus* (Nakatsu *et al.*, 2004). Un premier variant Mx1A avec une délétion de 18 paires de bases a été décrit, qui est en réalité un variant par épissage alternatif au niveau de la jonction entre l'exon 3 et l'intron 3 du gène Mx1 (Ellinwood *et al.*, 1998 ; Kojima *et al.*, 2003 ; Nakatsu *et al.*, 2004). L'activité anti-VSV de Mx1 et Mx1A reste inchangée (Nakatsu *et al.*, 2004). Un second variant par épissage alternatif a été plus récemment décrit, Mx1B (Yamada *et al.*, 2009). L'épissage se fait entre un exon alternatif E1' et l'exon 4, entraînant une délétion des 24 premiers acides aminés de la protéine Mx1 (exons 1 à 3) et leur substitution par 27 autres résidus (exon 1') (Yamada *et al.*, 2009). Cette modification entraîne l'apparition d'un signal de localisation nucléaire (NLS) qui rend ce variant Mx1B nucléaire, et rend en outre cette protéine inefficace contre le virus VSV, sauf si on lui supprime artificiellement son NLS (Yamada *et al.*, 2009).

Le spectre antiviral de la protéine Mx1 bovine s'étend au virus de la stomatite vésiculeuse (VSV) et au virus de la rage, tous deux membres de la famille des *Rhabdoviridae* et au virus influenza de type A, de la famille des *Orthomyxoviridae*. Elle reste sans effet, semble-t-il, sur les virus de la famille des *Paramyxoviridae* (Nakatsu *et al.*, 2004 ; Baise *et al.*, 2004 ; Leroy *et al.*, 2005 et 2006 ; Garigliany *et al.*, soumis).

Concernant le cDNA Mx2 bovin, de 2.381 paires de bases, huit allèles différents ont été décrits pour seulement deux substitutions au niveau de la séquence protéique, G302S et

I354V (Babiker *et al.*, 2007). La protéine Mx2 bovine possède une activité anti-VSV proche, bien que légèrement moins prononcée, de celle de la protéine Mx1 bovine, mais ne possède par contre pas d'activité anti-influenza (Babiker *et al.*, 2007 ; Garigliany *et al.*, soumis).

2. Le protéome des virus influenza A

2.1. The polymerase complex

2.1.1. Segment 1: Polymerase basic protein 2.

Influenza viruses, as all negative-stranded RNA viruses, encode their own RNA-dependent RNA polymerase and package it during the budding process. The complete 3D-structure of influenza virus polymerase is unknown, but a low resolution description is available that shows its heterotrimeric nature, globular shape and binding with the nucleoprotein at different sites (Area *et al.*, 2004; Torreira *et al.*, 2007). Separation of the three monomers by isoelectrofocalization revealed the basic nature of two and the acidic nature of the third, which gave them their names: polymerase basic proteins 1 and 2 and polymerase acidic protein (Horisberger, 1980). The 759 amino acid-long polymerase basic protein 2 (PB2) is encoded by genomic segment 1. It binds polymerase basic protein 1 (PB1), nucleoprotein and the cap structures of cell mRNAs. PB2 is therefore directly involved in the cap-snatching and transcription processes. It possesses its own nuclear localization signal (NLS).

2.1.1.a. Polymerase basic protein 1 and polymerase acidic protein binding sites

Within the polymerase heterotrimer, no specific direct interaction between PB2 and polymerase acidic protein (PA) was detected *in vitro* until very recently (Digard *et al.*, 1989; Hemerka *et al.*, 2009). PB1 binds both other monomers which, in turn, mainly bind PB1. Therefore, PB1 is predicted to occupy the core of the polymerase structure, the other two monomers binding on it. Using a panel of PB2 mutants, a first PB1 binding site was located in the PB2 amino-terminal segment extending up to residue 124 (Perales *et al.*, 1999). A second putative PB1 binding site spanning between residues 206 and 259 was picked up by deletion assays in which a weak co-immunoprecipitation with PB1 was found (Ohtsu *et al.*, 2002). Readdressing the same question, Poole and colleagues (2004) confirmed the binding ability of segment 1-124, refuted that of the 206-259 stretch and discovered a new, C-terminal, binding site (580-759). Moreover, each N- and C-terminal PB1 binding site overlaps a nucleoprotein binding site, which results in a competition between nucleoprotein (NP) and PB1 for

PB2-binding, the latter showing a higher affinity (Poole *et al.*, 2004). Using another panel of small fragments, Sugiyama and colleagues (2009) limited the PB1-binding site of PB2 within residues 1-37. These residues are organized as three successive α helices, which are imbricated with three corresponding α helices of the PB2-binding site (678-757) of PB1 (Sugiyama *et al.*, 2009). Further studies on the tridimensional structure of the interaction sites of PB2 and PB1 revealed the central role of E2, R3 and E6 of PB2, and K698 and D725 of PB1 in interprotein salt bridges formation, but their mutation does not seem to affect drastically the PB2-PB1 complex formation (Sugiyama *et al.*, 2009). I4, L7, L10 of PB2, V715, I746 and I750 of PB1 were all essential for PB2-PB1 interaction, and are probably involved in apolar contacts (Sugiyama *et al.*, 2009).
No specific PA-binding site was determined in PB2 but both proteins were shown to interact (Hemerka *et al.*, 2009). Further, this interaction was shown to occur in the cytoplasm with subsequent nuclear translocation to the nucleus of the heterodimer (Hemerka *et al.*, 2009).

2.1.1.b. Nucleoprotein-binding sites

The influenza polymerase was shown to associate with viral ribonucleoproteins (Klumpp *et al.*, 1997), and this binding is mediated by an interaction between the polymerase components and the nucleoprotein. Deletions experiments led to the detection of two nucleoprotein-binding regions within PB2; they extend between residues 1 and 269 on the one hand and between residues 580 to 683 on the other (Poole *et al.*, 2004). Those regions still remain poorly defined and considerably overlap the aforementioned PB1-binding sites but, functionally speaking, a competition between NP and PB1 for PB2 binding is clearly established. The conservation degree of both sites does not differ significantly from that of the whole PB2 (personal results).

2.1.1.c. Cap-binding domain

Influenza mRNAs are synthesized using the cap structures of cellular mRNAs as primers. Cellular mRNAs are bound by their cap and cleaved 10 to 13 nucleotides from their 5' end by the viral polymerase and these fragments are then used as a primer to transcribe the influenza genome into mRNAs. This process is referred to as the "cap-snatching" (Plotch *et al.*, 1981). The first attempt at detecting a cap-binding domain in

the viral polymerase complex consisted in the comparison of the three subunits amino acid sequences with known cap-binding domains from human and yeast proteins. This approach pointed at two amino acid stretches (552-565 and 633-650) within PB2 (de la Luna *et al.*, 1989). Binding of cap structures by PB2 was later confirmed by UV cross-linking studies which rather pointed at segments 242-282 and 538-577 designated cap-binding N- and C-sites, respectively (Honda *et al.*, 1999). The cap-binding C-site was then restricted to the 544-SVLVNTYQWIIRN-556 peptide (Li *et al.*, 2001), which contains a tryptophan and a tyrosine residue, two aromatic amino acids that in other cap-binding proteins have been shown to interact with the m7G of the cap (Matsuo *et al.*, 1997). This PB2 peptide is part of a larger tryptophan-rich region of PB2 (W537, Y550, W552, W557, W564) (Li *et al.*, 2001). Alanine substitution of W552 resulted in a mutant polymerase that was defective in cap-binding activity, possessing only ~25% of the activity of wild-type polymerase complexes. Besides W552, it has not been possible to evaluate the contribution of other aromatic residues because their substitution by alanine prevented PB2 complexation with PB1 and PA (Li *et al.*, 2001). Thus, at least one of the PB2 537-564 segment tryptophans functions in cap binding, indicating that this domain is probably similar to that of other known cap-binding proteins. As substitution of aromatic residues F363 and F404 by non aromatic residues also alters the PB2 cap-binding ability (Fechter *et al.*, 2003), a third segment (363-404) has been incriminated too (middle-site). Altogether, the experimental data available therefore suggest that PB2 contains a tripartite (N-, middle- and C-sites) cap-binding domain. As expected, these distinct domains form a single entity when considering the tridimensional structure of the protein (Guilligay *et al.*, 2008). Residues 320, 325, 332, 337, 339, 355, 357, 361, 378, 404, 429, 431 and 432 appear to form a pocket in which m^7GTP was found to take place (Guilligay *et al.*, 2008; Figure 1).

Residues K586, R589, R597, R604, K627, R630 and R690 would be involved in the formation of a basic pocket which serves as a RNA binding site (Kuzuhara *et al.*, 2009).

2.1.1.d. Nuclear Localization Signals

Since transcription and replication of influenza genomic RNA occur in the cell nucleus, polymerase proteins have to be nuclear. PB2 was the first polymerase component identified as being able to self translocate to the nucleus and to possess a nuclear localization signal (Jones *et al.*, 1986). The PB2 nuclear localization signal was

assigned, by deletion assays, to two discrete sequences made of residues 449-495 (NLS1) and 736-KRKR-739 (NLS2), the integrity of both being necessary for strict PB2 nuclear localization (Perales *et al.*, 1999; Mukaigawa & Nayak, 1991). However, when the PB2 C-terminal 678-759 fragment is expressed alone, it accumulates in the cell nucleus, suggesting the primacy of NLS2 (Tarendeau *et al.*, 2007). This strictly nucleotropic C-terminal fragment is made of a hydrophobic core consisting of a three-stranded antiparallel *β*-sheet onto which a small amphipathic *α*-helix is packed (Tarendeau *et al.*, 2007) (Figure 2). The NLS2 is located immediately after *β*-strand 3, all its residues being exposed, except for the side chain of K736 which is partially buried (Tarendeau *et al.*, 2007). The same PB2 fragment was also shown to bind human importin *α*5 (or Ran binding protein 5), which is a nuclear import receptor that recognizes cargo proteins carrying conventional basic monopartite and bipartite NLSs and facilitates their transport into the nucleus (Deng *et al.*, 2006; Dingwall & Laskey, 1991; Tarendeau *et al.*, 2007). On the other hand, a D701N mutation, associated with an improved pathogenicity in mammals, was shown to enhance the binding of PB2 to importin *α*1 (Gabriel *et al.*, 2008). As bipartite NLSs contain two clusters of basic residues connected by linkers of variable lengths, other mutation experiments were conducted to establish whether, beside the 736-KRKR-739 stretch, the more distal 752-KRIR-755 peptide could also be involved in the nuclear injection process. These studies led to the conclusion that it does (Tarendeau *et al.*, 2007), suggesting that the PB2 736-KRKR-X12-KRIR-755 domain is likely to function as a classical bipartite NLS.

Recent studies confirm the role played by NLS2 in importin binding (Boivin & Hart, 2011). Mutations D701N, R702K and S714R were all associated with enhanced binding to both human and avian *α*1 importins (Gabriel *et al.*, 2008; Boivin & Hart, 2011). Further, the addition of the domain surrounding residue PB2 627 (see further) diminished the association to *α* importins compared to NLS2 alone. This is associated to a steric clash due to the "627 domain", which could play a role in the regulation of the viral polymerase activity (Figure 3). On the other hand, affinity of this 627-NLS domain to avian *α*1 importin was stronger than for human *α*1 importin with both human-like and avian-like mutations (Boivin & Hart, 2011).

The Hsp90 (heat shock protein 90) or RAF-1 (RNA polymerase Activating Factor 1) protein was shown to interact with PB2 and to promote viral RNA synthesis (Momose *et al.*, 2002). Hsp90 binds PB2 through its N-terminal chaperone domain and the acidic domain of its middle region (Momose *et al.*, 2002). It plays a chaperone function on the

maturation of other cellular proteins and was shown to relocate from cytoplasm to nucleus upon influenza infection, via its binding to PB2 (Momose *et al.*, 2002). But Hsp90 also binds PB1 and PB2-PB1 complexes but not PB2-PB1-PA complexes, these results suggesting that Hps90 helps for the maturation of native influenza polymerase complexes and for their nuclear transport (Naito *et al.*, 2007). It is thought to be freed from PB2 and/or PB1 upon formation of polymerase heterotrimeric PB2-PB1-PA complexes (Naito *et al.*, 2007). Deng and colleagues (2006) showed that the nuclear import factor Ran binding protein 5 (or importin α5) interacts with PB1 and PB1-PA complexes but not with PB2-PB1 or PB2-PB1-PA complexes, it is possible that the viral polymerase proteins use different host factors to reach the cell nucleus and to form active trimeric polymerase complexes. But, as explained here above, this last result is in contradiction with observations of Tarendeau and colleagues (2007), which identified a binding of importin α5 to the C-terminal end of PB2.

2.1.1.e. Mitochondrial targeting signal

Small amounts of PB2 were fortuitously found to accumulate in mitochondria (Fodor *et al.*, 2004). A mitochondrial targeting signal (MTS) was localized within the PB2 amino-terminus and fine mapping indicated that the 22 first N-terminal amino acids and mostly two leucine residues (L7 and L10) were essential for mitochondrial localization (Carr *et al.*, 2006). The fact that the first 13 N-terminal residues are predicted to form an α-helix (Carr *et al.*, 2006) strengthens the experimental data because such structures are commonly found in MTSs (Stojanovski *et al.*, 2003). Moreover, functional studies showed that mutations in the PB2 MTS that prevent translocation of the protein to mitochondria lead to the dissipation of the organelle's membrane potential (Carr *et al.*, 2006). PB2 could therefore participate to the maintenance of mitochondrial integrity during influenza virus infection, possibly by counterbalancing the PB1-F2 proapoptotic function. Personal alignments of PB2 sequences available in GenBank showed a global high conservation of the PB2 MTS which indirectly confirms the conclusions reached *in vitro*.

PB2 protein from avian strains does not localize in mitochondria by opposition to that of human strains, due to a polymorphism at position 9 of PB2 (N in human and D in avian strains) (Graef *et al.*, 2010). This difference did not affect replication efficiency *in vitro* but the lack of mitochondrial localization was linked to an enhanced stimulation of

IFN*β* production and attenuation in animal models. Further, PB2 protein localizing in mitochondria was associated to mitochondrial antiviral signaling protein (MAVS), which is a known crucial factor of the IFN*β* pathway (Graef *et al.*, 2010).
If each of the polymerase subunits (PB2, PB1 and PA) was shown to interact with Interferon *β* Promoter Stimulator 1 (IPS-1), the binding by PB2 was the strongest and resulted in the most significant inhibition of IFN*β* production (Iwai *et al.*, 2010). Residues 120 to 256 of PB2 appeared as the most important for IPS-1 binding. This interaction provides another way for PB2 to inhibit the IFN*β* pathway (Iwai *et al.*, 2010).

2.1.1.f. Interaction with cytosolic chaperonin containing TCP-1 (CCT) protein

Purification of plasmid-expressed PB2 protein from human embryonic kidney 293 cells allowed the identification of several new cellular partners of PB2 protein: cytosolic chaperonin containing TCP-1 (CCT), stress-induced phosphoprotein 1 (STIP1), FK506 binding protein 5 (FKBP5), *α*- and *β*-tubulin, Hsp60, and mitochondrial protein p32 (Fislova *et al.*, 2010). Among these, the association of PB2 and CCT was further studied and revealed that the inhibition of CCT had a negative impact on influenza replication with diminished PB2 protein and viral RNA accumulation, suggesting a chaperone role for CCT on PB2 for its folding and probably its incorporation into the polymerase complex (Fislova *et al.*, 2010). Large deletion mutants were used to better define the PB2 domain involved in CCT binding and the central 181-522 domain was necessary for a positive co-immunoprecipitation of both proteins (Fislova *et al.*, 2010).

2.1.1.g. Interaction with cyclin T1/CDK9.

All three polymerase subunits (PB2, PB1 and PA) were shown to coprecipitate with cyclin T1/CDK9 (Zhang *et al.*, 2010). This interaction allows the viral polymerase to indirectly bind cellular RNA polymerase II, and suppression or overexpression of cyclin T1/CDK9 resulted in an inhibition or upregulation of the transcription activity of influenza vRNP, suggesting a regulating role of cyclin T1/CDK9 on influenza transcription (Zhang *et al.*, 2010).

2.1.1.h. Residues seen as determinants of pathogenicity for mammals

In vivo, avian strains replicate efficiently in avian hosts but are restricted in their replication in the respiratory tracts of mammalian hosts (Murphy *et al.*, 1982). Comparison of the replication efficiency *in vitro* of the human strain A/Los Angeles/2/87 and of a single gene reassortant virus genetically made of the PB2 encoding gene from the avian strain A/Mallard/NY/78 and the complementary seven gene segments from the same human strain led to the discovery that the "avian PB2" clearly caused an abatement of the replication efficiency in mammalian cells but not in avian cells (Clements *et al.*, 1992). After the poorly replicative reassortant virus was repeatedly passaged in mammalian cells and a highly replicative variant was isolated, it was established that the gain of replicative function was associated with a single mutation causing the substitution of the glutamate residue at position 627 by a lysine residue (Subbarao *et al.*, 1993). Since then, this E627K mutation has been correlated with an exacerbation of growth of H5N1 influenza A viruses in the mouse respiratory tract and lung (Hatta *et al.*, 2007; Munster *et al.*, 2007; Shinya *et al.*, 2007). Furthermore, the same E627K substitution has been associated with the increased pathogenicity of chicken H7N7 and avian H5N1 for humans (Fouchier *et al.*, 2004; Hatta *et al.*, 2001). Recent results have brought interesting mechanistic clues that are compatible with a specific gain of virulence for mammalian hosts. Replacement of glutamate by lysine at position 627 was shown to boost the transcription/replication activity in mammalian – but not avian – cells, probably by improving the NP binding properties of PB2 (Labadie *et al.*, 2007), which is consistent with the fact that residue 627 belongs to the second NP-binding site previously described (Poole *et al.*, 2004). Importantly, if a lysine at position 627 is commonly found in different avian strains, including H5N1 strains, there is no known human isolate having a glutamate. Thus, the E627K substitution is not a marker of human adaptation, but should rather be considered as a main determinant of pathogenicity for mammals. In some human isolates, a K627R substitution is also observed, which suggests that the true determinant of pathogenicity for humans is rather a polar positive (basic) residue at position 627 rather than lysine itself (personal results). A lysine residue at position 627 of PB2 was shown to confer influenza virus the ability to grow efficiently at 33°C, i.e. the temperature at the level of upper airways of mammals, by comparison with strains with a glutamate at this position, which need higher temperatures (> 37°C – in birds and in

lower airways of mammals) (Hatta *et al.*, 2007). The E627K mutation was associated *in vivo* with enhanced systemic infection and alteration of the T-cell immune response, leading to a more virulent phenotype (Fornek *et al.*, 2009).

Comparison between genomes of a highly pathogenic H7N7 avian influenza virus which is low-pathogenic for mice and its lethal mouse-adapted descendant revealed a constellation of 9 amino acid substitutions among which 3 were located in PB2: T333I, D701N and S714R (Gabriel *et al.*, 2005). Assaying of multiple reassortant viruses led to the discovery that (i) D701N and S714R alone moderately enhance polymerase activity *in vitro* but do not exacerbate pathogenicity *in vivo*, (ii) simultaneous possession of D701N and S714R exacerbates pathogenicity *in vivo* and (iii) the presence of S714R was a prerequisite for the expression of other virulence-conferring mutations, especially that affecting the nucleoprotein (N319K) (Gabriel *et al.*, 2005). This confirms the role played by residues of NLS2 in host adaptation and their interplay with residues of the "627 domain" (Boivin & Hart, 2011). Adaptation of the avian H7N7 Dobson strain to mouse cells also yielded the D701N substitution (Yao *et al.*, 2001). This last mutation was recently shown to increase the binding of PB2 to importin α1 in mammalian cells, the N319K mutation in NP enhancing the importin α1 binding by NP in the same way (Gabriel *et al.*, 2008). These two mutations increase the nuclear transport of PB2 and NP in mammalian, but not in avian, cells (Gabriel *et al.*, 2008). Interestingly, the E627K substitution was not detected in these experimental settings, suggesting that different evolution ways can conduct to acquisition of a lethal phenotype. Human H5N1 influenza A viruses isolated in Hong Kong in 1997 contained amino acid changes at positions 199, 627, 661 and 667 of PB2, but their objective contribution to pathogenicity has not been established yet (Hiromoto *et al.*, 2000). A lysine to glutamine substitution at position 355 was also reported to cause an abatement of the virulence of H5N1 strains for mice and humans (Hiromoto *et al.*, 2000; Yao et al, 2001; Katz *et al.*, 2000). Mutation PB2 T271A was also associated with enhanced polymerase activity and growth efficiency in mammals (Bussey *et al.*, 2010). Further evidence of the role played by residues PB2 271 and 627 was provided by Foeglein and colleagues (2011). Taken together, it is clear that PB2-enhancing mutations dramatically increase virulence in mammals and it is probable that acquisition of virulence for mammals requires a host-specific fine tuning between PB2 and NP.

2.1.1.i. Conclusion

The PB2 protein is a component of the influenza polymerase complex and plays an essential role in the cap-snatching and transcription processes (Figure 4). It binds PB1, and to a lesser extent PA. It also binds the nucleoprotein, this binding being involved in the association of the polymerase complex with viral ribonucleoproteins within influenza virions, and Hsp90 protein. It is nuclear and possesses at least one NLS. It also accumulates in mitochondriae thanks to the presence of a mitochondrial targeting signal, and is thought to exercise an anti-apoptosis activity at this level. Finally, PB2 is clearly involved in the host specificity and in the virulence of influenza virus, notably depending on the nature of residue 627.

2.1.2. Segment 2: Polymerase basic protein 1

The 757 amino acid-long polymerase basic protein 1 is the most conserved influenza A virus protein (97% of mean identities) (personal investigations). It is encoded by genomic segment 2. Within the polymerase heterotrimer, it binds the other two subunits and constitutes the core of this proteic complex (Ohtsu *et al.*, 2002). PB1 possesses its own NLS, binds both the 3' and 5' conserved ends of vRNA strands and ensures RNA-dependent RNA polymerization and would participate to the endonucleasic activity involved in the cap-snatching process (Biswas & Nayak, 1994; Fodor *et al.*, 2004; Jung & Brownlee, 2006; Li *et al.*, 2001).

PB1 is thought to be critically implicated in influenza virus virulence, since the emergence of the Asian (H2N2, 1957) and Hong-Kong (H3N2, 1968) pandemic strains was permitted through the acquisition of new genomic segments, among which PB1 (Wright & Webster, 2001). Intriguingly, two specific substitutions (K198R and I317M) were associated with diminished virulence in mice (Katz *et al.*, 2000).

PB1 is, together with NS1, a target for protein kinase C (PKC) phosphorylation (Mahmoudian *et al.*, 2009). Further, PKC inhibitor Gö6976 treatment resulting in a sharp decrease in the influenza transcription efficiency, PKC-dependent phosphorylation of PB1 is thought to regulate the polymerase activity (Mahmoudian *et al.*, 2009).

2.1.2.a. Polymerase basic protein 2-binding site

Using coexpression of full-length PB2 and PB1 deletion variants followed by co-immunoprecipitation studies, Biswas and Nayak (1996) detected two N-terminal PB1 segments involved in PB2 binding (49-144 and 252-320). The second segment overlaps the RNA polymerase motif I (298-311) and is assumed to permit the well-positioning of PB2 and PB1 polymerase catalytic site for efficient nucleotide addition (Biswas & Nayak, 1996). In other studies, C-terminal binding sites were detected, either between positions 506 and 659 (Gonzalez *et al.*, 1996) or between 601 and 757 (Toyoda *et al.*, 1996). Ohtsu and colleagues (2002) restricted the carboxy-terminal motif between residues 718 and 732. Further studies confirmed the importance of these C-terminal residues in PB2-binding, since the 712-746 motif was shown to efficiently bind PB2 (Poole *et al.*, 2006). Personal alignments of all PB1 sequences available reveal that this 712-746 domain was highly conserved among influenza A strains (only some V719I or M and I728V substitutions were detected, mutations in other residues being extremely rare) which is indeed compatible with a functional importance. There remains that, in the 3D-structure of the trimeric polymerase, both N- and C-terminal PB1 domains aforementioned could form a single PB1-PB2 interaction structure. The C-terminal extremity of PB1 is thought to present an α-helical structure (Poole *et al.*, 2006). The interaction between two herpes simplex virus polymerase proteins was shown to be mediated by an α-helical domain, and this interaction was susceptible to peptide inhibition and to small molecule inhibitors of the polypeptide interface, resulting in an antiviral activity (Poole *et al.*, 2006). A recent example was provided by Ghanem and colleagues (2007) who showed that the expression of a short peptide corresponding to the PA-binding site of PB1 protein blocked the viral polymerase activity (see further). A similar strategy might be used to design influenza polymerase inhibitors (Poole *et al.*, 2006), the very high conservation of PB2 and PB1 proteins (97% of mean identities each, among influenza A viruses) making them first-choice targets for antiviral therapy.
Recent structural resolution of the PB2-PB1 interaction site confirmed the involvement of three α helices formed by residues 1-37 of PB2 and three α helices made by residues 678-757 of PB1 in the complex formation (Sugiyama *et al.*, 2009). Residues 698, 715, 725, 746 and 750 of PB1 are thought to play a central role in salt bridges and apolar contacts formation with PB2 residues (Sugiyama *et al.*, 2009; see previously).

2.1.2.b. Polymerase acidic protein-binding site

The N-terminal end of PB1 was shown to be implicated in the binding to polymerase acidic protein subunit, precisely the first 25 (Ohtsu *et al.*, 2002), 48 (Perez & Donis, 1995) or 78 (Gonzalez *et al.*, 1996) amino acids. Furthermore, alanine substitution of N4, L7, L8, F9, L10, V12 and P13 led to a dramatically diminished co-immunoprecipitation with PA (Ohtsu *et al.*, 2002). Strikingly, the region 1-25 of PB1 exhibits higher variation than the rest of the protein (personal observations). Among the 7 critical residues previously identified by alanine substitution, only L10 was strictly conserved and L7 and F9 were highly conserved, substitutions of other residues being N4K/I, L8I/V (infrequent), V12I/M/A (infrequent) and P13S. Strikingly, the V12A substitution, which alters PB1-PA interaction *in vitro* (Ohtsu *et al.*, 2002), was found in several natural strains. Thus, a research effort seems still needed to reconcile all available data regarding the PA binding site of PB1.

A peptide corresponding to the 25 first residues of PB1 (thus targeting the PB1-binding site on PA protein) was shown to inhibit the influenza polymerase activity and to interfere with viral growth (Ghanem *et al.*, 2007). This last study confirms the importance of residues 1-25 of PB1 in PA-binding.

2.1.2.c. vRNA promoter binding sites

Transcription of genomic segments into mRNAs uses capped 5' ends of cellular mRNAs that are bound and cleaved by the viral polymerase, this process being referred to as the "cap-snatching" (Li *et al.*, 1998). Initiation of capped RNA primers elongation by the viral trimeric polymerase requires its prior activation by the successive binding of vRNA 5' 13-nucleotide-long and 3' 12-nucleotide-long extremities (forming the viral promoter) on the PB1 subunit. Accordingly, PB1 contains a specific vRNA binding site for each vRNA end.

The vRNA 5' end-binding site ("RCHRGDTQIQTRRSF") spans between residues 560 and 574, a stretch in which R571 and R572 play a critical role (Li *et al.*, 1998). vRNA 5' end fixation on this site induces an allosteric change of the polymerase complex that activates the cap-binding activity of PB2 and the 3' vRNA-binding capacity of PB1 itself (Li *et al.*, 1998). Replacement of R571 or R572 by alanine completely abolished vRNA 5' end fixation and subsequent endonuclease activity (Li *et al.*, 1998). The 560-

574 sequence is globally highly conserved among influenza A strains archived in GenBank (personal results). R572 was systematically conserved but some strains presented a K or, more surprisingly (and less frequently), an E or a G residue instead of the expected R at position 571 (RNA- and DNA-binding domains are commonly made of basic residues that interact with negatively-charged phosphate residues of nucleic acids). Interestingly, binding of vRNA 5' end on PB1 also depends on the formation of a PB1-PA complex for full efficiency (Lee *et al.*, 2002).

The demarcation of the PB1 vRNA 3' end-binding site is still debated. Amino acid sequence alignments first revealed an octapeptide (249-RGFVYFVE-256) homologous to the ribonucleoprotein 1 motif (RNP1) found in different RNA-binding proteins. Consistent with the known crucial role of RNP1 phenylalanine residues in such proteins, the binding of RNA by PB1 was abolished by alanine substitution of F251 or F254 (Li *et al.*, 1998). Also, according to personal sequences alignments, F251 and F254 were strictly conserved in all but one (F254S in A/FPV/Rostock/1934 [H7N1]) PB1 sequences available which reemphasizes the critical need of these two F residues. However, further alanine substitution assays do not confirm the absolute requirement of these phenylalanine residues for vRNA-binding (Jung & Brownlee, 2006). Moreover, comparison of the vRNA promoter binding sites between influenza A, B, C and Thogoto viruses highlights two domains directly flanking the aforementioned octapeptide (233-248 and 257-281) which show more conservation than the octapeptide itself, suggesting that the vRNA 3' end-binding site could be longer than initially thought (Jung & Brownlee, 2006). Mutational analyses and UV cross-linking assays this time revealed the critical importance of R233, R238, R239 and R249 in the octapeptide N-terminal flank for vRNA 3' and 5' ends binding, while there were no essential residues in the conserved C-terminal flank (269-281) (Jung & Brownlee, 2006). Residues R233 and R238 were also shown to fix vRNA 5' end in the absence of 3' end, whereas R239 and R249 only fix vRNA when both ends are present, suggesting the importance of the corkscrew secondary structure of the vRNA promoter to be detected and bound by the viral polymerase (Jung & Brownlee, 2006). This 233-249 motif, called "N1 region", is thus more likely to bind 5' end of vRNAs than 3' end (Jung & Brownlee, 2006).

These data suggest that vRNA 5' end binds to PB1 segments 233-249 and 560-574 (the vRNA 5' end-binding site mentioned above) and that the vRNA's corkscrew secondary structure brings its 3' end adjacent to its own 5' end with (perhaps without) the help of the 249-256 octapeptide (Jung & Brownlee, 2006).

A new motif of basic residues was more recently associated with RNA binding, being more specifically essential for mRNA synthesis (transcription) without affecting cRNA production (Kerry *et al.*, 2008). Alanine substitution of K669, R670 or R672 resulted in an abatement of PB1 binding to vRNA promoter and to capped RNAs, resulting in a diminished transcription efficiency (Kerry *et al.*, 2008).

2.1.2.d. Motifs involved in RNA-dependent RNA polymerization

The nucleotide addition activity of influenza virus polymerase is ensured by PB1, which includes the four consensus motifs typical of RNA-dependent RNA polymerases encoded by plus or minus polarity single- and double-stranded RNA viruses and of RNA-dependent DNA polymerases (reverse transcriptases) encoded by retroid elements (Poch *et al.*, 1989). The four consensus motifs found in PB1 are the following (I to IV): 298-ISFTITGDNTKWNE-311, 399-GTASLSPGMMMGMF-412, 438-WDGLQSSDDFALIVNA-453 and 474-GINMSKKKSYI-484. The strict conservation of D305 (motif I), G406 (II), 444-SDD-446 (III) and K481 (IV) in all influenza A strains sequenced to date (personal investigations) confirms the previously suspected crucial role of these residues in PB1-driven RNA-dependent RNA polymerization (Biswas & Nayak, 1994).

2.1.2.e. Motif involved in RNA endonucleasic cleavage

The RNA endonucleasic activity ensuring the cap-snatching process in which host mRNAs are cleaved 10 to 13 nucleotides from their 5' end to generate a pool of primers for viral mRNA synthesis was long thought to be taken up by PB1 (Hagen et al, 1994; Li *et al.*, 1998). The putative PB1 endonucleasic cleavage motif displays a RNase H-like type and is made of the segment 508-ELPSFGVSGINESAD-522 where amino acids E508, E519 and D522 form the typical "EED" triad found in other RNase H-like endonucleases. Substitution of one of these three amino acids completely abolishes PB1 endonucleasic activity. The EED triad of all RNase H-like endonucleases is spread over 50-60 residues and binds one or more divalent metal ions to become activated. In the case of PB1, the triad is far more compact (15 residues) and its activation also depends of the refolding triggered by the binding of vRNA's 5' and 3' ends (Hagen *et al.*, 1994). This allosteric change also positions the active endonucleasic site at the right distance

from the cap-binding site of PB2 which permits the cleavage to take place 10 to 13 nucleotides from the 5' cap-structure of host mRNAs (Li *et al.*, 2001).
However, recent structural data and mutational analyses tend to locate the endonuclease catalytic site of the polymerase complex on the N-terminal extremity of PA (Dias *et al.*, 2009; Crépin *et al.*, 2010).

2.1.2.f. Nuclear Localization Signals

The PB1 nuclear localization signal was first assigned, by deletion assays, to two discrete sequences made of residues 180-195 (NLS1) and 202-252 (NLS2) (Nath & Nayak, 1990). Each PB1 NLS contains a short basic stretch (RKRR and KKKQR, respectively) similar to the SV40 virus NLS, which consists of a proline followed by a stretch of basic residues (PKKKRKV). Deletion of one or the other PB1 NLS led to a mixed cytoplasmic/nuclear picture, whereas deletion of both caused exclusive cytoplasmic localization (Nath & Nayak, 1990). Therefore, instead of having two NLSs, it was hypothesized that the PB1 nuclear targeting signal rather consists in a nucleoplasmin-like type NLS with two basic clusters separated by a short amino acid spacer, both intact subunits being necessary for nuclear localization (Dingwall & Laskey, 1991). However, this view is challenged by recent experimental data and sequence alignments. Introduction of point mutations inside the putative bipartite NLS did not affect nuclear localization of the protein (Fodor & Smith, 2004). Moreover, the same authors showed that PA was required for efficient nuclear localization of PB1. Inversely, nuclear transport of PA had been shown to be enhanced by PB1 (Nieto *et al.*, 1992). Thus, both proteins could have to gather in a complex to ensure their nuclear injection or retention. Also, our sequence alignments from influenza virus strains sequenced so far revealed some significant natural variation in the putative bipartite NLS. For the 187-RKRR-190 stretch (NLS1), R187 was sometimes replaced by K, K188 by R, R189 by K, G or I and R190 by G, the substitution by non basic residues being relatively infrequent (personal observations). With respect to the second 207-KKKQR-211 stretch (NLS2), K207 was sometimes substituted by E, R or Q, K208 by R, I or E, K209 by R or N, Q210 by H or N and R211 by K, G, M or S. Interestingly, H210 and K211 were typically found in recent epidemic human H1N1 strains. NLS2 was globally less conserved than NLS1, but the substitutions, even by non basic residues, generally did not alter the polybasic nature of the stretch.

A third motif (668-PKRNRSI-674) was proposed as a potential NLS in a computer search. In the same way as for NLS1 and NLS2, introduction of point mutations within this putative NLS3 did not affect subcellular localization of PB1 protein (Fodor & Smith, 1994). Besides, PB1 was shown to bind the Ran binding protein 5 (RanBP5 or importin α5), and this binding was needed for nuclear accumulation of PB1-PA complexes (Deng *et al.*, 2006). RanBP5 was able to bind PB1-PA complexes but not PB2-PB1 or PB2-PB1-PA complexes. PB2 interacts with the Hsp90 protein and it is thought that Hsp90 acts as a chaperone for the maturation of native polymerase complexes (Naito *et al.*, 2007). Thus, Hsp90 and RanBP5 are both most likely to play an important role in the maturation and nuclear translocation of influenza polymerase proteins. The existence of PB2-PA complexes was recently demonstrated, meaning that the formation of a full polymerase complex does not necessarily involve a first PB1-PA interaction (Hemerka *et al.*, 2009). Both NLS1 and NLS2 of PB1 are required for full RanBP5 binding, and introduction of mutations in these motifs affects nuclear localization of PB1 and viral growth efficiency (Hutchinson *et al.*, 2011). It has to be noted here that PB1-F2 protein interacts with PB1 and that this interaction is required for the nuclear retention of PB1 protein at the end of the infection cycle (Mazur *et al.*, 2008).

2.1.2.g. Conclusion

PB1 appears as the central element of the influenza polymerase complex, both structurally and functionally. It binds PB2, PA and cellular RanBP5 protein, interacts with viral genomic RNA ends, and exercises the RNA-dependent RNA polymerase activity and is thought to participate to the endonucleasic activity needed for the cap-snatching of cellular mRNAs (Figure 5). All these critical functions are consistent with its very high conservation among influenza A strains.

2.1.3. Segment 2: PB1-F2 protein

Most influenza A virus isolates (>99%) carry an additional open reading frame overlapping the PB1 gene (ORF2) that encodes a small protein designated PB1-F2 (Chen *et al.*, 2001; Zell *et al.*, 2007). The ORF2 start codon is made of nucleotides 119-121 (ORF1 numbering) and 15 different in-frame stop codons were already detected,

yielding 8, 11, 25, 27, 34, 43, 57, 59, 63, 72, 79, 81, 87, 90 or 101 amino acid-long possible PB1-F2 peptides/proteins (Zell *et al.*, 2007). Seventy-nine and more amino acid-long PB1-F2s are considered to be functionally intact. In a collection of 2226 influenza A virus strains, 87% encoded intact PB1-F2s, among which 96%, 81% and 75% of avian, human and porcine strains did, respectively (Zell *et al.*, 2007). Strikingly, however, PB1-F2 of all H1N1 human strains isolated since 1950 was truncated (57 amino acid-long) (Zell *et al.*, 2007). Intact PB1-F2 protein displays a number of unique features, namely variable expression levels among infected cells, mitochondrial localization, apoptotic or proapoptotic properties and rapid proteasome-dependent degradation (Chen *et al.*, 2001). It interacts with PB1 and is thought to be necessary for the influenza polymerase activity (Mazur *et al.*, 2008). Thus, PB1-F2 participates to the fitness of influenza virus, *in vitro* but also most probably *in vivo*. The interaction with PB1 is responsible for the nuclear retention of PB1 at the end of the infectious cycle (Mazur *et al.*, 2008). The N-terminal part of PB1-F2 (1-50) is required for full PB1 protein expression and polymerase activity (Kosik *et al.*, 2011).

Interestingly, deletion of PB1-F2 was not systematically associated with attenuation of influenza virus in mouse models, meaning that the effect of PB1-F2 on virulence might be strain-specific (McAuley *et al.*, 2010).

PB1-F2 was also responsible for IFNβ stimulation via the NF-κB pathway, without implication of AP-1 or IRF3, making PB1-F2 an antagonist of NS1 and PB2 protein, which downregulate type I IFN expression (Le Goffic *et al.*, 2010).

2.1.3.a. Structure

Full-length PB1-F2s were first predicted to contain two α-helices between residues 54-62 and 73-82 (Chen *et al.*, 2001; Gibbs *et al.*, 2003). The predicted helix at amino acids 73 to 82 was found to contain an 11 amino acids sequence with obvious similarity to the amphipathic α-helix of the human T-cell leukaemia virus type 1 (HTLV-1) p13II protein, which is responsible for mitochondrial targeting of this protein (Ciminale *et al.*, 1999). A further study using recombinant PB1-F2 and Nuclear Magnetic Resonance (NMR) spectroscopy in the presence of membrane mimetics showed that the whole 55-85 segment forms an α-helix more compact than originally thought (Bruns *et al.*, 2007) (Figure 6). Furthermore, a much weaker helix-like structure is adopted by segment 9 to 20, which is separated from the 55-85 helix by an essentially random coil region (Bruns

et al., 2007). PB1-F2 was also shown to self-associate, with a highest affinity in aqueous solution than when hydrophobicity rises (Bruns *et al.*, 2007). Both an N-terminal and a C-terminal oligomerization domains were required for self-association, residues 68 to 72 being probably involved (Bruns *et al.*, 2007).
Further, PB1-F2 from several strains was able to switch from a disordered state to *α*-helix and *β*-sheet structures in a membrane environment, with amyloid fibers formation in infected cells (Chevalier *et al.*, 2010).

2.1.3.b. Mitochondrial Targeting Signal

The PB1-F2 protein essentially locates within mitochondriae (Chen *et al.*, 2001). The mitochondrial targeting signal (MTS) was first assigned to residues 65 to 87 (Gibbs *et al.*, 2003). Deletion of amino acids 69, 70 and 71 completely abolished mitochondrial localization (Gibbs *et al.*, 2003). Five positively charged residues (R or K at positions 73, 75, 78, 79 and 81) were also required for effective mitochondrial targeting (Chen *et al.*, 2004; Gibbs *et al.*, 2003), which is reminiscent of the arginine-rich domains inserted in other apoptosis-inducing proteins like Human Immunodeficiency Virus Vpr (Chen *et al.*, 2004). Another study by Yamada and colleagues (2004) revealed that the segment extending between residues 46 and 75 was necessary and sufficient for full efficiency of mitochondrial localization and that, in the 63-75 stretch, K73 and R75 were minimally required. Sequences alignments by the authors revealed that residues at positions 73 and 75 were not fully conserved. The K73R and R75H substitutions were often found, but those two residues are basic too, which confirms that the crucial requirement for mitochondrial targeting is the presence of a basic amphipathic *α*-helix.

2.1.3.c. Proapoptotic function

Examination of the effects of PB1-F2 on planar lipid membranes, on mitochondria and on the induction of cell apoptosis has led to the conclusion that the basic amphipathic *α*-helix directly destabilizes and permeabilizes the mitochondrial inner membrane (Chanturiya *et al.*, 2004; Zamarin *et al.*, 2005). Mechanistically speaking, intact PB1-F2 is thought to oligomerize in a way creating pores through the mitochondrial membrane (Chanturiya *et al.*, 2004; Zamarin *et al.*, 2005). *In vivo*, knocking out of PB1-F2 resulted in an accelerated clearance of the virus from mouse lungs without affecting its

replication rate (Zamarin *et al.*, 2006), which gives some credit to the hypothesis stating that PB1-F2 could be excreted and cause apoptosis of recruited immune cells (Chen *et al.*, 2001). As all the pandemic strains of the last century contained a new PB1 genomic segment, PB1-F2 has also been associated to pandemic properties (Zamarin *et al.*, 2006), but the demonstration of a cause-to-effect link is lacking so far.

2.1.3.d. Conclusion

PB1-F2 is a proapoptotic protein of variable length, not required for viral replication but most probably needed for full virulence. It is encoded by an alternative reading frame of the PB1 ORF. Its proapoptotic properties are due to the presence of a mitochondrial targeting signal, thought to be a basic amphipathic α-helix that would permeabilize the mitochondrial inner membrane. It interacts with PB1 and is required for the full activity of the viral polymerase.

2.1.4. Segment 3: Polymerase acidic protein.

The 716 residue-long viral polymerase acidic protein subunit participates to transcription and replication processes, being notably necessary to the endonuclease activity of the polymerase (Lamb & Krug, 2001). It is encoded by genomic segment 3. It binds to PB1 and PB2 and a cellular transcription cofactor (hCLE), includes a nucleotide-binding site and nuclear localization signals and displays proteasic and endonucleasic activities *in vitro*.
Mutations of residues 85, 186 and 336 of PA were associated with an enhanced polymerase activity of avian-origin polymerase in mammalian cells (Bussey *et al.*, 2011). Isoleucine at position 85 conferred faster growth efficiency in human A549 cells while M at position 336 was associated with a higher virulence in mice (Bussey *et al.*, 2011). The detailed role these residues may play remains unknown. In another study, residue 186 of PA was again shown as critical for compatibility with PB1 and PB2 and for polymerase activity (Wanitchang *et al.*, 2010).

2.1.4.a. Polymerase basic protein 1 and polymerase basic protein 2 binding sites

Using co-immunoprecipitation of deletion mutants, the PA PB1-binding site has been

mapped between residues 668 and 692 (Ohtsu *et al.*, 2002). The model fitting all results obtained from studies addressing the question of inter-subunits binding-sites stands that PB1 occupies the core of the polymerase complex, binds the PA C-terminal moiety through its N-terminal end and adheres to both PB2 ends via its C-terminal segment (Ohtsu *et al.*, 2002).

Targeting this PB1-binding site with a short peptide corresponding to residues 1-25 of PB1 (PA-binding site of PB1) blocked the polymerase activity and inhibited viral spread, which opens the way to new antiviral therapy strategies (Ghanem *et al.*, 2007).

The first 100 N-terminal residues of PA are thought to constitute the PB2-binding site of the protein (Hemerka *et al.*, 2009). The PB2-PA interaction occurs in the cell cytoplasm and the dimer is subsequently translocated into the nucleus (Hemerka *et al.*, 2009). Similarly, residue 97 of PA was shown essential for polymerase activity and virulence in mice (Song *et al.*, 2010).

2.1.4.b. hCLE-binding site

In a yeast two-hybrid screen, PA, alone or aggregated in the polymerasic complex, interacted with a human cell protein called hCLE, which is homologous to the yeast Cdc68 family of transcriptional activators (Huarte *et al.*, 2001). The bipartite hCLE-binding site of PA spans between residues 493 to 512 and 557 to 574. The hCLE protein functions as a positive modulator of RNA polymerase II activity (Perez-Gonzalez *et al.*, 2006). Therefore, PA could bring the viral polymerase close to the sites of synthesis of the cellular 5'-capped premessengers and, thus, accelerate the cap-snatching process.

2.1.4.c. Nucleotide-binding site

The PA amino acid sequence does not display unequivocal homology with other proteins *in silico*, but shows a weak relatedness to different nucleotide-binding proteins like some transcription factors or DNA/RNA polymerases (de la Luna *et al.*, 1989). For instance, the 502-509 motif ("GFIIKGRS") roughly corresponds to the canonical nucleotide-binding motif "GXXXXGKT/S". Unfortunately, to our knowledge, functional studies confirming nucleotide binding are still lacking. Assessing the conservation of this 502-509 motif among naturally occurring strains, we found that, although several residues were not strictly conserved, physico-chemical properties of

the residue occupying each position were most frequently conserved, suggesting a functional relevance. The only substitutions detected were the following: F503L (infrequent), I504V or L, I505V, L or T, K506R, R508K and S509A (infrequent) (personal investigations). Besides, residue K102 was shown to affect the cap-binding properties of the viral polymerase (Hara *et al.*, 2006). Since the PA protein was never shown to interact with cap structures in cross-linking experiments, by opposition to PB2 and PB1, it is most likely that the K102A mutation interferes with cap-binding by an indirect way, possibly by inducing a conformational change of PB2 or PB1 affecting their own cap-binding properties.

2.1.4.d. Nuclear Localization Signals

Nuclear transport of PA was first shown to be enhanced by PB1 and NS proteins (Nieto *et al.*, 1992). Inversely, PA was also required for efficient nuclear localization of PB1 (Fodor & Smith, 2004). Thus, both proteins could have to interact to ensure their nuclear injection or retention. Deletion analysis of the PA subunit revealed that two discontinuous segments must be simultaneously present to observe nuclear localization: residues 124-139 (NLS1) and residues 186-247 (NLS2) (Nieto *et al.*, 1994). NLS1 sequence corresponds to classic nucleoplasmin-like motifs in which two short clusters of basic residues are separated by a tens amino acids (RREVHIYYLEKANKIK), whereas no previously known nuclear localization motif is detectable within NLS2. NLS1 is also globally more conserved than NLS2 among influenza A strains. Residues R124 and R125 were sometimes replaced by lysine (which did not affect basic properties of the stretch) and K139 was almost invariable. Residue K137 was sometimes replaced by lysine but also sometimes by glutamine (very rare). Personal sequences alignments confirmed the very high conservation of NLS1, which is consistent with its putative role.

2.1.4.e. Proteasic activity

When expressed alone from cloned cDNA, PA induces a generalized proteolysis and reduces its own concentration (Sanz-Ezquerro *et al.*, 1995). The first amino-terminal 247 residues were shown to cause this proteolysis with the same rate and extent (Sanz-Ezquerro *et al.*, 1996). Furthermore, purified PA also exercises a chymotrypsin-type

serine protease activity for which the C-terminal part of PA seems to be critical (Hara *et al.*, 2001). Thus, it could be that two discrete domains are involved in two different proteasic activities.

With respect to the N-terminal segment, alanine/glycine substitution studies led to the detection of three residues critically involved in generalized proteolysis: T157 (Perales *et al.*, 2000), T162 (Huarte *et al.*, 2003; Perales *et al.*, 2000) and E154 (Sanz-Ezquerro *et al.*, 1995 & 1996). Moreover, the T157A mutation delayed nuclear transport of PA, impaired virus multiplication in cell culture, altered viral pathogenesis in mice and abolished viral replication without altering transcription, which suggests an important role in replication processes or in the transcription-replication switch (Huarte *et al.*, 2003; Perales *et al.*, 2000). As PA was found to be phosphorylated *in vivo* and to be a substrate for Casein Kinase II *in vitro*, T157 and T162 might function as phosphorylation sites (Sanz-Ezquerro *et al.*, 1998), which leads to the hypothesis that the phosphorylation state of PA might control the proteasic activity and/or conformational changes of the polymerase complex leading to the transcription-replication shift (Huarte *et al.*, 2003). Whether there is a causal link between proteolysis and other altered functions is not known so far. However, there is no evidence of any generalized proteolysis during influenza virus infection. Therefore, if this PA-driven proteasic activity has a functional significance, it should be highly regulated. The precise catalytic site is still unknown; T157 might participate directly (experimental evidence is still lacking) or indirectly by affecting the folding of PA. Our sequence alignments showed that T157 was sometimes replaced by S or I and T162 by N, A or I in naturally occurring strains, which questions the real importance of these residues in the biology of the virus. Conversely, E154 was strictly conserved (personal results).

With respect to the C-terminal segment, the chymotrypsin-type serine protease activity expressed by recombinant PA was shown to be critically dependent on S624 (Hara *et al.*, 2001). By analogy with the catalytic triad of chymotrypsin (H57-D102-S195), it was suggested that H510-D547-S624 was the PA's equivalent. Toyoda *et al.* (2003) showed that S624 was not essential for viral growth *in vivo* and *in vitro* but was required for maximal efficiency. Similarly, in another set of studies, S624A mutation did not affect virus yielding (Fodor *et al.*, 2002). However, alignment of available influenza A PA sequences revealed a strict conservation of H510 and S624, suggesting that their essential function has been missed in published experimental settings (personal investigations). By opposition, D547 was replaced by asparagine or glutamate in some

strains.

2.1.4.f. Role in the endonucleasic activity of viral polymerase

A set of studies suggests that some PA residues participate to the endonucleasic modification of capped mRNAs. Those are D108, K134 (Hara *et al.*, 2006) and H510 (Fodor *et al.*, 2002). D108A and K134A mutations resulted in a decrease in transcriptional activity (mRNA synthesis) of the viral polymerase *in vitro*, probably by affecting PB1 endonuclease activity (Hara *et al.*, 2006). Mechanistically speaking, it was hypothesized that D108, an acidic residue, could cooperate with residues E508, E519 and D522 from PB1 subunit to bind Mg2+ ions that are crucial to the polymerase endonucleasic activity (Hara *et al.*, 2006). This proposed essential role of D108 and K134 is compatible with their full conservation in influenza strains sequenced so far (personal observations). H510 is located just downstream the afore discussed nucleotide-binding motif (502-509) (de la Luna *et al.*, 1989; Zurcher *et al.*, 1996). H510 is hypothesized to be close to the endonuclease catalytic site of the PB1 subunit in the 3D structure. Since H510 could be replaced by another basic residue without loss of transcriptional activity, this amino acid – even if conserved among influenza A strains – is most likely not directly involved in catalysis (Fodor *et al.*, 2002).

The description of the crystal structure of the first 196 N-terminal PA residues showed a structural homology of PA with nucleases of the PD-(D/E)XK superfamily (Crépin *et al.*, 2010). Structural and mutational analysis confirmed the role of D108 and K134, but also of H41, E80, E119 and I120

in the endonuclease activity of PA and of the whole influenza polymerase, giving PA a central role in the cap-snatching process instead of PB1 (Dias *et al.*, 2009; Crépin *et al.*, 2010). The PA endonuclease active site was further shown to bind two Mn^{2+} ions, with a 500-fold higher affinity than for Mg^{2+} ions (Crépin *et al.*, 2010).

2.1.4.g. Conclusion

PA protein, the smallest component of the influenza polymerase complex, is involved in the transcription and replication processes, involved in the cap-snatching mechanism (notably by its hCLE- and nucleotide binding sites) and required for the endonuclease activity of the polymerase (Figure 7). It seems to possess a proteasic activity *in vitro*, the role of which has still to be determined.

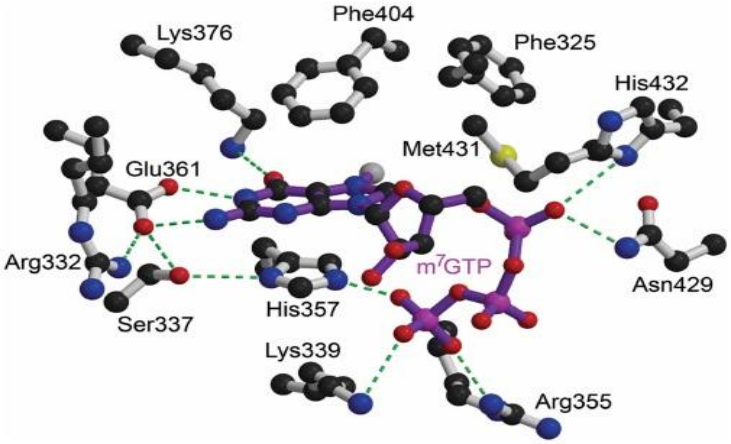

Figure 1: Tridimensional structure of the Cap-binding domain of PB2 protein bound to m^7GTP (Guilligay *et al.*, 2008).

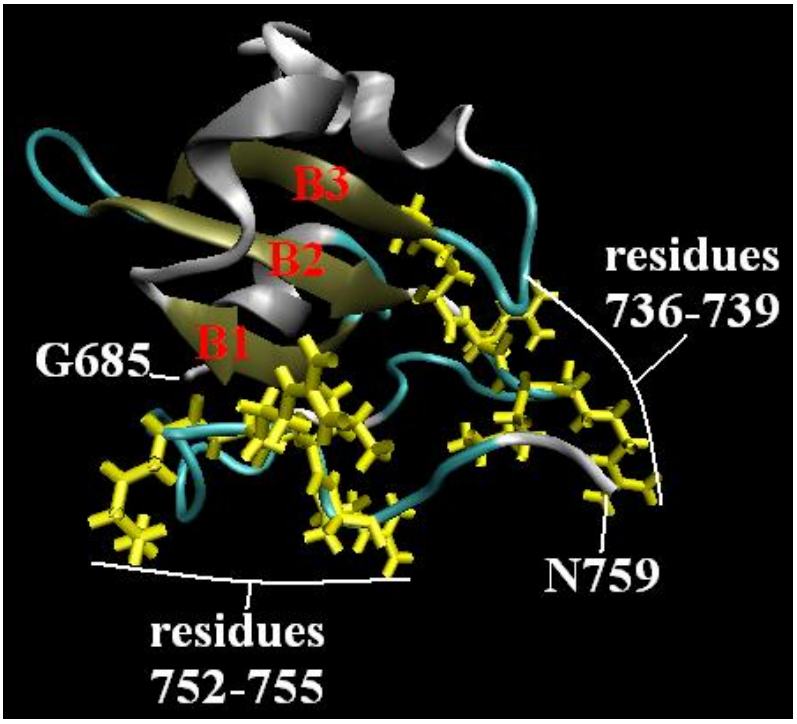

Figure 2: Structure of the 685-759 C-terminal domain of influenza PB2 protein. This domain is made of a hydrophobic three-stranded *β*-sheet core (B1, B2 and B3) surrounded by small *α*-helices. Residues forming the bipartite NLS2 (736-KRKR-739 and 752-KRIR-755) are all exposed at the surface of this domain and this NLS is thus most likely functional (Tarendeau *et al.*, 2007). 3D-structure from Tarendeau *et al.* (2007) – pdb code: 2GMO. Figure performed with VMD (Humphrey *et al.*, 1996).

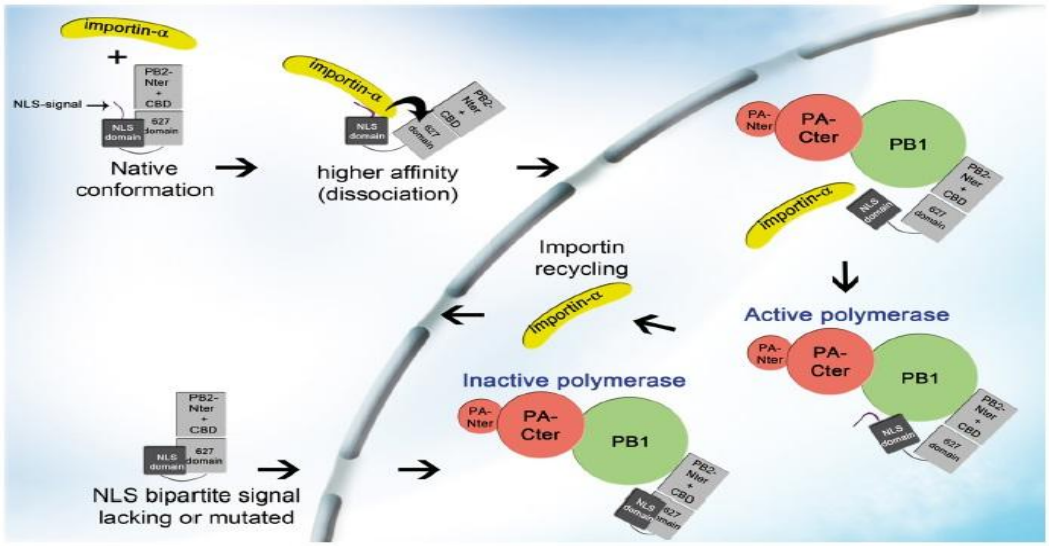

Figure 3: Interplay between the NLS domain (promoting importin *α* binding) and the 627 domain (decreasing PB2 affinity for importin *α*) of PB2 in importin *α* binding affinity regulation and polymerase activity (Boivin & Hart, 2011).

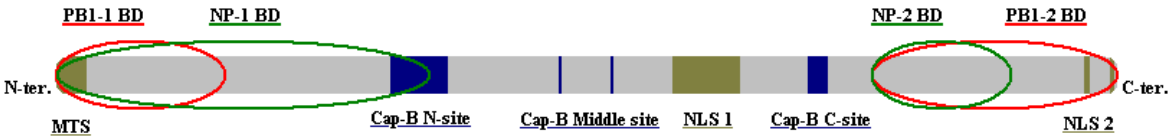

Figure 4: Functional domains of PB2 protein. PB2 is 759 residue-long (Lamb & Krug, 2001). It binds PB1 (PB1-1 BD: 1-124 and PB1-2 BD: 580-759) and NP (NP-1 BD: 1-269 and NP-2 BD: 580-683) (Poole *et al.*, 2004). It plays an essential role in the transcription process by binding cap-structures of cellular mRNAs (Cap-B N-site: 242-282, Cap-B Middle site: F363 and F404, and Cap-B C-site: 544-556) (Fechter *et al.*, 2003; Honda *et al.*, 1999; Li *et al.*, 2001). PB2 possesses two NLSs (NLS1: 449-495 and NLS2: 736-739/752-755) and one MTS (1-22) (Carr *et al.*, 2006; Mukaigawa & Nayak, 1991; Tarendeau *et al.*, 2007).

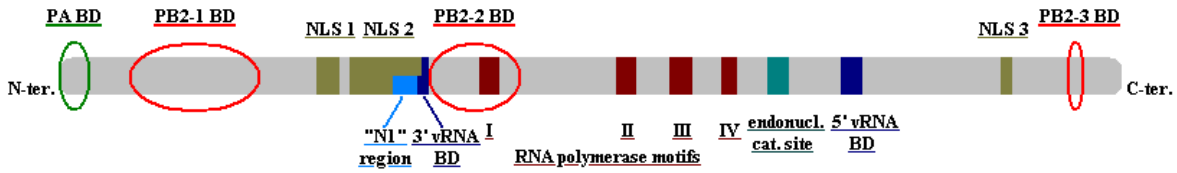

Figure 5: Functional domains of PB1 protein. PB1 is a 757 amino acid-long protein which binds PB2 (PB2-1 BD: 49-144, PB2-2 BD: 252-320, and PB2-3 BD: 712-746, the most important being probably PB2-3 BD), PA (PA BD: 1-25) (Ohtsu *et al.*, 2002; Biswas & Nayak, 1996; Poole *et al.*, 2007) and Ran binding protein 5 (Deng *et al.*, 2006). It ensures the RNA polymerase activity of the polymerase complex (RNA pol. motifs I: 298-311, II: 399-412, III: 438-453, and IV: 474-484) and binds vRNA segments (N1 region: 233-249, 3' vRNA BD: 249-256, and 5' vRNA BD: 560-574) (Biswas & Nayak, 1994; Li *et al.*, 1998; Jung & Brownlee, 2006). PB1 also contains a putative endonuclease catalytic site involved in the cap-snatching process (508-522) (Li *et al.*, 2001) and different NLSs (NLS1: 180-195, NLS2: 202-252 and NLS3: 668-674) (Fodor & Smith, 2004; Nieto *et al.*, 1992).

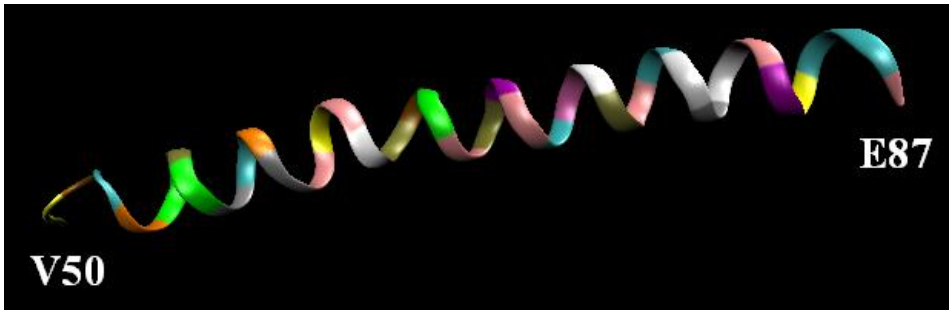

Figure 6: Structure of the C-terminal domain of PB1-F2 protein. The structure is typically α-helical. 3D-structure from (Bruns *et al.*, 2007) – pdb code: 2HN8. Figure performed with VMD (Humphrey *et al.*, 1996).

Figure 7: Functional domains of PA protein. It contains 716 residues (Lamb & Krug, 2001), binds PB1 (PB1 BD: 668-692) and hCLE protein, a human transcriptional activator (hCLE BD: 493-512 and 557-574) (Huarte *et al.*, 2001; Ohtsu *et al.*, 2002). It plays an active role in the endonuclease activity of the polymerase complex (the first 196 residues, notably D108 and K134, and possibly H510), together with PB1 protein (Crépin *et al.*, 2010; Hara *et al.*, 2006). PA is supposed to bind nucleic acids (putative nucleotide-binding sequence: 502-509) (de la Luna *et al.*, 1989). It displays two distinct protease activities/domains (N-terminal proteolytic domain: 1-247 and C-terminal proteolytic domain: triad H510, D547 and S624). It also possesses two NLSs (NLS1: 124-139 and NLS2: 186-247) (Nieto *et al.*, 1994).

2.1.5. References

Area E, Martin-Benito J, Gastaminza P, *et al.* 3D structure of the influenza virus polymerase complex: localization of subunit domains. *Proc Natl Acad Sci U S A* 2004; 101: 308-313.

Biswas SK, Nayak DP. Influenza virus polymerase basic protein 1 interacts with influenza virus polymerase basic protein 2 at multiple sites. *J Virol* 1996; 70: 6716-6722.

Biswas SK, Nayak DP. Mutational analysis of the conserved motifs of influenza A virus polymerase basic protein 1. *J Virol* 1994; 68: 1819-1826.

Boivin S, Hart DJ. Interaction of the influenza A virus polymerase PB2 C-terminal region with importin alpha isoforms provides insights into host adaptation and polymerase assembly. *J Biol Chem* 2011; 286: 10439-10448.

Bruns K, Studtrucker N, Sharma A, *et al.* Structural characterization and oligomerization of PB1-F2, a proapoptotic influenza A virus protein. *J Biol Chem* 2007; 282: 353-363.

Bussey KA, Desmet EA, Mattiacio JL, *et al.* PA Residues in the 2009 H1N1 Pandemic Influenza Virus Enhance Avian Influenza Virus Polymerase Activity in Mammalian Cells. *J Virol* 2011; 85: 7020-7028.

Carr SM, Carnero E, Garcia-Sastre A, *et al.* Characterization of a mitochondrial-targeting signal in the PB2 protein of influenza viruses. *Virology* 2006; 344: 492-508.

Chanturiya AN, Basanez G, Schubert U, *et al.* PB1-F2, an influenza A virus-encoded proapoptotic mitochondrial protein, creates variably sized pores in planar lipid membranes. *J Virol* 2004; 78: 6304-6312.

Chen GW, Yang CC, Tsao KC, *et al.* Influenza A virus PB1-F2 gene in recent Taiwanese isolates. *Emerg Infect Dis* 2004; 10: 630-636.

Chen W, Calvo PA, Malide D, *et al.* A novel influenza A virus mitochondrial protein that induces cell death. *Nat Med* 2001; 7: 1306-1312.

Chevalier C, Al Bazzal A, Vidic J, *et al.* PB1-F2 influenza A virus protein adopts a beta-sheet conformation and forms amyloid fibers in membrane environments. *J Biol Chem* 2010; 285: 13233-13243.

Ciminale V, Zotti L, D'Agostino DM, *et al.* Mitochondrial targeting of the p13II protein coded by the x-II ORF of human T-cell leukemia/lymphotropic virus type I

(HTLV-I). *Oncogene* 1999; 18: 4505-4514.

Clements ML, Subbarao EK, Fries LF, *et al.* Use of single-gene reassortant viruses to study the role of avian influenza A virus genes in attenuation of wild-type human influenza A virus for squirrel monkeys and adult human volunteers. *J Clin Microbiol* 1992; 30: 655-662.

Crépin T, Dias A, Palencia A, *et al.* Mutational and metal binding analysis of the endonuclease domain of the influenza virus polymerase PA subunit. *J Virol* 2010; 84: 9096-9104.

de la Luna S, Martinez C, Ortin J. Molecular cloning and sequencing of influenza virus A/Victoria/3/75 polymerase genes: sequence evolution and prediction of possible functional domains. *Virus Res* 1989; 13: 143-155.

Deng T, Engelhardt OG, Thomas B, *et al.* Role of ran binding protein 5 in nuclear import and assembly of the influenza virus RNA polymerase complex. *J Virol* 2006; 80: 11911-11919.

Dias A, Bouvier D, Crépin T, *et al.* The cap-snatching endonuclease of influenza virus polymerase resides in the PA subunit. *Nature* 2009; 458:;914-918.

Digard P, Blok VC, Inglis SC. Complex formation between influenza virus polymerase proteins expressed in Xenopus oocytes. *Virology* 1989; 171: 162-169.

Dingwall C, Laskey RA. Nuclear targeting sequences--a consensus? *Trends Biochem Sci* 1991; 16: 478-481.

Fechter P, Mingay L, Sharps J, *et al.* Two aromatic residues in the PB2 subunit of influenza A RNA polymerase are crucial for cap binding. *J Biol Chem* 2003; 278: 20381-20388.

Fislová T, Thomas B, Graef KM, *et al.* Association of the influenza virus RNA polymerase subunit PB2 with the host chaperonin CCT. *J Virol* 2010; 84: 8691-8699.

Fodor E, Crow M, Mingay LJ, *et al.* A single amino acid mutation in the PA subunit of the influenza virus RNA polymerase inhibits endonucleolytic cleavage of capped RNAs. *J Virol* 2002; 76: 8989-9001.

Fodor E, Smith M. The PA subunit is required for efficient nuclear accumulation of the PB1 subunit of the influenza A virus RNA polymerase complex. *J Virol* 2004; 78: 9144-9153.

Foeglein A, Loucaides EM, Mura M, *et al.* Influence of PB2 host-range determinants on the intranuclear mobility of the influenza A virus polymerase. *J Gen Virol* 2011;

92: 1650-1661.

Fornek JL, Gillim-Ross L, Santos C, *et al.* A single-amino-acid substitution in a polymerase protein of an H5N1 influenza virus is associated with systemic infection and impaired T-cell activation in mice. *J Virol* 2009; 83: 11102-11115.

Fouchier RA, Schneeberger PM, Rozendaal FW, *et al.* Avian influenza A virus (H7N7) associated with human conjunctivitis and a fatal case of acute respiratory distress syndrome. *Proc Natl Acad Sci U S A* 2004; 101: 1356-1361.

Gabriel G, Dauber B, Wolff T, *et al.* The viral polymerase mediates adaptation of an avian influenza virus to a mammalian host. *Proc Natl Acad Sci U S A* 2005; 102: 18590-18595.

Gabriel G, Herwig A, Klenk HD. Interaction of Polymerase Subunit PB2 and NP with Importin alpha1 Is a Determinant of Host Range of Influenza A Virus. *PLoS Pathog* 2008; 4: e11.

Ghanem A, Mayer D, Chase G, *et al.* Peptide-mediated interference with influenza A virus polymerase. *J Virol* 2007; 81: 7801-7804.

Gibbs JS, Malide D, Hornung F, *et al.* The influenza A virus PB1-F2 protein targets the inner mitochondrial membrane via a predicted basic amphipathic helix that disrupts mitochondrial function. *J Virol* 2003; 77: 7214-7224.

Gonzalez S, Zurcher T, Ortin J. Identification of two separate domains in the influenza virus PB1 protein involved in the interaction with the PB2 and PA subunits: a model for the viral RNA polymerase structure. *Nucleic Acids Res* 1996; 24: 4456-4463.

Graef KM, Vreede FT, Lau YF, *et al.* The PB2 subunit of the influenza virus RNA polymerase affects virulence by interacting with the mitochondrial antiviral signaling protein and inhibiting expression of beta interferon. *J Virol* 2010; 84: 8433-8445.

Guilligay D, Tarendeau F, Resa-Infante P, *et al.* The structural basis for cap binding by influenza virus polymerase subunit PB2. *Nat Struct Mol Biol* 2008; 15: 500-506.

Hagen M, Chung TD, Butcher JA, *et al.* Recombinant influenza virus polymerase: requirement of both 5' and 3' viral ends for endonuclease activity. *J Virol* 1994; 68: 1509-1515.

Hara K, Schmidt FI, Crow M, *et al.* Amino acid residues in the N-terminal region of the PA subunit of influenza A virus RNA polymerase play a critical role in protein stability, endonuclease activity, cap binding, and virion RNA promoter binding. *J*

Virol 2006; 80: 7789-7798.

Hara K, Shiota M, Kido H, *et al.* Influenza virus RNA polymerase PA subunit is a novel serine protease with Ser624 at the active site. *Genes Cells* 2001; 6: 87-97.

Hatta M, Gao P, Halfmann P, *et al.* Molecular basis for high virulence of Hong Kong H5N1 influenza A viruses. *Science* 2001; 293: 1840-1842.

Hatta M, Hatta Y, Kim JH, *et al.* Growth of H5N1 influenza A viruses in the upper respiratory tracts of mice. *PLoS Pathog* 2007; 3: 1374-1379.

Hemerka JN, Wang D, Weng Y, *et al.* Detection and characterization of influenza A virus PA-PB2 interaction through a bimolecular fluorescence complementation assay. *J Virol* 2009; 83: 3944-3955.

Hiromoto Y, Yamazaki Y, Fukushima T, *et al.* Evolutionary characterization of the six internal genes of H5N1 human influenza A virus. *J Gen Virol* 2000; 81: 1293-1303.

Honda A, Mizumoto K, Ishihama A. Two separate sequences of PB2 subunit constitute the RNA cap-binding site of influenza virus RNA polymerase. *Genes Cells* 1999; 4: 475-485.

Horisberger MA. The large P proteins of influenza A viruses are composed of one acidic and two basic polypeptides. *Virology* 1980; 107: 302-305.

Huarte M, Falcon A, Nakaya Y, *et al.* Threonine 157 of influenza virus PA polymerase subunit modulates RNA replication in infectious viruses. *J Virol* 2003; 77: 6007-6013.

Huarte M, Sanz-Ezquerro JJ, Roncal F, *et al.* PA subunit from influenza virus polymerase complex interacts with a cellular protein with homology to a family of transcriptional activators. *J Virol* 2001; 75: 8597-8604.

Humphrey W, Dalke, A., Schulten, K. VMD - Visual Molecular Dynamics. *J. Molec. Graphics* 1996; 14: 33-38.

Hutchinson E, Orr O, Man Liu S, *et al.* Characterisation of the interaction between the influenza A virus polymerase subunit PB1 and the host nuclear import factor Ran Binding Protein 5. *J Gen Virol* 2011 [Epub ahead of print].

Iwai A, Shiozaki T, Kawai T, *et al.* Influenza A virus polymerase inhibits type I interferon induction by binding to interferon beta promoter stimulator 1. *J Biol Chem* 2010; 285: 32064-32074.

Jones IM, Reay PA, Philpott KL. Nuclear location of all three influenza polymerase proteins and a nuclear signal in polymerase PB2. *Embo J* 1986; 5: 2371-2376.

Jung TE, Brownlee GG. A new promoter-binding site in the PB1 subunit of the influenza A virus polymerase. *J Gen Virol* 2006; 87: 679-688.

Katz JM, Lu X, Tumpey TM, *et al.* Molecular correlates of influenza A H5N1 virus pathogenesis in mice. *J Virol* 2000; 74: 10807-10810.

Kerry PS, Willsher N, Fodor E. A cluster of conserved basic amino acids near the C-terminus of the PB1 subunit of the influenza virus RNA polymerase is involved in the regulation of viral transcription. *Virology* 2008; 373: 202-210.

Klumpp K, Ruigrok RW, Baudin F. Roles of the influenza virus polymerase and nucleoprotein in forming a functional RNP structure. *Embo J* 1997; 16: 1248-1257.

Košík I, Krejnusová I, Bystrická M, *et al.* N-terminal region of the PB1-F2 protein is responsible for increased expression of influenza A viral protein PB1. *Acta Virol* 2011; 55: 45-53.

Kuzuhara T, Kise D, Yoshida H, *et al.* Structural basis of the influenza A virus RNA polymerase PB2 RNA-binding domain containing the pathogenicity-determinant lysine 627 residue. *J Biol Chem* 2009; 284: 6855-6860.

Labadie K, Dos Santos Afonso E, Rameix-Welti MA, *et al.* Host-range determinants on the PB2 protein of influenza A viruses control the interaction between the viral polymerase and nucleoprotein in human cells. *Virology* 2007; 362: 271-282.

Lamb RA, Krug RM. Orthomyxoviridae: The viruses and their replication. In Fields Virology, Knipe DM, Howley PM, Martin MA, Griffin DE, Lamb RA (eds). Lippincott Williams & Wilkins: Boston, 2001; 1487-1531.

Lee MT, Bishop K, Medcalf L, *et al.* Definition of the minimal viral components required for the initiation of unprimed RNA synthesis by influenza virus RNA polymerase. *Nucleic Acids Res* 2002; 30: 429-438.

Le Goffic R, Bouguyon E, Chevalier C, *et al.* Influenza A virus protein PB1-F2 exacerbates IFN-beta expression of human respiratory epithelial cells. *J Immunol* 2010; 185: 4812-4823.

Li ML, Ramirez BC, Krug RM. RNA-dependent activation of primer RNA production by influenza virus polymerase: different regions of the same protein subunit constitute the two required RNA-binding sites. *Embo J* 1998; 17: 5844-5852.

Li ML, Rao P, Krug RM. The active sites of the influenza cap-dependent endonuclease are on different polymerase subunits. *Embo J* 2001; 20: 2078-2086.

Mahmoudian S, Auerochs S, Gröne M, *et al.* Influenza A virus proteins PB1 and NS1

are subject to functionally important phosphorylation by protein kinase C. *J Gen Virol* 2009; 90: 1392-1397.

Matsuo H, Li H, McGuire AM, *et al.* Structure of translation factor eIF4E bound to m7GDP and interaction with 4E-binding protein. *Nat Struct Biol* 1997; 4: 717-724.

Mazur I, Anhlan D, Mitzner D, *et al.* The proapoptotic influenza A virus protein PB1-F2 regulates viral polymerase activity by interaction with the PB1 protein. *Cell Microbiol* 2008.

McAuley JL, Chipuk JE, Boyd KL, *et al.* PB1-F2 proteins from H5N1 and 20 century pandemic influenza viruses cause immunopathology. *PLoS Pathog* 2010; 6: e1001014.

Momose F, Naito T, Yano K, *et al.* Identification of Hsp90 as a stimulatory host factor involved in influenza virus RNA synthesis. *J Biol Chem* 2002; 277: 45306-45314.

Mukaigawa J, Nayak DP. Two signals mediate nuclear localization of influenza virus (A/WSN/33) polymerase basic protein 2. *J Virol* 1991; 65: 245-253.

Munster VJ, de Wit E, van Riel D, *et al.* The molecular basis of the pathogenicity of the Dutch highly pathogenic human influenza A H7N7 viruses. *J Infect Dis* 2007; 196: 258-265.

Murphy BR, Hinshaw VS, Sly DL, *et al.* Virulence of avian influenza A viruses for squirrel monkeys. *Infect Immun* 1982; 37: 1119-1126.

Naito T, Momose F, Kawaguchi A, *et al.* Involvement of Hsp90 in assembly and nuclear import of influenza virus RNA polymerase subunits. *J Virol* 2007; 81: 1339-1349.

Nath ST, Nayak DP. Function of two discrete regions is required for nuclear localization of polymerase basic protein 1 of A/WSN/33 influenza virus (H1 N1). *Mol Cell Biol* 1990; 10: 4139-4145.

Nieto A, de la Luna S, Barcena J, *et al.* Complex structure of the nuclear translocation signal of influenza virus polymerase PA subunit. *J Gen Virol* 1994; 75 (Pt 1): 29-36.

Nieto A, de la Luna S, Barcena J, *et al.* Nuclear transport of influenza virus polymerase PA protein. *Virus Res* 1992; 24: 65-75.

Ohtsu Y, Honda Y, Sakata Y, *et al.* Fine mapping of the subunit binding sites of influenza virus RNA polymerase. *Microbiol Immunol* 2002; 46: 167-175.

Perales B, de la Luna S, Palacios I, *et al.* Mutational analysis identifies functional domains in the influenza A virus PB2 polymerase subunit. *J Virol* 1996; 70: 1678-

1686.

Perales B, Sanz-Ezquerro JJ, Gastaminza P, *et al.* The replication activity of influenza virus polymerase is linked to the capacity of the PA subunit to induce proteolysis. *J Virol* 2000; 74: 1307-1312.

Perez DR, Donis RO. A 48-amino-acid region of influenza A virus PB1 protein is sufficient for complex formation with PA. *J Virol* 1995; 69: 6932-6939.

Perez-Gonzalez A, Rodriguez A, Huarte M, *et al.* hCLE/CGI-99, a human protein that interacts with the influenza virus polymerase, is a mRNA transcription modulator. *J Mol Biol* 2006; 362: 887-900.

Plotch SJ, Bouloy M, Ulmanen I, *et al.* A unique cap(m7GpppXm)-dependent influenza virion endonuclease cleaves capped RNAs to generate the primers that initiate viral RNA transcription. *Cell* 1981; 23: 847-858.

Poch O, Sauvaget I, Delarue M, *et al.* Identification of four conserved motifs among the RNA-dependent polymerase encoding elements. *Embo J* 1989; 8: 3867-3874.

Poole E, Elton D, Medcalf L, *et al.* Functional domains of the influenza A virus PB2 protein: identification of NP- and PB1-binding sites. *Virology* 2004; 321: 120-133.

Poole EL, Medcalf L, Elton D, *et al.* Evidence that the C-terminal PB2-binding region of the influenza A virus PB1 protein is a discrete alpha-helical domain. *FEBS Lett* 2007; 581: 5300-5306.

Sanz-Ezquerro JJ, de la Luna S, Ortin J, *et al.* Individual expression of influenza virus PA protein induces degradation of coexpressed proteins. *J Virol* 1995; 69: 2420-2426.

Sanz-Ezquerro JJ, Fernandez Santaren J, Sierra T, *et al.* The PA influenza virus polymerase subunit is a phosphorylated protein. *J Gen Virol* 1998; 79: 471-478.

Sanz-Ezquerro JJ, Zurcher T, de la Luna S, *et al.* The amino-terminal one-third of the influenza virus PA protein is responsible for the induction of proteolysis. *J Virol* 1996; 70: 1905-1911.

Shinya K, Watanabe S, Ito T, *et al.* Adaptation of an H7N7 equine influenza A virus in mice. *J Gen Virol* 2007; 88: 547-553.

Song MS, Pascua PN, Lee JH, *et al.* The polymerase acidic protein gene of influenza a virus contributes to pathogenicity in a mouse model. *J Virol* 2009; 83: 12325-12335.

Stojanovski D, Johnston AJ, Streimann I, *et al.* Import of nuclear-encoded proteins into mitochondria. *Exp Physiol* 2003; 88: 57-64.

Sugiyama K, Obayashi E, Kawaguchi A, *et al.* Structural insight into the essential PB1-PB2 subunit contact of the influenza virus RNA polymerase. *Embo J* 2009; 28: 1803-1811.

Subbarao EK, London W, Murphy BR. A single amino acid in the PB2 gene of influenza A virus is a determinant of host range. *J Virol* 1993; 67: 1761-1764.

Tarendeau F, Boudet J, Guilligay D, *et al.* Structure and nuclear import function of the C-terminal domain of influenza virus polymerase PB2 subunit. *Nat Struct Mol Biol* 2007; 14: 229-233.

Torreira E, Schoehn G, Fernandez Y, *et al.* Three-dimensional model for the isolated recombinant influenza virus polymerase heterotrimer. *Nucleic Acids Res* 2007; 35: 3774-3783.

Toyoda T, Adyshev DM, Kobayashi M, *et al.* Molecular assembly of the influenza virus RNA polymerase: determination of the subunit-subunit contact sites. *J Gen Virol* 1996; 77: 2149-2157.

Toyoda T, Hara K, Imamura Y. Ser624 of the PA subunit of influenza A virus is not essential for viral growth in cells and mice, but required for the maximal viral growth. *Arch Virol* 2003; 148: 1687-1696.

Wanitchang A, Jengarn J, Jongkaewwattana A. The N terminus of PA polymerase of swine-origin influenza virus H1N1 determines its compatibility with PB2 and PB1 subunits through a strain-specific amino acid serine 186. *Virus Res* 2011; 155: 325-333.

Wright PF, Webster RG. Orthomyxoviruses. In Fields Virology, Knipe DM, Howley PM, Martin MA, Griffin DE, Lamb RA (eds). Lippincott Williams & Wilkins: Boston, 2001; 1533-1579.

Yamada H, Chounan R, Higashi Y, *et al.* Mitochondrial targeting sequence of the influenza A virus PB1-F2 protein and its function in mitochondria. *FEBS Lett* 2004; 578: 331-336.

Yao Y, Mingay LJ, McCauley JW, *et al.* Sequences in influenza A virus PB2 protein that determine productive infection for an avian influenza virus in mouse and human cell lines. *J Virol* 2001; 75: 5410-5415.

Zamarin D, Garcia-Sastre A, Xiao X, *et al.* Influenza virus PB1-F2 protein induces cell death through mitochondrial ANT3 and VDAC1. *PLoS Pathog* 2005; 1: e4.

Zamarin D, Ortigoza MB, Palese P. Influenza A virus PB1-F2 protein contributes to viral pathogenesis in mice. *J Virol* 2006; 80: 7976-7983.

Zell R, Krumbholz A, Eitner A, *et al.* Prevalence of PB1-F2 of influenza A viruses. *J Gen Virol* 2007; 88: 536-546.

Zhang J, Li G, Ye X. Cyclin T1/CDK9 interacts with influenza A virus polymerase and facilitates its association with cellular RNA polymerase II. *J Virol* 2010; 84: 12619-12627.

Zurcher T, de la Luna S, Sanz-Ezquerro JJ, *et al.* Mutational analysis of the influenza virus A/Victoria/3/75 PA protein: studies of interaction with PB1 protein and identification of a dominant negative mutant. *J Gen Virol* 1996; 77: 1745-1749.

2.2. Surface proteins

2.2.1. Hemagglutinin

Hemagglutinin (HA) is the most abundant (400 to 500 units per virion) and immunogenic surface protein of influenza A virus (Lamb & Krug, 2001). It mediates the attachment of the virus to the cell surface by binding to terminal sialic acids of glycoproteins and glycolipids, which confers the hemagglutination properties that gave it its name. HA is also responsible for the fusion between viral and endosomal membranes that permits the penetration of viral ribonucleoproteins into the cytoplasm. Those crucial features give HA a central place in the virus replication cycle.

Hemagglutinin is an integral type I transmembrane glycoprotein of about 550 amino acids forming rod-shaped homotrimers of Mr 220,000. The monomer is made of a 512 residues N-terminal ectodomain, a 24 to 28 aa transmembrane domain and a 10 to 55 residue cytoplasmic tail (Verhoeyen *et al.*, 1980; Wilson *et al.*, 1981). It is synthesized as a single precursor HA_0 polypeptide (Mr 76,000) and undergoes posttranslational glycosylation (from 3 to 11 oligosaccharide chains addition) and palmitoylation (Naeve & Williams, 1990; Naim & Roth, 1993; Schmidt, 1982). The HA_0 precursor is cleaved either at the cell surface by trypsin-type proteases or intracellulary by subtilisin-type enzymes, depending on the features of its cleavage site (Steinhauer, 1999). The resultant two parts of the protein (HA_1 and HA_2) are disulfide bonded by C14 of HA_1 and C137 of HA_2 (H3 numbering). HA_1 displays five immunodominant and hypervariable epitopes and HA_2, which is more conserved between strains than HA_1, anchors the protein into the viral membrane and contains the fusion peptide (Kovacova *et al.*, 2002; Wilson *et al.*, 1981).

HA exists as 16 different antigenic forms that are used, along with neuraminidase (NA) varieties, to define the influenza A virus subtypes. The different subtypes are divided in two classes on the basis of their HA, the "H1 group" containing H1, H2, H5, H6, H8, H9, H11, H12, H13 and H16 subtypes, and the "H3 group" gathering H3, H4, H7, H10, H14 and H15 subtypes (Nobusawa *et al.*, 1991; Russell *et al.*, 2004; Suzuki & Nei, 2002; Tatulian & Tam, 2000; Thoennes *et al.*, 2008). Besides, HAs are further categorized into five clades. H1 clade (H1, H2, H5 and H6), H9 clade (H8, H9 and H12) and H13 clade (H11, H13 and H16) for group 1; H3 clade (H3, H4 and H14) and H7 clade (H7, H10 and H15) for group 2 (Nobusawa *et al.*, 1991; Russell *et al.*, 2004;

Thoennes *et al.*, 2008). Structural peculiarities correlate with this classification (Ha *et al.*, 2002). For example, the structure of H3, H5 and H9 HAs typically differs in the rotation degree of the membrane-distal subdomains relative to the central stem (cf. *infra*).

All subtypes may be found infecting birds; humans are naturally only infected by strains from H1, H2 and H3 subtypes (although H5, H7 and H9 strains have been found in humans during avian influenza outbreaks); swine strains are at least of four types H1, H2, H3 and H9; and horse strains are of H3 and H7 subtypes.

2.2.1.a. General structure

The first description of the structure of HA was made in 1981 by Wilson and colleagues, working on the A/Hong Kong/1968 (H3N2) strain. Proteolytic cleavage of the H3 HA yields HA_1 and HA_2 chains made of 328 and 221 aa, respectively. The A/Hong Kong/1968 (H3N2) HA is glycosylated at seven sites and these carbohydrates are essentially located near the viral membrane end of the molecule in the tertiary structure (Wilson *et al.*, 1981). Six disulfide bonds were detected, five intra-chain and one between chains (Wilson *et al.*, 1981).

The A/Hong Kong/1968 (H3N2) strain HA trimer was solubilized from the viral membrane by bromelain digestion, which removes the C-terminal part of HA_2 (after residue 175 of HA_2 including the transmembrane domain (186-211) and the cytoplasmic tail (212-221)). The trimer is a 135 Å-long rod-shaped cylinder, from 15 to 40 Å in radius (Wilson *et al.*, 1981) (Figure 1). The HA monomer consists of two different domains: a long fibrous stem region at its base made of residues from HA_1 and HA_2 and a head globular domain only containing residues from HA_1. In the HA trimer, the stem domain is a cylindrical compact stalk centered on a 76 Å triple-stranded coiled coil formed by three long α-helices (one per monomer) of 53 aa (Stevens *et al.*, 2004; Wilson *et al.*, 1981) (Figure 1). Residues 11 to 51 and 276 to 329 of HA_1 and 1 to 176 of HA_2 are implicated in the stem domain (H1 numbering). The cleavage site of HA_0 is also present in the stem region (Wilson *et al.*, 1981) (Figure 1).

The first N-terminal 63 residues of HA_1 first progress from the membrane surface in an almost extended 96 Å-long conformation and then assume a compact structure participating to the globular domain which contains a three-turn helix and is stabilized by a disulfide bond (54-76) (Wilson *et al.*, 1981). Residues 116 to 261 form an 8-

stranded antiparallel *β*-sheet structure that constitutes the framework of the globular domain. Some projected loops between those strands generate important antigenic regions. By analogy with the hemagglutinin-esterase-fusion (HEF) protein of influenza C viruses, which displays the activities mediated by the hemagglutinin and the neuraminidase of influenza A and B viruses, the overall 3D-structure of influenza A HA protein can be divided into a R (for *receptor-bindin*g) domain at the top of the molecule, an E' (for *vestigial esterase*) domain just beyond the R domain and a F (for *fusion-mediating*) domain (Rosenthal *et al.*, 1998). The globular region is bond to the fibrous stem by two disulfide bonds (52-277 and 281-305, H3 numbering). After the 8-stranded *β*-sheet structure, the C-terminal segment of HA_1 runs 60 Å towards the viral membrane antiparallely to the N-terminal segment of HA_1 (Wilson *et al.*, 1981).

The stem region is essentially made of 2 antiparallel *α*-helices (Figure 1). A short 29 Å *α*-helix "A" (residues 38-56 of HA_2) first pulls ahead from the membrane, is followed by a short extended segment (HA_2 59-76) and then a long (76 Å, 14 turns) *α*-helix "B" (residues 74-126) that runs back towards the membrane (Wilson *et al.*, 1981). Those 2 *α*-helices thus adopt an antiparallel disposition, the smaller being located along the membrane half of the long one. The base of the stem is made of a compact globular structure containing a 5-stranded antiparallel *β*-sheet structure (Wilson *et al.*, 1981). It is constituted by the N-terminal segment of HA_1 flanked on both sides by a strand formed by the extended chain of HA_2 (Wilson *et al.*, 1981). A 3-turn *α*-helix is present in the last part of bromelain-digested HA_2 (residue 175 of HA_2), but it might be absent from "normal" HA (Wilson *et al.*, 1981).

The trimer is essentially stabilized by the central coiled coil structure in which helices twist 100° around each other in a left-handed superhelix (Wilson *et al.*, 1981) (Figure 1). The distal (in relation to the viral membrane) half of the coil is more tightly packed with numerous nonpolar residues in van der Waals interaction (I77, L80, V84, L91, L98, L99, L102), whereas the base of the coil is more expanded, with many polar residues (H106, D109, D112, S113, N116, Q120, R123).

Structure of influenza HA subtypes essentially differs by the variable rotation level between the membrane-distal subdomain and the central stem. This variation might be linked to different conformations of the loop between *α*-helices A and B (Russell *et al.*, 2004).

2.2.1.b. Pattern of glycosylation

- *Description and variation*

The majority of carbohydrate side chains of HAs are located in the basal half of the stem region (Wilson *et al.*, 1981). The glycosylation sites consist of a "NXT/S" sequence. Some carbohydrate side chains consist of *N*-acetyl glucosamine and mannose, while others also contain galactose and fucose (Wilson *et al.*, 1981). None of the carbohydrates is terminated by sialic acid because of the activity of neuraminidase (Schulze, 1997; Wilson *et al.*, 1981). Carbohydrates cover about 20% of the HA trimer surface, covered residues being essentially hydrophilic (60%) with many S and T (33%) and many interactions between those residues and carbohydrates are present (Wilson *et al.*, 1981). At first sight, glycosylation of HAs probably stabilizes the quaternary structure of the trimer and may cover potential cleavage sites, thus protecting HAs against degradative enzymes, the best known example being the control of the accessibility of the HA_0 cleavage site (see after). Artificial addition of a new glycosylation site in an HA sequence was also shown to be able to alter its folding, membrane transport, and stability (Gallagher *et al.*, 1988).

Considerable variation is found in the glycosylation pattern among influenza A strains and within a said strain derived from different hosts or cell types. Overall, HAs of influenza strains grown on mammalian cells, even if the parental virus was laboratory-adapted with few glycosylations, always present a great part of the HA trimer surface covered by carbohydrates. At first sight, these observations are thought to result from species- or cell-specific glycosylating machineries (Schulze, 1997). However, some data are poorly understood. For example, current H1 human strains often present 4 glycosylations on the tip of the HA while past and current avian and swine H1 strains do not display any. Whether the difference between human and avian/porcine H1 strains is due to host selective pressure or to the existence of 2 different H1 lineages evolving since the re-emergence of H1 subtype in 1977 is unknown (Schulze, 1997). More strikingly, differences were documented between human H3 strains isolated before and after 1975, the latter presenting an additional glycosylation site at position 126 (near antigenic region A) close to the RBS (receptor binding site) pocket (Abe *et al.*, 2004).

The pattern of glycosylation probably constitutes an underestimated virulence factor since it can regulate the receptor binding affinity of HA, its antigenicity, the

accessibility of its cleavage site, and the host/cell range of the influenza virus.

- *Receptor binding affinity is glycosylation-dependent*

A reduction in receptor binding has been associated with the combination of a histidine to asparagine substitution close to the RBS and attachment of large complex glycans to asparagine (Mir-Shekari *et al.*, 1997). Similarly, when N-linked oligosaccharides attached to N123 and N149 of fowl plague influenza virus HA were deleted by site-specific mutagenesis, receptor binding was enhanced to such an extent that release by receptor-destroying enzymes became severely impeded or completely inhibited (Ohuchi *et al.*, 1997). In a different experimental setting, reassortant fowl plague virus A/FPV/Rostock/34 (H7N1) expressing those mutant HAs displayed higher affinity for sialic acids too and the sialidase activity of the N1 NA was too weak to permit new virions to be released from the cell surface (Wagner *et al.*, 2000). Conversely, reassortant HA-mutant viruses possessing a N2 subtype NA, with a stronger sialidase activity, were readily rescued, the N2 NA being able to overcome the higher affinity of mutant HA for its receptor (Wagner *et al.*, 2000). These results point out a close "balance" between HA and NA, which might account for the observation that some HA- and NA-subtypes associations are never found in naturally occurring influenza strains. Similar conclusions were reached with a H7 HA lacking glycosylation at position 158 (Baigent & McCauley, 2001). Altogether, these findings indicate that the oligosaccharides attached to asparagine residues located on the tip of HA regulate the receptor affinity in a manner that controls the ability of HA to both bind and dissociate from its receptor. Thus, elimination of a glycosylation site of an HA that is associated with a long-stalked NA allows the virus to bind and enter cells more rapidly, which therefore helps to escape the immune pressure (Nohinek *et al.*, 1985; Schulze, 1997; Yewdell *et al.*, 1986).

Another example is the contribution to mammalian adaptation of a mutation in position 160 of a H5N1 virus HA which abolishes a glycosylation site and affect the receptor binding properties, once again confirming the importance of glycosylation pattern for virulence (Gao *et al.*, 2009). The importance of glycosylation on receptor binding and immune response was further provided by Wang and colleagues (2009).

- *Glycosylation pattern and antigenicity*

Four to five glycosylation sites are conserved among HAs of avian and porcine strains, whereas human H1 strains usually present up to 8 or 9 glycosylations. Several of these optional glycosylation sites are located on the globular head. These findings stress the role of glycosylation in the control of host range and suggest that oligosaccharides on the tip of HA are important to the survival of H1 viruses in humans but not in birds or pigs, presumably because they help the virus to escape the human immune pressure (Inkster *et al.*, 1983). Accordingly, it was suggested that strains with heavily glycosylated – thus possibly less immunogenic – HA should be avoided in the formulation of vaccines. This is far from being clear however, as data brought by Bright and colleagues (2003) using a DNA-based vaccine targeting an avian H5N1 strain were not compatible with that hypothesis. Taking the opposite point of view, the question of whether the classic preparation of human influenza vaccines in embryonated hens'eggs, which confers an avian-type glycosylation pattern to the antigens to be injected, yields the most efficient way to evoke a protection against wild-type human strains is still open to debate.

There is growing evidence of the role played by glycosylation in the "shielding" of antigenic regions of the HA globular head and subsequent escape from immune response (Das *et al.*, 2010).

- *Host/cell range might be glycosylation-dependent*

H3N2 influenza A viruses isolated from Vero cells (African Green Monkey Kidney, ATCC CCL-81), MDCK cells or chicken embryos showed different agglutination properties on chicken erythrocytes and growth properties in chicken eggs, i.e. Vero-adapted variants were dramatically deficient in those two properties while MDCK- and chicken embryos-adapted variants were not (Romanova *et al.*, 2003). The sole difference between the HA_1 fragments of these three variants was the glycosylation pattern, with more oligosaccharides of high mannose type in the Vero-adapted variant than in both other ones. Furthermore, removal of some mannose residues of the Vero-adapted strain by an exomannosidase restored its ability to agglutinate chicken erythrocytes (Romanova *et al.*, 2003). However, the H1N1 variants isolated by the same group from Vero, MDCK cells or eggs did not differ in carbohydrate composition,

agglutination properties or ability to infect eggs, thus showing that the glycosylation dependence of an HA function depends on the cell-type/HA-subtype pair rather than on the sole cell type.

The loss of two potential glycosylation sites at positions 165 and 246 of A/Phillipines/1/82 HA significantly increased virulence of the virus for mice, which could be linked to enhanced access to HA cleavage site (see hereafter; Hartley *et al.*, 1994). The lack of these glycosylations renders the virus less sensitive to neutralization by lung-derived mannose-binding lectins of mice (Hartley *et al.*, 1994). Similarly, a point mutation at position 246 of HA of a H3N2 influenza strains resulted in the loss of a glycosylation site, resistance to murine collectins and increased virulence in mice (Reading *et al.*, 2009).

2.2.1.c. Cleavage of the HA_0 precursor

Proteolytic cleavage of HA_0 is necessary to activate the hemagglutinin by permitting its subsequent acid pH-mediated conformational change, which confers its membrane fusion activity. The cleavage site is made of one to six basic residues directly preceding a conserved glycine. Its accessibility to proteases depends on the glycosylation pattern of residues 22, 165 and 246 of HA_1. After cleavage, the unique R residue or the polybasic stretch is removed by a host carboxypeptidase, but this excision is not critical for subsequent functioning of cleaved HA (Garten & Klenk, 1983).

- *Cleavage motifs*

When the cleavage site is made of a "Q/EXRG" recognition motif, thus with a single basic amino acid, HA_0 is typically activated extracellularly by proteases with trypsin-like activity (Steinhauer, 1999). The local availability of extracellular trypsin-like proteases is therefore crucial for virus propagation, explaining why influenza virus strains of which the HA display a single amino acid at the cleavage site limit their spread in hosts or tissues where the appropriate proteases are encountered and require incorporation of exogenous trypsin in the cell culture medium *in vitro*. In the human respiratory tract, the serine protease tryptase Clara produced by Clara cells of the bronchiolar epithelium and miniplasmin produced by the epithelial cells of the upward divisions of bronchioles are the most likely local proteases responsible for HA_0

cleavage (Kido *et al.*, 1992; Murakami *et al.*, 2001; Bertram *et al.*, 2010). Endogenous inhibitors of these proteases, like sectretory leukoprotease inhibitor and pulmonary surfactant are known inhibitors of influenza replication *in vitro* and *in vivo* (Bertram *et al.*, 2010). As most bacteria also produce proteases, a synergistic effect of bacterial respiratory infections in regard to the cleavage of HA is also suspected (Steinhauer, 1999; Bertram *et al.*, 2010). In the chick embryo, a preparation routinely used to amplify influenza viruses, a calcium dependent serine endoprotease highly homologous to the blood clotting factor X is responsible for the cleavage (Gotoh *et al.*, 1990). The fortuitous observation that the mouse adapted variant of the human A/WS/33 strain was able to grow *in vitro* without incorporation of trypsin, despite the monobasic cleavage motif of its HA_0, led to the discovery that the companion NA was able to recruit plasminogen, which, upon activation, was able to cleave the HA_0 precursor (Lazarowitz *et al.*, 1973). This activity of plasminogen was promoted by interaction between plasminogen and annexin-2 (LeBouder *et al.*, 2010). Even if applicable to some extent to other strains, this plasminogen-binding mechanism is probably a very particular way of HA activation of this selected neurovirulent mouse-adapted strain. It is confirmed by a recent study on the same A/WSN/33 H1N1 strain, confirming the importance of the cleavage site for plasminogen activation and subsequent neurovirulence (Sun *et al.*, 2010).

Further, in human cells of the upper respiratory tract, cleavage was shown to be cell type-dependent, which led to the identification of the role played by membrane bound proteases like type II transmembrane serine proteases (TTSPs) TMPRSS2 and TMPRSS4 and human airway trypsin-like protease (HAT) (Bertram *et al.*, 2010). Expression of these proteases in MDCK in trypsin-free culture conditions was sufficient to allow the amplification of influenza virus (Bertram *et al.*, 2010).

When the cleavage site is made of a stretch of consecutive basic amino acids, HA_0 is typically activated intracellularly in the medial and/or trans-Golgi network, by proteases with subtilisin-like activity (Stieneke-Grober *et al.*, 1992). These latter, among which furin, are ubiquitously distributed within the body which permits the HA_0 activation in cells of any type and thus opens avenues for polysystemic propagation. The minimum consensus motif for recognition is "R/KXK/RR-GLF" (Stieneke-Grober *et al.*, 1992). Only strains of the H5 and H7 subtypes have been found to present more than one basic residue at the cleavage site.

It is thus clear that cleavage site characteristics and the cell- and tissue-specificity of the

expression of the various proteases able to cleave HA determine the tropism of influenza virus (Bertram *et al.*, 2010).

- *Aptitude for cleavage and virulence*

The classification of avian influenza strains as *highly* (HPAI) or *low* (LPAI) pathogenic avian influenza is based on a clinical appraisal of the virulence of the virus, the so-called "intravenous pathogenicity index" (IVPI). According to the OIE (World Organisation for Animal Health), is considered as an HPAI strain: "Any influenza virus that is lethal for six, seven or eight of eight 4-8-week-old susceptible chickens within 10 days following intravenous inoculation with 0.2 ml of a 1/10 dilution of a bacteria-free, infective allantoic fluid" (OIE, 2004). In birds, such a maximum virulence is frequently associated with H5 or H7 strains containing up to 6 basic amino acids at the cleavage site (for example: recent strains of Asian H5N1 avian influenza) which may lead to the erroneous interpretation that the presence of a polybasic site is necessary and sufficient for a strain to be highly pathogenic. However, some "polybasic" avian strains with peculiar glycosylation patterns do not display the highly pathogenic phenotype because of an altered accessibility of the cleavage site (see after). Recent studies confirm that addition of a polybasic cleavage site is not sufficient to confer a highly pathogenic phenotype (Stech *et al.*, 2009). Aptitude to cleavage is controlled by substitution, by insertion, or by glycosylation pattern-associated variation in cleavage site accessibility.

- *Insertion/substitution mechanisms*

A mechanism for the insertion of basic residues in the cleavage site has been discovered in H5N2 strains that derived from a non pathogenic avian strain and caused an outbreak in Central America in the middle of the nineties. The early isolates of this H5N2 strain possessed the sequence "PQRETRG" at the cleavage site (Perdue *et al.*, 1997; Steinhauer, 1999). Pathogenic isolates emerging from these had an E to K substitution at position P-3 in relation to the cleavage site and a RK insertion at position P-3 and P-4. One strain showed two repetitive insertions, resulting in a "RKRK" motif. By studying different isolates, it was determined that the E to K substitution preceded the two insertions and that the E to K substitution was due to a single nucleotide substitution (G to A) at position 5 of a six-nucleotide motif ("AAGA**A**A", mRNA sense), which motif

is directly repeated once in strains with the aforementioned "RK" insertions and twice in the strain with the "RKRK" motif) (Perdue *et al.*, 1997). These observations led to the hypothesis that this local abundance of purine residues and short stretch of poly(A) might adopt a stable secondary structure (hairpin) which could temporary stop the RNA polymerase during copying of the positive-sense template RNA. Then, by releasing and repriming of RNA or by slippage of the polymerase, insertions and mutations could be added in the RNA sequence. Such mechanisms have already been suggested for other RNA viruses (Bebenek *et al.*, 1989; Cattaneo *et al.*, 1989; Garcia-Barreno *et al.*, 1990; Thomas *et al.*, 1988; Vidal *et al.*, 1990). Interestingly, many HPAI H5 and H7 strains contain such sequences, with purine-rich codons "AAA" or "AAG" (lysine) and "AGA" or "AGG" (arginine) (Perdue *et al.*, 1997), which strengthens the credibility of this hypothesis.

- *Control of accessibility by carbohydrates*

Structure analysis of the HA_0 precursor also revealed the importance of the accessibility of the HA_1-HA_2 junction for cleavage and, thus, for virulence. In most strains, the monobasic cleavage site is buried inside a cavity and is partially hindered by a carbohydrate side chain, resulting in inefficient furin cleavage and low-pathogenic phenotype. In some H5N1 strains however, the carbohydrate chain is absent (due to substituted residue HA_1 22) and, despite a monobasic cleavage site, they show a highly-pathogenic phenotype (Kawaoka & Webster, 1989; Steinhauer, 1999), suggesting that a better exposition permits efficient furin cleavage. Also, insertion of additional basic residues is supposed, even in the presence of the carbohydrate, to result in a far better exposition of the cleavage site and thus more efficient furin cleavage. For example, deletion of residues p-5 and p-6 of the polybasic cluster ("RKRKKR") of the A/Turkey/Ireland/83 strain (which possesses a carbohydrate chain bonded to residue HA_1 22) prevented its intracellular cleavage (Kawaoka & Webster, 1989; Steinhauer, 1999). Overall, nearly all highly pathogenic strains contain insertion of basic residues and lack the HA_1 22 glycosylation site by comparison with low-pathogenic strains.

- *Cleavage-dependent activation*

A R329Q HA mutant was produced to determine the structure of the H3 uncleaved HA_0

from the 1968 Hong Kong strain (A/Aichi/2/68) (Chen *et al.*, 1998). The HA_0 3D-structure is nearly superimposable on the structure of cleaved HA, with the exception of 19 residues, the six C-terminal residues of HA_1 (323-328), R329Q, and the 12 first (N-terminal) amino acids of HA_2 (H3 count). These residues form a prominent surface loop projecting residues HA_1 327 to HA_2 5 away from the surface of the molecule, making them accessible to proteases (Chen *et al.*, 1998; Steinhauer, 1999). The corresponding loop of avian H5 HAs is exposed in a similar manner. In contrast to H3 and H5 subtypes, only a miniloop structure was observed in the 1918 H1N1 HA, with M17 of HA_2 at the tip of it (Stevens *et al.*, 2004). This protruded part of the loop is located close to the carbohydrate linked to residue N20 (N22 in H3 numbering) of HA_1 that is known to control HA cleavage properties as afore discussed.

When the HA_0 cleavage occurs, the first ten residues of the newly released N-terminal end of HA_2 (positively charged) are internalized into a negatively charged adjacent deep cavity in which they make up to five hydrogen bonds. This cavity, which is hidden in the trimer interior before cleavage, systematically contains D109, D112 and K51 (HA_2, H3 numbering), whatever the HA subtype (Ha *et al.*, 2002). Other residues (17, 106 and 111) are mainly clade-specific (Ha *et al.*, 2002; Russell *et al.*, 2004). When pH diminishes up to the fusion pH (pH 5-6), those residues are protonated which abolishes those hydrogen bonds and frees the fusion peptide (Russell *et al.*, 2004).

This relocation of the fusion peptide upon cleavage, which thus hinders a series of ionisable residues, is supposed to create the pH-subordinated trigger that will permit the subsequent projection of the fusion peptide and associated activation of fusion activity upon acidification (Ha *et al.*, 2002). This working hypothesis is strengthened by the demonstration that mutations of these amino acids led to a higher membrane-fusion pH (Daniels *et al.*, 1985; Steinhauer *et al.*, 1995; Thoennes *et al.*, 2008; Wharton *et al.*, 1986). Alanine substitution of HA_2 residues D109 or D112 increases the fusion pH by 0.3 or 0.5, respectively (Thoennes *et al.*, 2008). The D109G, D109E, D112G, D112E and D112N substitutions also led to an increased fusion pH (Daniels *et al.*, 1985; Steinhauer *et al.*, 1996). Residues K51 and Q105 are also involved (Thoennes *et al.*, 2008). The hydrogen bonds made by these residues with residues of the fusion peptide are thus clearly implicated in triggering the fusion process when pH diminishes (Thoennes *et al.*, 2008). The histidine residues around W21 becoming positively-charged at acidic pH, they could cause the sudden expulsion of the positively-charged fusion peptide away from the cavity when pH diminishes (Stevens *et al.*, 2004).

Influenza viruses contain a proton channel (the matrix protein 2, "M2") which maintains the *Trans* Golgi Network pH above the fusion pH of intracellularly-cleavable HAs of HPAI strains to prevent their premature activation (Ciampor *et al.*, 1992; Grambas & Hay, 1992; Steinhauer *et al.*, 1991; Sugrue *et al.*, 1990). Comparison of the M2 ion channel activity of different HPAI strains revealed the possibility of an interplay between the M2 pH-modulating activity and the HA fusion pH according to which any increase in the fusion pH of HA is balanced by an increase in the M2 pH-modulating activity and inversely (Betakova *et al.*, 2005).

Overall, the molecular physiology of influenza HA_0 cleavage/activation suggests two potential pharmaceutical targets: the cleavage itself on the one hand and the availability of the pocket for fusion peptide relocation on the other.

2.2.1.d. Receptor Binding Site

- *Structure, function and polymorphism*

The HA receptor binding site (RBS) consists of a small cavity at the top of the molecule binding sialic acids (Figure 2). All but one of the residues forming the RBS are very conserved among influenza A strains (Kovacova *et al.*, 2002; Nobusawa *et al.*, 1991; Watowich *et al.*, 1994; Weis *et al.*, 1988; Wilson *et al.*, 1981). The bottom of the cavity is made of the phenolic hydroxyl group of Y98 and aromatic rings of W153 and its rear is delineated by E190 and L194, protruding from a short helix, with H183 and T155 (H3 numbering) (Masuda *et al.*, 1999; Sauter *et al.*, 1989; Sauter *et al.*, 1992; Weis *et al.*, 1988). Only the latter, T155, displays a relatively low conservation degree. Among the 191 strains studied by Kovacova and colleagues (2002), roughly half presented a threonine residue, whereas the other half frequently possessed a hydrophobic residue (V, L or I), or a histidine (in some H1, H2, H3 and H4 strains). The RBS is further demarcated by 2 edges, a right one made of "GVTAA" in H1/H3 HAs (131-135/134-138) and a left one consisting in "RGQAGR" (221-226/224-229) (Kovacova *et al.*, 2002). Taking all HA subtypes into consideration yields the consensus sequences "GVSSA" and "RGQSGR", respectively (Kovacova *et al.*, 2002).

Residues critically engaged in hydrogen bonding or van der Waals contacts with sialic acid were detected by structural analysis. In the H3 subtype, the carboxylate group of sialic acid is hydrogen bonded to S136 and to the amide of peptide bond 137 (Skehel &

Wiley, 2000) (Figure 7). Other hydrogen bonds are implicated between the 9-hydroxyl group and H183 and E190 and between the 8-hydroxyl group and Y98. Y98 and H183 are hydrogen bonded to each other and this binding is essential for sialic acid binding (Martin *et al.*, 1998). The 5-acetamido nitrogen of sialic acid binds the carbonyl of peptide bond 135 and its methyl group forms van der Waals contacts with W153. The acetamido carbonyl and the 7-hydroxyl group of sialic acid are hydrogen bonded and both develop van der Waals contacts with L194. The 4-hydroxyl group is directed outward and does not seem to play any role in the interaction (Skehel & Wiley, 2000). The corresponding residues in H1 HAs are Y91, W150, T152, H180, E187, L191 and Y192. Directed mutagenesis of H3 HA showed that only three mutations abolish sialic acid binding/hemagglutination: Y98F, H183F, and L194A. As mutations of E190 and S228 (that both interact with the 9-hydroxyl group of sialic acid) are not critical, the 9-hydroxyl group is probably not required for binding (Kelm *et al.*, 1992). Furthermore, because alanine substitution of W153 and Y195, which are engaged in a hydrogen-bonded network with H183 and Y98, results in a partial loss of binding (Martin *et al.*, 1998), H183 and Y98 seem to be the most important residues for sialic acid binding (Skehel & Wiley, 2000).

- *Specificity*

Another essential feature of the hemagglutinin receptor with crucial biological implications is its sialic acid-type specificity. Sialic acids (SA) are found at terminal ends of *N-glycans*, *O-glycans* and glycosphingolipids (Suzuki, 2005). The main two types among the ~40 different molecules of SAs found in nature are 5-*N*-acetylneuraminic acid (Neu5Ac) and 5-*N*-glycolylneuraminic acid (Neu5Gc), differing by the functional group at the C-5 position (Masuda *et al.*, 1999; Suzuki, 2005). Neu5Gc has been found in equine and swine trachea, in duck intestine but not in human respiratory epithelium. Influenza A and B viruses essentially use trisaccharides monosialo-lactosamine types I and II (SAα2-3(6)Galβ1-3(4)GlcNAcβ1-) on glycoproteins and gangliosides as receptors (Suzuki, 2005). Different types of linkage between Neu5Ac and the subjacent galactose residue exist among different species. The two main types are Neu5Ac-α(2,3)-Gal and Neu5Ac-α(2,6)-Gal. The ability of the HA RBS to bind a particular type of SA linkage determines, at least partially, the host range specificity of influenza viruses. HAs from avian strains mainly recognize α(2,3)

linkages (as equine strains do) and those from human strains *α*(2,6) linkages. As swine strains are able to bind both *α*(2,3)- and *α*(2,6)-linked sialic acids, pigs were thought to serve as "mixing vessel" for avian and human viruses. The "mixing vessel" hypothesis proposes that emerging human pandemic strains are produced by reassortment of genomic segments (including HA) of an avian virulent strain and a "classical" human strain, thus resulting in a human-adapted strain with some new virulent genes (Lamb & Krug, 2001). Such "antigenic shifts" were observed for the 1957 H2N2, 1968 H3N2 and 2009 H1N1 pandemic strains. But it seems that the 1918 H1N1 pandemic strain was derived directly from an avian virus, which adapted itself to humans (Taubenberger, 2006). On the other hand, it was shown that *α*(2,3)-linked SA is expressed in human ciliated airway and type II alveolar epithelial cells, which is not consistent with the mixing vessel hypothesis. The intestine of chicken and quail also contains *α*(2,6) receptors and it is now clear that these birds can serve as mixing vessel for the reassortment of avian and human influenza viruses, and this is most likely what happened in 1957 and 1968 (Guo *et al.*, 2007). Therefore, a new pandemic human strain can emerge by evolution from an avian strain without need of any intermediate host between birds and humans.

In spite of this last point, the HA *α*(2,3) *vs.* *α*(2,6) specificity probably remains an important factor of host-adaptation and adaptation of the specificity is probably required for full virulence. A demonstration of this was provided by Matrosovich and colleagues (2007) who showed that avian-like specificity attenuated a H3N2 virus in cultures of human airway epithelium. Similar results were obtained for H9N2 strains (Wan *et al.*, 2007). Besides, recognition of the Neu5Gc-*α*(2,3)-Gal moiety is critical for the efficient replication of influenza A viruses in horses and in ducks (Suzuki *et al.*, 2000). Therefore, an important question is that of the residues of the RBS critically involved in the preference for such or such SA-Gal moiety. The majority of the studies that have addressed this question focused on the H3 HA.

- *H3 hemagglutinin SA-α(2,3)- vs. SA-α(2,6)- linkage specificity*

A determinant role of L226 (H3 numbering) in the sialyl specificity was suggested by a set of studies in which variants from a parental strain were selected that showed a switched specificity. Firstly, incorporation of horse *α*-2 macroglobulin serum glycoprotein into the culture medium of cell monolayers infected with the A/Hong

Kong/68 strain (H3 subtype, SA-*α*(2,6)-Gal-specific) resulted in the isolation of a mutant strain with a higher *α*(2,3) binding affinity than the parental wild-type strain (Roberts *et al.*, 1998). The HA of the mutant clone had an altered RBS, with a L226Q substitution. In another experimental setup, amplification of a mutant clone of the A/duck/Ukraine/1/63 strain with acquired SA-*α*(2,6)-Gal-specificity similarly implicating a Q to L substitution at position 226 through a single passage in the allantoic membrane of the chicken embryo that have SA-*α*(2,3)-Gal receptor resulted in a reversion to the initial SA-*α*(2,3)-Gal-specific phenotype and Q226 genotype (Rogers *et al.*, 1995). The determinant role of L226 in the sialyl linkage specificity was confirmed by Ito and colleagues (1997) by culturing human influenza SA-*α*(2-6)-Gal-specific isolates in embryonated chicken eggs. The resulting viruses maintained high SA-*α*(2,6)-Gal specificity following up to two amniotic passages. However, further passages in either the amnion or the allantois resulted in the acquisition of, or a complete shift to, SA-*α*(2,3)- specificity. This change in specificity was also accompanied by appearance of variants with L to Q substitution at position 226. Structural studies, focusing either on the RBS or on the glycosaccharidic receptor, generated results compatible with the suspected crucial role of the residue at position 226. On the one hand, the L226Q substitution was proved to alter the RBS's 3D-structure (Weis *et al.*, 1988). On the other, the modality of the linkage between Neu5Ac and galactose was shown to considerably modify intra-saccharide van der Waals and hydrogen bonds and thus the conformation of the glycosaccharide (Skehel & Wiley, 2000). Therefore, as leucine 226 is located on the left edge of the RBS, near the glycosidic linkage of the receptor sialyl linkage, an effect of its substitution on HA sialyl linkage specificity is structurally plausible. Sequences alignments tend to confirm the importance of residue 226 in host specificity. Considering H3 subtype, we found that L226 is often replaced by V, I, and rarely by Q or F, the vast majority of human influenza A strains thus carrying a non-polar aliphatic residue at position 226. Human H3 HAs present a serine residue at position 228 in almost all cases (see hereafter). Conversely, avian H3 strains all present a Q226 and a G228. Recent data confirm the importance of Q226L and G228S substitutions in H3 HA for human adaptation (Tambunan *et al.*, 2010). These data suggest that these two residues are critical for human adaptation in H3 subtype viruses.

A role of S205 (H3 numbering) in the sialyl specificity was suggested by a study in which the application of a selective pressure using antibodies directed against the viral HA changed the binding specificity (Suzuki *et al.*, 1989). This switch in specificity was

accompanied by the substitution of serine (*α*(2,3)-Gal-specific) to tyrosine (*α*(2,6)-Gal-specific) at position 205. This position is located in the antigenic site D of H3. Although distant from the RBS, the residue at this position is proximate to the RBS of the next subunit, explaining why replacement of serine by a bulky tyrosine can affect the RBS function.

Other differences in residues in the neighborhood of the H3 hemagglutinin receptor were associated with linkage-type specificity, among which residues 193 and 218 (Daniels *et al.*, 1987; Ping *et al.*, 2010).

- *H3 hemagglutinin Neu5Ac-α(2,3)- vs. Neu5Gc-α(2,3)- specificity*

Anders and colleagues (1986) first detected an association between the T155Y substitution among early (1968-1971) and late (1972 and after) naturally occurring H3 strains and the *in vitro* recognition of sialylsugar chains containing Neu5Gc. As human, swine and equine upper airways significantly differ in their sialic acid species composition, Neu5Ac only in humans, balanced Neu5Ac and Neu5Gc in pigs (1:1) and predominant Neu5Gc among horses (9:1), the comparison of the binding properties of host-specific influenza virus strains was of particular interest. As expected, equine and swine influenza strains were shown to be able to bind Neu5Gc-galactose on glycolipids whereas human strains were not (Masuda *et al.*, 1999; Suzuki *et al.*, 1997). Moreover, equine strains were subsequently found to harbor a strictly conserved T155, whereas both threonine or tyrosine are found among swine strains and only tyrosine is present in human strains (Suzuki, 2005).

In addition to L226, another important residue is probably associated with human adaptation, S228 (H3 numbering). Duck-adapted human H3 strains contain glutamine and glycine residues at these positions respectively, which could be due to the presence of Neu5Gc in addition to Neu5Ac in duck's intestine (Ito *et al.*, 2000). Interestingly, the same residues are found at the same positions (Q222 and G224, corresponding to Q226 and G228 in H3 numbering) in HPAI H5N1 viruses isolated from poultry and humans in Vietnam and Thailand in 2004 (Li *et al.*, 2004).

Masuda and colleagues (Masuda *et al.*, 1999) also emphasized the critical importance of residues H143 and G158, localized near the RBS of HA_1, for recognition of Neu5Gc. The T155Y and E158G in H3 HA were recently confirmed to facilitate virus binding to Neu5Gc (Takahashi *et al.*, 2009).

- *Specificity of non-H3 HAs RBS for SAs and their linkage type*

In strains belonging to the H1 subtype, residues 226 and 228 are not implicated in receptor specificity since both human and avian strains contain most frequently glutamine and glycine (like avian H3 strains) at those positions, respectively (Nobusawa *et al.*, 1991; Vines *et al.*, 1998). Moreover, some human H1s (such as A/PR/8/34) bind both linkage types (Rogers *et al.*, 1983; Suzuki *et al.*, 1987). The reason why residues 226 and 228 of the left edge of the RBS are involved in the HA specificity and indirectly in the host-adaptation of H3 subtype HAs and not for the H1 subtype remains to be explained. Conversely, residues at positions 186 and 225 (H1 numbering) were suggested to influence the linkage specificity: avian strains present a P186 and a G225, whereas S186 and D225 were found in human strains (Matrosovich *et al.*, 1997). However, working with the available database, we found a P186 and G225 in many human strains and a S186 in many avian strains, which suggests that the presumed cause-to-effect link between the residues present at these positions and linkage specificity remains to be confirmed. Reid and colleagues (1999) showed that the E190D substitution was the sole difference between swine and avian-adapted swine H1 strains (Reid *et al.*, 1999; Stevens *et al.*, 2004). Residue 226 of the hemagglutinin from H9N2 strains was shown to determine the replication in human airway epithelium and is thus implicated in the host-adaptation (Wan & Perez, 2007). Importance of the E190D and G225D in H1 HA was recently reported (Tambunan *et al.*, 2010).

The D222G mutation in the HA of pandemic 2009 H1N1 virus was associated with acquisition of a dual α(2,3) and α(2,6) receptor specificity (Chutinimitkul *et al.*, 2010). Q223R mutation greatly enhanced infectivity in human cells of 2009 H1N1 virus (Wang *et al.*, 2010). Even if not part of the RBS, residues 200 and 227 also seem important, since the T200A and E227A mutations in swine-origin pandemic 2009 H1N1 virus were associated with modified α(2,6) affinity (de Vries *et al.*, 2011).

2.2.1.e. Antigenic sites

Five hypervariable antigenic sites (A to E) have been mapped on the globular head of the H3 HA (Both & Sleigh, 1981; Raymond *et al.*, 1986; Wiley *et al.*, 1981; Wrigley *et al.*, 1983). These sites consist of protruding loops at the extremity of the hemagglutinin spike. These loops can support amino acid substitutions without affecting the correct

folding of the protein. They constantly evolve to permit the virus to escape the host's immune response and, with the five antigenic sites of the neuraminidase, are responsible for "antigenic drift". Site A is formed by a protruding loop constituted by amino acids 133 to 137 and 140 to 146; site B comprises residues 155 to 160 and 186 to 197; site C contains the disulfide bond between C52 and C277 and different residues around it; site D is located at the interface between monomers and notably comprises residues 172, 174, 201, 205, 207, 217, 220, 226, 242 and 244; site E is near the bottom of the globular distal domain between sites A and C and is constituted by residues 62, 63, 78, 81 and 83 (Both & Sleigh, 1981; Wiley *et al.*, 1981; Wrigley *et al.*, 1983).

Five antigenic sites were also detected in the H1 HA: *Sa, Sb, Ca_1, Ca_2* and *Cb* (Caton *et al.*, 1982).

Another mechanism contributing to evading the host's immune response is the presence of variable carbohydrate side chains that are post-translationally added to the HA molecule (see above). As these carbohydrate chains are synthesized by cellular enzymes, they are not immunogenic by themselves (they are antigenically "self") but may cover and hinder an immunogenic portion of the HA surface. On the other hand, antigenic drift may create new glycosylation sites inside an antigenic site which may in turn prevent antibody fixation on this site (Skehel & Wiley, 2000).

All these data question the pertinence of using embryonated hens'eggs (that favors selection of α(2,3)-linkage type receptors instead of α(2,6)) to amplify human influenza viruses for vaccine production. Since the adaptation to another linkage-type was shown to modify the receptor site of HA, it also may affect the neighboring antigenic sites at the top of the HA spike, and the vaccine virus might thus not harbor the antigens able to evoke a fully effective protection against the wild-type virus. For this reason, virus amplification for human vaccination should maybe better be done in mammalian cells.

2.2.1.f. Fusion-associated segments

- *Description*

Cleavage of the HA_0 precursor is necessary to permit the subsequent pH-dependent activation of the HA membrane fusion activity. The activation process basically consists in an irreversible conformational change of the HA_2 segment, occurring in the late endosomal compartment where the pH drops between 5.0 and 6.0. The first 20 amino

acids of the N-terminus of the HA_2 segment generated after the cleavage of HA_0 constitute the hydrophobic fusion peptide. Upon activation, this latter is sharply relocated towards and into the endosomal membrane which causes its fusion with the viral membrane. Therefore, HA_2, which previously had its C-terminal end anchoring the HA molecule in the virus membrane, is now additionally anchored in the cell endosomal membrane by its N-terminal end. This double anchoring mediates the fusion between both membranes (Bizebard *et al.*, 1995; Durrer *et al.*, 1996; Ruigrok *et al.*, 1988; Sammalkorpi *et al.*, 2007; Sauter *et al.*, 1989; Skehel *et al.*, 1986; Thoennes *et al.*, 2008; Tsurudome *et al.*, 1992; Weber *et al.*, 1994).

- *Refolding events activating fusing power*

Structurally speaking, three major changes occur in HA_2 during the pH-dependent refolding (Bullough *et al.*, 1994; Carr *et al.*, 1993; Chen *et al.*, 1999). First, there is an extension of the central triple-stranded coiled coil of the native HA_2 (made of residues 76-105 before and of residues 38-105 after) due to the participation of residues 38-75 that previously formed an extended loop and a short α-helix. This extension relocates and exposes the fusion peptide at about 100 Å from its initial position. Secondly, the segment 105-129 participating to the long α-helix of native HA_2 undergoes a rearrangement in which the stretch 105-110 is converted into a reverse run and the second half of the helix (112-129) becomes folded up on the first half in an antiparallel manner. This results in the relocation of the C-terminal end of HA_2 over 100 Å in relation to residues 76-105 which remain in an identical coiled-coil structure in both conformations. The last event affects residues 141-175 that are just distal to a short β-sheet hairpin (residues 130-133 and 137-140). As the latter follows the folded-up-on-itself α-helix afore described, segment 141-175 is refolded from a compact conformation to a structure that extents toward the central coiled-coil, in an antiparallel fashion in relation to adjacent α-helices. Those three conformational changes tend to induce the bending in half of the HA_2 subunit, rendering the viral membrane anchor (C-terminal end of HA_2) and the fusion peptide (N-terminal end) closer to each other (Hughson, 1997).

- *Fusion peptide*

The 22 first residues of HA_2 were shown to insert into the cell endosomal membrane (Durrer *et al.*, 1996; Thoennes *et al.*, 2008). This so-called fusion peptide (HA_2 residues 1-20) is a glycine-rich sequence that forms a series of 4 contiguous reverse turns (Wilson *et al.*, 1981). It is one of the most conserved regions among HAs of influenza A virus strains, especially the first 11 residues: 1-GLFGAIAGFIENGWEGMIDG-20. Some strains were reported to differ from this quasi-consensus motif, particularly some H3-subtype strains that present a L2I or an A5E/V substitution. In some cases, the I6K, A7T, I10T or E11Q substitutions are also found, but we found that G1 and G8 are strictly conserved. In the second half (residues 12 to 20), there is a greater variability but G13, G16 and G20 are strictly conserved too. Thus, G5 is the sole of the 6 glycine residues that can be substituted in some influenza A strains, according to our alignment results (using the BLAST tool of the Influenza Virus Resource of the National Center for Biotechnology Information (Bao *et al.*, 2008). In spite of this high natural conservation, a series of experimental substitutions did not affect the fusion activity (Skehel & Wiley, 2000). For example, E11V and E15V substitutions do not affect the fusion activity, suggesting that those two charged residues are not essential (Steinhauer *et al.*, 1995). Conversely, experimental substitution of glycine 1 by any other residue than alanine completely abolishes fusion activity *in vitro* (Qiao *et al.*, 1999; Steinhauer *et al..*, 1995). Moreover, deletion of either G1 or L2 led to the loss of fusion activity (Garten *et al.*, 1991; Steinhauer *et al..*, 1995), which emphasizes the critical importance of the peptide length for fusion.

At neutral (7.4) and acidic pHs (5.0), the structure of the fusion peptide is essentially helical amphipathic (Han *et al.*, 2001). At pH 5.0, the HA fusion peptide presents a sharp bend and an additional 3_{10}-helix (C-terminal residues), which repositions the C-terminal residues, including the charged residues E15 and D19 (Han *et al.*, 2001). This rotation of E15 and D19 induces a deeper insertion of the fusion peptide into the lipid bilayer and is thus thought to play an essential role in triggering the penetration of the HA fusion peptide into the target membrane (Han *et al.*, 2001). The hydrophobic side chains of residues 2, 6 and 10 of the fusion peptide are thought to interact with the target lipid membrane (Langley *et al.*, 2009). The peculiar inversed V-shape or "kink" structure adopted by wild-type fusion peptide is highly susceptible to mutation since the following substitutions are linked to complete disruption of this structure: G1E, G1S,

G1V, G4V, E11A and W14A (Li *et al.*, 2010). These mutants rather adopt a linear *α*-helical conformation, not compatible with the fusion peptide function (Li *et al.*, 2010). In this helical hairpin "kink" structure, residues from the N-terminal half of the fusion peptide interact with those of the distal part for stabilization (Lorieau *et al.*, 2011).

- *Fusion process*

The influenza hemagglutinin is a typical example of viral class I fusion glycoprotein. The complete membrane fusion seems to be preceded by formation of HA clusters consisting in complexes of 3 to 6 trimers (Skehel & Wiley, 2000; Thoennes *et al.*, 2008). Free energy released by the refolding of HA and eventually by the formation of such complexes could be used for membrane fusion, and the fusion activity is enhanced by oligomerization (Chang *et al.*, 2008; Lau *et al.*, 2004; Rand & Parsegian, 1986; Sammalkorpi & Lazaridis, 2007; Siegel & Epand, 1997). It is clear that hydrogen bonds between residues of the fusion peptide and surrounding residues are implicated in triggering the fusion process when pH diminishes (thus disrupting these hydrogen bonds) (Thoennes *et al.*, 2008).

The HA C-terminal transmembrane anchor is hypothesised to play a role in fusion too since its replacement by a glycosylphosphatidylinositol anchor only promotes hemi-fusion (Kemble *et al.*, 1994; Melikyan *et al.*, 1995 & 1997). Hemi-fusion is an intermediate state consisting in the fusion of the proximal, but not distal leaflets of the two juxtaposed lipid bilayers (Tatulian & Tamm, 2000). The HA transmembrane domain is thus thought to disrupt the intermediate hemi-fusion state and to promote the formation of complete pores. Recent experiments confirm that the transmembrane domain of HA exerts with the fusion peptide a synergistic effect on membrane perturbation to promote fusion (Chang *et al.*, 2008). Other studies showed that the replacement of the HA transmembrane domain by that of the F glycoprotein of Sendai virus did not affect the fusion activity of the chimeric protein (Schroth-Diez *et al.*, 1998). Thus, the fusion-promoting activity of the HA transmembrane domain does not need a perfect conservation of its amino acids sequence. Neither its three conserved palmitoylated cysteines (Melikyan *et al.*, 1997), nor the connected cytoplasmic tail (Jin *et al.*, 1997) participate in the fusion mechanism. Interestingly, the 30 residue synthetic peptide used by Tatulian and Tamm (2000) as a prototypic HA transmembrane domain (see after) strongly tended to self-associate in oligomers that resist heat and SDS.

Therefore, the HA transmembrane domain could play a role in the aggregation of the non-covalently linked HA trimers. Such oligomers also seem to order the lipids surrounding them and to be attracted by ordered lipids (Tatulian & Tamm, 2000). Ordering of the lipids around HA transmembrane domain is thought to dehydrate the membrane (as does the HA fusion peptide) and thus to locally modify its physical properties (decrease of the hydratation pressure between interacting membranes) and, indirectly, to permit fusion.

It was further shown that fusion peptides of trimeric HA insert deeply and obliquely in the target membrane (Sammalkorpi & Lazaridis, 2007). Monomeric fusion peptides present an average angle to the membrane plane of 12.4°, while the insertion is more oblique (between 25 and 45°) for trimeric fusion peptides (Sammalkorpi & Lazaridis, 2007). Peptide-peptide interactions may play an essential role in the membrane insertion and the fusion process, which is confirmed by the fact that oligomerization enhances the fusion activity (Chang *et al.*, 2008; Lau *et al.*, 2004; Sammalkorpi & Lazaridis, 2007).

2.2.1.g. Membrane-addressing domain

- *Description and polymorphism*

Another important function of the influenza HA transmembrane domain is to address neosynthesized HAs to the cell apical membrane and to promote their insertion and assembly into lipid rafts (Skibbens *et al.*, 1988). Lipid rafts are membrane subdomains more ordered than the rest of the membrane by a greater richness in cholesterol and sphingomyelin; they function as platforms for signal transduction and constitute the budding site of many enveloped viruses (Takeda *et al.*, 2003).

A peptide corresponding to the HA transmembrane domain (amino acids 185 to 211 of HA_2) is essentially hydrophobic but also contains several polar residues (essentially serine residues, and some cysteines and threonines); its structure being largely α-helical (Tatulian and Tamm, 2000). Some of these polar/hydrophilic residues (particularly those present in the N-terminal half) are very conserved among influenza A strains; they seem to be exposed on the same side of the helical structure, which should permit water to penetrate deeply in the lipid bilayer suggesting ion canal properties (Tatulian and Tamm, 2000). Different hydrophobic residues are also highly (but not completely) conserved, such as I186, L187, I189, L197 and W208 of HA_2. G204 and C210 (the first of the three

palmitoylated cysteines) display a high degree of conservation too (Tatulian and Tamm, 2000). These conserved residues can arbitrarily be assigned to 3 segments. At the N-terminal end, there is an helical turn with the very conserved 5-mer "ILxIo" among H1, H2, H5, H6, H8, H9, H11, H12 and H13 subtypes ("H1 group", see above) and "ILoIx" among other subtypes (the "H3 group") (x: most frequently S, but also T or A; o: large aromatic residue) (Tatulian and Tamm, 2000). In this region, I189 was shown to mediate the folding of HA in the membrane (Lin *et al.*, 1998). The central conserved segment displays the motif 193-hASSL-197 (H1 group) or 193-hSCFL-197 (H3 group) (h being a branched aliphatic residue), the substitution L197V being found in some strains. At the C-terminal end, G204, W208 and C210 are, as aforementioned, very well conserved. It has to be noted here that the HA transmembrane domain was shown to be active on folding and trimerization of the HA (Lazarovits *et al.*, 1990). Alanine substitution of I514 (I189 of HA_2) and Y515 (Y190 of HA_2) severely impaired transport of the mutant HA from the ER to the Golgi network, trimerization being a prerequisite for export of HA from the ER (Lin *et al.*, 1998).

The influenza matrix protein 1 (M1) was shown to colocalize with HA in immunofluorescence studies (Ali *et al.*, 2000; Barman *et al.*, 2001). During the budding process, the M1 protein constitutes the physical link between surface glycoproteins (HA and NA) and the internal components of new virions (notably the ribonucleoproteins) (Ali *et al.*, 2000; Nayak *et al.*, 2004). The production of chimeric constructs of HA with parts of the Sendai virus F protein permitted to show that both the cytoplasmic tail and the transmembrane domain of HA are implicated in M1-binding (Ali *et al.*, 2000; Barman *et al.*, 2001).

- *Apical sorting and lipid raft insertion*

In addition to its membrane fusion function, the amino acid sequence of the transmembrane domain is crucial for apical sorting and lipid raft association. Those last two properties fail to completely correlate since some mutant HAs present a random sorting in spite of a high degree of lipid raft association, while others were efficiently transported apically without significant lipid raft association (Lin *et al.*, 1998). Deletion of the cytoplasmic tail reduces association to lipid rafts but does not alter the apical sorting (Zhang *et al.*, 2000). A C543Y substitution was shown to induce a predominant baso-lateral sorting of HA (Brewer & Roth, 1991), but does not impede the apical

sorting of HA since more than 99% of the virions bud from the cellular apex (Barman *et al.*, 2003; Mora *et al.*, 2002). Other mechanisms are thus thought to prevent baso-lateral sorting and/or to favour apical budding of influenza particles.

HA possesses two apical sorting signals, one in the transmembrane domain and one in the ectodomain, the latter being probably a glycan (Nayak *et al.*, 2004). Targeted mutagenesis experiments limited the apical sorting signal within the middle of the transmembrane domain (Nayak *et al.*, 2004). Alanine substitution of I511 and V512 caused a random sorting phenotype (Lin *et al.*, 1998). Disruption of microtubule network was also shown to induce baso-lateral instead of apical sorting of influenza HA.

Mutagenesis studies limited the lipid raft association signal within the external and cytoplasmic thirds of the transmembrane domain (Nayak *et al.*, 2004). The most important residues seem to be those residing in the outer leaflet of the viral membrane (Tatulian & Tamm, 2000). Studies by Lin *et al.* (1998) revealed the importance of residues I511 (corresponding to I186 of HA_2), V512 (corresponding to residue 187 of HA_2, most frequently replaced by L), T517 (192 of HA_2), V518 (193), G520 (195) and S521 (196). For example, alanine substitution of residues G520 and S521 led to HA exclusion from lipid rafts, which caused a baso-lateral sorting phenotype in the absence of baso-lateral sorting signal (Lin *et al.*, 1998). These residues are moderately conserved, the most frequent mutations being T517A (especially in H3 subtype) and G520S. Alanine substitution experiments also emphasized the importance of residues 530-538 (H3 numbering; 205-213 of HA_2) for lipid raft association, along with the requirement of HA molecules concentration by lipid rafts for efficient budding and subsequent fusion. Palmitoylation of the three C-terminal cysteine residues of the transmembrane domain is required for insertion of HA into lipid rafts (Tatulian & Tamm, 2000). Other conserved residues of the C-terminal end of the transmembrane domain were not associated to lipid raft concentration of HA, but may have other functions. For example, W208 (W residues are frequently associated with lipid bilayers interfaces) could be essential for correct positioning of transmembrane helices in the lipid bilayer (Wimley & White, 1996).

It is thus now clear that influenza HA is, upon synthesis, directly addressed to the cellular apex through its own apical sorting signals and tends to accumulate into lipid rafts microdomains, which enriches the membrane of the future virions with cholesterol and sphingolipids. Together with NA, HA is thus a key element to concentrate the viral

ribonucleoproteins at the budding site, via the M1 protein. Further studies are needed to delineate more precisely the apical sorting and lipid raft association domains of influenza HA.

2.2.2. Neuraminidase

Neuraminidase is a type II integral membrane glycoprotein of about 450 residues, its C-terminal end is exposed at the outer aspect of the virus membrane and its N-terminal end supports the transmembrane domain (residues 7-35) and the cytoplasmic tail (1-6) (Lamb & Krug, 2001). It is encoded by genomic segment 6. NA forms mushroom-shaped homotetramers (Mr about 220,000), each monomer with a stalk region penetrating into the membrane and a distal box-shaped globular head (100x100x60 Å). The monomers are disulfide-linked via the cysteine 49 (N1 numbering) of the stalk which stabilizes the quaternary structure, even if this stabilization is not absolutely necessary for the formation of enzymatically active tetramers (Hausmann *et al.*, 1997). Calcium ions and hydrophobic contacts between monomers also contribute to stabilization of tetrameric NA (Varghese *et al.*, 1983). NA is the second most important target of the host immune response and as such is also involved with hemagglutinin in the antigenic drift/shift processes. Those antigenic properties permitted to distinguish between nine different NA subtypes (N1 to N9), which are used in combination with HA subtypes to define influenza virus A subtypes. Each virion contains about 100 neuraminidase proteins. Sequence and structural data tend to class influenza A NA subtypes into two clusters: group-1 (including N1, N4, N5 and N8) and group-2 (N2, N3, N6, N7 and N9) (Russell *et al.*, 2006).

NA exerts an acetylneuraminyl hydrolase (or "neuraminidase") enzymatic activity essential for the budding process of new virions. This enzymatic activity catalyses the cleavage of the *α*-ketosidic (*α*2, *α*3 or *α*6) junction between terminal sialic acid (5-*N*-acetylneuraminic acid) and the subjacent *D*-galactose ("Gal") or *D*-galactosamine. This cleavage permits (i) release of new virions, which without NA would remain bonded by their hemagglutinins to membrane glycoproteins sialic acids and would aggregate on it and (ii) removal of sialic acids from viral components (Griffin *et al.*, 1983; Palese *et al.*, 1974). Residues 275 and 431 of N2 NA were shown to be involved in Neu5Ac*α*-2,6-Gal versus Neu5Gc*α*-2,6-Gal specificity (Kobasa *et al.*, 1999) but *in vivo* importance of these data remains unknown. NA was also hypothesized to facilitate the virus passage

through the mucin layer to reach the epithelial cells of the respiratory tract (Burnet *et al.*, 1947; Burnet, 1948; Gottschalk, 1958 & 1972; Matrosovich *et al.*, 2004). In addition, many avian influenza NAs have been shown to induce hemagglutination, via a second sialic acid binding site, but this function does not seem to have implications in the virus life cycle (Hausmann *et al.*, 1995; Kobasa *et al.*, 1997; Laver *et al.*, 1984). However, as human influenza strains systematically fail to present such hemagglutination properties, it is very likely that adaptations at this level are needed for an avian strain to become human-adapted. Recent data suggest that the second sialic acid binding site in avian N1 neuraminidase could be involved in receptor recognition and catalytic efficiency (Sung *et al.*, 2010).

2.2.2.a. General structure

Structure of NA was first investigated by Varghese *et al.* (1983) who crystallised and X-rayed a N2 subtype NA (A/Tokyo/3/67 NA) fragment obtained by pronase digestion of virions, which liberates the NA tetramer without its 74 or 77 N-terminal residues, i.e. without cytoplasmic tail, transmembrane domain and stalk region. Globular head of each NA subunit contains six 4-stranded *β*-sheet structures that are organized in a "propeller"-like structure in which each sheet constitutes a blade of the propeller (Colman, 1994; Varghese *et al.*, 1983) (Figure 3). The first strand of each sheet, which is the closest from the propeller axis, is parallel to this axis, and the last strand, the farthest from the axis, is nearly perpendicular to this axis and thus to the first, central strand (Varghese *et al.*, 1983). Each sheet is thus characterized by a typical twisted conformation. The last (outermost) strand of one sheet is then followed by the first (central) strand of the next sheet (Varghese *et al.*, 1983). The different strands are linked by connecting loops. Many of the antigenically and enzymatically essential amino acids are contained in those connecting loops (Colman *et al.*, 1983; Colman, 1994).

The globular head also contains the catalytic site of neuraminidase activity at the centre of its top, just above the central strands of each *β*-sheet. This site consists of a pocket bordered by 12 loops, among which 6 are connecting strand 4 of one sheet to strand 1 of the following *β*-sheet and the other six strands 2 and 3 of each sheet (Colman *et al.*, 1983) (Figure 3). Many charged residues are present in and around the pocket. They are of 2 types: some are in direct contact with the substrate, and others participate to the structure of the active site, although the distinction between both types is not so clear

(Colman *et al.*, 1983; Colman, 1994). The conserved charged residues are R118, E119, D151, R152, D198, R224, Q227, D243, H274, Q276, Q277, R292, D330, K350 and Q425 (Colman *et al.*, 1983). Close to the sialic acid-binding site, one finds other conserved residues: Y121 (F in N1, N5 and N8 strains), W178 and L134. Although a slight preference for α2-3 linkages has been noticed, the neuraminidase activity presents fairly low linkage specificity (Corfield *et al.*, 1982 & 1983). Among these residues, only Y (or F) 121, L134, W178, D243, R292 and D330 are strictly invariable. The less conserved is D198, which is frequently replaced by N or E (personal investigations).

Many intrachain disulfide bonds are found in the neuraminidase protein (for N2 neuraminidase: C92-C417, C124-C129, C175-C193, C183-C230, C232-C237, C278-C291, C280-C289, C318-C337 and C421-C447) (Varghese *et al.*, 1983). Intrachain disulfide linkage between C257 (278 in N2 numbering) and C270 (291 in N2) in N1 subtype NA is crucial for the correct folding of NA, its absence leading to rapid degradation of the protein (Hausmann *et al.*, 1997).

Subunit interfaces support the binding of metal (calcium) ions, located in the vicinity of R113 and D141, as judged from N2 neuraminidase of A/Tokyo/3/67 strain (Varghese *et al.*, 1983).

Other residues (R344 and F466, N2 numbering) seem to be implicated in the low-pH stability of neuraminidase, probably by affecting calcium ion binding since they are located near the calcium ion-binding sites (Gulati *et al.*, 2002). Low-pH resistance of NA could be necessary in avian strains to resist stomach acidic environment before reaching the intestine. As such, residues at positions 344 and 466 could be important as host-range determinants and as factors of virulence as well (Suzuki, 2005). Also, the finding that, among influenza A virus strains isolated *in vivo*, only a R or K residue can be found at position 344 and only a F or a L (or Y in some rare strains) can be found at position 466 (personal results), which makes the amino acid at these positions less variable than anywhere else in NA, emphasizes the essential importance of the residues present at these two positions. Since these residues seem to be conserved in influenza strains of mammalian origin too, it is probable that NA low-pH resistance is needed during the maturation process of native NAs in the acidic conditions prevailing in the endosomal compartment or the *trans* Golgi network. Finally, it must be underlined that the glycosylation pattern (cf. after) of NA is far from being constant, which influences its structure, function and host adaptation. For instance, four glycosylation sites are present in the Tokyo/3/67 N2 NA (Varghese *et al.*, 1983), while seven glycosylations are

present in avian N1 subtype neuraminidases (Reid *et al.*, 2000).

2.2.2.b. Globular head (residues 74-450)

- *Catalytic site*

Crystallographic studies determined that the catalytic site binds the *α*-anomer of Neu5Ac in a half-chair conformation, where the carboxylate group at C2 is displaced from its axial low-energy position (on the floor of the pocket) to an equatorial location and the glycosidic oxygen from its equatorial position to an axial (pointing out) orientation (Colman, 1994). As in the HA receptor binding site, the pyranose binds to the bottom of the pocket by its hydrophobic face (this is the sole similarity between the HA receptor binding site and the NA catalytic site). In its equatorial position, the carboxylate group of Neu5Ac is surrounded by residues R118, 292 and 371 of NA and the glycosidic group is near the carboxylate oxygens of residue D151 of NA (Colman, 1994). The hydroxyl group in position C4 of the sugar is contained in a pocket bordered by residues E119 and E227. The *N*-acetyl group on C5 is hydrogen-bonded to the NA pocket. The glycerol chain of Neu5Ac makes hydrophobic contacts with the hydrocarbon side chain of R224 (Varghese *et al.*, 1992). Hydroxyls on C8 and C9 interact with E276 whereas C7 hydroxyl has no contact with the NA (Colman, 1994; Varghese *et al.*, 1992). Little is known about the precise mechanism of the neuraminidase activity reaction. Results seem to converge to the mechanistic pattern of a general acid, such as a H_20 molecule activated by D151, in attacking the glycosidic linkage with formation of a carboxonium ion intermediate (Chong *et al.*, 1992; Colman, 1994). Conformational differences were found in the NA catalytic site between group-1 and group-2 NAs (Russell *et al.*, 2006), essentially at the level of the loop around residue 150 (the "150-loop", made of residues 147 to 152). The particular 150-loop conformation in N1 neuraminidase (group-1) creates an adjacent cavity which is not present in N9 neuraminidase (group-2). The side chain of V149, a group-1 specific residue, is directed away from the active site, while for I149 (group-2 specific) the side chain points towards this active site (Russell *et al.*, 2006). The inter-group conserved residues 119 and 151 present a different conformation of their side chain depending on the group. These differences in the orientation of side chains of different residues and the presence of a cavity near the 150-loop in group-1 NAs make the group-1 active site

about 5 Å wider than for group-2 NAs (Russell *et al.*, 2006). These results are consistent with the differences in drug susceptibility of neuraminidases in relation to their group (see hereafter), and suggest that the inhibiting activity of neuraminidase inhibitors (NAI) could be enhanced by adapting them more precisely to the active site of group-1 or group-2 NAs (Amaro *et al.*, 2007; Landon *et al.*, 2008; Russell *et al.*, 2006).

Sequence analyses revealed that D151 (N2 numbering), like other previously thought strictly conserved residues (A203, T225 and E375), present a relatively high level of variation among influenza A N1 and N2 subtypes sequences available in GenBank (McKimm-Breschkin *et al.*, 2003). D151 is the most variable and, as said here above, might be replaced by G, E, N, or V, which does not correlate with its presumed essential role in the catalysis of neuraminidase activity (McKimm-Breschkin *et al.*, 2003). Conversely, none of the naturally occurring strains studied by McKimm-Breschkin *et al.* (2003) presented one of the mutations known to be responsible for resistance to neuraminidase inhibitors (E119V, R292K, H274Y, R152K, N2 numbering). Thus, wild-type influenza A strains were all susceptible to NAIs. Currently, we know that some clinical isolates of treated human patients were shown to present one of these mutations (de Jong *et al.*, 2006; ECDC, 2005; Monto *et al.*, 2006; Yen *et al.*, 2005; Zurcher *et al.*, 2006). Other mutations were since associated with resistance to neuraminidase inhibitors and, at the present time, one can distinguish mutations of catalytic residues or of framework residues, some of which are NA subtype(group)-specific mutations and some are drug-specific (oseltamivir *vs.* zanamivir) (Ferraris & Lina, 2008). It was shown that resistance to NAI could also be acquired by mutations in HA, leading to a reduced binding of HA to sialic acids and thus to a less important need of sialidase activity to allow new virions to escape from the infected cell surface (Gubavera *et al.*, 1996; McKimm-Breschkin *et al.*, 1996; Staschke *et al.*, 1995). Mutations of the NA catalytic residues presently known to induce a resistance to neuraminidase inhibitors are: D151E (low resistance to oseltamivir only), R152K, R224K, E276D, R292K and R371K (N2 numbering), most of which dramatically diminish the sialidase activity of NA. Substitutions of framework residues are E119V (oseltamivir-specific), E119G (zanamivir-specific), E119A/D (mostly zanamivir-specific), D198N, I222V (weak resistance to oseltamivir only), H274Y (oseltamivir-specific in N1 and N9 subtypes, not relevant in N2 subtype) and N294S (weak resistance to oseltamivir only) (Ferraris & Lina, 2008; Zurcher *et al.*, 2006). Most of these framework mutations only slightly affected the neuraminidase activity. The most frequent mutations found after inhibitor

treatment vary depending on the NA subtype, since R292K and E119V are preponderant in N2 NA, while H274Y is the most frequent mutation in N1 subtype (Ferraris & Lina, 2008). In addition, influenza strains were shown to be more sensitive either to oseltamivir or to zanamivir, depending on their NA. During the first three years of NAI use (1999 to 2002), human H3N2 and H1N2 influenza A strains tended to be more sensitive to oseltamivir, while H1N1 strains were more susceptible to zanamivir (Ferraris *et al.*, 2005; Hurt *et al.*, 2004; Monto *et al.*, 2006). It appears that the higher susceptibility to oseltamivir or zanamivir may also vary within a given NA subtype. NAI resistant strains were until now shown to be less infective and less transmissible in mice and ferret (Herlocher *et al.*, 2002; Ives *et al.*, 2002). But it seems that if NAI resistant strains with mutations of catalytic residues are effectively less virulent, viruses bearing substitutions in framework residues could be less altered, since an E119V mutant was as transmissible as the wild-type parental H3N2 strain (Herlocher *et al.*, 2004). Further, the I222V substitution was shown to compensate the E119V mutation (Simon *et al.*, 2011). Recent H5N1 NAI-resistant strains retain their fitness both *in vitro* and in mice (Yen *et al.*, 2007). H274Y oseltamivir-resistant mutants of H5N1 virus are highly attenuated in ferrets, but the N294S mutation was associated with only partial attenuation of lethality in mice and ferrets and with oseltamivir- but not zanamivir-resistance (Kiso *et al.*, 2011). It is thus possible that in the near future some NAI resistant strains could appear with one or more mutation(s) among framework residues and with an unaltered fitness, which could be of concern in the present context of a H5N1 pandemic threat (Ferraris & Lina, 2008).

Though not part of the catalytic site, residues 234, 241, 257 and 286 were shown to be essential for H5N1 NA function and viral particle release, together with residue 345, which is located in an antigenic site on the rim of the enzyme pocket (Tisoncik *et al.*, 2011).

- *Antigenic sites*

The antibody response against NA fails to neutralize virus infectivity since NA is not required for the virus to penetrate the target cell (Kilbourne *et al.*, 1968), but it diminishes virus titers and limits the extent of lung lesions, thus playing an important role in influenza epidemiology (Li *et al.*, 1993). Theoretically, antibodies directed against the enzymatic active site should present a better inhibiting capacity but such

antibodies are rare. This might be due to the fact that the enzymatic pocket is too small to permit the generation of specific antibodies (Colman *et al.*, 1987; Colman, 1994). This antibody-antigen interface classically involves a dozen of hydrogen bonds and contacts between some 15 amino acids of the target protein and the antibody (Davies *et al.*, 1993). Mutation of one of those residues was shown, by studies using monoclonal antibodies, to be sufficient to alter the antigen recognition to the point that a said monoclonal antibody becomes ineffective in antigen binding (Webster *et al.*, 1982 & 1987). This is the molecular basis of the antigenic drift. Since the sole globular head surface conserved between NA subtypes is precisely the enzymatic pocket, the other surfaces being occupied by variable loops, no cross-reactive inter-subtypes recognition may be seen for a given antiserum.

Five epitopes were described on N1 and N2 NAs: residues 328-332 (N1 region I), 339-344 (J), 365-369 (L), 385-399 (M), 430-434 (N) in N1 and residues 197-199 or 198-221 (N2 region D'), 328-339 (F'), 344-347 (G'), 368-369 (I') and 400-403 (K') of N2 NA. Similar results were obtained for N8 and N9 NAs (Saito *et al.*, 1994; Webster *et al.*, 1987).

- *Host-adaptation*

There is no doubt that NA is involved in the host-adaptation and virulence of influenza virus, as demonstrated for example by the 1957 H2N2 pandemic strain, of which the NA gene – of avian origin – was introduced by reassortment in the genome of a less pathogenic human strain (Wright & Webster, 2001). Residue 223 of N1 neuraminidase was linked to pathogenicity in mice because an isoleucine to threonine substitution at this position diminishes virulence in mice of 1997 highly pathogenic H5N1 strains (Katz *et al.*, 2000). Besides, the NA activity – which depends on the length of the stalk region (see after) – and the presence or not of a second sialic acid binding site (discussed previously) also determine the host-adaptation and pathogenicity (Baigent & McCauley, 2001; Wagner *et al.*, 2000).

- *Glycosylation pattern*

The glycosylation pattern is more critical for the NA correct folding than it is for HA (Saito *et al.*, 2000). For example, abolishing glycosylation by targeted mutagenesis of

D83 (66 in N1 numbering) or D398 (213 in N1) of subtype 8 NA prevented the expression of structurally or functionally mature NA (Saito *et al.*, 1997). Functional studies of N8 NA lacking the glycosylation site D144 also revealed that the glycosylation pattern of a correctly folded NA controls its substrate specificity (Saito *et al.*, 1997). The neuraminidase activity itself was shown to depend on glycosylation. The carbohydrate at position 144 (N8 numbering) is located close to the catalytic site and its absence diminishes or even completely abolishes neuraminidase activity (Hausmann *et al.*, 1997; Lentz *et al.*, 1987). Conversely, a N to I substitution at position 213 of N1 NA led to an over threefold increase in neuraminidase activity, probably by inducing an allosteric modification (Hausmann *et al.*, 1997).

Another amazing example of the importance of NA glycosylation was detected in studies of the neurovirulence of the A/WSN/33 and A/NWS/33 strains (see previously). Their hemagglutinin possesses a single arginine residue at its cleavage site, their activation in the brain thus necessitating a mechanism different from that typical of highly pathogenic avian influenza HAs. Moreover, these two strains do not require incorporation of trypsin in the medium to grow on cells *in vitro*. It turned out that their NA, lacking a glycosylation site at position 130 (corresponding to position 146 in N2 subtype NA) that is conserved in all other influenza virus neuraminidases, is able to bind plasminogen, the activation of which in plasmin permitting the cleavage, and thus the activation of WSN HA (Goto *et al.*, 2001). In addition to this specific glycosylation pattern, a plasminogen-binding HA-cleaving NA must possess a C-terminal lysine residue, which is a feature shared by plasminogen-binding proteins (Goto *et al.*, 2001).

Deletion of NA's glycosylation sites does not affect the transport of the protein to the cell surface (Hausmann *et al.*, 1997), except if carbohydrate at position 146 of N2 NA is eliminated, which confers a transport-defective phenotype (Lentz *et al.*, 1987). An interesting feature of the transport of NA to the cell surface is that it is significantly slower than HA transport and thus could be rate-limiting in new virion assembly (Hausmann *et al.*, 1997).

2.2.2.c. Stalk region (residues 36-73)

The region spanning residues 36-73 of N2 NA, located between membrane anchoring and pronase digestion sites, is heavily glycosylated and is referred to as the stalk region. The stalk is relatively thin (Varghese *et al.*, 1983) and contributing amino acids are

highly variable (Blok & Air, 1980). The stalk length influences the ability of NA to cleave sialic acid. The stalk region holds the globular head away from the virus envelope. Short-stalked NAs, whose active site is too close to the viral envelope are unable to reach their substrate on the cell surface and are consequently inefficient in releasing new virions from the cell surface (Baigent & McCauley, 2001; Els *et al.*, 1985). There seems to exist an interplay between the neuraminidase activity and the affinity of HA for sialic acids. Influenza strains with a high affinity HA need a full-length neuraminidase to overcome this affinity during the budding process, while low affinity HAs are associated with short-stalked NAs (Baigent & McCauley, 2001; Wagner *et al.*, 2000). Moreover, the stalk length may affect the host range and cell culture specificity of the influenza virus (Luo *et al.*, 1993; Vines *et al.*, 1998). Deletions of up to 28 residues and insertions of up to 41 aa did not prevent the formation of infectious virions. But it most probably affects the *in vivo* virulence. For example, the 1918 N1 NA possessed a full-length stalk region (thus without any deletion). It was also characterized by one cysteine residue and four glycosylation sites, like in all wild avian strains and most mammalian strains NAs (Reid *et al.*, 2000). Short stalk length in the NA of H5N1 virus was associated with enhanced virulence in mice (Matsuoka *et al.*, 2009). Banks *et al.* (2001) and Campitelli *et al.* (2004) showed that stalk deletion occurs in N1, N2 and N3 neuraminidases in domestic birds only, and never in wild birds. Replication of an H2N2 strain in chicken was supported by deletion of 27 residues in the NA stalk region (Sorrell *et al.*, 2010).

NA deletions are frequent and exist as numerous different types in avian strains, and are correlated with gallinaceous hosts and certain amino acid features on the HA protein (Li *et al.*, 2011).

2.2.2.d. Transmembrane and apical sorting domains

Membrane anchoring consists of a 29 residue sequence located near the N-terminus of NA (amino acids 7 to 35, N2 numbering). Influenza virus envelope was shown to be enriched with cholesterol and glycosphingolipids by comparison with cellular membrane composition (Scheiffelle *et al.*, 1999; Zhang *et al.*, 2000). In infected cells and in cells expressing plasmid-encoded viral envelope proteins, each viral envelope protein is found to essentially accumulate at the normal budding site (cellular apex in polarized cells). Apical sorting signals have been found in each of these envelope

proteins, although such signal has still to be defined in the matrix protein 2 (Nayak *et al.*, 2004). HA and NA each possess two apical signals: one within the transmembrane domain and one in the ectodomain, which is probably a glycan (Nayak *et al.*, 2004). The cytoplasmic tail (which contains the baso-lateral signal in the case of vesicular stomatitis virus) of NA and HA does not contain any apical sorting signal. HA and NA were furthermore shown to associate with lipid rafts, and this property depends on their transmembrane domain (Kundu *et al.*, 1996; Lin *et al.*, 1998). Precise analysis of the NA transmembrane domain revealed that the apical signal is made of the association of residues from multiple regions (and not formed by a single cluster in the primary structure of the protein), residues 9 to 27 of NA being sufficient for apical sorting (Barman & Nayak, 2000). The external half of the NA transmembrane domain is critical for lipid raft association. Although both lipid raft association and apical sorting determinants are present in the transmembrane domain and overlap, they are distinct (Barman & Nayak, 2000). For example, a deleted NA without its cytoplasmic tail displays a diminished association with lipid rafts but a still preferentially apical sorting (Zhang *et al.*, 2000). Alanine substitution of the first 3 N-terminal residues of NA led to elongated virus particles, without affecting lipid raft association (see hereafter). Replacement of the NA transmembrane domain by that of the human transferrin receptor also gave elongated particles with an altered budding process (Nayak *et al.*, 2004). Taken together, these data suggest that NA plays an important role in the budding process which seems independent of lipid raft association.

2.2.2.e. Cytoplasmic tail

The NA cytoplasmic tail, as that of HA, is highly conserved among strains (residues 1-MNPNQK-6) and is thought to play an essential role in the budding process (Colman, 1989). However, our sequence alignments show that several substitutions can be found in some strains: N2D, I or P, P3S or T, N4S, Q5R, K or L, and K6R. Deletion experiments with HA and/or NA lacking their cytoplasmic tail led to a dramatic alteration of viral morphology (many elongated and distended structures), a decreased virus yield, and an increased amount of matrix protein 2 per virion (Jin *et al.*, 1997). Those modifications are particularly marked in double HA- and NA-deletion mutants. Altered morphology in such mutant viruses is linked to the compromised interaction between HA and NA cytoplasmic tails on the one hand and the matrix protein 1 on the

other, which is a major determinant of particle shape (Barman *et al.*, 2001; Nayak *et al.*, 2004; Roberts *et al.*, 1998). Deletion of the NA- (but not HA-) cytoplasmic tail alone is sufficient for morphology alteration (Jin *et al.*, 1997). The accumulation of the M2 protein is attributed to a diminution of the normal exclusion of this protein provided by the cytoplasmic tails of NA and HA.

2.2.3. Matrix protein 2

The matrix protein 2 is a 97 residue transmembrane type III protein (Mr 14,000), with a 24 aa N-terminal extracytoplasmic end, a 19 residue hydrophobic transmembrane domain and a C-terminal cytoplasmic tail of 54 residues (Lamb *et al.*, 1985). It is encoded by a spliced mRNA derived from the genomic segment 7 (Lamb & Krug, 2001). The active form is a homo-tetramer (Sakaguchi *et al.*, 1997) stabilized by disulfide bonds between cysteines located in the extracytoplasmic region, and formed either by disulfide-linked monomers or by association of two disulfide-linked dimers (Holsinger & Lamb, 1991; Sakaguchi *et al.*, 1997; Sugrue & Hay, 1991). C17 and C19 of the M2 ectodomain are involved in these disulfide bonds between monomers but these bonds most likely stabilize the tetramer rather than directly cause its formation since noncovalent tetrameric structures have been found by electrophoresis (Tian *et al.*, 2002). Extensive studies of the characteristics and behaviour of M2 tetramers in lipid bilayers concluded that the M2 tetramer protrudes of about 1-1.5 nm from the bilayer surface at both its N- and C-terminal ends and is less than 4 nm in diameter (Hughes *et al.*, 2004).

When incorporated into planar membranes, a peptide corresponding to the M2 transmembrane domain was shown to promote amantadine-susceptible proton translocation (Duff & Ashley, 1992), suggesting an H+ ion channel activity. This M2 ion channel activity is proton-specific (M2 permeability to Na^+, for example, was estimated to be $6x10^7$ less than that to H^+) and pH-dependent, being activated at low pH such as that prevailing in the endosomal compartment or the *trans* Golgi network (Chizhmakov *et al.*, 1996; Pinto *et al.*, 1992; Wang *et al.*, 1993). The antiviral drug amantadine accelerated the discovery of the key role of M2 protein in influenza virus biological cycle because it specifically blocks its activity by occupying the lumen of the M2 ion channel. The key role of the M2 protein consists in permitting the intra-virion acidification that is needed to free the viral ribonucleoproteins (vRNPs) from the viral

matrix (M1) during the centripetal traffic of virion-containing endosomes (Helenius, 1992) (Figure 4). A second important role has been assigned to M2 in HPAI strains. As their native HAs are directly cleaved by intracellular furin-type proteases upon synthesis, they are immediately prone to be activated and promote fusion by acidic pH. To prevent such activation in the *trans* Golgi network, the M2 protein is thought to keep the pH above the threshold of activation (Ciampor *et al.*, 1992; Grambas *et al.*, 1992; Takeuchi & Lamb, 1994).

The remarkably low amount of M2 incorporated in each virion (20 to 60 molecules) sharply contrasts with its high level of expression on the infected cell surface and with the amounts of HAs per virion, suggesting an "exclusion" of the M2 protein when the virion is assembled (Lamb *et al.*, 1985; Sauter *et al.*, 1992; Zebedee & Lamb, 1988). Hemagglutinins and NAs are known to associate with lipid rafts which accumulate at foci where the budding proceeds. Therefore, a first possibility could be that M2 fails to specifically associate with lipid rafts, which would result in the lower concentration observed. HAs and NAs also possess apical sorting signals and binding sites to the M1 protein (Ali *et al.*, 2000; Nayak *et al.*, 2004) and when their C-terminal end is truncated by reverse genetics the amount of M2 protein per virion increases, raising the possibility that M2 exclusion depends on interactions between cytoplasmic tails (Ives *et al.*, 2002). Moreover, as Sendaï virus F protein is systematically excluded from influenza virions whereas chimeric M2-Sendaï F proteins are incorporated only when their extracellular domain is that of M2, incorporation of the latter into virions might also depend on interactions between M2 and HA/NA transmembrane or ectodomains. As in this case the cytoplasmic tail of the chimeric protein is not the one of the influenza M2 protein, the incorporation of M2 into virions probably does not require M1-M2 interactions (which need the presence of the M2 cytoplasmic tail).

M2 was shown to possess a cholesterol recognition/interaction amino acid consensus (CRAC) motif (46-LFFKCIYRRFK-56) in its cytoplasmic tail which would be necessary to its incorporation into virions. It appears that the CRAC motif is not required for virus replication but contributes to virulence (Stewart *et al.*, 2010). These results are consistent with the identification of an interaction of M2 with caveolin-1, a cholesterol-binding protein enriched in lipid rafts, via residues 47-55 (Zou *et al.*, 2009).

M2 was shown to interact with Hsp40 and $P58^{IPK}$ *in vitro* and *in vivo*, regulating the PKR signaling pathway (Guan *et al.*, 2010).

2.2.3.a. Structure

- *Transmembrane region*

The highly hydrophobic transmembrane region spanning residues 25 to 43 was shown to be largely α-helical and most probably left-handed, which tends to confirm the hypothesis supporting that M2-transmembrane domain consists in a left four-helix bundle with one helix per monomer (Kovacs & Cross, 1997) (Figure 5). In their experiments, Kovacs and Cross (1997) found the membrane-bound M2 proteins tilt 33° with respect to the lipid bilayer. Zhong *et al.* (1998) performed molecular dynamics simulations with a 25 residue peptide containing the M2 transmembrane domain which forms a parallel α-helix bundle in the octane portion of a "membrane-like" water/octane system. They confirmed the left-handed bundle hypothesis and identified a funnel-like motif, filled with water, formed by the bundle at its N-terminus (Zhong *et al.*, 1998). The funnel motif starts at residue V27 and ends at H37. The four helices are hydrogen bonded to each other at their C-termini. The stability of the funnel-like structure needs hydration of residues S23 and D24 at the rim of the funnel (Zhong *et al.*, 1998). These two residues, which are located at the lipid/solvent interface, are – if not hydrated – involved by their side chains in hydrogen bonds in which S23 of one monomer is linked to the D24 of the adjacent monomer. S23 and D24 are largely conserved but sometimes replaced by N or E (personal results). Hydration of the dehydrated metastable conformation breaks these bonds and opens the N-terminus of the bundle which takes the typical more stable funnel-like conformation. At the C-terminus, D44 of one monomer is hydrogen bonded by its side chain to the side guanidine moiety of R45 of a neighboring monomer (Zhong *et al.*, 1998) and this linkage is present whatever the hydration status. In the metastable dehydrated conformation with none of the H37 protonated, the imidazole groups of each H37 residue are located inside the bundle which clutters up the channel's lumen. The peptides forming the supercoil tilted on about 27±5° with respect to the interface, a result that is coherent with data generated by Kovacs and Cross (1997). Another study showed that the M2 monomeric transmembrane domain is a very uniform α-helix of about 3,56 residues per turn, with a helical tilt from one to the other of about 38° in a hydrated lipid bilayer (Wang *et al.*, 2001).

- *Cytoplasmic tail*

Structural data suggest that residues 45-62 form a very amphipathic helix which interacts with the hydrophobic/hydrophilic interface of the bilayer, with a tilt angle of about 80°, meaning that its direction is almost parallel to the bilayer plan (Tian *et al.*, 2003). In the tetrameric form, these amphipathic helices are thus thought to radiate from the channel on the membrane surface. Apart from being involved in virion packaging and morphogenesis (see below), the cytoplasmic tail is known to be removed upon activation of caspase-2, leading to a Mr 12,000 truncated form of M2 (Zhirnov *et al.*, 2002), and two substitutions (P64S and L67P) were proposed to be associated with enhanced virulence of human H5N1 isolates in Hong Kong in 1997 (Hiromoto *et al.*, 2000).

2.2.3.b. Ion channel structure and function

- *pH-dependent conductance*

Assessment of ion selectivity and membrane currents across the M2 channel was performed in *in vitro* expression systems or in reconstituted systems combining recombinant M2 and either lipid bilayers, liposomes or water/hydrophobic substance interfaces. Zhong *et al.* (2000) identified two conducting states of the M2 ion channel. The M2 ion channel activity first increases when pH diminishes from 7.0 to 5.0 and then drops below pH 5.0 (Chizhmakov *et al.*, 1996; Kovacs & Cross, 1997; Pinto *et al.*, 1992; Wang *et al.*, 1993). Thus, a high pH_{out} closes the channel, while a low pH_{out} activates it.

Interestingly, M2 was also shown to permit the efflux of K^+ or Na^+ cations from virions, probably to maintain electric neutrality. Furthermore, as the pH inside the M2-containing vesicle diminishes, the proton conductance decreases, but the cation efflux increases. This reciprocal inhibition/activation is thought to allow internal acidification at the beginning, while the activation of cations efflux when internal acidic pH is achieved permits to restore the electric neutrality and trapping of protons inside the virion (Leiding *et al.*, 2010).

- *Critical residues controlling pH-sensing and conductance*

As mentioned before, dehydration of residues S23 and R24 closes the N-terminus of the channel, whereas their hydration restores its opening (Zhong *et al.*, 1998). This is thus a first possible triggering mechanism for the activation of the M2 ion channel activity under low pH conditions. As the M2 pK_a (5.77) is very close to that of its H37 imidazole moiety, it was hypothesized that the pH-dependent activation of M2 was explained by the protonation of H37 (Wang *et al.*, 1995). Mutation experiments indeed emphasized the importance of this residue in the M2 activity and in the proton selectivity of the channel. For example, H37 replacement by glycine, alanine, glutamate, serine or threonine increased transport of Na^+ and K^+ ions (Gandhi *et al.*, 1999; Pinto *et al.*, 1997; Wang *et al.*, 1995). Moreover, adding imidazole in the buffer solution containing these substituted mutants of H37 partially re-established the ion selectivity (Venkataraman *et al.*, 2005). Because two diagonally opposite deprotonated H37 expose their rings facing each other and thus obstruct the channel lumen, while the other two H37 are stacked above these two (Zhong *et al.*, 2000), the role of protonation of H37 in the tuning of proton conductance appeared credible too (Figure 5). Sansom *et al.* (1997) proposed the protonation of H37 of all four M2 monomers within a tetramer creates a sufficient hydratation of the channel lumen to conduct protons. However, whereas both single-protonated and doubly-protonated H37 states are stable, the four-protonated state is not (Zhong *et al.*, 1998).

New light was shed by Tang and colleagues (2002) who reported the effect of point mutations inside the M2 transmembrane domain on membrane currents. Their results are compatible with a minimalist Shaker-type channel-like mechanism, with the pH-sensor role assumed by H37 and the effector "gate-control" role played by W41 (Tang *et al.*, 2002). A W41C mutation exacerbated the membrane currents, suggesting that the voluminous indole group of W41 limited the permeability to protons and thus the current amplitude across the channel. A W41F mutant caused the same phenotype while a W41Y mutation nearly restored the behaviour of the wild-type M2 (Tang *et al.*, 2002). Finally, when a voluminous group resembling tryptophan was added on the side chain of the cysteine in the W41C mutant, the narrowing of the channel was partially restored. These results led to the following paradigm: under high extracytoplasmic pH conditions, H37 is deprotonated and W41 adopts a conformation that obstructs the channel, closing the gate; when external pH drops, H37 becomes protonated permitting

an H^+ influx, then the indole side chain of W41 rotates towards the side chain of H37 which opens the gate and let the H^+ ions to reach the cytoplasmic side of the membrane (Tang *et al.*, 2002) (Figure 5). The rotation of the indole W41 side chain could be due to its implication in cation-π interaction with the protonated H37 (Tang *et al.*, 2002). The crucial role of H37 in proton conductance was recently confirmed (Wang *et al.*, 2011). According to our sequence alignments, W41 is conserved in all influenza A strains sequenced so far.

- *Proton transport*

Two mechanisms are proposed to account for proton transportation across the channel: the gating and the shuttle mechanisms.

According to the gating mechanism, each H37 residue would acquire one proton during the channel activation, rendering them positively-charged and resulting in their repulsion from each other, which opens the pore (Sansom *et al.*, 1997). The M2 pore would then be filled by water molecules generating an immobile water column ("proton wire") from the outer to the inner end of the channel. H^+ ions would be transported through the channel by passing from one water molecule to another. This mechanistic hypothesis is corroborated by the fact that mutation of residues lining the pore (V27, S31, G34, F38 and W41) does not prevent the proton transport, implying that they are not directly implicated (Mould *et al.*, 2000; Sansom *et al.*, 1997), and by molecular dynamic studies that confirmed the presence of immobile water molecules in the open pore (Smondyrev & Voth, 2002).

According to the shuttle mechanism, H37 residues are directly involved in the H^+ relay through the channel. During activation, the imidazole side chain is supposed to accept protons and become temporarily bi-protonated (with ε- and δ-hydrogens). It then would tend to release one of these at the other end of the ion channel to restore electroneutrality. The proton flow would then result from the cyclic capture and release by the imidazole side chains of H37 residues (Pinto *et al.*, 1997). This hypothesis is supported by energy minimization simulations (Lau *et al.*, 2004). The existence of bi-protonated H37 in the activated state was confirmed, which thus agrees with both hypotheses (Okada *et al.*, 2001).

More recently, a refinement of the gating model was introduced in which the new data brought by Okada *et al.* (2001) and Nishimura *et al.* (2002) were taken into account.

According to these authors, *(i)* the distance between the Nδ-H37 and the Cγ-W41 in the closed conformation is less than 3.9 Å, *(ii)* bi-protonation of H37 results in an hydrogen-π interaction between its own δ-hydrogen and the indole group of W41 and *(iii)* bi-protonated H37 undergoes a small rotation of its χ^2 angle that causes a sufficient enlargement of the pore to permit penetration of water molecules (Hu *et al.,* 2006). In the open channel conformation, one or maybe two of the H37 would be bi-protonated and would thus be stabilized by cation-π interaction with the nearest W41 residue. This last hypothesis is the most attractive because it would explain both the pH-sensing function of H37, which becomes protonated when external pH diminishes under 6.0, and the "gating" role of W41, which protrudes its side chain towards the lumen in the closed state and towards H37, thus opening the pore, in the open state. Interplay between H37 and W41 in the M2 activation process was also confirmed by tryptophane fluorescence assays (Czatobar *et al.,* 2004). Two pH-dependent changes in fluorescence were recorded: an increase in fluorescence involving W15 of the N-terminal domain when pH diminishes from 8.0 to approximately 6.0, the role of which remains to be determined, and a constant decrease in fluorescence of W41 under pH 6.0 which is blocked by amantadine and disappears upon H37A substitution (Czatobar *et al.*, 2004). As amantadine did not quench the W41 fluorescence of the H37A mutant, they concluded to a quenching of the W41 fluorescence by H37 in the wild-type M2 protein.
The crucial pH-sensor role of H37 was confirmed by Hu *et al.* (2006). At neutral pH, the four H37 of the M2 homotetramer form two dimers, stacked on each other. When pH diminishes, the protonation of three of these histidine residues would be necessary to change the conformation into the acidic state. In other words, it is the protonation of the third H37 residue that is responsible for the acidic activation of M2 proton channel properties (Hu *et al.*, 2006). The protonation of the first two histidines disrupts the first dimer, but the second dimer maintains the ion channel in its closed state. When the third histidine becomes protonated, the second dimer disrupts too and this allows the channel to open (Hu *et al.,* 2006).

- *Variation in proton conductance among strains*

The amplitude of the proton conductance of a wild-type M2 tetramer is about 10^5 protons per second at pH 5.7 (the pH found in endosomes), which is very low (Lin et al;, 2001; Vijayvergiya *et al.,* 2004). Higher conductance values were observed in some

strains. For example, mutations known to confer amantadine-resistance (V27A, V27S, A30T, S31N and G34E, see below) were shown to act by increasing the proton flux across M2 (Grambas *et al.*, 1992). Important differences were also noted in M2 ion channel function between the Rostock and Weybridge Fowl Plague viruses, two closely related H7 highly pathogenic avian strains (in such HPAI strains, M2 also possesses a protective role of native HAs by regulating *trans* Golgi Network pH). The Rostock M2 is less stable at low pH than the other but this is compensated by a sevenfold greater proton conductance than that afforded by the Weybridge M2 (Chizhmakov *et al.*, 2003; Grambas *et al.*, 1992). Three aa substitutions were found in the M2 transmembrane domain of these two strains: V27I, F38L and D44N (Betakova *et al.*, 2005). The gain-in-function mutation was later assigned to the D44N mutation and it finally turned out that this substitution also conferred amantadine-resistance (Betakova *et al.*, 2005). Although not unequivocally established yet, there seems to be, in HPAI strains, an interesting interplay between the HA fusion pH and the M2 pH-modulating activity, an increased fusion pH of HA being associated with a mutated M2 protein with increased pH-modulating capacity and inversely (Betakova *et al.*, 2005). Intriguingly, mutations of residues L26, S31, I33, L38 and L40 of the transmembrane domain generated a set of M2s of which the majority was more stable than the wild-type, while the remaining (L26A and L40F) were as stable as the wild-type (Stouffer *et al.*, 2005), suggesting that natural selection prioritizes function before stability.

- *Amantadine-resistance mutations*

Amantadine (1-aminoadamantane hydrochloride) and rimantadine (*α*-methyl-1-adamantane methylamine hydrochloride) are two antiviral drugs established as effective in prophylaxis and treatment of influenza infections (Oxford & Galbraith, 1980). At high concentration, these molecules raise the pH of endosome and thus prevent the pH-induced activation of HAs and the subsequent fusion mechanism, but this property is shared by many amines (Daniels *et al.*, 1985). At therapeutic concentrations, the antiviral effect of amantadine and rimantadine consists in the prevention of the internal acidification of entering virions in the endosome, thus precluding the detaching of vRNPs from the matrix M1 protein (Bukrinskaya *et al.*, 1982; Martin & Helenius, 1991). In HPAI strains, amantadine was also shown to alter the hemagglutinin maturation process. The amantadine-resistant phenotype was first shown to co-segregate

with the segment 7 of viral genome (Hay *et al.*, 1979; Lubeck *et al.*, 1978). Later, Hay *et al.* (1986) identified causal mutations in the M2 protein at positions 27, 30, 31 and 34. By expressing the A/Udorn/72 M2 protein in *Xenopus Laevis* oocytes and by measuring total membrane currents in wild-type and a panel of M2 mutants, Holsinger and colleagues (1994) confirmed the role of these residues by showing that V27A, V27S, A30T, S31N and G34E substitutions conferred resistance to the drug. The M2 transmembrane domain forms an α-helix in which residues 27, 30, 31, 34, 37, 38 and 41 are all on the same side of the helix, exposed in the lumen of the tetrameric M2 ion channel (Holsinger *et al.*, 1983). Mutation of these residues is therefore expected to result in an altered conductance of the M2 ion channel. Interestingly, point mutations performed by reverse genetics to render an influenza strain resistant to amantadine may diminish the M2 ion channel activity or increase it depending on the strain and of the neighboring residues in the lumen of the ion channel (Grambas *et al.*, 1992; Holsinger *et al.*, 1994). This experimental result is compatible with the observation that amantadine-resistance acquisition by different strains involves mutation of different residues. As aforementioned, recent comparison of the M2 function in Rostock and Weybridge H7 substrains by Betakova *et al.* (2005) led to the discovery of a new amantadine resistance-conferring mutation: D44N.

A second, low affinity, binding site of amantadine was described at the lipid interface of the M2 tetrameric pore (Rosenberg & Casarotto, 2010).

2.2.3.c. Putative Matrix protein 1-binding site

A monoclonal antibody (mAb14C2) directed against the extracellular N-terminus of the M2 protein was shown to restrict growth, viral assembly and release of influenza A/Udorn/72 strain (Hughey *et al.*, 1995; Treanor *et al.*, 1990; Zebedee & Lamb, 1988; Zebedee & Lamb, 1989). It also prevented formation of filamentous particles (Roberts *et al.*, 1998). mAb14C2-resistant strains were shown to present amino acid substitutions either in the M2 (S71T and K78Q) or M1 (A41V) coding sequences and displayed a filamentous morphology even in the presence of the mAb14C2 antibody (Roberts *et al.*, 1998). As they are located in the cytoplasmic tail of M2, residues 71 and 78 are thought to belong to the M1-binding site on M2. This interaction of M1 with M2 and with other viral membrane proteins (HA and NA) is consistent with the central role played by M1 in the packaging process (Nayak *et al.*, 2004). S71 is conserved in all influenza A

strains. K78 is most of the time replaced by Q, suggesting that the K78Q substitution is probably independent of the presence of the anti-M2 antibody. We found that K78 can be replaced in other strains by H, N, E or L.

McCown *et al.* (2003) showed that reducing expression of M2 protein by RNA interference led to a reduction of both total and infectious virion production, reemphasizing the role of M2 in processes underlying the packaging of new virions. The same authors later showed that an M2 mutant lacking its 28 C-terminal residues (M_2STOP70) produced four times less progeny particles, but 1000 times less infectious virions (McCown & Pekosz, 2005). The ion channel conductance of this mutant M2 was not affected, nor was the viral morphology altered, but nucleoprotein incorporation and RNA content of new virions were diminished. In addition, expression in *trans* of wild-type M2 protein rescued the mutated virus for the production of unaltered virions (McCown & Pekosz, 2005). Taken together, these data suggest that M2's cytoplasmic tail participates to the packaging of new virions. The M2 protein is a type III integral membrane protein which requires a segment of the cytoplasmic tail for the transmembrane domain to be recognized by the signal recognition particles and then translocated in the endoplasmic reticulum membrane (Hull *et al.*, 1988). In the experiments led by McCown and Pekosz (2005), only the 28 last residues of the 54 residue-long cytoplasmic tail of M2 were truncated and the mutated M2 protein was effectively expressed on the surface of infected cells. As a M_2STOP90 mutant replicated as effectively as the wild-type virus, it is hypothesized that the residues 70-89 support the M2 packaging function (McCown & Pekosz, 2005). Interestingly, this segment includes the residues 71 and 78 initially implicated in virion assembly and morphogenesis by Roberts *et al.* (1998). As M1 incorporation was not affected into M2-mutated new virions, it is likely that M1 is packaged essentially by binding to HA, NA and lipids more than to M2. But the M1-M2 interaction appears to be essential for efficient packaging of vRNPs into progeny virions. Recent studies showed that the residues 45-69 of M2 are essential for M1-binding, while residues 70 to 77 affect the efficiency of the packaging process of vRNPs (McCown & Pekosz, 2006). Among the last residues, tyrosine seem to play an essential role in the packaging process, since a Y76A was highly attenuated *in vitro*, with sharp decrease in NP incorporation into virions, while an adaptative S71Y mutation appeared after several passages of the Y76A mutant, which conferred a normal phenotype. Tyrosine residues in the M2 cytoplasmic tail are thus crucial for proper packaging of NP (Grantham *et al.*, 2010).

These results do not exclude a role for distal residues (70-97) in M1-binding, but these residues seem to be dispensable for this function. On the other hand, it appears that M1-binding alone may not be enough to stimulate infectious virus production (McCown & Pekosz, 2006).

2.2.4. Conclusion

HA, the most abundant surface glycoprotein of influenza virus, is an essential component of the virus life cycle by binding the virus to its receptor at the cell surface and permitting the viral entry into the cytoplasm. It is a main antigenic determinant and is used with NA to define influenza A subtypes. The sialic acid specificity is involved in the host adaptation of the virus, even if not as critical as originally thought, and the cleavability of HA_0 precursor is clearly a crucial part of the virulence. These features are modulated by the glycosylation pattern of HA. HA binds the M1 protein which brings the internal components of future virions to the budding site, at the cellular apex (Figure 6).

Neuraminidase, the second surface glycoprotein of influenza virus, is used with hemagglutinin to determine the subtypes of influenza A virus. It forms homotetramers and its main role is to allow new virions to be freed from the infected cell surface at the end of the replication cycle, by cutting off sialic acids of cellular glycoproteins. The existence of a balance between hemagglutinin affinity for sialic acids and neuraminidase activity (short-stalked NAs being less active than full-length NAs) explains why some HA and NA subtypes associations are not found among influenza viruses. Like hemagglutinin, neuraminidase plays an important role in addressing the viral ribonucleoproteins to the budding site, notably by interaction with the M1 protein (Figure 7).

M2 protein is the third surface protein of influenza virus. It forms homotetrameric H^+ ion channels, which activate when pH_{out} is acidic, typically in endosomes and in the *trans* Golgi network. The main role of M2 protein is to allow the internal acidification of entering virion in the endosomal compartment, which is needed to free the vRNPs form the viral matrix. Residues H37 and W41 are directly involved in the pH-dependent opening of the ion channel. The M2 activity is selectively inhibited by the antiviral drug amantadine. Some M2 mutant proteins are resistant to the effect of amantadine, these mutations acting by increasing the ion channel conductance. M2 protein binds to M1

protein and is clearly involved in the budding process and in the virion morphology (Figure 8).

2.2.5. References

Abe Y., Takashita E., Sugawara K., Matsuzaki Y., Muraki Y., Hongo S., Effect of the addition of oligosaccharides on the biological activities and antigenicity of influenza A/H3N2 virus hemagglutinin, J Virol (2004) 78:9605-9611.

Air G.M., Els M.C., Brown L.E., Laver W.G., Webster R.G., Location of antigenic sites on the three-dimensional structure of the influenza N2 virus neuraminidase, Virology (1985) 145:237-248.

Air G.M., Laver W.G., Webster R.G., Els M.C., Luo M., Antibody recognition of the influenza virus neuraminidase, Cold Spring Harb Symp Quant Biol (1989) 54 Pt 1:247-255.

Ali A., Avalos R.T., Ponimaskin E., Nayak D.P., Influenza virus assembly: effect of influenza virus glycoproteins on the membrane association of M1 protein, J Virol (2000) 74:8709-8719.

Amaro R.E., Minh D.D., Cheng L.S., Lindstrom W.M., Jr., Olson A.J., Lin J.H., Li W.W., McCammon J.A., Remarkable loop flexibility in avian influenza N1 and its implications for antiviral drug design, J Am Chem Soc (2007) 129:7764-7765.

Anders E.M., Scalzo A.A., Rogers G.N., White D.O., Relationship between mitogenic activity of influenza viruses and the receptor-binding specificity of their hemagglutinin molecules, J Virol (1986) 60:476-482.

Baigent S.J., McCauley J.W., Glycosylation of haemagglutinin and stalk-length of neuraminidase combine to regulate the growth of avian influenza viruses in tissue culture, Virus Res (2001) 79:177-185.

Banks J., Speidel E.S., Moore E., Plowright L., Piccirillo A., Capua I., Cordioli P., Fioretti A., Alexander D.J., Changes in the haemagglutinin and the neuraminidase genes prior to the emergence of highly pathogenic H7N1 avian influenza viruses in Italy, Arch Virol (2001) 146:963-973.

Bao Y., Bolotov P., Dernovoy D., Kiryutin B., Zaslavsky L., Tatusova T., Ostell J., Lipman D., The influenza virus resource at the National Center for Biotechnology Information, J Virol (2008) 82:596-601.

Barman S., Nayak D.P., Analysis of the transmembrane domain of influenza virus neuraminidase, a type II transmembrane glycoprotein, for apical sorting and raft association, J Virol (2000) 74:6538-6545.

Barman S., Ali A., Hui E.K., Adhikary L., Nayak D.P., Transport of viral proteins to the apical membranes and interaction of matrix protein with glycoproteins in the assembly of influenza viruses, Virus Res (2001) 77:61-69.

Barman S., Adhikary L., Kawaoka Y., Nayak D.P., Influenza A virus hemagglutinin containing basolateral localization signal does not alter the apical budding of a recombinant influenza A virus in polarized MDCK cells, Virology (2003) 305:138-152.

Bebenek K., Abbotts J., Roberts J.D., Wilson S.H., Kunkel T.A., Specificity and mechanism of error-prone replication by human immunodeficiency virus-1 reverse transcriptase, J Biol Chem (1989) 264:16948-16956.

Bertram S., Glowacka I., Steffen I., Kühl A., Pöhlmann S., Novel insights into proteolytic cleavage of influenza virus hemagglutinin, Rev Med Virol (2010) 20:298-310.

Betakova T., Ciampor F., Hay A.J., Influence of residue 44 on the activity of the M2 proton channel of influenza A virus, J Gen Virol (2005) 86:181-184.

Bizebard T., Gigant B., Rigolet P., Rasmussen B., Diat O., Bosecke P., Wharton S.A., Skehel J.J., Knossow M., Structure of influenza virus haemagglutinin complexed with a neutralizing antibody, Nature (1995) 376:92-94.

Blok J., Air G.M., Comparative nucleotide sequences at the 3' end of the neuraminidase gene from eleven influenza type A viruses, Virology (1980) 107:50-60.

Both G.W., Sleigh M.J., Conservation and variation in the hemagglutinins of Hong Kong subtype influenza viruses during antigenic drift, J Virol (1981) 39:663-672.

Brewer C.B., Roth M.G., A single amino acid change in the cytoplasmic domain alters the polarized delivery of influenza virus hemagglutinin, J Cell Biol (1991) 114:413-421.

Bright R.A., Ross T.M., Subbarao K., Robinson H.L., Katz J.M., Impact of glycosylation on the immunogenicity of a DNA-based influenza H5 HA vaccine, Virology (2003) 308:270-278.

Bukrinskaya A.G., Vorkunova N.K., Kornilayeva G.V., Narmanbetova R.A., Vorkunova G.K., Influenza virus uncoating in infected cells and effect of rimantadine, J Gen Virol (1982) 60:49-59.

Bullough P.A., Hughson F.M., Skehel J.J., Wiley D.C., Structure of influenza haemagglutinin at the pH of membrane fusion, Nature (1994) 371:37-43.

Burnet F.M., McCrea J.F., Anderson S.G., Mucin as a substrate of enzyme action by viruses of the mumps of influenza group., Nature (Lond) (1947) 160:404-405.

Burnet F.M., Mucins and mucoids in relation to influenza virus action. IV. Inhibition by purified mucoid of infection and hemagglutinin with the strain WSE., Aust J Exp Biol Med Sci (1948) 25:227-233.

Campitelli L., Mogavero E., De Marco M.A., Delogu M., Puzelli S., Frezza F., Facchini M., Chiapponi C., Foni E., Cordioli P., Webby R., Barigazzi G., Webster R.G., Donatelli I., Interspecies transmission of an H7N3 influenza virus from wild birds to intensively reared domestic poultry in Italy, Virology (2004) 323:24-36.

Carr C.M., Kim P.S., A spring-loaded mechanism for the conformational change of influenza hemagglutinin, Cell (1993) 73:823-832.

Caton A.J., Brownlee G.G., Yewdell J.W., Gerhard W., The antigenic structure of the influenza virus A/PR/8/34 hemagglutinin (H1 subtype), Cell (1982) 31:417-427.

Cattaneo R., Kaelin K., Baczko K., Billeter M.A., Measles virus editing provides an additional cysteine-rich protein, Cell (1989) 56:759-764.

Chang D.K., Cheng S.F., Kantchev E.A., Liu Y.T., Lin C.H., Membrane interaction and structure of the transmembrane domain of influenza hemagglutinin and its fusion peptide complex, BMC Biol (2008) 6:2.

Chen J., Lee K.H., Steinhauer D.A., Stevens D.J., Skehel J.J., Wiley D.C., Structure of the hemagglutinin precursor cleavage site, a determinant of influenza pathogenicity and the origin of the labile conformation, Cell (1998) 95:409-417.

Chen J., Skehel J.J., Wiley D.C., N- and C-terminal residues combine in the fusion-pH influenza hemagglutinin HA(2) subunit to form an N cap that terminates the triple-stranded coiled coil, Proc Natl Acad Sci U S A (1999) 96:8967-8972.

Chizhmakov I.V., Geraghty F.M., Ogden D.C., Hayhurst A., Antoniou M., Hay A.J., Selective proton permeability and pH regulation of the influenza virus M2 channel expressed in mouse erythroleukaemia cells, J Physiol (1996) 494 (Pt 2):329-336.

Chizhmakov I.V., Ogden D.C., Geraghty F.M., Hayhurst A., Skinner A., Betakova T., Hay A.J., Differences in conductance of M2 proton channels of two influenza viruses at low and high pH, J Physiol (2003) 546:427-438.

Chong A.K., Pegg M.S., Taylor N.R., von Itzstein M., Evidence for a sialosyl cation transition-state complex in the reaction of sialidase from influenza virus, Eur J Biochem (1992) 207:335-343.

Chutinimitkul S., Herfst S., Steel J., Lowen A.C., Ye J., van Riel D., Schrauwen E.J., Bestebroer T.M., Koel B., Burke D.F., Sutherland-Cash K.H., Whittleston C.S., Russell C.A., Wales D.J., Smith D.J., Jonges M., Meijer A., Koopmans M., Rimmelzwaan G.F., Kuiken T., Osterhaus A.D., García-Sastre A., Perez D.R., Fouchier R.A., Virulence-associated substitution D222G in the hemagglutinin of 2009 pandemic influenza A(H1N1) virus affects receptor binding, J Virol (2010) 84:11802-11813.

Ciampor F., Bayley P.M., Nermut M.V., Hirst E.M., Sugrue R.J., Hay A.J., Evidence that the amantadine-induced, M2-mediated conversion of influenza A virus hemagglutinin to the low pH conformation occurs in an acidic trans Golgi compartment, Virology (1992) 188:14-24.

Colman P.M., Varghese J.N., Laver W.G., Structure of the catalytic and antigenic sites in influenza virus neuraminidase, Nature (1983) 303:41-44.

Colman P.M., Laver W.G., Varghese J.N., Baker A.T., Tulloch P.A., Air G.M., Webster R.G., Three-dimensional structure of a complex of antibody with influenza virus neuraminidase, Nature (1987) 326:358-363.

Colman P.M., Influenza virus neuraminidase: Enzyme and antigen, In: Krug R.M. (Eds.), The influenza viruses, New York, Plenum Press, 1989, pp. 175-218.

Colman P.M., Influenza virus neuraminidase: structure, antibodies, and inhibitors, Protein Sci (1994) 3:1687-1696.

Corfield A.P., Wember M., Schauer R., Rott R., The specificity of viral sialidases. The use of oligosaccharide substrates to probe enzymic characteristics and strain-specific differences, Eur J Biochem (1982) 124:521-525.

Corfield A.P., Higa H., Paulson J.C., Schauer R., The specificity of viral and bacterial sialidases for alpha(2-3)- and alpha(2-6)-linked sialic acids in glycoproteins, Biochim Biophys Acta (1983) 744:121-126.

Czabotar P.E., Martin S.R., Hay A.J., Studies of structural changes in the M2 proton channel of influenza A virus by tryptophan fluorescence, Virus Res (2004) 99:57-61.

Daniels P.S., Jeffries S., Yates P., Schild G.C., Rogers G.N., Paulson J.C., Wharton S.A., Douglas A.R., Skehel J.J., Wiley D.C., The receptor-binding and membrane-fusion properties of influenza virus variants selected using anti-haemagglutinin monoclonal antibodies, Embo J (1987) 6:1459-1465.

Daniels R.S., Downie J.C., Hay A.J., Knossow M., Skehel J.J., Wang M.L., Wiley D.C.,

Fusion mutants of the influenza virus hemagglutinin glycoprotein, Cell (1985) 40:431-439.

Das S.R., Puigbò P., Hensley S.E., Hurt D.E., Bennink J.R., Yewdell J.W., Glycosylation focuses sequence variation in the influenza A virus H1 hemagglutinin globular domain, PLoS Pathog (2010) 6:e1001211.

Davies D.R., Chacko S., Antibody structure, Accounts of Chemical Research (1993) 26:421-427.

de Jong M.D., Simmons C.P., Thanh T.T., Hien V.M., Smith G.J., Chau T.N., Hoang D.M., Chau N.V., Khanh T.H., Dong V.C., Qui P.T., Cam B.V., Ha do Q., Guan Y., Peiris J.S., Chinh N.T., Hien T.T., Farrar J., Fatal outcome of human influenza A (H5N1) is associated with high viral load and hypercytokinemia, Nat Med (2006) 12:1203-1207.

de Vries R.P., de Vries E., Moore K.S., Rigter A., Rottier P.J., de Haan C.A., Only two residues are responsible for the dramatic difference in receptor binding between swine and new pandemic H1 hemagglutinin, J Biol Chem (2011) 286:5868-5875.

Duff K.C., Ashley R.H., The transmembrane domain of influenza A M2 protein forms amantadine-sensitive proton channels in planar lipid bilayers, Virology (1992) 190:485-489.

Durrer P., Galli C., Hoenke S., Corti C., Gluck R., Vorherr T., Brunner J., H+-induced membrane insertion of influenza virus hemagglutinin involves the HA_2 amino-terminal fusion peptide but not the coiled coil region, J Biol Chem (1996) 271:13417-13421.

ECDC Influenza Team, H5N1 virus resistant to oseltamivir isolated from Vietnamese patient, Euro Surveill (2005) 10:E051020 051022.

Els M.C., Air G.M., Murti K.G., Webster R.G., Laver W.G., An 18-amino acid deletion in an influenza neuraminidase, Virology (1985) 142:241-247.

Fanning T.G., Reid A.H., Taubenberger J.K., Influenza A virus neuraminidase: regions of the protein potentially involved in virus-host interactions, Virology (2000) 276:417-423.

Ferraris O., Kessler N., Lina B., Sensitivity of influenza viruses to zanamivir and oseltamivir: a study performed on viruses circulating in France prior to the introduction of neuraminidase inhibitors in clinical practice, Antiviral Res (2005) 68:43-48.

Ferraris O., Lina B., Mutations of neuraminidase implicated in neuraminidase inhibitors resistance, J Clin Virol (2008) 41:13-19.

Fleury D., Wharton S.A., Skehel J.J., Knossow M., Bizebard T., Antigen distortion allows influenza virus to escape neutralization, Nat Struct Biol (1998) 5:119-123.

Fouchier R.A., Munster V., Wallensten A., Bestebroer T.M., Herfst S., Smith D., Rimmelzwaan G.F., Olsen B., Osterhaus A.D., Characterization of a novel influenza A virus hemagglutinin subtype (H16) obtained from black-headed gulls, J Virol (2005) 79:2814-2822.

Gallagher P., Henneberry J., Wilson I., Sambrook J., Gething M.J., Addition of carbohydrate side chains at novel sites on influenza virus hemagglutinin can modulate the folding, transport, and activity of the molecule, J Cell Biol (1988) 107:2059-2073.

Gandhi C.S., Shuck K., Lear J.D., Dieckmann G.R., DeGrado W.F., Lamb R.A., Pinto L.H., Cu(II) inhibition of the proton translocation machinery of the influenza A virus M2 protein, J Biol Chem (1999) 274:5474-5482.

Gao Y., Zhang Y., Shinya K., Deng G., Jiang Y., Li Z., Guan Y., Tian G., Li Y., Shi J., Liu L., Zeng X., Bu Z., Xia X., Kawaoka Y., Chen H., Identification of amino acids in HA and PB2 critical for the transmission of H5N1 avian influenza viruses in a mammalian host, PLoS Pathog (2009) 5:e1000709.

Garcia-Barreno B., Portela A., Delgado T., Lopez J.A., Melero J.A., Frame shift mutations as a novel mechanism for the generation of neutralization resistant mutants of human respiratory syncytial virus, Embo J (1990) 9:4181-4187.

Garten W., Klenk H.D., Characterization of the carboxypeptidase involved in the proteolytic cleavage of the influenza haemagglutinin, J Gen Virol (1983) 64 (Pt 10):2127-2137.

Garten W., Vey M., Ohuchi R., Ohuchi M., Klenk H.D., Modification of the cleavage activation of the influenza virus hemagglutinin by site-specific mutagenesis, Behring Inst Mitt (1991) 12-22.

Goto H., Wells K., Takada A., Kawaoka Y., Plasminogen-binding activity of neuraminidase determines the pathogenicity of influenza A virus, J Virol (2001) 75:9297-9301.

Gotoh B., Ogasawara T., Toyoda T., Inocencio N.M., Hamaguchi M., Nagai Y., An endoprotease homologous to the blood clotting factor X as a determinant of viral

tropism in chick embryo, Embo J (1990) 9:4189-4195.

Gottschalk A., The influenza virus neuraminidase, Nature (1958) 181:377-378.

Gottschalk A., Historical introduction., In: Gottschalk A. (Eds.), Glycoproteins, their composition, structure and function., Amsterdam, Elsevier, 1972, pp. 2-3.

Grambas S., Hay A.J., Maturation of influenza A virus hemagglutinin--estimates of the pH encountered during transport and its regulation by the M2 protein, Virology (1992) 190:11-18.

Grantham M.L., Stewart S.M., Lalime E.N., Pekosz A. Tyrosines in the influenza A virus M2 protein cytoplasmic tail are critical for production of infectious virus particles, J Virol (2010) 84:8765-8776.

Griffin J.A., Basak S., Compans R.W., Effects of hexose starvation and the role of sialic acid in influenza virus release, Virology (1983) 125:324-334.

Guan Z., Liu D., Mi S., Zhang J., Ye Q., Wang M., Gao G.F., Yan J., Interaction of Hsp40 with influenza virus M2 protein: implications for PKR signaling pathway, Protein Cell (2010) 1:944-955.

Gubareva L.V., Bethell R., Hart G.J., Murti K.G., Penn C.R., Webster R.G., Characterization of mutants of influenza A virus selected with the neuraminidase inhibitor 4-guanidino-Neu5Ac2en, J Virol (1996) 70:1818-1827.

Gulati U., Hwang C.C., Venkatramani L., Gulati S., Stray S.J., Lee J.T., Laver W.G., Bochkarev A., Zlotnick A., Air G.M., Antibody epitopes on the neuraminidase of a recent H3N2 influenza virus (A/Memphis/31/98), J Virol (2002) 76:12274-12280.

Guo C.T., Takahashi N., Yagi H., Kato K., Takahashi T., Yi S.Q., Chen Y., Ito T., Otsuki K., Kida H., Kawaoka Y., Hidari K.I., Miyamoto D., Suzuki T., Suzuki Y., The quail and chicken intestine have sialyl-galactose sugar chains responsible for the binding of influenza A viruses to human type receptors, Glycobiology (2007) 17:713-724.

Ha Y., Stevens D.J., Skehel J.J., Wiley D.C., H5 avian and H9 swine influenza virus haemagglutinin structures: possible origin of influenza subtypes, Embo J (2002) 21:865-875.

Han X., Bushweller J.H., Cafiso D.S., Tamm L.K., Membrane structure and fusion-triggering conformational change of the fusion domain from influenza hemagglutinin, Nat Struct Biol (2001) 8:715-720.

Hartley C.A., Reading P.C., Ward A.C., Anders E.M., Changes in the hemagglutinin

molecule of influenza type A (H3N2) virus associated with increased virulence for mice, Arch Virol (1997) 142:75-88.

Hausmann J., Kretzschmar E., Garten W., Klenk H.D., N1 neuraminidase of influenza virus A/FPV/Rostock/34 has haemadsorbing activity, J Gen Virol (1995) 76 (Pt 7):1719-1728.

Hausmann J., Kretzschmar E., Garten W., Klenk H.D., Biosynthesis, intracellular transport and enzymatic activity of an avian influenza A virus neuraminidase: role of unpaired cysteines and individual oligosaccharides, J Gen Virol (1997) 78 (Pt 12):3233-3245.

Hay A.J., Kennedy N.C., Skehel J.J., Appleyard G., The matrix protein gene determines amantadine-sensitivity of influenza viruses, J Gen Virol (1979) 42:189-191.

Helenius A., Unpacking the incoming influenza virus, Cell (1992) 69:577-578.

Herlocher M.L., Carr J., Ives J., Elias S., Truscon R., Roberts N., Monto A.S., Influenza virus carrying an R292K mutation in the neuraminidase gene is not transmitted in ferrets, Antiviral Res (2002) 54:99-111.

Herlocher M.L., Truscon R., Elias S., Yen H.L., Roberts N.A., Ohmit S.E., Monto A.S., Influenza viruses resistant to the antiviral drug oseltamivir: transmission studies in ferrets, J Infect Dis (2004) 190:1627-1630.

Hiromoto Y., Yamazaki Y., Fukushima T., Saito T., Lindstrom S.E., Omoe K., Nerome R., Lim W., Sugita S., Nerome K., Evolutionary characterization of the six internal genes of H5N1 human influenza A virus, J Gen Virol (2000) 81:1293-1303.

Holsinger L.J., Lamb R.A., Influenza virus M2 integral membrane protein is a homotetramer stabilized by formation of disulfide bonds, Virology (1991) 183:32-43.

Holsinger L.J., Nichani D., Pinto L.H., Lamb R.A., Influenza A virus M2 ion channel protein: a structure-function analysis, J Virol (1994) 68:1551-1563.

Hu J., Fu R., Nishimura K., Zhang L., Zhou H.X., Busath D.D., Vijayvergiya V., Cross T.A., Histidines, heart of the hydrogen ion channel from influenza A virus: toward an understanding of conductance and proton selectivity, Proc Natl Acad Sci U S A (2006) 103:6865-6870.

Hughes T., Strongin B., Gao F.P., Vijayvergiya V., Busath D.D., Davis R.C., AFM visualization of mobile influenza A M2 molecules in planar bilayers, Biophys J (2004) 87:311-322.

Hughey P.G., Roberts P.C., Holsinger L.J., Zebedee S.L., Lamb R.A., Compans R.W., Effects of antibody to the influenza A virus M2 protein on M2 surface expression and virus assembly, Virology (1995) 212:411-421.

Hughson F.M., Enveloped viruses: a common mode of membrane fusion?, Curr Biol (1997) 7:R565-569.

Hull J.D., Gilmore R., Lamb R.A., Integration of a small integral membrane protein, M2, of influenza virus into the endoplasmic reticulum: analysis of the internal signal-anchor domain of a protein with an ectoplasmic NH2 terminus, J Cell Biol (1988) 106:1489-1498.

Humphrey W., Dalke A., Schulten K., VMD - Visual Molecular Dynamics, J. Molec. Graphics (1996) 14:33-38.

Hurt A.C., Barr I.G., Hartel G., Hampson A.W., Susceptibility of human influenza viruses from Australasia and South East Asia to the neuraminidase inhibitors zanamivir and oseltamivir, Antiviral Res (2004) 62:37-45.

Ibricevic A., Pekosz A., Walter M.J., Newby C., Battaile J.T., Brown E.G., Holtzman M.J., Brody S.L., Influenza virus receptor specificity and cell tropism in mouse and human airway epithelial cells, J Virol (2006) 80:7469-7480.

Inkster M.D., Hinshaw V.S., Schulze I.T., The hemagglutinins of duck and human H1 influenza viruses differ in sequence conservation and in glycosylation, J Virol (1993) 67:7436-7443.

Ito T., Suzuki Y., Takada A., Kawamoto A., Otsuki K., Masuda H., Yamada M., Suzuki T., Kida H., Kawaoka Y., Differences in sialic acid-galactose linkages in the chicken egg amnion and allantois influence human influenza virus receptor specificity and variant selection, J Virol (1997) 71:3357-3362.

Ito T., Suzuki Y., Suzuki T., Takada A., Horimoto T., Wells K., Kida H., Otsuki K., Kiso M., Ishida H., Kawaoka Y., Recognition of N-glycolylneuraminic acid linked to galactose by the alpha2,3 linkage is associated with intestinal replication of influenza A virus in ducks, J Virol (2000) 74:9300-9305.

Ives J.A., Carr J.A., Mendel D.B., Tai C.Y., Lambkin R., Kelly L., Oxford J.S., Hayden F.G., Roberts N.A., The H274Y mutation in the influenza A/H1N1 neuraminidase active site following oseltamivir phosphate treatment leave virus severely compromised both *in vitro* and *in vivo*, Antiviral Res (2002) 55:307-317.

Jin H., Leser G.P., Zhang J., Lamb R.A., Influenza virus hemagglutinin and

neuraminidase cytoplasmic tails control particle shape, Embo J (1997) 16:1236-1247.

Kawaoka Y., Webster R.G., Interplay between carbohydrate in the stalk and the length of the connecting peptide determines the cleavability of influenza virus hemagglutinin, J Virol (1989) 63:3296-3300.

Kelm S., Paulson J.C., Rose U., Brossmer R., Schmid W., Bandgar B.P., Schreiner E., Hartmann M., Zbiral E., Use of sialic acid analogues to define functional groups involved in binding to the influenza virus hemagglutinin, Eur J Biochem (1992) 205:147-153.

Kemble G.W., Danieli T., White J.M., Lipid-anchored influenza hemagglutinin promotes hemifusion, not complete fusion, Cell (1994) 76:383-391.

Kido H., Yokogoshi Y., Sakai K., Tashiro M., Kishino Y., Fukutomi A., Katunuma N., Isolation and characterization of a novel trypsin-like protease found in rat bronchiolar epithelial Clara cells. A possible activator of the viral fusion glycoprotein, J Biol Chem (1992) 267:13573-13579.

Kilbourne E.D., Laver W.G., Schulman J.L., Webster R.G., Antiviral activity of antiserum specific for an influenza virus neuraminidase, J Virol (1968) 2:281-288.

Kiso M., Ozawa M., Le M.T., Imai H., Takahashi K., Kakugawa S., Noda T., Horimoto T., Kawaoka Y., Effect of an asparagine-to-serine mutation at position 294 in neuraminidase on the pathogenicity of highly pathogenic H5N1 influenza A virus, J Virol (2011) 85:4667-4672.

Kobasa D., Rodgers M.E., Wells K., Kawaoka Y., Neuraminidase hemadsorption activity, conserved in avian influenza A viruses, does not influence viral replication in ducks, J Virol (1997) 71:6706-6713.

Kobasa D., Kodihalli S., Luo M., Castrucci M.R., Donatelli I., Suzuki Y., Suzuki T., Kawaoka Y., Amino acid residues contributing to the substrate specificity of the influenza A virus neuraminidase, J Virol (1999) 73:6743-6751.

Kovacova A., Ruttkay-Nedecky G., Haverlik I.K., Janecek S., Sequence similarities and evolutionary relationships of influenza virus A hemagglutinins, Virus Genes (2002) 24:57-63.

Kovacs F.A., Cross T.A., Transmembrane four-helix bundle of influenza A M2 protein channel: structural implications from helix tilt and orientation, Biophys J (1997) 73:2511-2517.

Kundu A., Avalos R.T., Sanderson C.M., Nayak D.P., Transmembrane domain of influenza virus neuraminidase, a type II protein, possesses an apical sorting signal in polarized MDCK cells, J Virol (1996) 70:6508-6515.

Lamb R.A., Zebedee S.L., Richardson C.D., Influenza virus M2 protein is an integral membrane protein expressed on the infected-cell surface, Cell (1985) 40:627-633.

Lamb R.A., Krug R.M., *Orthomyxoviridae*: The viruses and their replication, In: Knipe D.M., Howley P.M., Martin M.A., Griffin D.E.,Lamb R.A. (Eds.), Fields Virology, Boston, Lippincott Williams & Wilkins, 2001, pp. 1487-1531.

Landon M.R., Amaro R.E., Baron R., Ngan C.H., Ozonoff D., McCammon J.A., Vajda S., Novel druggable hot spots in avian influenza neuraminidase H5N1 revealed by computational solvent mapping of a reduced and representative receptor ensemble, Chem Biol Drug Des (2008) 71:106-116.

Langley W.A., Thoennes S., Bradley K.C., Galloway S.E., Talekar G.R., Cummings S.F., Varecková E., Russell R.J., Steinhauer D.A., Single residue deletions along the length of the influenza HA fusion peptide lead to inhibition of membrane fusion function, Virology (2009) 394:321-330.

Lau W.L., Ege D.S., Lear J.D., Hammer D.A., DeGrado W.F., Oligomerization of fusogenic peptides promotes membrane fusion by enhancing membrane destabilization, Biophys J (2004) 86:272-284.

Laver W.G., Colman P.M., Webster R.G., Hinshaw V.S., Air G.M., Influenza virus neuraminidase with hemagglutinin activity, Virology (1984) 137:314-323.

Lazarovits J., Shia S.P., Ktistakis N., Lee M.S., Bird C., Roth M.G., The effects of foreign transmembrane domains on the biosynthesis of the influenza virus hemagglutinin, J Biol Chem (1990) 265:4760-4767.

Lazarowitz S.G., Goldberg A.R., Choppin P.W., Proteolytic cleavage by plasmin of the HA polypeptide of influenza virus: host cell activation of serum plasminogen, Virology (1973) 56:172-180.

LeBouder F., Lina B., Rimmelzwaan G.F., Riteau B., Plasminogen promotes influenza A virus replication through an annexin 2-dependent pathway in the absence of neuraminidase, J Gen Virol (2010) 91:2753-2761.

Leiding T., Wang J., Martinsson J., DeGrado W.F., Arsköld S.P., Proton and cation transport activity of the M2 proton channel from influenza A virus, Proc Natl Acad Sci U S A (2010) 107:15409-15414.

Lentz M.R., Webster R.G., Air G.M., Site-directed mutation of the active site of influenza neuraminidase and implications for the catalytic mechanism, Biochemistry (1987) 26:5351-5358.

Li J., Das P., Zhou R., Single mutation effects on conformational change and membrane deformation of influenza hemagglutinin fusion peptides, J Phys Chem B (2010) 114:8799-8806.

Li J., Zu Dohna H., Cardona C.J., Miller J., Carpenter T.E., Emergence and genetic variation of neuraminidase stalk deletions in avian influenza viruses, PLoS One (2011) 6:e14722.

Li K.S., Guan Y., Wang J., Smith G.J., Xu K.M., Duan L., Rahardjo A.P., Puthavathana P., Buranathai C., Nguyen T.D., Estoepangestie A.T., Chaisingh A., Auewarakul P., Long H.T., Hanh N.T., Webby R.J., Poon L.L., Chen H., Shortridge K.F., Yuen K.Y., Webster R.G., Peiris J.S., Genesis of a highly pathogenic and potentially pandemic H5N1 influenza virus in eastern Asia, Nature (2004) 430:209-213.

Li S., Schulman J., Itamura S., Palese P., Glycosylation of neuraminidase determines the neurovirulence of influenza A/WSN/33 virus, J Virol (1993) 67:6667-6673.

Lin S., Naim H.Y., Rodriguez A.C., Roth M.G., Mutations in the middle of the transmembrane domain reverse the polarity of transport of the influenza virus hemagglutinin in MDCK epithelial cells, J Cell Biol (1998) 142:51-57.

Lin T.I., Schroeder C., Definitive assignment of proton selectivity and attoampere unitary current to the M2 ion channel protein of influenza A virus, J Virol (2001) 75:3647-3656.

Lorieau J.L., Louis J.M., Bax A., Helical hairpin structure of influenza hemagglutinin fusion peptide stabilized by charge-dipole interactions between the N-terminal amino group and the second helix, J Am Chem Soc (2011) 133:2824-2827.

Lubeck M.D., Schulman J.L., Palese P., Susceptibility of influenza A viruses to amantadine is influenced by the gene coding for M protein, J Virol (1978) 28:710-716.

Luo G., Chung J., Palese P., Alterations of the stalk of the influenza virus neuraminidase: deletions and insertions, Virus Res (1993) 29:321.

Martin J., Wharton S.A., Lin Y.P., Takemoto D.K., Skehel J.J., Wiley D.C., Steinhauer D.A., Studies of the binding properties of influenza hemagglutinin receptor-site mutants, Virology (1998) 241:101-111.

Martin K., Helenius A., Transport of incoming influenza virus nucleocapsids into the nucleus, J Virol (1991) 65:232-244.

Masuda H., Suzuki T., Sugiyama Y., Horiike G., Murakami K., Miyamoto D., Jwa Hidari K.I., Ito T., Kida H., Kiso M., Fukunaga K., Ohuchi M., Toyoda T., Ishihama A., Kawaoka Y., Suzuki Y., Substitution of amino acid residue in influenza A virus hemagglutinin affects recognition of sialyl-oligosaccharides containing N-glycolylneuraminic acid, FEBS Lett (1999) 464:71-74.

Matrosovich M., Matrosovich T., Uhlendorff J., Garten W., Klenk H.D., Avian-virus-like receptor specificity of the hemagglutinin impedes influenza virus replication in cultures of human airway epithelium, Virology (2007) 361:384-390.

Matrosovich M.N., Gambaryan A.S., Teneberg S., Piskarev V.E., Yamnikova S.S., Lvov D.K., Robertson J.S., Karlsson K.A., Avian influenza A viruses differ from human viruses by recognition of sialyloligosaccharides and gangliosides and by a higher conservation of the HA receptor-binding site, Virology (1997) 233:224-234.

Matrosovich M.N., Matrosovich T.Y., Gray T., Roberts N.A., Klenk H.D., Neuraminidase is important for the initiation of influenza virus infection in human airway epithelium, J Virol (2004) 78:12665-12667.

McCown M., Diamond M.S., Pekosz A., The utility of siRNA transcripts produced by RNA polymerase I in down regulating viral gene expression and replication of negative- and positive-strand RNA viruses, Virology (2003) 313:514-524.

McCown M.F., Pekosz A., The influenza A virus M2 cytoplasmic tail is required for infectious virus production and efficient genome packaging, J Virol (2005) 79:3595-3605.

McCown M.F., Pekosz A., Distinct domains of the influenza a virus M2 protein cytoplasmic tail mediate binding to the M1 protein and facilitate infectious virus production, J Virol (2006) 80:8178-8189.

McKimm-Breschkin J., Trivedi T., Hampson A., Hay A., Klimov A., Tashiro M., Hayden F., Zambon M., Neuraminidase sequence analysis and susceptibilities of influenza virus clinical isolates to zanamivir and oseltamivir, Antimicrob Agents Chemother (2003) 47:2264-2272.

McKimm-Breschkin J.L., McDonald M., Blick T.J., Colman P.M., Mutation in the influenza virus neuraminidase gene resulting in decreased sensitivity to the neuraminidase inhibitor 4-guanidino-Neu5Ac2en leads to instability of the

enzyme, Virology (1996) 225:240-242.

Melikyan G.B., White J.M., Cohen F.S., GPI-anchored influenza hemagglutinin induces hemifusion to both red blood cell and planar bilayer membranes, J Cell Biol (1995) 131:679-691.

Melikyan G.B., Brener S.A., Ok D.C., Cohen F.S., Inner but not outer membrane leaflets control the transition from glycosylphosphatidylinositol-anchored influenza hemagglutinin-induced hemifusion to full fusion, J Cell Biol (1997) 136:995-1005.

Mir-Shekari S.Y., Ashford D.A., Harvey D.J., Dwek R.A., Schulze I.T., The glycosylation of the influenza A virus hemagglutinin by mammalian cells. A site-specific study, J Biol Chem (1997) 272:4027-4036.

Monto A.S., McKimm-Breschkin J.L., Macken C., Hampson A.W., Hay A., Klimov A., Tashiro M., Webster R.G., Aymard M., Hayden F.G., Zambon M., Detection of influenza viruses resistant to neuraminidase inhibitors in global surveillance during the first 3 years of their use, Antimicrob Agents Chemother (2006) 50:2395-2402.

Mora R., Rodriguez-Boulan E., Palese P., Garcia-Sastre A., Apical budding of a recombinant influenza A virus expressing a hemagglutinin protein with a basolateral localization signal, J Virol (2002) 76:3544-3553.

Mould J.A., Li H.C., Dudlak C.S., Lear J.D., Pekosz A., Lamb R.A., Pinto L.H., Mechanism for proton conduction of the M(2) ion channel of influenza A virus, J Biol Chem (2000) 275:8592-8599.

Murakami M., Towatari T., Ohuchi M., Shiota M., Akao M., Okumura Y., Parry M.A., Kido H., Mini-plasmin found in the epithelial cells of bronchioles triggers infection by broad-spectrum influenza A viruses and Sendai virus, Eur J Biochem (2001) 268:2847-2855.

Naeve C.W., Williams D., Fatty acids on the A/Japan/305/57 influenza virus hemagglutinin have a role in membrane fusion, Embo J (1990) 9:3857-3866.

Naim H.Y., Roth M.G., Basis for selective incorporation of glycoproteins into the influenza virus envelope, J Virol (1993) 67:4831-4841.

Nayak D.P., Hui E.K., Barman S., Assembly and budding of influenza virus, Virus Res (2004) 106:147-165.

Nobusawa E., Aoyama T., Kato H., Suzuki Y., Tateno Y., Nakajima K., Comparison of complete amino acid sequences and receptor-binding properties among 13

serotypes of hemagglutinins of influenza A viruses, Virology (1991) 182:475-485.

Nohinek B., Gerhard W., Schulze I.T., Characterization of host cell binding variants of influenza virus by monoclonal antibodies, Virology (1985) 143:651-656.

Office International des Epizooties, Manual of Diagnostic Tests and Vaccines for Terrestrial Animals, Paris, Special Ed. OIE, 2004.

Ohuchi M., Ohuchi R., Feldmann A., Klenk H.D., Regulation of receptor binding affinity of influenza virus hemagglutinin by its carbohydrate moiety, J Virol (1997) 71:8377-8384.

Okada A., Miura T., Takeuchi H., Protonation of histidine and histidine-tryptophan interaction in the activation of the M2 ion channel from influenza a virus, Biochemistry (2001) 40:6053-6060.

Oxford J.S., Galbraith A., Antiviral activity of amantadine: a review of laboratory and clinical data, Pharmacol Ther (1980) 11:181-262.

Palese P., Tobita K., Ueda M., Compans R.W., Characterization of temperature sensitive influenza virus mutants defective in neuraminidase, Virology (1974) 61:397-410.

Perdue M.L., Garcia M., Senne D., Fraire M., Virulence-associated sequence duplication at the hemagglutinin cleavage site of avian influenza viruses, Virus Res (1997) 49:173-186.

Ping J., Dankar S.K., Forbes N.E., Keleta L., Zhou Y., Tyler S., Brown E.G., PB2 and hemagglutinin mutations are major determinants of host range and virulence in mouse-adapted influenza A virus, J Virol (2010) 84:10606-10618.

Pinto L.H., Holsinger L.J., Lamb R.A., Influenza virus M2 protein has ion channel activity, Cell (1992) 69:517-528.

Pinto L.H., Dieckmann G.R., Gandhi C.S., Papworth C.G., Braman J., Shaughnessy M.A., Lear J.D., Lamb R.A., DeGrado W.F., A functionally defined model for the M2 proton channel of influenza A virus suggests a mechanism for its ion selectivity, Proc Natl Acad Sci U S A (1997) 94:11301-11306.

Qiao H., Armstrong R.T., Melikyan G.B., Cohen F.S., White J.M., A specific point mutant at position 1 of the influenza hemagglutinin fusion peptide displays a hemifusion phenotype, Mol Biol Cell (1999) 10:2759-2769.

Rand R.P., Parsegian V.A., Mimicry and mechanism in phospholipid models of membrane fusion, Annu Rev Physiol (1986) 48:201-212.

Raymond F.L., Caton A.J., Cox N.J., Kendal A.P., Brownlee G.G., The antigenicity and evolution of influenza H1 haemagglutinin, from 1950-1957 and 1977-1983: two pathways from one gene, Virology (1986) 148:275-287.

Reading P.C., Pickett D.L., Tate M.D., Whitney P.G., Job E.R., Brooks A.G., Loss of a single N-linked glycan from the hemagglutinin of influenza virus is associated with resistance to collectins and increased virulence in mice, Respir Res (2009) 10:117.

Reid A.H., Fanning T.G., Hultin J.V., Taubenberger J.K., Origin and evolution of the 1918 "Spanish" influenza virus hemagglutinin gene, Proc Natl Acad Sci U S A (1999) 96:1651-1656.

Reid A.H., Fanning T.G., Janczewski T.A., Taubenberger J.K., Characterization of the 1918 "Spanish" influenza virus neuraminidase gene, Proc Natl Acad Sci U S A (2000) 97:6785-6790.

Rindler M.J., Ivanov I.E., Sabatini D.D., Microtubule-acting drugs lead to the nonpolarized delivery of the influenza hemagglutinin to the cell surface of polarized Madin-Darby canine kidney cells, J Cell Biol (1987) 104:231-241.

Roberts P.C., Lamb R.A., Compans R.W., The M1 and M2 proteins of influenza A virus are important determinants in filamentous particle formation, Virology (1998) 240:127-137.

Rogers G.N., Paulson J.C., Daniels R.S., Skehel J.J., Wilson I.A., Wiley D.C., Single amino acid substitutions in influenza haemagglutinin change receptor binding specificity, Nature (1983) 304:76-78.

Rogers G.N., Daniels R.S., Skehel J.J., Wiley D.C., Wang X.F., Higa H.H., Paulson J.C., Host-mediated selection of influenza virus receptor variants. Sialic acid-alpha 2,6Gal-specific clones of A/duck/Ukraine/1/63 revert to sialic acid-alpha 2,3Gal-specific wild type in ovo, J Biol Chem (1985) 260:7362-7367.

Romanova J., Katinger D., Ferko B., Voglauer R., Mochalova L., Bovin N., Lim W., Katinger H., Egorov A., Distinct host range of influenza H3N2 virus isolates in Vero and MDCK cells is determined by cell specific glycosylation pattern, Virology (2003) 307:90-97.

Rosenberg M.R., Casarotto M.G., Coexistence of two adamantane binding sites in the influenza A M2 ion channel, Proc Natl Acad Sci U S A (2010) 107:13866-13871.

Rosenthal P.B., Zhang X., Formanowski F., Fitz W., Wong C.H., Meier-Ewert H., Skehel J.J., Wiley D.C., Structure of the haemagglutinin-esterase-fusion

glycoprotein of influenza C virus, Nature (1998) 396:92-96.

Rudino-Pinera E., Tunnah P., Crennell S.J., Webster R.G., Laver W.G., Garman E.F., The Crystal Structure of Type a Influenza Virus Neuraminidase of the N6 Subtype Reveals the Existence of Two Separate Neu5Ac Binding Sites, To be published. DOI: 10.2210/pdb1w21/pdb (2005).

Ruigrok R.W., Aitken A., Calder L.J., Martin S.R., Skehel J.J., Wharton S.A., Weis W., Wiley D.C., Studies on the structure of the influenza virus haemagglutinin at the pH of membrane fusion, J Gen Virol (1988) 69 (Pt 11):2785-2795.

Russell R.J., Gamblin S.J., Haire L.F., Stevens D.J., Xiao B., Ha Y., Skehel J.J., H1 and H7 influenza haemagglutinin structures extend a structural classification of haemagglutinin subtypes, Virology (2004) 325:287-296.

Russell R.J., Haire L.F., Stevens D.J., Collins P.J., Lin Y.P., Blackburn G.M., Hay A.J., Gamblin S.J., Skehel J.J., The structure of H5N1 avian influenza neuraminidase suggests new opportunities for drug design, Nature (2006) 443:45-49.

Saito T., Taylor G., Laver W.G., Kawaoka Y., Webster R.G., Antigenicity of the N8 influenza A virus neuraminidase: existence of an epitope at the subunit interface of the neuraminidase, J Virol (1994) 68:1790-1796.

Saito T., Kawano K., Loss of glycosylation at Asn144 alters the substrate preference of the N8 influenza A virus neuraminidase, J Vet Med Sci (1997) 59:923-926.

Saito T., Yamaguchi I., Effect of glycosylation and glucose trimming inhibitors on the influenza A virus glycoproteins, J Vet Med Sci (2000) 62:575-581.

Sakaguchi T., Tu Q., Pinto L.H., Lamb R.A., The active oligomeric state of the minimalistic influenza virus M2 ion channel is a tetramer, Proc Natl Acad Sci U S A (1997) 94:5000-5005.

Sammalkorpi M., Lazaridis T., Configuration of influenza hemagglutinin fusion peptide monomers and oligomers in membranes, Biochim Biophys Acta (2007) 1768:30-38.

Sansom M.S., Kerr I.D., Smith G.R., Son H.S., The influenza A virus M2 channel: a molecular modeling and simulation study, Virology (1997) 233:163-173.

Sauter N.K., Bednarski M.D., Wurzburg B.A., Hanson J.E., Whitesides G.M., Skehel J.J., Wiley D.C., Hemagglutinins from two influenza virus variants bind to sialic acid derivatives with millimolar dissociation constants: a 500-MHz proton nuclear magnetic resonance study, Biochemistry (1989) 28:8388-8396.

Sauter N.K., Hanson J.E., Glick G.D., Brown J.H., Crowther R.L., Park S.J., Skehel J.J.,

Wiley D.C., Binding of influenza virus hemagglutinin to analogs of its cell-surface receptor, sialic acid: analysis by proton nuclear magnetic resonance spectroscopy and X-ray crystallography, Biochemistry (1992) 31:9609-9621.

Scheiffele P., Rietveld A., Wilk T., Simons K., Influenza viruses select ordered lipid domains during budding from the plasma membrane, J Biol Chem (1999) 274:2038-2044.

Schmidt M.F., Acylation of viral spike glycoproteins: a feature of enveloped RNA viruses, Virology (1982) 116:327-338.

Schroth-Diez B., Ponimaskin E., Reverey H., Schmidt M.F., Herrmann A., Fusion activity of transmembrane and cytoplasmic domain chimeras of the influenza virus glycoprotein hemagglutinin, J Virol (1998) 72:133-141.

Schulze I.T., Effects of glycosylation on the properties and functions of influenza virus hemagglutinin, J Infect Dis (1997) 176 Suppl 1:S24-28.

Siegel D.P., Epand R.M., The mechanism of lamellar-to-inverted hexagonal phase transitions in phosphatidylethanolamine: implications for membrane fusion mechanisms, Biophys J (1997) 73:3089-3111.

Simon P., Holder B.P., Bouhy X., Abed Y., Beauchemin C.A., Boivin G., The I222V neuraminidase mutation has a compensatory role in replication of an oseltamivir-resistant influenza virus A/H3N2 E119V mutant, J Clin Microbiol (2011) 49:715-717.

Skehel J.J., Daniels R.S., Hay A.J., Ruigrok R., Wharton S.A., Wrigley N.G., Weiss W., Willey D.C., Structural changes in influenza virus haemagglutinin at the pH of membrane fusion, Biochem Soc Trans (1986) 14:252-253.

Skehel J.J., Wiley D.C., Receptor binding and membrane fusion in virus entry: the influenza hemagglutinin, Annu Rev Biochem (2000) 69:531-569.

Skibbens J.E., Roth M.G., Matlin K.S., Differential extractability of influenza virus hemagglutinin during intracellular transport in polarized epithelial cells and nonpolar fibroblasts, J Cell Biol (1989) 108:821-832.

Smondyrev A.M., Voth G.A., Molecular dynamics simulation of proton transport through the influenza A virus M2 channel, Biophys J (2002) 83:1987-1996.

Sorrell E.M., Song H., Pena L., Perez D.R., A 27-amino-acid deletion in the neuraminidase stalk supports replication of an avian H2N2 influenza A virus in the respiratory tract of chickens, J Virol (2010) 84:11831-11840.

Staschke K.A., Colacino J.M., Baxter A.J., Air G.M., Bansal A., Hornback W.J., Munroe

J.E., Laver W.G., Molecular basis for the resistance of influenza viruses to 4-guanidino-Neu5Ac2en, Virology (1995) 214:642-646.

Stech O., Veits J., Weber S., Deckers D., Schröer D., Vahlenkamp T.W., Breithaupt A., Teifke J., Mettenleiter T.C., Stech J., Acquisition of a polybasic hemagglutinin cleavage site by a low-pathogenic avian influenza virus is not sufficient for immediate transformation into a highly pathogenic strain, J Virol (2009) 83:5864-5868.

Steinhauer D.A., Wharton S.A., Skehel J.J., Wiley D.C., Hay A.J., Amantadine selection of a mutant influenza virus containing an acid-stable hemagglutinin glycoprotein: evidence for virus-specific regulation of the pH of glycoprotein transport vesicles, Proc Natl Acad Sci U S A (1991) 88:11525-11529.

Steinhauer D.A., Wharton S.A., Skehel J.J., Wiley D.C., Studies of the membrane fusion activities of fusion peptide mutants of influenza virus hemagglutinin, J Virol (1995) 69:6643-6651.

Steinhauer D.A., Martin J., Lin Y.P., Wharton S.A., Oldstone M.B., Skehel J.J., Wiley D.C., Studies using double mutants of the conformational transitions in influenza hemagglutinin required for its membrane fusion activity, Proc Natl Acad Sci U S A (1996) 93:12873-12878.

Steinhauer D.A., Role of hemagglutinin cleavage for the pathogenicity of influenza virus, Virology (1999) 258:1-20.

Stevens J., Corper A.L., Basler C.F., Taubenberger J.K., Palese P., Wilson I.A., Structure of the uncleaved human H1 hemagglutinin from the extinct 1918 influenza virus, Science (2004) 303:1866-1870.

Stewart S.M., Wu W.H., Lalime E.N., Pekosz A., The cholesterol recognition/interaction amino acid consensus motif of the influenza A virus M2 protein is not required for virus replication but contributes to virulence, Virology (2010) 405:530-538.

Stieneke-Grober A., Vey M., Angliker H., Shaw E., Thomas G., Roberts C., Klenk H.D., Garten W., Influenza virus hemagglutinin with multibasic cleavage site is activated by furin, a subtilisin-like endoprotease, Embo J (1992) 11:2407-2414.

Stouffer A.L., Nanda V., Lear J.D., DeGrado W.F., Sequence determinants of a transmembrane proton channel: an inverse relationship between stability and function, J Mol Biol (2005) 347:169-179.

Sugrue R.J., Bahadur G., Zambon M.C., Hall-Smith M., Douglas A.R., Hay A.J., Specific structural alteration of the influenza haemagglutinin by amantadine,

Embo J (1990) 9:3469-3476.

Sugrue R.J., Hay A.J., Structural characteristics of the M2 protein of influenza A viruses: evidence that it forms a tetrameric channel, Virology (1991) 180:617-624.

Sun X., Tse L.V., Ferguson A.D., Whittaker G.R., Modifications to the hemagglutinin cleavage site control the virulence of a neurotropic H1N1 influenza virus, J Virol (2010) 84:8683-8690.

Sung J.C., Van Wynsberghe A.W., Amaro R.E., Li W.W., McCammon J.A., Role of secondary sialic acid binding sites in influenza N1 neuraminidase, J Am Chem Soc (2010) 132:2883-2885.

Suzuki T., Horiike G., Yamazaki Y., Kawabe K., Masuda H., Miyamoto D., Matsuda M., Nishimura S.I., Yamagata T., Ito T., Kida H., Kawaoka Y., Suzuki Y., Swine influenza virus strains recognize sialylsugar chains containing the molecular species of sialic acid predominantly present in the swine tracheal epithelium, FEBS Lett (1997) 404:192-196.

Suzuki Y., Nagao Y., Kato H., Suzuki T., Matsumoto M., Murayama J., The hemagglutinins of the human influenza viruses A and B recognize different receptor microdomains, Biochim Biophys Acta (1987) 903:417-424.

Suzuki Y., Kato H., Naeve C.W., Webster R.G., Single-amino-acid substitution in an antigenic site of influenza virus hemagglutinin can alter the specificity of binding to cell membrane-associated gangliosides, J Virol (1989) 63:4298-4302.

Suzuki Y., Ito T., Suzuki T., Holland R.E., Jr., Chambers T.M., Kiso M., Ishida H., Kawaoka Y., Sialic acid species as a determinant of the host range of influenza A viruses, J Virol (2000) 74:11825-11831.

Suzuki Y., Nei M., Origin and evolution of influenza virus hemagglutinin genes, Mol Biol Evol (2002) 19:501-509.

Suzuki Y., Sialobiology of influenza: molecular mechanism of host range variation of influenza viruses, Biol Pharm Bull (2005) 28:399-408.

Takahashi T., Hashimoto A., Maruyama M., Ishida H., Kiso M., Kawaoka Y., Suzuki Y., Suzuki T., Identification of amino acid residues of influenza A virus H3 HA contributing to the recognition of molecular species of sialic acid, FEBS Lett (2009) 583:3171-3174.

Takeda M., Leser G.P., Russell C.J., Lamb R.A., Influenza virus hemagglutinin concentrates in lipid raft microdomains for efficient viral fusion, Proc Natl Acad

Sci U S A (2003) 100:14610-14617.

Takeuchi K., Lamb R.A., Influenza virus M2 protein ion channel activity stabilizes the native form of fowl plague virus hemagglutinin during intracellular transport, J Virol (1994) 68:911-919.

Tambunan U.S., Ramdhan., Identification of sequence mutations affecting hemagglutinin specificity to sialic acid receptor in influenza A virus subtypes, Bioinformation (2010) 5:244-249.

Tang Y., Zaitseva F., Lamb R.A., Pinto L.H., The gate of the influenza virus M2 proton channel is formed by a single tryptophan residue, J Biol Chem (2002) 277:39880-39886.

Tatulian S.A., Tamm L.K., Secondary structure, orientation, oligomerization, and lipid interactions of the transmembrane domain of influenza hemagglutinin, Biochemistry (2000) 39:496-507.

Taubenberger J.K., The origin and virulence of the 1918 "Spanish" influenza virus, Proc Am Philos Soc (2006) 150:86-112.

Thoennes S., Li Z.N., Lee B.J., Langley W.A., Skehel J.J., Russell R.J., Steinhauer D.A., Analysis of residues near the fusion peptide in the influenza hemagglutinin structure for roles in triggering membrane fusion, Virology (2008) 370:403-414.

Thomas S.M., Lamb R.A., Paterson R.G., Two mRNAs that differ by two nontemplated nucleotides encode the amino coterminal proteins P and V of the paramyxovirus SV5, Cell (1988) 54:891-902.

Tian C., Tobler K., Lamb R.A., Pinto L.H., Cross T.A., Expression and initial structural insights from solid-state NMR of the M2 proton channel from influenza A virus, Biochemistry (2002) 41:11294-11300.

Tian C., Gao P.F., Pinto L.H., Lamb R.A., Cross T.A., Initial structural and dynamic characterization of the M2 protein transmembrane and amphipathic helices in lipid bilayers, Protein Sci (2003) 12:2597-2605.

Tisoncik J.R., Guo Y., Cordero K.S., Yu J., Wang J., Cao Y., Rong L., Identification of critical residues of influenza neuraminidase in viral particle release, Virol J (2011) 8:14.

Treanor J.J., Tierney E.L., Zebedee S.L., Lamb R.A., Murphy B.R., Passively transferred monoclonal antibody to the M2 protein inhibits influenza A virus replication in mice, J Virol (1990) 64:1375-1377.

Tsurudome M., Gluck R., Graf R., Falchetto R., Schaller U., Brunner J., Lipid

interactions of the hemagglutinin HA_2 NH2-terminal segment during influenza virus-induced membrane fusion, J Biol Chem (1992) 267:20225-20232.

Varghese J.N., Laver W.G., Colman P.M., Structure of the influenza virus glycoprotein antigen neuraminidase at 2.9 A resolution, Nature (1983) 303:35-40.

Varghese J.N., McKimm-Breschkin J.L., Caldwell J.B., Kortt A.A., Colman P.M., The structure of the complex between influenza virus neuraminidase and sialic acid, the viral receptor, Proteins (1992) 14:327-332.

Venkataraman P., Lamb R.A., Pinto L.H., Chemical rescue of histidine selectivity filter mutants of the M2 ion channel of influenza A virus, J Biol Chem (2005) 280:21463-21472.

Verhoeyen M., Fang R., Jou W.M., Devos R., Huylebroeck D., Saman E., Fiers W., Antigenic drift between the haemagglutinin of the Hong Kong influenza strains A/Aichi/2/68 and A/Victoria/3/75, Nature (1980) 286:771-776.

Vidal S., Curran J., Kolakofsky D., A stuttering model for paramyxovirus P mRNA editing, Embo J (1990) 9:2017-2022.

Vijayvergiya V., Wilson R., Chorak A., Gao P.F., Cross T.A., Busath D.D., Proton conductance of influenza virus M2 protein in planar lipid bilayers, Biophys J (2004) 87:1697-1704.

Vines A., Wells K., Matrosovich M., Castrucci M.R., Ito T., Kawaoka Y., The role of influenza A virus hemagglutinin residues 226 and 228 in receptor specificity and host range restriction, J Virol (1998) 72:7626-7631.

Wagner R., Wolff T., Herwig A., Pleschka S., Klenk H.D., Interdependence of hemagglutinin glycosylation and neuraminidase as regulators of influenza virus growth: a study by reverse genetics, J Virol (2000) 74:6316-6323.

Wan H., Perez D.R., Amino acid 226 in the hemagglutinin of H9N2 influenza viruses determines cell tropism and replication in human airway epithelial cells, J Virol (2007) 81:5181-5191.

Wang C.C., Chen J.R., Tseng Y.C., Hsu C.H., Hung Y.F., Chen S.W., Chen C.M., Khoo K.H., Cheng T.J., Cheng Y.S., Jan J.T., Wu C.Y., Ma C., Wong C.H., Glycans on influenza hemagglutinin affect receptor binding and immune response, Proc Natl Acad Sci U S A (2009) 106:18137-18142.

Wang C., Takeuchi K., Pinto L.H., Lamb R.A., Ion channel activity of influenza A virus M2 protein: characterization of the amantadine block, J Virol (1993) 67:5585-5594.

Wang C., Lamb R.A., Pinto L.H., Activation of the M2 ion channel of influenza virus: a role for the transmembrane domain histidine residue, Biophys J (1995) 69:1363-1371.

Wang J., Kim S., Kovacs F., Cross T.A., Structure of the transmembrane region of the M2 protein H(+) channel, Protein Sci (2001) 10:2241-2250.

Wang J., Qiu J.X., Soto C., DeGrado W.F., Structural and dynamic mechanisms for the function and inhibition of the M2 proton channel from influenza A virus, Curr Opin Struct Biol (2011) 21:68-80.

Wang W., Castelán-Vega J.A., Jiménez-Alberto A., Vassell R., Ye Z, Weiss C.D., A mutation in the receptor binding site enhances infectivity of 2009 H1N1 influenza hemagglutinin pseudotypes without changing antigenicity, Virology (2010) 407:374-380.

Watowich S.J., Skehel J.J., Wiley D.C., Crystal structures of influenza virus hemagglutinin in complex with high-affinity receptor analogs, Structure (1994) 2:719-731.

Weber T., Paesold G., Galli C., Mischler R., Semenza G., Brunner J., Evidence for H(+)-induced insertion of influenza hemagglutinin HA_2 N-terminal segment into viral membrane, J Biol Chem (1994) 269:18353-18358.

Webster R.G., Hinshaw V.S., Laver W.G., Selection and analysis of antigenic variants of the neuraminidase of N2 influenza viruses with monoclonal antibodies, Virology (1982) 117:93-104.

Webster R.G., Brown L.E., Laver W.G., Antigenic and biological characterization of influenza virus neuraminidase (N2) with monoclonal antibodies, Virology (1984) 135:30-42.

Webster R.G., Air G.M., Metzger D.W., Colman P.M., Varghese J.N., Baker A.T., Laver W.G., Antigenic structure and variation in an influenza virus N9 neuraminidase, J Virol (1987) 61:2910-2916.

Weis W., Brown J.H., Cusack S., Paulson J.C., Skehel J.J., Wiley D.C., Structure of the influenza virus haemagglutinin complexed with its receptor, sialic acid, Nature (1988) 333:426-431.

Wharton S.A., Skehel J.J., Wiley D.C., Studies of influenza haemagglutinin-mediated membrane fusion, Virology (1986) 149:27-35.

Wiley D.C., Wilson I.A., Skehel J.J., Structural identification of the antibody-binding sites of Hong Kong influenza haemagglutinin and their involvement in antigenic

variation, Nature (1981) 289:373-378.

Wilson I.A., Skehel J.J., Wiley D.C., Structure of the haemagglutinin membrane glycoprotein of influenza virus at 3 A resolution, Nature (1981) 289:366-373.

Wimley W.C., White S.H., Experimentally determined hydrophobicity scale for proteins at membrane interfaces, Nat Struct Biol (1996) 3:842-848.

Wright P.F., Webster R.G., Orthomyxoviruses, In: Knipe D.M., Howley P.M., Martin M.A., Griffin D.E.,Lamb R.A. (Eds.), Fields Virology, Boston, Lippincott Williams & Wilkins, 2001, pp. 1533-1579.

Wrigley N.G., Brown E.B., Daniels R.S., Douglas A.R., Skehel J.J., Wiley D.C., Electron microscopy of influenza haemagglutinin-monoclonal antibody complexes, Virology (1983) 131:308-314.

Yen H.L., Herlocher L.M., Hoffmann E., Matrosovich M.N., Monto A.S., Webster R.G., Govorkova E.A., Neuraminidase inhibitor-resistant influenza viruses may differ substantially in fitness and transmissibility, Antimicrob Agents Chemother (2005) 49:4075-4084.

Yen H.L., Hoffmann E., Taylor G., Scholtissek C., Monto A.S., Webster R.G., Govorkova E.A., Importance of neuraminidase active-site residues to the neuraminidase inhibitor resistance of influenza viruses, J Virol (2006) 80:8787-8795.

Yen H.L., Ilyushina N.A., Salomon R., Hoffmann E., Webster R.G., Govorkova E.A., Neuraminidase inhibitor-resistant recombinant A/Vietnam/1203/04 (H5N1) influenza viruses retain their replication efficiency and pathogenicity *in vitro* and *in vivo*, J Virol (2007) 81:12418-12426.

Yewdell J.W., Caton A.J., Gerhard W., Selection of influenza A virus adsorptive mutants by growth in the presence of a mixture of monoclonal antihemagglutinin antibodies, J Virol (1986) 57:623-628.

Zebedee S.L., Lamb R.A., Influenza A virus M2 protein: monoclonal antibody restriction of virus growth and detection of M2 in virions, J Virol (1988) 62:2762-2772.

Zebedee S.L., Lamb R.A., Growth restriction of influenza A virus by M2 protein antibody is genetically linked to the M1 protein, Proc Natl Acad Sci U S A (1989) 86:1061-1065.

Zhang J., Leser G.P., Pekosz A., Lamb R.A., The cytoplasmic tails of the influenza virus spike glycoproteins are required for normal genome packaging, Virology (2000)

269:325-334.

Zhang J., Pekosz A., Lamb R.A., Influenza virus assembly and lipid raft microdomains: a role for the cytoplasmic tails of the spike glycoproteins, J Virol (2000) 74:4634-4644.

Zhirnov O.P., Ksenofontov A.L., Kuzmina S.G., Klenk H.D., Interaction of influenza A virus M1 matrix protein with caspases, Biochemistry (2002) 67:534-539.

Zhong Q., Husslein T., Moore P.B., Newns D.M., Pattnaik P., Klein M.L., The M2 channel of influenza A virus: a molecular dynamics study, FEBS Lett (1998) 434:265-271.

Zhong Q., Newns D.M., Pattnaik P., Lear J.D., Klein M.L., Two possible conducting states of the influenza A virus M2 ion channel, FEBS Lett (2000) 473:195-198.

Zou P., Wu F., Lu L., Huang J.H., Chen Y.H., The cytoplasmic domain of influenza M2 protein interacts with caveolin-1, Arch Biochem Biophys (2009) 486:150-154.

Zurcher T., Yates P.J., Daly J., Sahasrabudhe A., Walters M., Dash L., Tisdale M., McKimm-Breschkin J.L., Mutations conferring zanamivir resistance in human influenza virus N2 neuraminidases compromise virus fitness and are not stably maintained *in vitro*, J Antimicrob Chemother (2006) 58:723-732.

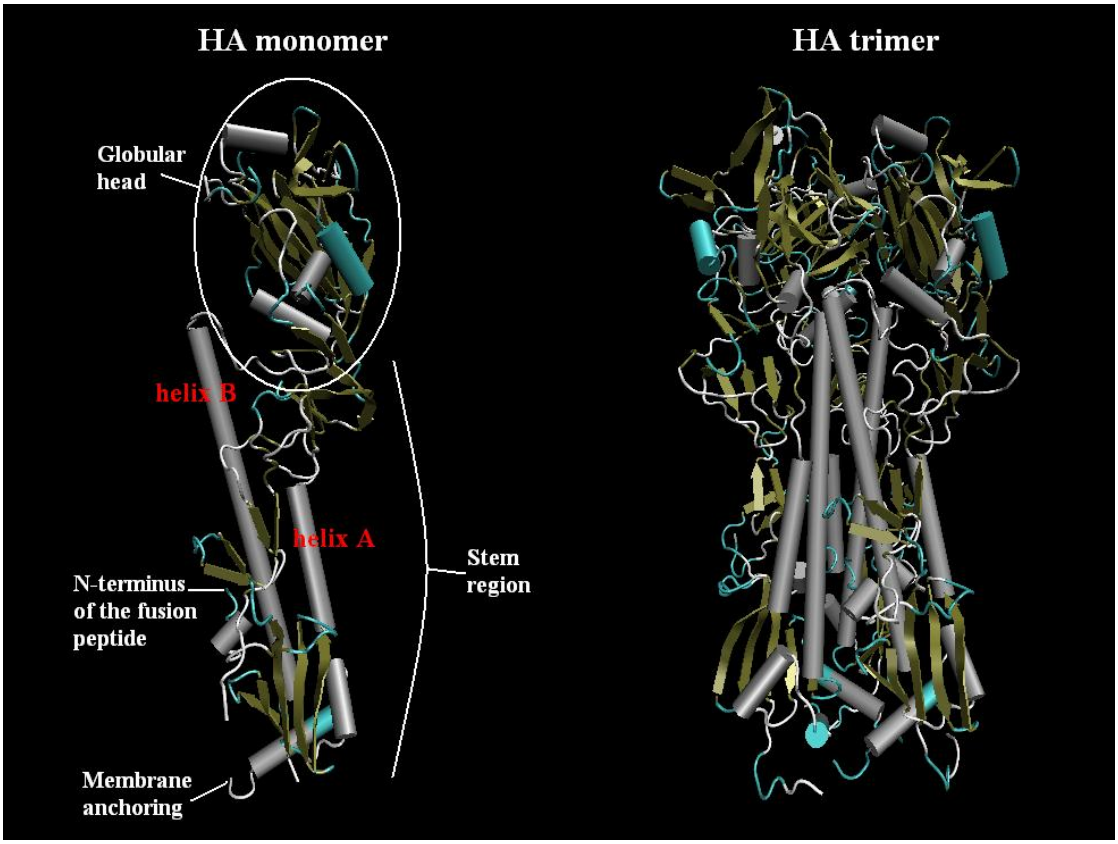

Figure 1: H3 monomer and trimer. The monomer structure (about 135Å in length) is divided into a distal globular head and a membrane-anchored stem region. The core of the globular head is essentially made of an 8-stranded *β*-sheet, while the stem region is axed on two long *α*-helices (A and B). The trimer is mainly stabilized by the twist of the helices of the stem region in a left-handed superhelix. 3D-structure from Fleury *et al.* (1998) – pdb code: 2VIU and Sauter *et al.* (1992) – pdb code: 1HGI. Figure performed with VMD (Humphrey *et al.*, 1996).

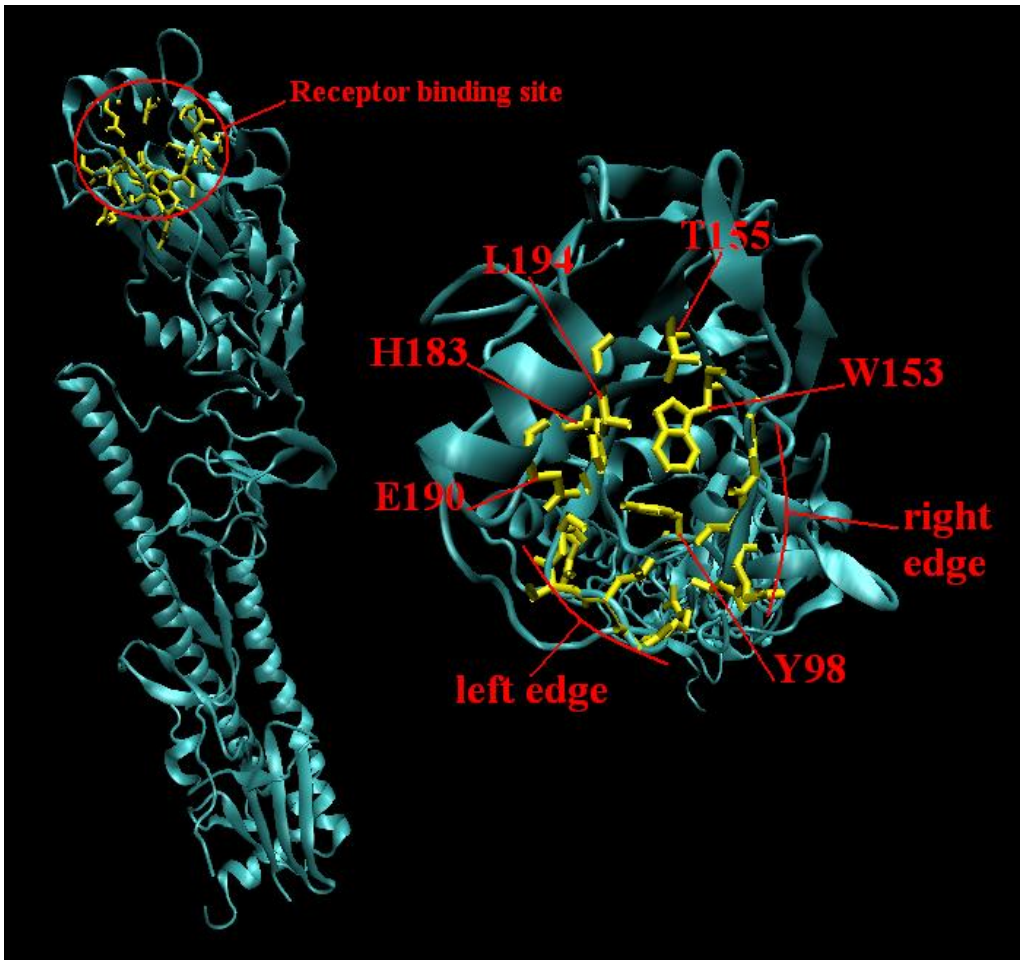

Figure 2: Receptor binding site of the influenza hemagglutinin. The RBS, at the top of the globular head of HA, is lined by a left and a right edge and is essentially made of residues Y98, S136 (right edge), W153, T155, H183, E190 and L194 (H3 numbering) (Ito *et al.*, 1999; Sauter *et al.*, 1989; Sauter *et al.*, 1992; Weis *et al.*, 1988). 3D-structure from Fleury *et al.* (1998) – pdb code: 2VIU. Figure performed with VMD (Humphrey *et al.*, 1996).

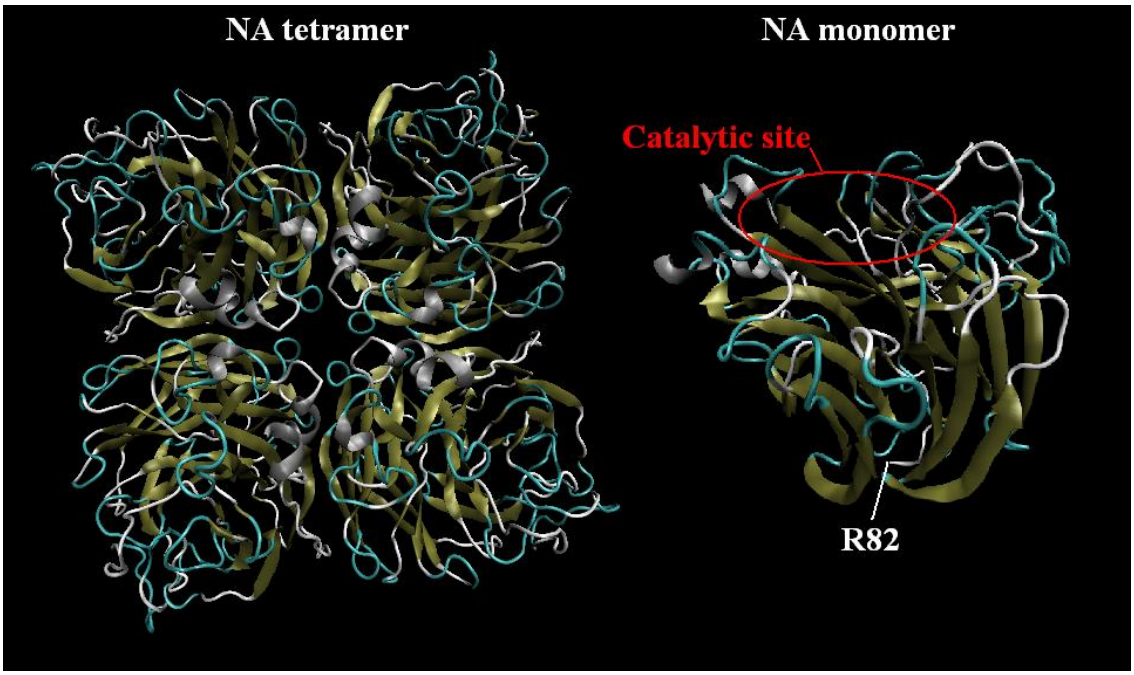

Figure 3: N6 subtype tetrameric and monomeric neuraminidase. Only the C-terminal part of NA, corresponding to the globular head, is represented here. The NA globular head contains six 4-stranded *β*-sheet structures organised in a "propeller"-like arrangement. The catalytic site is exposed on the top of the molecule, at the opposite side of the stem domain and membrane anchoring (linked to R82 in the full-length protein). 3D-structures from Rudino-Pinera *et al.* (2005) – pdb codes: 1V0Z and 1W21. Figure performed with VMD (Humphrey *et al.*, 1996).

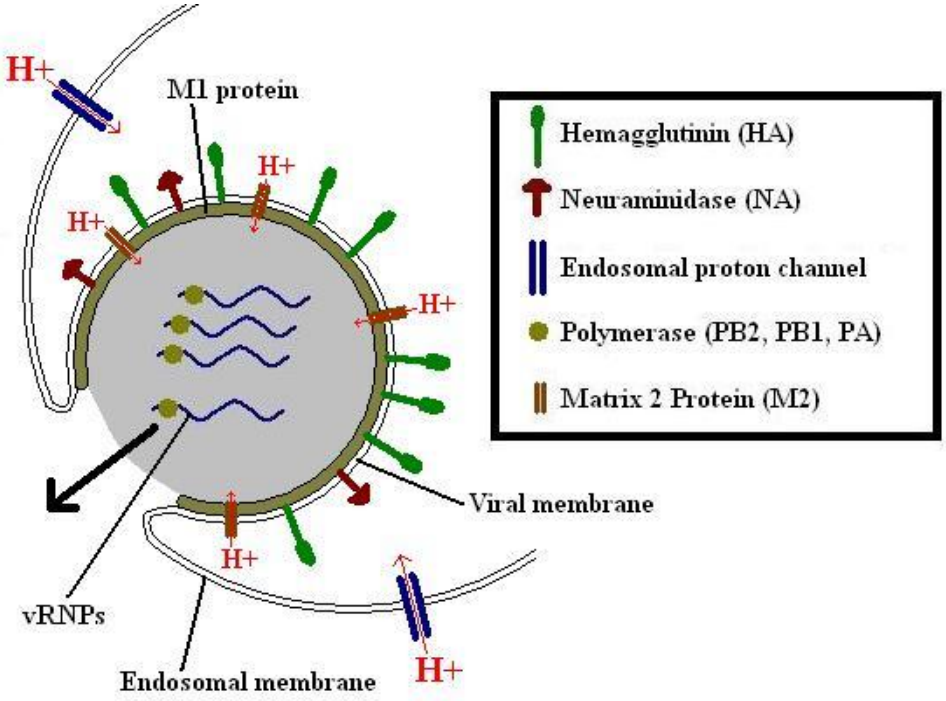

Figure 4: Role of the M2 proton channel in releasing vRNPs from the viral matrix during the first stages of the viral infectious cycle.

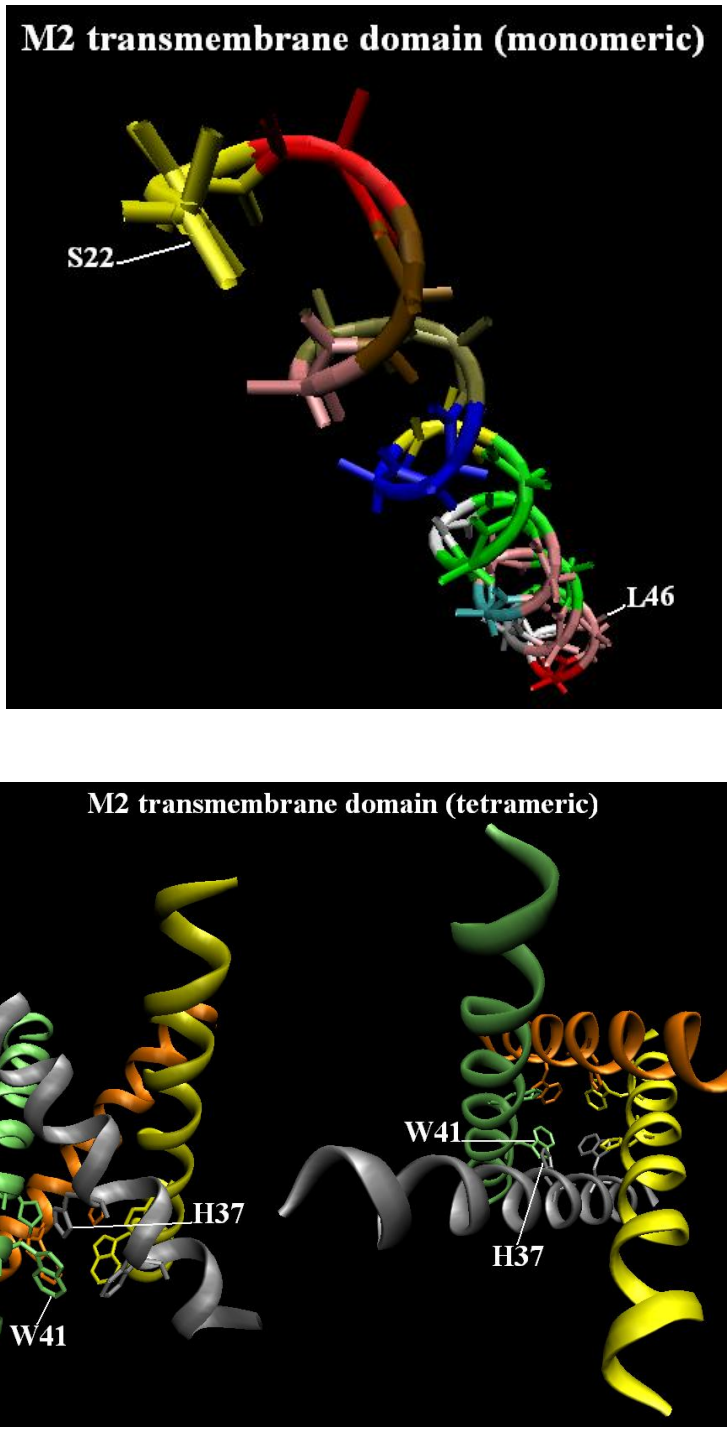

Figure 5: Structure of the M2 transmembrane domain. Positions of residues H37 and W41, which play an essential role in the ion channel activity, are emphasized. 3D-structures from Wang *et al.* (2001) – pdb code: 1MP6 and Nishimura *et al.* (2002) – pdb code: 1NYJ. Figure performed with VMD (Humphrey *et al.*, 1996).

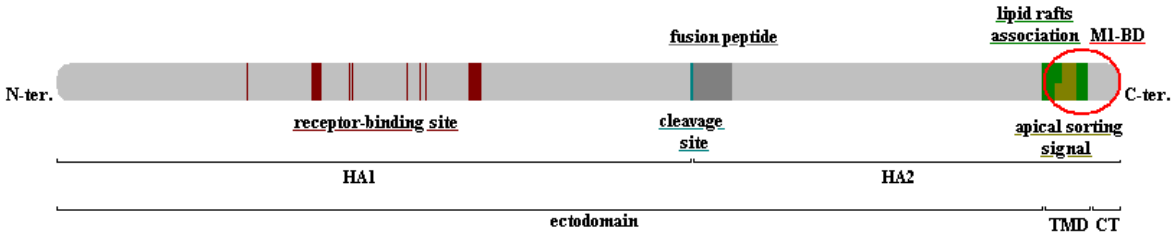

Figure 6: Functional domains of HA protein. The HA is about 550 amino acid-long. It is a transmembrane glycoprotein with an ectodomain (1-512), a transmembrane domain (513-539, the TMD is 24 to 28 residue-long), and a 10 to 55 residues cytoplasmic tail (Wilson *et al.*, 1981). The precursor protein HA_0 is cleaved by trypsin-like proteases into HA_1 (N-terminal fragment; about 330 residues) and HA_2 (C-terminal fragment; about 220 residues). It binds sialic acids (receptor-binding site: Y98, 131-GVTAA-135, S136, W153, T155, H183, Q190, L194 and 221-RGQAGR-226) (Kovacova *et al.*, 2002; Masuda *et al.*, 1999; Sauter *et al.*, 1989 & 1992; Skehel & Wiley, 2000; Weis *et al.*, 1988). The fusion peptide consists in the 20 first amino acids of HA_2. The apical sorting signal is in the middle of the transmembrane domain, while residues important for lipid raft association are present in the outer half (residues 511, 512, 517, 518, 520 and 521) and at the C-terminal extremity (residues 530-538) of this TMD (Lin *et al.*, 1998; Nayak *et al.*, 2004; Takeda *et al.*, 2003). The TMD and the cytoplasmic tail constitute the M1-binding domain of the influenza HA (Ali *et al.*, 2000).

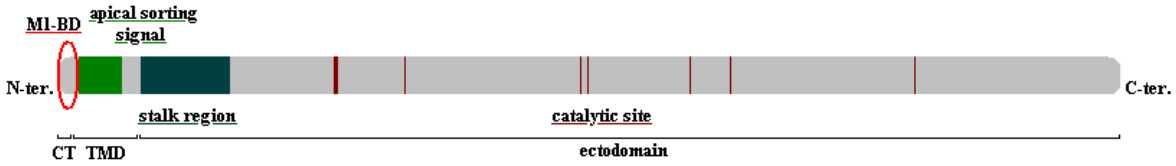

Figure 7: Functional domains of NA protein. NA is a type II integral transmembrane glycoprotein, with a 6 amino acids N-terminal cytoplasmic tail (CT), a 29 residues transmembrane domain (TMD, residues 7-35) and a long C-terminal ectodomain (Lamb & Krug, 2001). The ectodomain essentially contains the sialidase catalytic site (residues 118, 119, 151, 224, 227, 276, 292 and 371) (Colman, 1994). The stalk region is made of residues 36-73, while the other residues (74-450) form the globular head (Varghese *et al.*, 1983). The TMD contains an apical sorting signal (9-27) (Barman *et al.*, 2000). The cytoplasmic tail of NA binds the M1 protein (Barman *et al.*, 2001; Jin *et al.*, 1997).

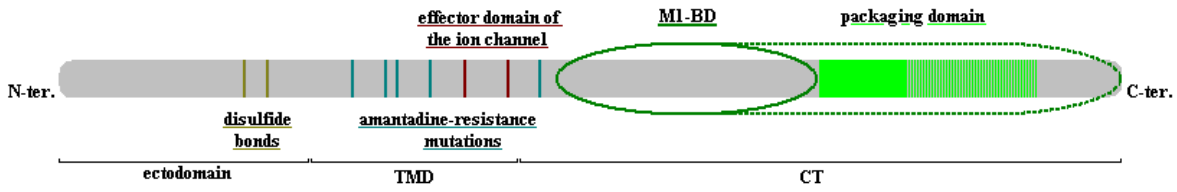

Figure 8: Functional domains of M2 protein. M2 is a transmembrane protein of 97 residues, with a 54 residues cytoplasmic tail and a 19 residues transmembrane domain (Lamb *et al.*, 1985). It binds M1 by its cytoplasmic tail (M1-BD: 45-69, with a less important role of residues 70-97) (McCown & Pekosz, 2006; Roberts *et al.*, 1998). The 70-89 motif, and most particularly residues 70-77, is thought to be implicated in the packaging process (packaging domain) (McCown & Pekosz, 2005 & 2006). The M2 protein forms tetramers, which are linked by disulfide bonds involving C17 and C19. H37 and W41 play an essential role in the activation and the proton specificity of the M2 ion channel activity (effector domain) (Tang *et al.*, 2002). Mutations linked to the acquisition of a resistance to the antiviral drug amantadine concern residues essentially located in the ion channel part of the protein (V27, A30, S31, G34 and D44) (Betakova *et al.*, 2005; Holsinger *et al.*, 1994).

2.3. Nucleoprotein

Influenza A virus nucleoprotein (NP) is a 498 amino acid-long protein showing an overall high degree of conservation between strains. It is the second most abundant protein of the virion (1000 units per virion) (Lamb & Krug, 2001). It contains many basic amino acids, is arginine-, serine- and glycine-rich and presents a net positive charge at neutral pH (pI 9.3), while the C-terminal 30 residues form a very acidic domain (pI 3.7) (Portela & Digard, 2002). The antigenicity of NP is used to differentiate influenza A, B and C (Lamb & Krug, 2001). A 27 Å resolution electron microscopic model of recombinant NP suggests that it adopts a banana-like curved shape, possibly with 2 different domains (Martin-Benito *et al.*, 2001). The description of the crystal structure of NP at a 3.2 Å resolution shed new lights on the manner by which it binds RNA and on the possible roles of the different functional domains of the protein (Ye *et al.*, 2006). NP forms oligomeric structures, binds polymerase basic proteins 1 and 2 (PB1 and PB2), matrix protein 1 (M1) and actin, displays two nuclear localization signals (NLS), and constitutes an essential component of viral ribonucleoproteins (vRNPs). RNA-free NP oligomers self-assemble in helices twisted back in a double helical hairpin, creating supercoiled structures with a terminal loop (Baudin *et al.*, 2001; Compans *et al.*, 1972; Heggeness *et al.*, 1982; Pons *et al.*, 1969; Ruigrok & Baudin, 1995). Working with recombinant vRNPs made of a vRNA-like genome of 248 nucleotides RNA, Martin-Benito *et al.* (2001) identified rings made of 8 to 9 monomers of NP. In these structures, vRNA is exposed outwards of the NP ring and the viral polymerases fix on the NP circle. In recombinant vRNPs made of a vRNA-like genome of 313 nucleotides, NP also self-assembles in circular or elliptic multimers (10-12 monomers), whereas recombinant RNPs with longer RNA molecules (over 400 nucleotides) are only helical (Ortega *et al.*, 2000). Those data suggest a model in which the core of vRNPs would be constituted by a helical multimeric structure of NP proteins, surrounded by the vRNA strand (Martin-Benito *et al.*, 2001; Ortega *et al.*, 2000). This model is consistent with the observation that, unlike *Paramyxoviridae*, the genome of influenza viruses is not resistant to RNAses, thus suggesting that the viral RNA is exposed outwards of the NP helix (Baudin *et al.*, 1994; Duesberg, 1969; Martin-Benito *et al.*, 2001; Ortega *et al.*, 2000; Ye *et al.*, 2006). The viral polymerase complex is located at one extremity of the vRNP and would be needed to maintain the RNA ends linked together (Klumpp *et al.*, 1997; Murti *et al.*, 1988).

2.3.1. Structure

The crystal structure of NP was recently resolved using multiple isomorphous replacement and anomalous scattering technology (MIRAS) (Ye *et al.*, 2006) (Figure 1). The monomer is essentially made of α-helices, adopts a curved shape and displays two main domains (head and body) formed by non-contiguous parts of the polypeptidic chain. Residues 150-272 and 438-452 contribute to the head domain and the body is formed by residues 21-149, 273-396 and 453-489 (Ye *et al.*, 2006). In addition, residues 402-428 form a tail loop containing three β-strands, the last two forming a β-hairpin (Ye *et al.*, 2006). The tail loop is attached to the head by a disordered, highly flexible linker region and intimately interacts with the body domain of a neighboring NP monomer (Figure 1). This interaction is mediated by intermolecular β-sheets, hydrophobic interactions and salt bridges. NP is able to oligomerize spontaneously, essentially as trimeric oligomers, either in the absence or in the presence of RNA. The monomer structure also presents a deep groove between head and body domains. In the oligomer, the groove is exposed outwards and is thought to form the RNA-binding domain (Ye *et al.*, 2006) (Figure 2).

2.3.2. Self-association domains

Viral RNPs conserve their physical structure after removal of RNA, which suggests that RNP backbone-forming NP oligomerization precedes RNA binding (Pons *et al.*, 1969; Kingsbury *et al.*, 1969). Moreover, *in vitro*, purified NP proteins multimerize into structures ranging from trimers to large complexes that are indistinguishable from normal vRNP structures by electron microscopy (Ruigrok & Baudin, 1995; Prokudina-Kantorovich & Semenova, 1996). Those data strongly suggest the existence of NP-NP binding sites. Deletion studies and *in vitro* binding assays pointed to two independent regions, one extending from residues 189 to 358 and the second from amino acids 371 to 498 (Elton *et al.*, 1999). With respect to the latter segment, opposite results were obtained when subsegments were studied. Removal of the 23 C-terminal residues enhanced NP self-association on the one hand (Elton *et al.*, 1999) and mutations that disorganize or delete the 402-428 tail loop were shown to abolish oligomerization on the other (Ye et al, 2006). Point mutations show that a R199A substitution decreased NP self-association threefold and a R416A substitution over tenfold, while a F479A (F479

being one of the 23 C-terminal residues of NP) substitution increased the binding affinity about fivefold (Elton *et al.*, 1999). Thus, it seems that the role of the 371-498 segment results from a balance between promotion of oligomerization by the *β*-strands-containing tail loop (Ye *et al.*, 2006) and inhibition by the C-terminal segment. As aforementioned, the 30 C-terminal residues of NP have a pI of 3.7 for the A/PR8/34 strain (Portela & Digard, 2002), while the full-length NP pI is 9.3. This C-terminal domain was shown to be necessary for normal virus gene expression since its removal or truncation abolished it (Elton *et al.*, 1999). The important role of this domain agrees with the fact that mutation of F479 or F488 inhibits cRNA synthesis (Elton *et al.*, 1999; Mena *et al.*, 1999). But in the case of the mutation of F488, no modification of the NP-NP affinity was present, suggesting that this C-terminal domain probably affects the transcription mechanism by another way. Sequence alignments show a very high conservation degree for F479 and F488, which agrees with the observed effect of mutation of these two residues. The only known exceptions are a F479L substitution in the NP protein of Rostock Fowl Plague Virus and a F488I substitution in the NP of some other strains (personal investigations). The global conservation of the 402-428 tail loop is very high (even if not higher than the rest of the NP protein), but some residues are variable, such as E421, R422 and A423.

The existence of distinct self-association sites in each NP molecule is consistent with the need to interact with more than one other monomer to construct the helical structures displayed by vRNPs (Ruigrok & Baudin, 1995).

Recent studies showed that four NP mutants (E339A, V408S P410S, R416A, and L418S P419S mutants) presented a complete abatement of RNP activities with NP unable to oligomerize. RNP activity of four other mutants (R267A, I406S, R422A, and E449A) was more than 50% decreased, NP being present as a mixture of unstable oligomers (Chan *et al.*, 2010). This confirms the role played by the NP tail loop in oligomerization and stabilization of oligomers.

2.3.3. RNA-binding domain

NP binds single-stranded RNAs with a high affinity and without sequence specificity (Baudin *et al.*, 1994; Scholtissek & Becht, 1971; Kingsbury *et al.*, 1987; Yamanaka *et al.*, 1990; Digard *et al.*, 1999). The NP-RNA interaction is cooperative, with a stoechiometry of about 1 NP molecule per 24 nucleotides (Compans, 1972; Ortega *et*

al., 2000; Yamanaka *et al.*, 1990). Deletion mapping of the putative RNA-binding domain first pointed to the N-terminal one-third of NP (residues 1-181), of which each half alone (1-77 or 79-180) also retained RNA-binding activity (Kobayashi *et al.*, 1994; Albo *et al.*, 1995). However, chemical fragmentation and amino acid sequencing of NP that had been UV cross-linked to radiolabelled RNA later showed that protein-RNA contacts occur throughout the length of the polypeptide. Single-codon mutagenesis identified five tryptophan, one phenylalanine, and two arginine residues as essential for high-affinity RNA binding. These mutationally sensitive residues are not localised to any particular region of NP but instead are distributed throughout the protein (Elton *et al.*, 1999), which suggests that high-affinity binding of RNA by NP requires the concerted interaction of multiple regions of the protein with RNA. The 3D-structure of NP recently made available revealed the existence of a deep groove made of many basic residues (R65, R150, R152, R156, R174, R175, R195, R199, R213, R214, R221, R236, R355, K357, R361 and R391) and exposed on the NP oligomer surface (Ye *et al.*, 2006) (Figures 2 and 3). This positively charged groove is therefore thought to be engaged in an electrostatic partnership with the polyanionic phosphate backbone of RNA. The distance between two adjacent grooves in oligomeric NP is about 70 Å, which is consistent with the aforementioned stoechiometry of one NP per 24 nucleotides (Ortega *et al.*, 2000; Ye *et al.*, 2006).

2.3.4. Polymerase basic proteins 1 and 2-binding sites

The existence of NP-PB2 interactions was first suggested after the detection of a correction mutation in the PB2 gene in a revertant of a thermo-sensitive virus with a lesion in the NP gene (Mandler *et al.*, 1991). Interactions of NP with both PB2 and PB1, but not with PA (polymerase acidic), polymerase subunits was later demonstrated by co-immunoprecipitation (Biswas *et al.*, 1998; Medcalf *et al.*, 1999). Structural informations on the vRNP structure confirmed the existence of close contacts between NP and the polymerase complex (Martin-Benito *et al.*, 2001).

Three different NP fragments (1-161, 255-341 and 340-498) were shown to bind PB2 while the fourth (160-256) did not, suggesting that NP contains at least three different PB2-binding sites that are not located in the 160-256 sequence; they were called PB2-binding site 1 (1-161), -2 (255-341) and -3 (340-498) (Portela & Digard, 2002). The existence of different PB2-binding sites is also consistent with studies by Poole *et al.*

(2004) which found two different NP-binding domains on PB2, thus confirming that these proteins interact with each other at different sites. Interestingly, deletion of the 33 C-terminal residues of NP increases its affinity for PB2, suggesting a masking of the PB2-binding site(s) by those 33 first C-terminal residues (Biswas *et al.*, 1998). Further studies are needed to delimit these sites more precisely.

2.3.5. Matrix protein 1-binding site

Co-expression of NP and M1 proteins was first shown to result in homo- rather than hetero-oligomeric structures (Zhao *et al.*, 1998). However, co-sedimentation studies later revealed a binding between NP and the M1 C-terminal domain (165-252) (Baudin *et al.*, 2001). It is hypothesized that the interaction might be limited to precise step(s) of the virus biological cycle and might depend on the NP phosphorylation status and/or on the NP cleavage by cellular caspases at the end of the replication cycle (Baudin *et al.*, 2001) (see further). Precise delineation of the M1-binding motif is still lacking so far.
The heat shock protein 70 (Hsp70) was shown to bind NP at 41°C and to block nuclear export of native vRNPs by preventing the M1-NP interaction (Hirayama *et al.*, 2004).

2.3.6. Actin-binding site

In influenza virus-infected cells, NP is resistant to detergent extraction, suggesting that it interacts with cytoskeletal elements (Avalos *et al.*, 1997). Furthermore, NP binds to filamentous actin *in vitro* with an affinity comparable to that of many cellular F-actin-binding proteins and, when expressed alone in cells, i.e. without any other influenza proteins, is associated with F-actin stress fibres with a stoechiometry of 1 NP per actin molecule (Digard *et al.*, 1999). Mutational studies revealed the crucial implication of residues F338, E339, D340, R342 and Q405 in the interaction with actin, of which four (338-342) lie within one of the most highly conserved blocks of amino acids between influenza A, B, C, and Dhori virus NPs (Fuller *et al.*, 1987), suggesting that it is functionally relevant. The fact that mutations of these residues simultaneously weaken F-actin binding and restore nuclear import, even in the absence of a functional N-terminal NLS (Digard *et al.*, 1999) implies a causative link between F-actin binding and cytoplasmic retention of NP. As NP protein accumulates in the cell nucleus at early times of infection and essentially in the cytoplasm at later times, Digard and colleagues

(1999) proposed that the interaction between NP and actin regulates the localization of RNPs by causing their cytoplasmic retention late in infection. Recent structural data however show that the putative actin-binding site is buried into the NP structure, which theoretically should hamper binding to F-actin (Ye *et al.*, 2006). Also, personal sequences alignments revealed some mutations of the residues critical for binding to F-actin exist in nature, even if rare (D340 is sometimes replaced by N or G, E339 by G and A/chicken/Hong Kong/NT366/03 [H9N2] contains the F338V and R342K mutations).

2.3.7. RAF-2p48-binding site

A 48 kDa polypeptide, RAF-2p48 (RNA polymerase Activating Factor-2p48), a cellular splicing factor belonging to the DEAD-box family of RNA-dependent ATPases previously designated BAT1 or UAP56, was identified as a NP-interacting protein in a yeast two-hybrid screen of a mammalian cDNA library (Palese *et al.*, 1997). *In vitro*, RAF-2p48 interacts with free NP but not with NP bound to RNA, increases vRNA synthesis and stimulates the NP-RNA association, probably acting as a chaperone for NP and being released upon interaction of NP with RNA. The NP 20 first N-terminal residues were proved to support binding to RAF-2p48 by deletions analyses and yeast two-hybrid assays (Momose *et al.*, 2001). RAF-2p48 was further shown to facilitate the encapsidation of nascent cRNA by NP as a molecular chaperone (Kawaguchi *et al.*, 2011).
Another "RAF" protein was identified as a chaperone protein for the influenza PB2 protein, the heat shock protein 90 (Hsp90) (Momose *et al.*, 2002).

2.3.8. Nuclear Localization Signals

Influenza vRNPs must enter the nucleus of their host cells to establish a productive infection (Lamb & Krug, 2001). The nuclear import of vRNPs occurs after the infecting influenza virion containing the incoming vRNPs is internalized into an endosome. The vRNPs are then released into the cytoplasm by fusion of the viral and endosomal membranes, which is triggered by the acidic environment of the endosome. Once in the cytoplasm, the vRNPs must use an exposed nuclear localization signal (NLS) to be taken up by the nuclear import machinery.

Nuclear import of NP-RNA complexes was shown to rely on the interaction of NP with two NP-interacting cellular proteins (O'Neill *et al.*, 1995; O'Neill & Palese, 1995). These proteins belong to the karyopherin α/importin 60 family of general transport factors involved in nuclear transport of NLS-containing proteins (Gorlich *et al.*, 1994; Moroianu *et al.*, 1995; Wang *et al.*, 1995; Weis *et al.*, 1995).

Two NP motifs function as NLSs when fused to cytoplasmic proteins (Wang *et al.*, 1997; Weber *et al.*, 1998). As deletion of both still results in nuclear accumulation of NP, the existence of a third NLS is suspected whose precise location is yet to be mapped (Bullido *et al.*, 2000). The first NLS, also termed the nonclassical NLS, is located at the N terminus of NP (residues 1-13, NLS1) and binds to importins α1 and α5 (Neumann *et al.*, 1997; Wang *et al.*, 1997). This N-terminal 1-13 sequence is highly conserved among influenza A strains but does not resemble classical NLS sequences found in other viral or cellular proteins (Wang *et al.*, 1997). The second NLS is located in the middle of the protein (residues 198-216, NLS2) (Weber *et al.*, 1998). NLS2 is less well characterized and was originally proposed to be a classical bipartite NLS. The recently-solved crystal structure of NP suggests that the unconventional 1-13 NLS1 is exposed at the outer periphery on the NP oligomers and is thus highly accessible to solvent and thus to cellular importins (Ye *et al.*, 2006). By opposition, both clusters of basic amino acids of the bipartite NLS2 (198-RK-199 and 213-RKTR-216) are separated from about 15 Å, which, theoretically speaking, should be a distance too short to allow efficient binding (minimal distance required in a classic bipartite NLS is 28 Å) (Fontes *et al.*, 2000; Ye *et al.*, 2006). Taking these structural data into account and because mutations of the second cluster of basic amino acids (positions 213, 214 and 216) of NLS2 are critical to the nuclear import of recombinant NP (Weber *et al.*, 1998), it is possible that the 213-RKTR-216 motif acts as a monopartite NLS.

The elucidation of the respective contribution of NLS1 and NLS2 to the nuclear import of influenza vRNPs has recently been addressed. Studying nuclear import of *in vitro* assembled NP–vRNA complexes in the absence or presence of competitive peptides carrying NLS1, Cros *et al.* (2005) found that the NLS1 peptide efficiently inhibited the nuclear import of these complexes. However, using vRNPs isolated from influenza A virions, Wu and colleagues (2007) found that both NLS1 and NLS2 contribute to the nuclear import of vRNPs. NLS1 and NLS2 act independently of each other, as inhibition of only one of the two NLSs still resulted in significant, though diminished, nuclear import of vRNPs. Similarly, Ozawa *et al.* (2007) found that mutation of either

NLS1 or NLS2 eliminated some nuclear import of influenza vRNPs but did not abolish it completely. In all these studies, however, the nuclear localization signal from NLS1 appeared to be a more potent mediator of nuclear import than that from NLS2. A comparative analysis of the levels of surface exposure of both NLSs on vRNPs by immunogold labelling recently produced an elegant confirmation of these functional studies: 71% of vRNPs were labelled with one to six gold particles located throughout the vRNP for NLS1, whereas less than 10% of vRNPs were labelled with an antibody against NLS2 (Wu *et al.*, 2007). These findings provide a structural basis for the enhanced ability of NLS1 in mediating nuclear import of influenza vRNPs.

The interaction of NP with cellular importin α5 was demonstrated and was shown to not interfere with RNA binding by NP (Boulo *et al.*, 2011), but this interaction impede oligomerizaion of NP, suggesting that neosynthesized NP enters the nucleus as a monomer. It was further shown that for efficient replication NP (together with PB2) of avian viruses interacts preferentially with importin α3, while that of mammalian viruses showed importin α7 specificity, suggesting a role of this relative affinity in host adaptation (Gabriel *et al.*, 2011).

NP is phosphorylated during the infection process by cellular kinases (Kistner *et al.*, 1989; Privalsky & Penhoet, 1977). Phosphorylation is a known mechanism of nuclear transport modulation and the use of inhibitors and activators of protein kinases was shown to influence NP localization in the cell (Neumann *et al.*, 1997; Whittaker & Helenius, 1998). As Arrese and Portela (1996) showed that the major phosphorylation site of NP was S3, S3A and S3D mutant NPs were produced to examine the role of phosphorylation. No significant difference was noted between wild-type and mutated NPs at the level of subcellular localization and RNA binding (Bullido *et al.*, 2000). Incidentally, we found that S3 is replaced by T, L or P in some naturally occurring influenza A strains which confirms that S3 phosphorylation status does probably not play a crucial role in the virus biology (personal results).

2.3.9. Cellular caspase cleavage site

NP is cleaved late in the cell infectious process by a cellular caspase (56 to 53 kDa) (Zhirnov & Bukrinskaya, 1984). The cleavage occurs at a classical caspase recognition site "E/DXD16*X" (X being any amino acid), which removes the first 16 amino-terminal residues (Zhirnov *et al.*, 1999). Only human-adapted strains were claimed to

retain an aspartate residue at position 16 and thus the caspase cleavability phenotype; D16 was subsequently considered a marker of human adaptation (Zhirnov *et al.*, 1999). However, personal sequences alignments revealed that D16 can also be found in some swine, equine, mouse or canine strains, which opposes such a human marker-of-adaptation status. But it seems that D16 is conserved in human strains and G(or S)16 is conserved in avian strains, so residue at this position could be used to distinguish human *vs.* avian influenza strains. Whether D16-associated NP cleavage phenotype plays a specific role in the influenza infectious cycle or is a simple consequence of the onset of apoptosis (and thus of caspases activation) is not completely elucidated. But recent studies show that the presence or absence of a cleavage site at position 16 of NP is essential for the virus fitness, since insertion of a cleavage-susceptible site in an avian strain or of a cleavage-resistant site in a human influenza strain reduced virulence for mice in both cases (Lipatov *et al.*, 2008). Compatibility between NP and the other proteins of the virus is thus needed for full virulence in a specific host (Lipatov *et al.*, 2008).

2.3.10. Nucleosome- or histone-binding site

Influenza vRNPs and purified NP were shown to bind cellular nucleosomes (Bui *et al.*, 2000). Studies by Takizawa and colleagues (2006) showed that the majority of vRNPs are associated with densely packed chromatin while new vRNP copies are rather released in the nucleoplasm. The role of the fixation of viral RNPs on the cellular chromatin is unknown. Theoretically, it could prevent the accessibility to cellular genes by disturbing the chromatin structure and thus indirectly favour the expression of viral genes, but this hypothesis has still to be confirmed (Garcia-Robles *et al.*, 2005). Since nucleosomes bind NP protein and whole vRNPs to the same extent, it is most likely that vRNPs interact with cellular histones through the nucleoprotein (Garcia-Robles *et al.*, 2005). The interaction with cellular chromatin was shown to be dependent of the binding of NP to nucleosomic rather than to linker histones (H1) or to DNA (Garcia-Robles *et al.*, 2005). Trypsin-treated histones (which lost their tail) are unable to fix influenza RNPs, suggesting that NP binds their tail (Garcia-Robles *et al.*, 2005). The influenza M1 protein was also shown to bind cellular histones, but at a different site from that used by NP, since trypsin-treated histones still bound M1 proteins (Garcia-Robles *et al.*, 2005).

2.3.11. cRNA rescue by nucleoprotein

The control of transcription and replication of viral RNA *in vivo* has been the subject of intense research since more than two decades. The viral life cycle comprises an early transcriptive phase followed later by a predominantly replicative phase. As the treatment of infected cells with cycloheximide, an inhibitor of protein synthesis, prevents the switch from the transcriptive to the replicative stage, it was first suggested that replication requires *de novo* protein synthesis (Barrett *et al.*, 1979; Hay et al;, 1977; Taylor *et al.*, 1977). As several temperature-sensitive NP mutants are defective in replication and RNA binding (Biswas *et al.*, 1998; Krug *et al.*, 1975; Mahy *et al.*, 1981; Markushin & Ghendon, 1984; Scholtissek , 1978; Thierry & Danos, 1982) and because biochemical studies suggested that NP is required for the synthesis of cRNA by preventing premature termination (Beaton & Krug, 1986; Krug *et al.*, 1989; Shapiro & Krug, 1988), neosynthesized NP was seen as a prime candidate for exercising the transcription-to-replication switch. A model, referred to as the *template modification model*, was put forward according to which soluble NP binds template RNA, modifying its structure and thereby altering transcription *vs.* replication initiation and termination (Fodor *et al.*, 1994; Hsu *et al.*, 1987; Klumpp *et al.*, 1997; Portela & Digard, 2002). However, using a cell-free system, purified virion-derived vRNPs were recently shown to transcribe both mRNA and cRNA in the absence of any non-virion-associated proteins (Vreede & Brownlee, 2007). Moreover, the addition of non-virion-associated polymerase or NP in the system had no effect on the transcription and replication activities of purified virion-derived vRNPs. Therefore, there is probably no switch between the synthesis of mRNA and cRNA *per se*, which theoretically implies that the absence of cRNA early in the viral infectious cycle demonstrated before could be attributable to a dramatically short half-life rather than to lack of synthesis. Consistent with this hypothesis, cRNA can be detected early in 293T cells infected with influenza A virus in the presence of cycloheximide if viral heterotrimeric polymerase and NP are preexpressed (Vreede *et al.*, 2004). This suggests that free (neosynthesized) viral polymerase and NP bind nascent cRNA and form a cRNP complex, thereby protecting it from degradation by host cell nucleases (RNAs lacking a 5' cap and a 3' poly(A) tail are rapidly degraded in the cell nucleus). This current model is referred to as the *stabilization* model (Vreede *et al.*, 2004).

2.3.12. Conclusion

The NP protein is a main structural component of viral ribonucleoproteins. Those are made of a helical core of nucleoproteins, surrounded by the viral RNA (Lamb & Krug, 2001). The RNA is bond in a deep groove between the head and body domains of each NP monomer (Ye *et al.*, 2006) (Figure 2). In the vRNP structure, NP also binds the PB2 and PB1 subunits of the viral polymerase (Biswas *et al.*, 1998; Portela & Digard, 2002) (Figure 3). NP possesses two nuclear localization signals, responsible for the nuclear import of entering vRNPs. It binds M1 protein, the binding of which is thought to play a role in the nuclear export of native vRNPs at the end of the viral replication cycle (Baudin *et al.*, 2001), cellular actin (Digard *et al.*, 1999), and nucleosomes (Garcia-Robles *et al.*, 2005). NP interacts with the splicing factor RAF-2p48, which is thought to stimulate the NP-RNA interaction (Momose *et al.*, 2001). NP of some influenza strains is cleaved at the end of the replication cycle by cellular caspases, the potential role of this cleavage being still unknown (Zhirnov *et al.*, 1999). Finally, in addition to its structural roles, NP was shown to enhance the replication of the influenza genome, probably by stabilizing the native cRNAs and protecting them from degradation (Vreede & Brownlee, 2007).

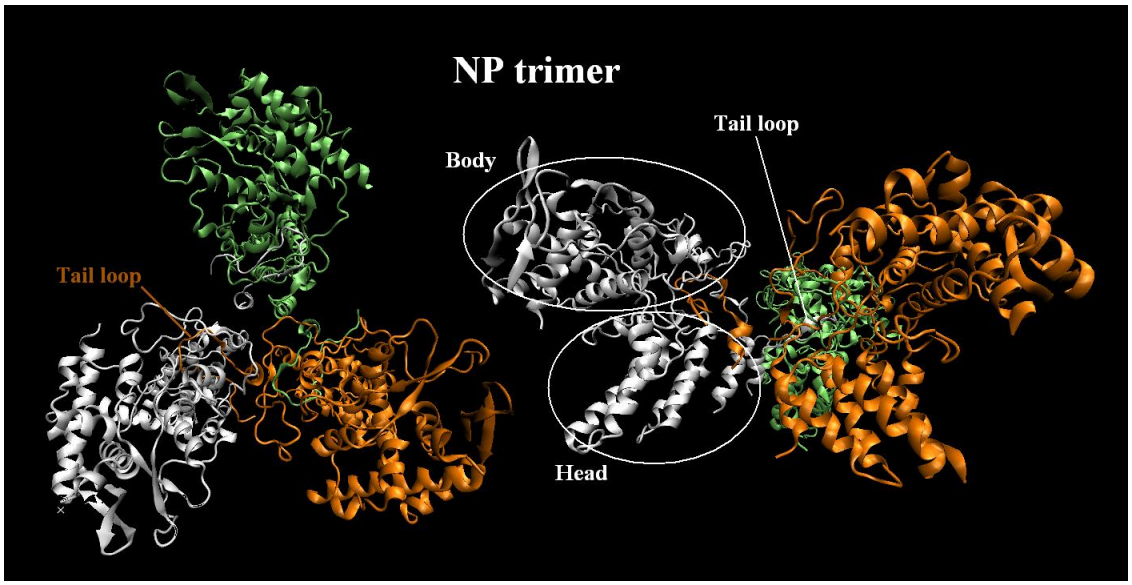

Figure 1: Structure of a trimer of nucleoproteins. Each NP monomer presents a head and a body domain. The tail loop of one monomer is inserted into the adjacent monomer. Adapted from Ye *et al.* (2006) – pdb code: 2IQH. Figure performed with VMD (Humphrey *et al.*, 1996).

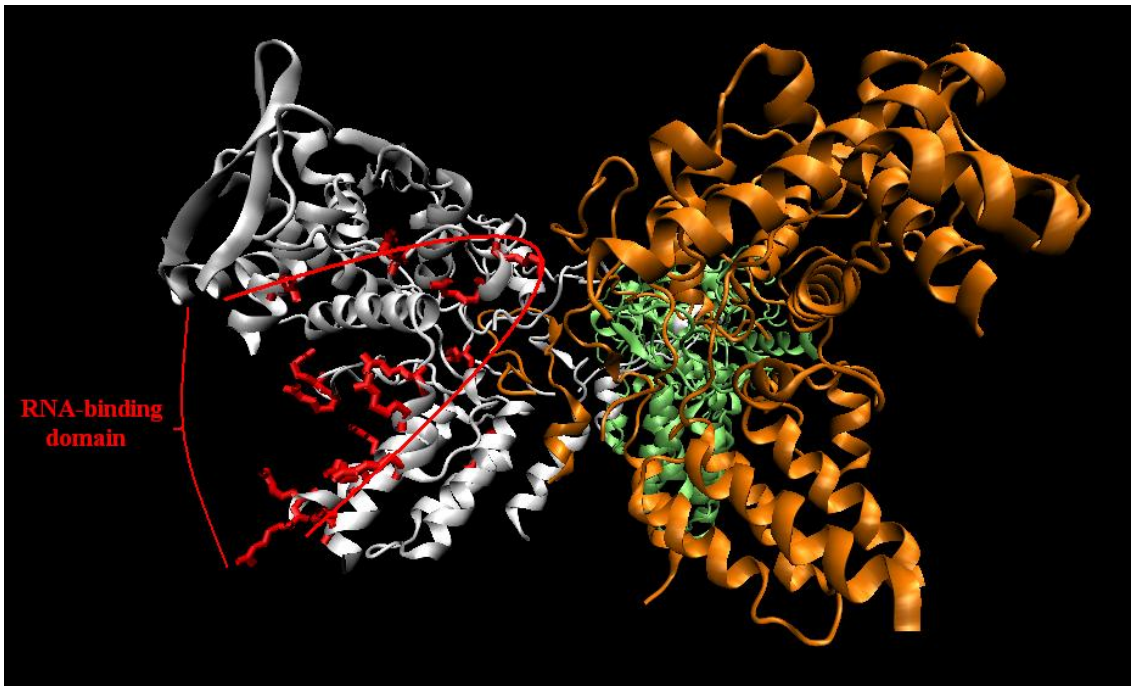

Figure 2: The RNA-binding domain of the influenza A NP protein. Residues involved in RNA-binding (R65, R150, R152, R156, R174, R175, R195, R199, R213, R214, R221, R236, R355, K357, R361, and R391) are all located in the deep groove between the head and the body of each NP monomer (Ye *et al.*, 2006). 3D-structure from Ye *et al.* (2006) – pdb code: 2IQH. Figure performed with VMD (Humphrey *et al.*, 1996).

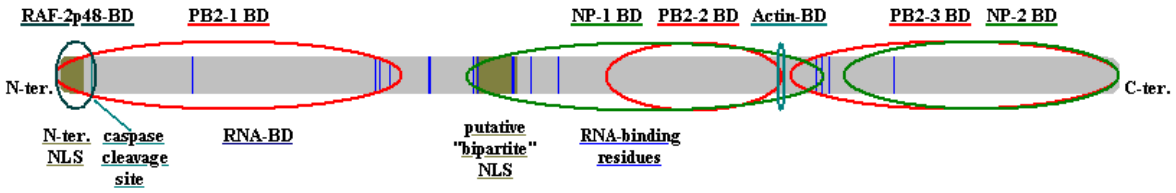

Figure 3: Functional domains of nucleoprotein (NP). NP contains 498 residues (Lamb & Krug, 2001). It binds PB2 (PB2-1 BD: 1-161, PB2-2 BD: 255-341, and PB2-3 BD: 344-498), PB1 (undefined domain), M1 (undefined domain), histones (undefined domain) and cellular F-actin (Actin-BD: residues 338, 339, 340, 342 (and 405)) (Baudin *et al.*, 2001; Biswas *et al.*, 1998; Digard *et al.*, 1999; Garcia-Robles *et al.*, 2005). It forms oligomers and possesses two NP-binding sites (NP-1 BD: 189-358, and NP-2 BD: 371-498), the most important residues being those forming the tail loop (402-428) (Elton *et al.*, 1999; Ye *et al.*, 2006). Two RNA-binding domains were initially described (RNA-BD 1: 1-77 and RNA-BD 2: 79-180), but further studies showed that residues involved in RNA-binding are spread throughout the whole protein and assembled in a deep groove (residues R65, R150, R152, R156, R174, R175, R195, R199, R213, R214, R221, R236, R355, K357, R361 and R391) (Albo *et al.*, 1995; Kobayashi *et al.*, 1994; Ye *et al.*, 2006). NP also binds the cellular splicing factor RAF-2p48 (RAF-2p48-BD: 1-20) (Momose *et al.*, 2001). NP possesses two NLSs (NLS1: 1-13, which is the most important, and a putative bipartite NLS2: 198-216) (Cros *et al.*, 2005; Weber *et al.*, 1998; Ye *et al.*, 2006). It also possesses a caspase cleavage site (D16) (Zhirnov *et al.*, 1999).

2.3.13. References

Albo C, Valencia A, Portela A. Identification of an RNA binding region within the N-terminal third of the influenza A virus nucleoprotein. *J Virol* 1995; 69: 3799-3806.

Arrese M, Portela A. Serine 3 is critical for phosphorylation at the N-terminal end of the nucleoprotein of influenza virus A/Victoria/3/75. *J Virol* 1996; 70: 3385-3391.

Avalos RT, Yu Z, Nayak DP. Association of influenza virus NP and M1 proteins with cellular cytoskeletal elements in influenza virus-infected cells. *J Virol* 1997; 71: 2947-2958.

Barrett T, Wolstenholme AJ, Mahy BW. Transcription and replication of influenza virus RNA. *Virology* 1979; 98: 211-225.

Baudin F, Bach C, Cusack S, *et al.* Structure of influenza virus RNP. I. Influenza virus nucleoprotein melts secondary structure in panhandle RNA and exposes the bases to the solvent. *Embo J* 1994; 13: 3158-3165.

Baudin F, Petit I, Weissenhorn W, *et al. In vitro* dissection of the membrane and RNP binding activities of influenza virus M1 protein. *Virology* 2001; 281: 102-108.

Beaton AR, Krug RM. Transcription antitermination during influenza viral template RNA synthesis requires the nucleocapsid protein and the absence of a 5' capped end. *Proc Natl Acad Sci U S A* 1986; 83: 6282-6286.

Biswas SK, Boutz PL, Nayak DP. Influenza virus nucleoprotein interacts with influenza virus polymerase proteins. *J Virol* 1998; 72: 5493-5501.*et al.*

Boulo S, Akarsu H, Lotteau V, *et al.* Human importin alpha and RNA do not compete for binding to influenza A virus nucleoprotein. *Virology* 2011; 409: 84-90.

Bui M, Wills EG, Helenius A, *et al.* Role of the influenza virus M1 protein in nuclear export of viral ribonucleoproteins. *J Virol* 2000; 74: 1781-1786.

Bullido R, Gomez-Puertas P, Albo C, *et al.* Several protein regions contribute to determine the nuclear and cytoplasmic localization of the influenza A virus nucleoprotein. *J Gen Virol* 2000; 81: 135-142.

Chan WH, Ng AK, Robb NC, *et al.* Functional analysis of the influenza virus H5N1 nucleoprotein tail loop reveals amino acids that are crucial for oligomerization and ribonucleoprotein activities. *J Virol* 2010; 84: 7337-7345.

Compans RW, Content J, Duesberg PH. Structure of the ribonucleoprotein of influenza virus. *J Virol* 1972; 10: 795-800.

Cros JF, Garcia-Sastre A, Palese P. An unconventional NLS is critical for the nuclear import of the influenza A virus nucleoprotein and ribonucleoprotein. *Traffic* 2005; 6: 205-213.

Digard P, Elton D, Bishop K, *et al.* Modulation of nuclear localization of the influenza virus nucleoprotein through interaction with actin filaments. *J Virol* 1999; 73: 2222-2231.

Duesberg PH. Distinct subunits of the ribonucleoprotein of influenza virus. *J Mol Biol* 1969; 42: 485-499.

Elton D, Medcalf E, Bishop K, *et al.* Oligomerization of the influenza virus nucleoprotein: identification of positive and negative sequence elements. *Virology* 1999; 260: 190-200.

Elton D, Medcalf L, Bishop K, *et al.* Identification of amino acid residues of influenza virus nucleoprotein essential for RNA binding. *J Virol* 1999; 73: 7357-7367.

Fodor E, Pritlove DC, Brownlee GG. The influenza virus panhandle is involved in the initiation of transcription. *J Virol* 1994; 68: 4092-4096.

Fontes MR, Teh T, Kobe B. Structural basis of recognition of monopartite and bipartite nuclear localization sequences by mammalian importin-alpha. *J Mol Biol* 2000; 297: 1183-1194.

Fuller FJ, Freedman-Faulstich EZ, Barnes JA. Complete nucleotide sequence of the tick-borne, orthomyxo-like Dhori/Indian/1313/61 virus nucleoprotein gene. *Virology* 1987; 160: 81-87.

Gabriel G, Klingel K, Otte A, *et al.* Differential use of importin-*α* isoforms governs cell tropism and host adaptation of influenza virus. *Nat Commun* 2011; 2: 156.

Garcia-Robles I, Akarsu H, Muller CW, *et al.* Interaction of influenza virus proteins with nucleosomes. *Virology* 2005; 332: 329-336.

Gorlich D, Prehn S, Laskey RA, *et al.* Isolation of a protein that is essential for the first step of nuclear protein import. *Cell* 1994; 79: 767-778.

Hay AJ, Lomniczi B, Bellamy AR, *et al.* Transcription of the influenza virus genome. *Virology* 1977; 83: 337-355.

Heggeness MH, Smith PR, Ulmanen I, *et al.* Studies on the helical nucleocapsid of influenza virus. *Virology* 1982; 118: 466-470.

Hirayama E, Atagi H, Hiraki A, *et al.* Heat shock protein 70 is related to thermal inhibition of nuclear export of the influenza virus ribonucleoprotein complex. *J Virol* 2004; 78: 1263-1270.

Hsu MT, Parvin JD, Gupta S, *et al.* Genomic RNAs of influenza viruses are held in a circular conformation in virions and in infected cells by a terminal panhandle. *Proc Natl Acad Sci U S A* 1987; 84: 8140-8144.

Humphrey W, Dalke, A., Schulten, K. VMD - Visual Molecular Dynamics. *J. Molec. Graphics* 1996; 14: 33-38.

Kawaguchi A, Momose F, Nagata K. Replication-coupled and host factor-mediated encapsidation of the influenza virus genome by viral nucleoprotein. *J Virol* 2011; 85: 6197-6204.

Kingsbury DW, Jones IM, Murti KG. Assembly of influenza ribonucleoprotein *in vitro* using recombinant nucleoprotein. *Virology* 1987; 156: 396-403.

Kingsbury DW, Webster RG. Some Properties of Influenza Virus Nucleocapsids. *J Virol* 1969; 4: 219-225.

Kistner O, Muller K, Scholtissek C. Differential phosphorylation of the nucleoprotein of influenza A viruses. *J Gen Virol* 1989; 70 (Pt 9): 2421-2431.

Klumpp K, Ruigrok RW, Baudin F. Roles of the influenza virus polymerase and nucleoprotein in forming a functional RNP structure. *Embo J* 1997; 16: 1248-1257.

Kobayashi M, Toyoda T, Adyshev DM, *et al.* Molecular dissection of influenza virus nucleoprotein: deletion mapping of the RNA binding domain. *J Virol* 1994; 68: 8433-8436.

Krug RM, Alonso-Caplen FV, Julkunen I, *et al.* Expression and replication of the influenza virus genome. In The influenza viruses, Krug RM (eds). Plenum Press: New York, 1989; 89-152.

Krug RM, Ueda M, Palese P. Temperature-sensitive mutants of influenza WSN virus defective in virus-specific RNA synthesis. *J Virol* 1975; 16: 790-796.

Lamb RA, Krug RM. *Orthomyxoviridae*: The viruses and their replication. In Fields Virology, Knipe DM, Howley PM, Martin MA, Griffin DE, Lamb RA (eds). Lippincott Williams & Wilkins: Boston, 2001; 1487-1531.

Lipatov AS, Yen HL, Salomon R, *et al.* The role of the N-terminal caspase cleavage site in the nucleoprotein of influenza A virus *in vitro* and *in vivo*. *Arch Virol* 2008; 153: 427-434.

Mahy BWJ, Barret T, Nichol ST, *et al.* Analysis of the functions of influenza virus genome RNA segments by the use of temperature-sensitive mutants of fowl plague virus. In The replication of negative strand viruses, Bishop DHL,

Compans RW (eds). Elsevier: Amsterdam, 1981; 379-387.

Mandler J, Muller K, Scholtissek C. Mutants and revertants of an avian influenza A virus with temperature-sensitive defects in the nucleoprotein and PB2. *Virology* 1991; 181: 512-519.

Markushin SG, Ghendon YZ. Studies of fowl plague virus temperature-sensitive mutants with defects in synthesis of virion RNA. *J Gen Virol* 1984; 65 (Pt 3): 559-575.

Martin-Benito J, Area E, Ortega J, *et al.* Three-dimensional reconstruction of a recombinant influenza virus ribonucleoprotein particle. *EMBO Rep* 2001; 2: 313-317.

Medcalf L, Poole E, Elton D, *et al.* Temperature-sensitive lesions in two influenza A viruses defective for replicative transcription disrupt RNA binding by the nucleoprotein. *J Virol* 1999; 73: 7349-7356.

Mena I, Jambrina E, Albo C, *et al.* Mutational analysis of influenza A virus nucleoprotein: identification of mutations that affect RNA replication. *J Virol* 1999; 73: 1186-1194.

Momose F, Basler CF, O'Neill RE, *et al.* Cellular splicing factor RAF-2p48/NPI-5/BAT1/UAP56 interacts with the influenza virus nucleoprotein and enhances viral RNA synthesis. *J Virol* 2001; 75: 1899-1908.

Momose F, Naito T, Yano K, *et al.* Identification of Hsp90 as a stimulatory host factor involved in influenza virus RNA synthesis. *J Biol Chem* 2002; 277: 45306-45314.

Moroianu J, Blobel G, Radu A. Previously identified protein of uncertain function is karyopherin alpha and together with karyopherin beta docks import substrate at nuclear pore complexes. *Proc Natl Acad Sci U S A* 1995; 92: 2008-2011.

Murti KG, Webster RG, Jones IM. Localization of RNA polymerases on influenza viral ribonucleoproteins by immunogold labeling. *Virology* 1988; 164: 562-566.

Neumann G, Castrucci MR, Kawaoka Y. Nuclear import and export of influenza virus nucleoprotein. *J Virol* 1997; 71: 9690-9700.

O'Neill RE, Jaskunas R, Blobel G, *et al.* Nuclear import of influenza virus RNA can be mediated by viral nucleoprotein and transport factors required for protein import. *J Biol Chem* 1995; 270: 22701-22704.

O'Neill RE, Palese P. NPI-1, the human homolog of SRP-1, interacts with influenza virus nucleoprotein. *Virology* 1995; 206: 116-125.

Ortega J, Martin-Benito J, Zurcher T, *et al.* Ultrastructural and functional analyses of recombinant influenza virus ribonucleoproteins suggest dimerization of nucleoprotein during virus amplification. *J Virol* 2000; 74: 156-163.

Ozawa M, Fujii K, Muramoto Y, *et al.* Contributions of two nuclear localization signals of influenza A virus nucleoprotein to viral replication. *J Virol* 2007; 81: 30-41.

Palese P, Wang P, Wolff T, *et al.* Host-viral protein-protein interactions in influenza virus replication. In Molecular aspects of host-pathogen interaction, McCrae MA, *et al.* (eds). Cambridge University Press: Cambridge, 1997; 327-340.

Pons MW, Schulze IT, Hirst GK, *et al.* Isolation and characterization of the ribonucleoprotein of influenza virus. *Virology* 1969; 39: 250-259.

Poole E, Elton D, Medcalf L, *et al.* Functional domains of the influenza A virus PB2 protein: identification of NP- and PB1-binding sites. *Virology* 2004; 321: 120-133.

Portela A, Digard P. The influenza virus nucleoprotein: a multifunctional RNA-binding protein pivotal to virus replication. *J Gen Virol* 2002; 83: 723-734.

Privalsky ML, Penhoet EE. Phosphorylated protein component present in influenza virions. *J Virol* 1977; 24: 401-405.

Prokudina-Kantorovich EN, Semenova NP. Intracellular oligomerization of influenza virus nucleoprotein. *Virology* 1996; 223: 51-56.

Ruigrok RW, Baudin F. Structure of influenza virus ribonucleoprotein particles. II. Purified RNA-free influenza virus ribonucleoprotein forms structures that are indistinguishable from the intact influenza virus ribonucleoprotein particles. *J Gen Virol* 1995; 76 (Pt 4): 1009-1014.

Scholtissek C, Becht H. Binding of ribonucleic acids to the RNP-antigen protein of influenza viruses. *J Gen Virol* 1971; 10: 11-16.

Scholtissek C. The genome of the influenza virus. *Curr Top Microbiol Immunol* 1978; 80: 139-169.

Shapiro GI, Krug RM. Influenza virus RNA replication *in vitro*: synthesis of viral template RNAs and virion RNAs in the absence of an added primer. *J Virol* 1988; 62: 2285-2290.

Takizawa N, Watanabe K, Nouno K, *et al.* Association of functional influenza viral proteins and RNAs with nuclear chromatin and sub-chromatin structure. *Microbes Infect* 2006; 8: 823-833.

Taylor JM, Illmensee R, Litwin S, *et al.* Use of specific radioactive probes to study

transcription and replication of the influenza virus genome. *J Virol* 1977; 21: 530-540.

Thierry F, Danos O. Use of specific single stranded DNA probes cloned in M13 to study the RNA synthesis of four temperature-sensitive mutants of HK/68 influenza virus. *Nucleic Acids Res* 1982; 10: 2925-2938.

Vreede FT, Brownlee GG. Influenza virion-derived viral ribonucleoproteins synthesize both mRNA and cRNA *in vitro. J Virol* 2007; 81: 2196-2204.

Vreede FT, Jung TE, Brownlee GG. Model suggesting that replication of influenza virus is regulated by stabilization of replicative intermediates. *J Virol* 2004; 78: 9568-9572.

Wang P, Palese P, O'Neill RE. The NPI-1/NPI-3 (karyopherin alpha) binding site on the influenza a virus nucleoprotein NP is a nonconventional nuclear localization signal. *J Virol* 1997; 71: 1850-1856.

Weber F, Kochs G, Gruber S, *et al.* A classical bipartite nuclear localization signal on Thogoto and influenza A virus nucleoproteins. *Virology* 1998; 250: 9-18.

Weis K, Mattaj IW, Lamond AI. Identification of hSRP1 alpha as a functional receptor for nuclear localization sequences. *Science* 1995; 268: 1049-1053.

Whittaker GR, Helenius A. Nuclear import and export of viruses and virus genomes. *Virology* 1998; 246: 1-23.

Wu WW, Sun YH, Pante N. Nuclear import of influenza A viral ribonucleoprotein complexes is mediated by two nuclear localization sequences on viral nucleoprotein. *Virol J* 2007; 4: 49.

Wu WW, Weaver LL, Pante N. Ultrastructural analysis of the nuclear localization sequences on influenza a ribonucleoprotein complexes. *J Mol Biol* 2007; 374: 910-916.

Yamanaka K, Ishihama A, Nagata K. Reconstitution of influenza virus RNA-nucleoprotein complexes structurally resembling native viral ribonucleoprotein cores. *J Biol Chem* 1990; 265: 11151-11155.

Ye Q, Krug RM, Tao YJ. The mechanism by which influenza A virus nucleoprotein forms oligomers and binds RNA. *Nature* 2006; 444: 1078-1082.

Zhao H, Ekstrom M, Garoff H. The M1 and NP proteins of influenza A virus form homo- but not heterooligomeric complexes when coexpressed in BHK-21 cells. *J Gen Virol* 1998; 79 (Pt 10): 2435-2446.

Zhirnov O, Bukrinskaya AG. Nucleoproteins of animal influenza viruses, in contrast to

those of human strains, are not cleaved in infected cells. *J Gen Virol* 1984; 65 (Pt 6): 1127-1134.

Zhirnov OP, Konakova TE, Garten W, *et al.* Caspase-dependent N-terminal cleavage of influenza virus nucleocapsid protein in infected cells. *J Virol* 1999; 73: 10158-10163.

2.4. The matrix protein 1

The matrix protein 1 (M1) is 252 amino acid-long. It is the most abundant protein in the virion (3000 units per virion) and the second most conserved after polymerase basic protein 1 (97% of mean identities) (Lamb & Krug, 2001) (personal results). Ultrastructural imaging revealed that it adopts a 6 nm-long thin rod-like shape, with one end connecting the viral membrane (Ruigrok *et al.*, 2000). It binds matrix protein 2 (M2), nucleoprotein (NP), nuclear export protein (NEP), lipids, and probably the cytoplasmic tail of hemagglutinin (HA) and neuraminidase (NA). On a functional point of view, M1 autonomously translocates in the nucleus by use of its own nuclear localization signal (NLS), displays transcription inhibition properties (Elster *et al.*, 1997; Watanabe *et al.*, 1996; Ye *et al.*, 1987 & 1989) and plays a crucial role in the export of newly synthesized viral ribonucleoproteins (vRNPs) from the nucleus (O'Neill *et al.*, 1998). Moreover, as ectopic expression of M1 proteins alone from a recombinant plasmid leads to the formation of tubular structures and even of virus-like particles, M1 proteins are thought to play a central role in the budding process (Gomez-Puertas *et al.*, 2000).

M1 is a target for SUMOylation at position K242, which modification is required for M1 interaction with vRNPs and nuclear export of these vRNPs (Wu *et al.*, 2011). It also interacts through its N-terminal domain with C1qA, which leads to the inhibition of classical complement pathway (Zhang *et al.*, 2009).

2.4.1. Structure

The full-length M1 protein is constituted of a compact globular N-terminal domain, a flexible linker region and an elongated C-terminal domain (Artz *et al.*, 2001). Purified M1 protein is almost systematically found cleaved at position 162, probably by contaminating proteases during the purification process, which yields only the N-terminal fragment in amenable quantities for 3D-structure determination by X-ray crystallography (Baudin *et al.*, 2001; Sha & Luo, 1997). It is constituted of a succession of helices separated by connecting loops, first 4 α-helices (H1-H4, "N domain"), then a 3_{10} helix (H5) and, again, 4 α-helices (H6-H9, "M domain") (Harris *et al.*, 2001; Sha & Luo, 1997) (Figure 1). Successive helices span residues 2 to 14 (H1), 18 to 33 (H2), 39 to 48 (H3), 54 to 67 (H4), 78 to 85 (H5), 91 to 105 (H6), 109 to 118 (H7), 121 to 133

(H8) and 140 to 158 (H9) (Sha & Luo, 1997). The C-terminal domain seems to be flexibly linked to the H9 α-helix of the N-terminal fragment. It has 38% α-helical content when measured by circular dichroism and seems to be very elongated which gives the M1 protein its rod-like shape (Artz *et al.*, 2001). The C-terminal domain is supposed to contain four α-helices: H10 from residues 155 to 173, H11 from 179 to 193, H12 from 199 to 219 and H13 from 233 to 251, as determined by tritium bombardment of intact influenza virions (Shishkov *et al.*, 1999).

The 3D-structure of the N-terminal fragment is roughly similar at an acidic (pH 4.0) or a neutral pH (Harris *et al.*, 2001; Sha & Luo, 1997), the most significant difference being the conformation/positioning of the flexible loops intercalated between H4 and H5, H5 and H6, H8 and H9 and of the C-terminal end itself (Harris *et al.*, 2001). Even with these changes, notably those affecting the H5-flanking loops, the N and M domains adopt a similar relative position at both pHs. This is supposed to be attributable to strong intradomain hydrophobic interactions (between H1 and H4 for the N domain, H6 and H9 for the M domain) which tend to result in interdomains hydrophobic contacts (Harris *et al.*, 2001). Confirmation of the α-helical content of M1 protein was confirmed by *in situ* structural characterization, within virions (Shishkov *et al.*, 2009).

Although M1 has been found once as an elongated monomer in solution (Artz *et al.*, 2001), the emerging concept stands that it typically forms dimers, with two monomers stacked on the top of each other (Sha & Luo, 1997) (Figure 2). The neutral dimer interfaces in two ways, either N-N or M-M (Harris *et al.*, 2001). Conversely, interfacing is only through M-M stacking in acidic dimers, with a relative rotation of the monomers by comparison with the neutral pH structure. This is attributed to an altered conformation of K35 and R36 in the connecting loop between H2 and H3, on the N domain at the top of the M1 monomer. Those asymmetric dimers ("stacked dimers") are able to assemble in M1 ribbons (acidic dimers tend to form tetramers) by translational stacking interactions in which H6 and H7 basic residues (R and K) are exposed on the same side of the ribbon (in both acidic and neutral structures), which significantly affects the RNA-binding properties of M1 (Harris *et al.*, 2001). In addition to stacking interface interactions, M1 molecules in the tetramers form interactions between the H5-flanking loops and that intercalated between H8 and H9. Those additional interactions are referred to as the M1-M1 twofold interface (Harris *et al.*, 2001). M1 monomers are linked at their staking interface (about 1,100 $Å^2$ and 880 $Å^2$ of buried surface areas in neutral and acidic dimers, respectively and 2,115 $Å^2$ in the twofold interface) by van der

Waals contacts and hydrogen bonds (Harris *et al.*, 2001). This interface is formed by a protrusion of hydrophobic residues (top residues) coming in contact with a depression of hydrophobic residues (bottom residues) in both N-N domain or M-M domain interfaces. T67 is hydrogen-bonded by its carbonyl moiety to the amide nitrogen of I51. N87 (in the loop after H5) is hydrogen-bonded by its side chain to the carbonyl of A137 (in the loop between H8 and H9). Dominant amino acids involved in polar and non polar interactions in the neutral dimer are L4, A33, L66, T67 and P69 of the top N domain, and P16, P19, P50, I51 and P59 of the bottom N domain; in the M domain, those residues are R105, I107 and T139 in the top face, and N87, A121 and I154 of the bottom face (Harris *et al.*, 2001). In the acidic dimer, equivalent residues of the M domain (no N-N interactions in this form) are R105, E106, I107 and T139 in the top face, and N87, N92, A121, A125 and I154 in the bottom face. Many interacting residues are thus conserved in both neutral and acidic forms. At the M domain interface of the acidic dimer, the hydrophobic depression of the bottom molecule is deeper and the protrusion of the top molecule is higher, which permits to engage three additional residues in hydrophobic interactions. This stronger M-M interaction excludes N domains from hydrophobic contacts, the latter being exposed to the solvent. In the acidic form, N87 is hydrogen-bonded to the carbonyl of E106 of the H6-H7 connecting loop, and the side chain of N92 forms an hydrogen bond with the carbonyl of R105 (Harris *et al.*, 2001). These differences in M1 monomers interactions at neutral *vs.* acidic pH are thought to play role during the uncoating process, which requires internal acidification of entering virions.

Deletion mutagenesis studies confirmed that the M domain (which is involved in M1-M1 interactions at both acidic and neutral pHs) is the main determinant of M1 self-association (Noton *et al.*, 2007).

As the side of the M1 monomer where the NLS and RNA-binding site are located is positively charged and the opposite side is negatively charged, it has been suggested that electrostatic forces could also play a role in the generation of M1 oligomeric structures (Artz *et al.*, 2001). In addition to the formation of ribbons by single M1 molecules, computational analysis showed that additional M1-M1 twofold interactions may occur, which could result in the formation of double ribbon of M1 dimers organizing into an helix of about 200 Å of diameter with 16 molecules per turn (Harris *et al.*, 2001). No potential hydrogen bond was found to stabilize the ribbon structure, but polar and van der Waals interactions might be present. As aforementioned, the basic

residues of H6 and H7 are systematically exposed on the same side of the molecule in all these different structures (Harris *et al.*, 2001). Thus, the M1 protein could form two major supra-structures, either an extended helix, or flexible strands (or ribbons). The existence of the later had been suggested by previous electron microscopy studies (Nermut, 1972; Oxford *et al.*, 1987; Ruigrok *et al.*, 1989 & 2000).
Ultrastructural studies revealed that M1 proteins coil around vRNPs and bind RNA cooperatively (Wakefield & Brownlee, 1989). As most basic residues are exposed on the same side of the helix, they are supposed to be engaged in the interfacing with vRNPs. The C-terminal domain is thought to be exposed on the inside of the helix.
Structure-function studies of M1 have unambiguously identified lipid-, M2-, protease-, histone-, RNA-, NP-, NEP-, HA-, and NA-binding sites along with protein kinase C phosphorylation sites.

2.4.2. Lipid-binding sites

The M1 protein interacts with lipidic membranes in *in vitro* assays or during influenza virus replication cycle (Bucher *et al.*, 1980; Gregoriades, 1980; Kretzschmar *et al.*, 1996; Zhang & Lamb, 1996). Co-sedimentation assays showed that the M1-membrane interaction disappeared when the salt concentration or the pH was raised, suggesting that the intimate nature of these interactions is electrostatic (Ruigrok *et al.*, 2000). Zhirnov (1992) had previously shown that M1 can be solubilized after destabilization of the viral membrane by high salt concentration or by acidic pH, which also tended to prove that M1-lipid interactions are electrostatic rather than hydrophobic. As only full length M1 protein and its N-terminal fragment (1-164) were shown to float with negatively charged liposomes, the N-terminal domain of M1 is most probably the main membrane-binding region (Baudin *et al.*, 2001). Conversely, as only the full length and the C-terminal end of M1 interact with vRNPs (Baudin *et al.*, 2001), the extremity of the 6 nm-long rods observed by Ruigrok *et al.* (2000) could be the N-terminal end and the opposite extremity could be the C-terminal end interacting with vRNPs (see further). The 101-RKLKR-105 NLS domain of M1 protein is thought to participate to lipid-binding (Baudin *et al.*, 2001), the positive basic residues of this cluster interacting with the negatively charged liposomes.

2.4.3. Putative M2-binding site and virion morphology-associated amino acids

The 14C2 anti-M2 monoclonal antibody (mAb) prevented the filamentous particles formation of the A/Udorn/72 strain and impaired its multiplication (Roberts *et al.*, 1998; Zebedee & Lamb, 1989). Variants of this 14C2 mAb-resistant strain with restored multiplication potential however retained the filamentous morphology. Two of these mutants presented a mutation in the M2 and another mutant in the M1 protein (A41V substitution) (Roberts *et al.*, 1998). A V31I substitution had previously been described in some variants (Zebedee & Lamb, 1989). Accordingly, these two residues (31 and 41) are thought to be part of a M2-binding site on the M1 protein. Furthermore, the M1 and M2 proteins and their interaction thus seem critical for viral morphology. Our sequences alignments show that A41 is almost invariable, while V31 is in some strains replaced by a phenylalanine residue (which conserves the hydrophobic properties of the residue at this position). The strict conservation of A41 is consistent with its putative role in M2-binding.

Classical laboratory grown influenza virus strains adopt a regular spherical morphology whereas strains isolated *in vivo* frequently assume elongated/filamentous shapes. There are however some exceptions to this rule, such as the A/Udorn/72 laboratory strain which adopts a filamentous morphology. Working on the parental A/WilsonSmith/33 influenza strain, which adopts a spherical morphology, Burleigh *et al.* (2005) demonstrated the importance of residues K95, K98, R101 and K102 for viral morphology. K95A mutants showed an enlarged but almost normal morphology at 33°C but were greatly enlarged and spherical at 37°C. K98A mutants behaved similarly but assumed more elongated forms at 37°C. R101A mutants were very similar to wild-type virions at 33°C, being only a little more pleiomorphic with some slightly disrupted particles. But at 37°C, many disrupted particles were present. For the K102A mutants, many different shapes were found at 33°C, with elongated and spherical particles as well. At 37°C, these mutants displayed a highly filamentous morphology (Burleigh *et al.*, 2005). These results suggest that either the said residues are involved in the budding process, or the alanine replacement at said positions results in a disruption of the M1 H6 structure, which alters its functions.

Besides, McCown and Pekosz (2005) showed that a functional revertant of a mutant M_2STOP70 virus, lacking the 28 C-terminal residues of M2, displayed a compensatory A22T change in the M1 protein. This result suggests that the potential M2-binding site

extends more widely toward the N-terminus of the M1 protein. The M_2STOP70 mutant is characterized by a drastic abatement of new infectious particles production and by a decrease of intraparticle NP and RNA incorporation, suggesting a role of the M1-M2 interaction in the efficient packaging of vRNPs (McCown & Pekosz, 2005). As the M1 incorporation was unaffected in these mutant progeny viruses, the packaging of M1 is most probably essentially due to its binding to HA, NA and to the lipid membrane, rather than to the M2 protein. In spite of a high level of conservation, A22 is in some strains replaced by a serine, a polar residue (by opposition to the hydrophobicity of alanine), showing that the properties of amino acid at position 22 can be modified in naturally occurring influenza A strains (personal investigations).

In conclusion, there is no doubt that M1 possesses a M2-binding site, which is still poorly defined at the amino acid level. M1 is also the most essential determinant of virion morphology, through oligomerization and complex interactions with the membrane, the M2 protein and the cytoplasmic tails of HA and NA (Ali *et al.*, 2000; Barman *et al.*, 2001; Jin *et al.*, 1997; Roberts *et al.*, 1998).

2.4.4. Protease-binding and inhibition domain

The M1 protein is able to bind trypsin-like serine- and cysteine-proteases by its N-terminal end (Timofeeva *et al.*, 2001; Zhirnov *et al.*, 1999). Since the binding is prevented by monoclonal antibodies targeting the 46-70 region and by an antiserum to region 21-45, this potential protease-binding domain is assigned to residues 21 to 70 of the M1 protein (Timofeeva *et al.*, 2001). Protein-protein binding assays on polystyrene plates and PVP membranes showed a specific binding between M1 and caspase-8 (and a weak binding with caspase-7), an essential mediator of the apoptosis pathway (Zhirnov *et al.*, 2002). Computational analysis identified a putative anti-caspase site in the N-terminal end of M1, similar to that of baculovirus p35 protein. As influenza virus was shown to induce cell apoptosis late in the infection (Hinshaw *et al.*, 1994; Takizawa *et al.*, 1993) and as M1 prevented the induction of apoptosis by Tumor Necrosis Factor α in human carcinoma Hep-2 cells (Zhirnov *et al.*, 2002), a caspase-8 inhibiting activity of the M1 protein is postulated. The apoptosis activation process starts with the auto-aggregation and activation of caspase-8 (Zhirnov *et al.*, 2002), which is controlled by its interaction with the death effector domain (DED) of the cellular FADD (Fas-Associated protein with a Death Domain) adapter protein associated with the apoptosis Fas-

receptor. Interestingly, a 35% homology was found between the amino acid stretch spanning residues 25-40 of the M1 N-terminal domain and the DED-domain of FADD (residues 44-67), which led to the hypothesis that M1 interferes with the FADD-caspase-8 interaction by binding the latter and thus prevents apoptosis in this way (Zhirnov *et al.*, 2002). On the other hand, influenza-induced cell death was shown to be dependent on the FADD/caspase-8 apoptosis pathway, via the activation of Protein Kinase R, which is prevented by the influenza NS1 protein (non structural protein 1) (Balachandran *et al.*, 2000). Whether M1 and NS1 proteins cooperate to prevent apoptosis or act independently on specific aspects of the apoptotic process remains to be studied.

2.4.5. Histone-binding

By co-immunoprecipitation and *in vitro* binding assays on nitrocellulose, the M1 protein was shown to selectively bind H2A, H2B, H3, H4 and, weakly, H1 histones (Zhirnov & Klenk, 1997). As this interaction was sensitive to acidic pH and high salt concentrations, the authors concluded the interaction was dependent on ionic forces and M1 protein conformation. Because histones contain many basic residues to interact with nucleic acids, the existence of acidic domains to be enrolled in histone binding was hypothesized. As M1 is essentially a basic protein (pI of about 8.8) of which most basic residues are located in the central and C-terminal parts of the protein, the N-terminal end is supposed to permit histone binding (Zhirnov & Klenk, 1997). Functional relevance of these interactions is unknown and remains to be demonstrated. Studies by Garcia-Robles and colleagues (2005) confirmed the binding of M1 to nucleosomes. A strong reduction of nucleosome-binding was associated with the 101-AALAA-105 NLS M1 mutant, which tends to show that this domain is critically involved, even if residues 101-105 are essentially basic (Garcia-Robles *et al.*, 2005). M1 proteins were also shown to bind histones at a site different from that used by NP proteins, since trypsin-treated histones (thus lacking their tail, which is enrolled in NP binding) still bound M1 proteins (Garcia-Robles *et al.*, 2005). Since vRNPs are associated with cellular chromatin in infected cells and since they have to be freed to be exported from the nucleus late in the infection cycle, the M1 could be required to displace the RNPs from the cellular histones (Garcia-Robles *et al.*, 2005; Ye *et al.*, 2006; Zhirnov & Klenk, 1997).

2.4.6. RNA-binding site and Nuclear Localization Signal

The M1 protein binds RNA even in the absence of NP, suggesting that its RNA-binding activity does not require prior M1-NP contacts (Wakefield & Brownlee, 1989). Using purified M1 protein and ^{32}P-labelled RNA probes, Wakefield and Brownlee (1989) concluded to a stoechiometric ratio of about one M1 protein per 200 nucleotides at saturation. M1 protein was also shown to fix RNA molecules devoid of the 3' and 5' influenza-specific sequences (Wakefield & Brownlee, 1989). Furthermore, cross-linking experiments showed the M1 RNA-binding activity is not sequence-specific (Elster *et al.*, 1997). Two disjoint RNA-binding domains have been identified: (i) the 95-105 polybasic window and (ii) the 148-162 Zn-finger motif. Within the former, an additional function-specific subdomain was picked up, a putative NLS (101-RKLKR-105).

2.4.6.a. The RNA-binding polybasic 95-105 window

The sequence spanning residues 95 to 105 ("RAVKLYRKLKR") was proposed to function as the M1 RNA-binding domain because it forms an α-helix with K and R residues systematically exposed on one side (Figure 1), which is predicted to favor interactions with the negatively charged phosphates of RNA molecules (Elster *et al.*, 1997; Watanabe *et al.*, 1996; Winter & Fields, 1980). Basic residues thought to be enrolled in RNA-binding (R95, K98, R101, K102, K104 and R105) are indeed all located on the same side of the M1 monomer, thus creating a continuous positively charged area with other neighboring charged residues (K47, R49, K57, R72, R76, R77, R78 and R134) (Artz *et al.*, 2001; Elster *et al.*, 1997; Watanabe *et al.*, 1996). This specific arrangement also causes the opposite side of the M1 monomer to be negatively charged, which participates to the oligomerization of M1 monomers. Among residues 95 to 105, sequences alignments show that the most conserved are L99, K102, L103, K104 and R105. In spite of a general very high conservation of this motif (consistent with the functional need of the presence of basic residues), observed substitutions are: R95K, A96S or G, V97A, K98R, N or M, Y100F (infrequent), R101K, G, T or Q. Thus, surprisingly, residue R101 is in some (rare) strains replaced by non basic amino acids, which raises questions about its implication in the multiple roles assigned to the 101-105 stretch (RNA-binding, NLS – see hereafter – , etc.).

The effect of several mutations within the 101-RKLKR-105 subdomain on the whole or

on specific steps of the biological cycle of the virus has been assessed. First, single asparagine substitution of K102 or K104 was shown to be lethal for the virus (Liu & Ye, 2002). Further, single serine substitution of R101 or R105 was nonlethal but caused a dramatic abatement of viral growth/yield (Liu & Ye, 2002). On the other hand, combining targeted mutation assays and immunofluorescence staining, Ye and colleagues (1995) showed that substitution of the 101-RKLKR-105 stretch by 101-SNLNS-105 sharply diminished M1 nuclear localization, thus implying that it also functions as an NLS. Incidentally, this "RKLKR" basic motif is very similar to the NLS of many other peptides (Chelsy *et al.*, 1989). Mechanistically speaking, it must be emphasized that the 3D-structure of the M1 NLS mutant (101-AALAA-105), which is simultaneously deficient for RNA-, membrane- and NEP-binding, nuclear translocation and M1-M1 oligomerization, is not different from that of wild-type M1 protein (Artz *et al.*, 2004), which suggests that the positive residues rather than the overall structure are responsible for the functions afforded by the 101-105 subdomain.

2.4.6.b. The RNA-binding Zn-finger motif

Beside the 95-105 polybasic window, Wakefield and Brownlee (1989) identified a second sequence (later restricted to the amino acid stretch 148 to 162: "CATCEQIADSQHRSH"), predicted to form a "Zn-finger", i.e. a structure typically found in nucleic acid-binding proteins. Mutations experiments targeting the two cysteine and the two histidine residues, either individually or in combination, in this Zn-finger motif only slightly altered viral growth, suggesting that it is not crucial for RNA-binding (Hui *et al.*, 2003; Liu & Ye, 2002). Conversely, the replacement of A155 by a glycine residue is lethal for the virus, which suggests A155 plays a critical role for an essential but yet unknown M1 protein function (Hui *et al.*, 2003). Alternatively, A155 replacement by a glycine (or D or T) could disrupt the α-helical structure of H9 and possibly destabilize the rest of the protein, thus resulting in altered functions (Hui *et al.*, 2003). Moreover, only a fraction of the M1 proteins (5-15%) are found to contain a Zn^{2+} ion and it is possible that Zn^{2+} ion-binding induces a conformational change of the M1 protein (Artz *et al.*, 2001; Elster *et al.*, 1994). The very high conservation of this Zn-finger motif among influenza A virus strains tends to prove it must play a significant biological role. Our sequences alignments show that in spite of a high conservation level for both cysteines and both histidines of the Zn-finger motif, these residues are not

completely conserved in some H1N2 or H3N2 strains. Substitutions found in some strains are: C151W, H159D or H162Y or L. Relevance of these results has still to be defined. It seems that the Zn-finger region adopts a α-helical structure (in the H9 α-helix) in the absence of Zn^{2+} ions at both acidic and neutral pHs. In the presence of Zn^{2+} at neutral pH however, this region takes a partially unfold conformation with a tetrahedral conformation where a central Zn^{2+} ion is surrounded by the two cysteine and the two histidine residues of the Zn-finger domain (Okada *et al.*, 2003). Furthermore, the Zn-finger region refolds into the initial α-helix and releases the Zn^{2+} ion when the pH is diminished under 5.9 (Okada *et al.*, 2003). This pH-dependent conformational change could therefore play a critical role in the uncoating process taking place in the incoming particles, which crucially requires the separation of vRNPs from the M1 proteins. Consistent with a physiological role of this domain, some alanine substitutions mutants of the Zn-finger motif were shown to be very attenuated *in vivo* in mice, but also in mouse and human lung cells culture, while there was no attenuation in MDCK cells or embryonated chicken eggs (Hui *et al.*, 2006). Thus, this Zn-finger motif seems to be implicated in the virulence and host-adaptation of the virus (Hui *et al.*, 2006).

2.4.7. Viral ribonucleoprotein and/or nucleoprotein-binding

Only full-length M1 protein or its C-terminal domain were shown to fix vRNPs (Baudin *et al.*, 2001). Furthermore, M1 or its C-terminal domain (165-252) co-sediments with purified NP, thus in the absence of viral RNA and viral polymerase subunits PB1, PB2 (polymerase basic proteins 1 and 2) and PA (polymerase acidic protein) (Baudin *et al.*, 2001). As the binding site of naked RNA is located in the M1 N-terminal fragment (see above) and as the C-terminal end of M1 contains the vRNP- and NP-binding-sites, it is most likely that M1 binds to vRNPs by binding to NP and not to RNA or to the polymerasic complex (Baudin *et al.*, 2001). This hypothesis agrees with previous studies showing that M1 binds vRNPs (with lower affinity) even after RNase treatment (Ye *et al.*, 1999). Other results, however, argue against this view. First, Ye and colleagues (1999) found the 76 N-terminal residues of M1 protein were also able to bind vRNPs, even with a low affinity. Secondly, coexpressed M1 and NP proteins form distinct homo-oligomeric structures, but do not aggregate into hetero-oligomers (Zhao *et al.*, 1998). A possible explanation could be that M1-NP interactions, if any, are restricted to specific step(s) of the virus biological cycle, e.g. the budding process

(Baudin *et al.*, 2001). Such M1-NP interactions were recently confirmed by deletion mutagenesis, showing that the M1 88-165 M domain possesses a substantial NP-binding activity *in vitro*, approaching that observed for the full-length protein. This last result tends to demonstrate, at least *in vitro*, that M1 binds vRNPs essentially by binding the NP protein (Noton *et al.*, 2007).

Binding of vRNPs by the M1 protein is altered by manipulations of the solution's salt concentration and pH, the affinity of M1 for vRNPs being minimum at high salt concentration and low pH (Ye *et al.*, 1999). This result is compatible with the crucial requirement of internal acidification of entering virions for the vRNPs to be freed from the M1 protein, which is a prerequisite for their injection into the cytoplasm (cf. M2 protein). In this respect, although M1 inhibits transcription by fixing on vRNPs (Elster *et al.*, 1997; Watanabe *et al.*, 1999; Ye *et al.*, 1987 & 1989), its C-terminal domain expressed alone cannot (Baudin *et al.*, 2001). It might be that M1 super-structures formation is necessary to effectively bind vRNPs in a way that prevents their transcription (Baudin *et al.*, 2001). The M1:vRNP stoechiometry is still unknown, but all studies agree with the fact that a single vRNP binds several M1 proteins (Baudin *et al.*, 2001; Watanabe *et al.*, 1999; Ye *et al.*, 1999).

The M1 protein also binds cellular cytoskeletal elements. This requires the concomitant presence of other viral components (probably vRNPs and/or NP, which bind actin filaments) and is thought to play a role in the viral budding process (Avalos *et al.*, 1997; Nayak *et al.*, 2004) (Figure 3).

2.4.8. Nuclear export protein-binding

As the virus NS2 protein (recently renamed "nuclear export Protein", "NEP") binds vRNPs only in the presence of M1, and as M1 and NEP coprecipitate, the existence of a NEP-binding site on M1 is suspected (O'Neill *et al.*, 1998; Yasuda *et al.*, 1993). By a two-hybrid system assay, the C-terminal 90-252 M1 segment was shown to be able to bind the NEP protein (Ward *et al.*, 1995). A subsequent filter-binding assay permitted the location of the binding partner domain within the NEP protein within its 70 C-terminal residues (Ward *et al.*, 1995).

The interaction between M1 and the NEP protein is essential for the nuclear export of native vRNPs. The M1 protein is suspected to function as an adapter molecule between vRNPs and NEP proteins, the latter being involved in interactions with the nuclear

export cell machinery (Akarsu *et al.*, 2003) (Figures 3 and 4). In this respect, a 101-AALAA-105 mutant of M1 is severely impaired in NEP-binding, which is probably attributable to the loss of basic residues at this position rather than to a structural alteration as the mutant and wild-type proteins display the same 3D-structure (Akarsu *et al.*, 2003; Artz *et al.*, 2004). To further define the crucial M1 basic residues involved in NEP-binding, half-site mutants were created (101-AALKR-105 and 101-RKLAA-105). Both displayed an intermediate level of NEP-binding, thus suggesting that at least one basic residue in each half-site contributes to NEP-binding (Akarsu *et al.*, 2003).

It has to be noted here that the C-terminal half of the M1 protein was shown to interact with the Hsc70 (heat shock cognate 70) protein, a constitutive form of the Hsp70 (heat shock protein 70) family, and the suppression of this interaction by RNA interference impedes the nuclear export of M1 and NP proteins at the end of the replication cycle. This Hsc70 protein would therefore be an important factor for influenza replication (Watanabe *et al.*, 2006).

2.4.9. Hemagglutinin- and neuraminidase-binding

Membrane-bound M1 protein was shown to become predominantly detergent-resistant in the presence of HA and NA and to be TX-100-soluble when those proteins are absent (Ali *et al.*, 2000; Barman *et al.*, 2001). HA and NA are two lipid raft-associated glycoproteins, which explains their detergent-resistance. Theoretically, a binding of M1 to the cytoplasmic tail (and/or transmembrane domain) of these two glycoproteins is therefore likely to confer such a detergent-resistance to M1. Such an M1-HA interaction was indeed suggested by colocalization studies (Ali *et al.*, 2000). The simultaneous binding of M1 to both vRNPs and membrane glycoproteins is consistent with a central role in the budding process, the M1 protein forming the physical link between internal and external components of new virions. This view is reinforced by the previous observations on the role of M1 on the one hand and the HA/NA's cytoplasmic tails on the other on virion morphology (Jin *et al.*, 1997; Liu *et al.*, 1995; Pattnaik *et al.*, 1986). The shared affinity of M1 for vRNPs, NA and HA also helps to understand how native vRNPs reach the lipid-raft microdomains – which are enriched in HAs and NAs – where the budding process takes place (Nayak *et al.*, 2004) (Figure 3). In the presence of monensin, a drug that blocks the protein exocytic pathway in the mid-Golgi region, both HA and M1 proteins were essentially (not exclusively) found in the perinuclear

Golgi region and absent from the cell membrane. Even if the colocalization was not perfect, it clearly suggests that the physical association of M1 and HA occurs early in the maturation process of HA (Ali *et al.*, 2000; Nayak *et al.*, 2004).

2.4.10. Protein Kinase C phosphorylation sites

M1 protein is phosphorylated during the influenza virus replication cycle, essentially at serine residues, by unknown kinases (Gregoriades *et al.*, 1984 & 1990). The potential regulatory role of the phosphorylation level of M1 on its proviral activities is still unknown as well. Using yeast two-hybrid assays and screening of an HeLa cDNA expression library, Reinhardt and Wolff (2000) found an interaction of M1 with the RACK-1 protein (Receptor of the Activated C Kinase), a protein that anchors Protein Kinase C (PKC) on membranes and cytoskeleton near its substrate. The M1-RACK-1 interaction is conserved among avian, human and swine influenza A strains, which suggests a specific role during the replication cycle (Reinhardt & Wolff, 2000). Moreover, the compound GF109203X, a specific PKC inhibitor, dramatically reduced the level of M1 phosphorylation, suggesting that PKC is the main, if not the sole, M1-phosphorylating enzyme *in vivo* (Reinhardt & Wolff, 2000). Conserved PKC M1 target sites are S70, S161 and T185. Personal results show that, in spite of a very high conservation degree of these three residues, only T185 is fully conserved. S70N and S161P substitutions are found in some H6N1 avian strains, while a S161A substitution is found in the A/canine/Florida/43/2004 (H3N8) strain.

2.4.11. The mouse winning tiercé

A set of M1 mutants were associated to viral adaptation to the mouse host. Two amino acid substitutions (A41V and T139A) were identified in mouse neurovirulent variants of the parental A/WS/33 strain (Ward, 1995). Similarly, the same T139A substitution confers an enhanced virulence to the mouse-adapted A/FM/1/47 strain virus and the A41V substitution correlates with enhanced mouse virulence in independent experimental settings (Gao *et al.*, 1999; Smeenk & Brown, 1994; Ward, 1996). Furthermore, a V15I substitution correlates with enhanced pathogenicity of recent H5N1 avian strains for mice (Hiromoto *et al.*, 2000; Katz *et al.*, 2000). Last but not least, a silent "TTT" to "TTC" codon substitution (coding for F32) in the A/FM/1/47

mouse-adapted strain increases its virulence (Smeenk & Brown, 1994). Our sequence alignments show that the V15I (or L) substitution is frequent among avian and swine strains, a V15M substitution being less frequent. The T139A substitution is not only found in mouse-adapted A/FM/1/47 but also in different avian and swine H3N2 strains and in the A/duck/Honk Kong/319/1978 (H2N2) strain. Significance of these mutations if any, in avian and swine strains has still to be assessed (personal investigations).

2.4.12. Conclusion

The M1 protein, the most abundant protein of the influenza virion, in addition to its structural role in the virion, plays multiple functions during the replication cycle (Figure 5). It is essential for the nuclear export of new vRNPs at the end of the cycle, in collaboration with the NEP protein. It is the key protein of the budding process, driving the vRNPs from the nucleus to the cell surface, at the budding site and, by interaction with lipids, HA, NA, M2 and vRNPs, plays an active role in the encapsidation and the budding of new viral particles. Its very high conservation and its crucial roles in the viral replication make the M1 protein a first choice target for antiviral therapy.

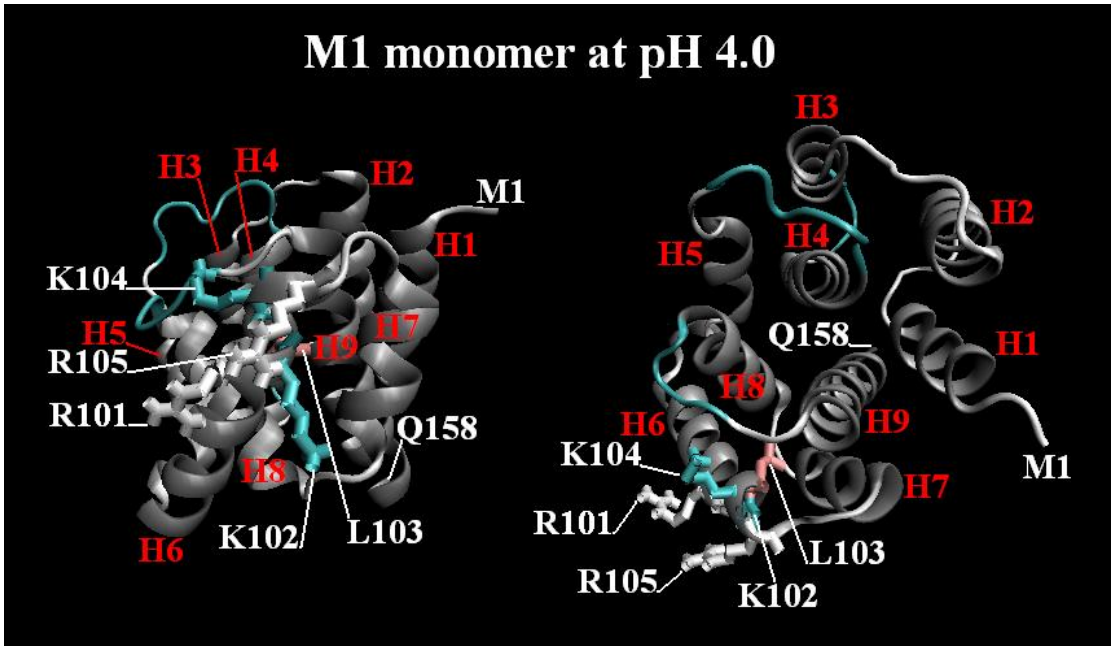

Figure 1: Structure of the 1-162 N-terminal fragment of the Matrix protein 1 of influenza A virus at acidic pH. Residues 101-RKLKR-105 on helix 6 are all on the same side of the protein. Adapted from Sha & Luo (1997) – pdb code: 1AA7. Figure performed with VMD (Humphrey *et al.*, 1996).

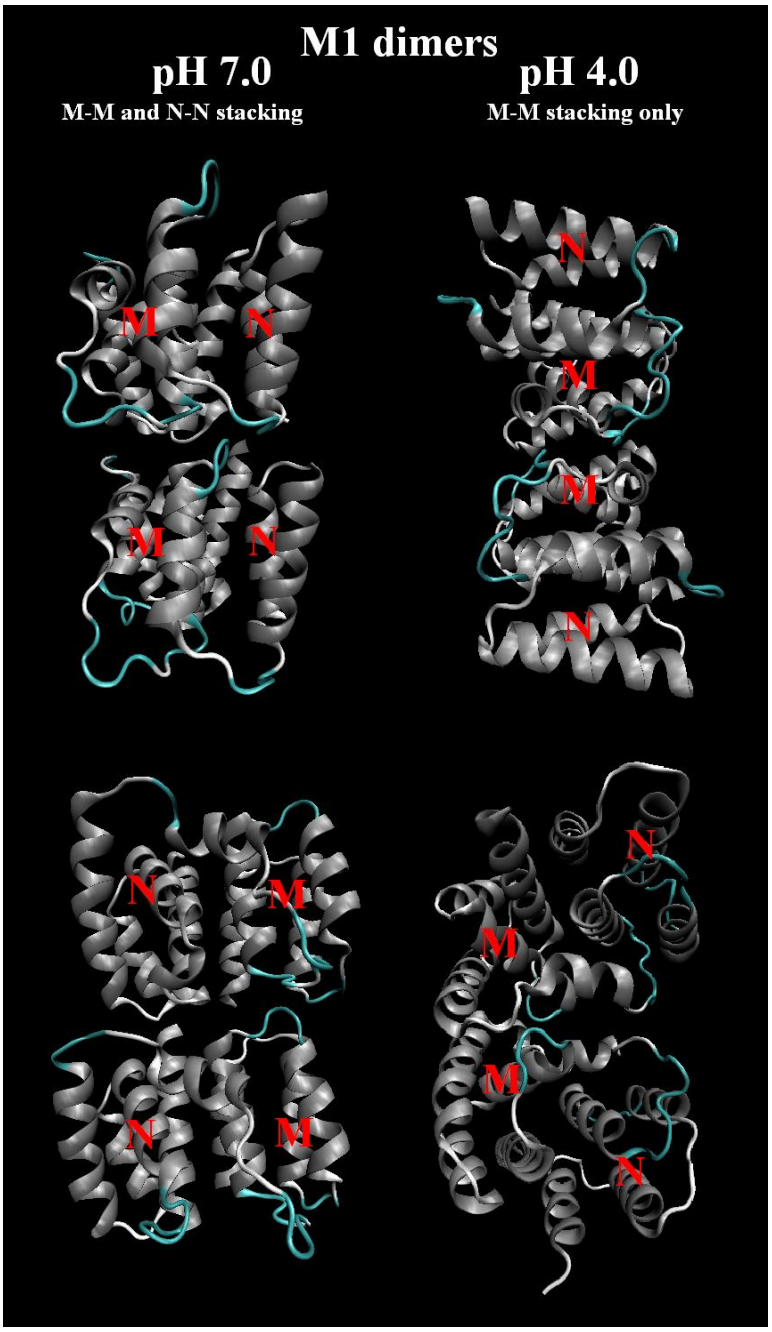

Figure 2: Structure of the M1 protein dimers (fragment 1-162), at neutral and acidic pH. 3D-structure from Sha & Luo (1997) – pdb code: 1AA7 and Artz *et al.* (2001) – pdb code: 1EA3. Figure performed with VMD (Humphrey *et al.*, 1996).

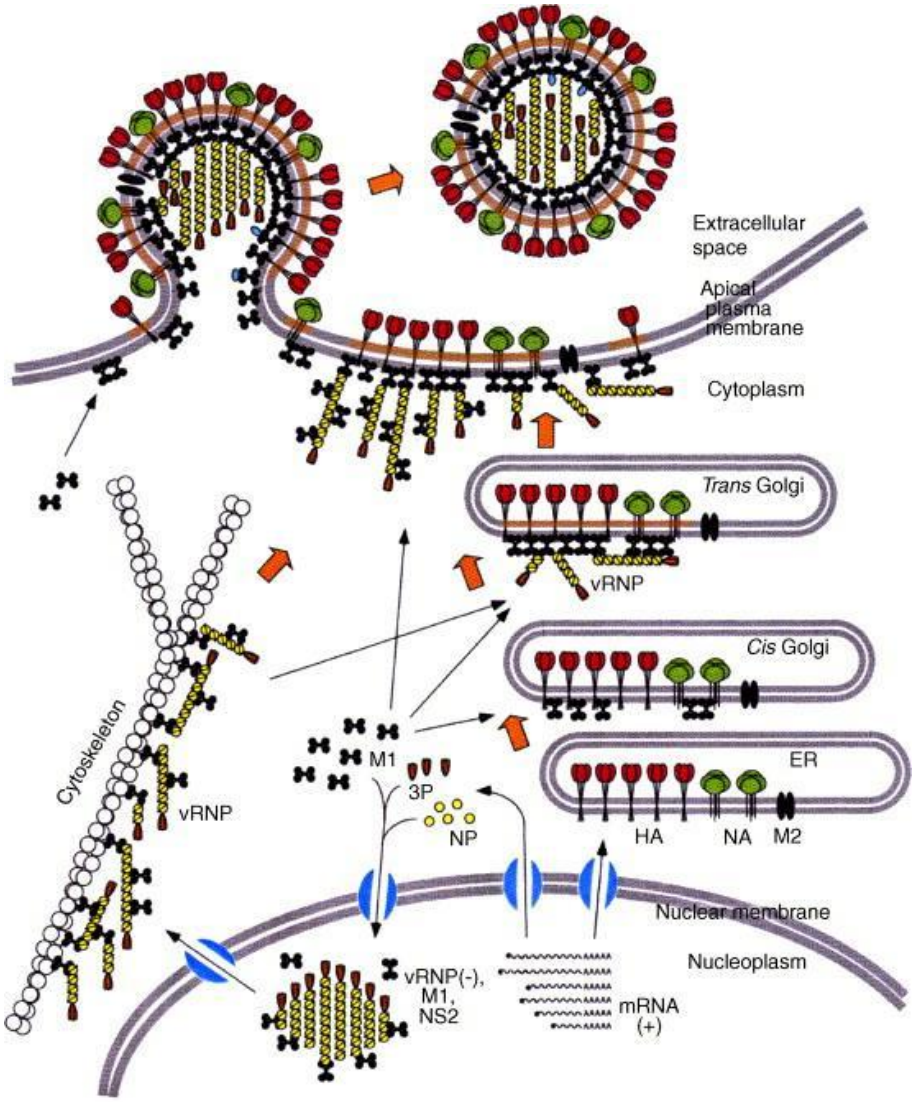

Figure 3: Role of the M1 protein in the nuclear export of native viral ribonucleoproteins and in the budding process. Nuclear export of vRNPs at the end of the replication cycle is performed through the interaction of NEP protein (formerly "NS2") with cellular exportins, the NEP protein being physically linked to vRNPs via the M1 protein. The M1 protein is thought to permit the vRNPs to reach the cell surface at the budding site, notably by interaction with the cytoskeleton. There, the M1 protein forms a bridge between the surface elements of the future virions (HA, NA, M2 and viral membrane) and the internal elements among which the vRNPs. Reproduced with permission of Nayak *et al.* (2004).

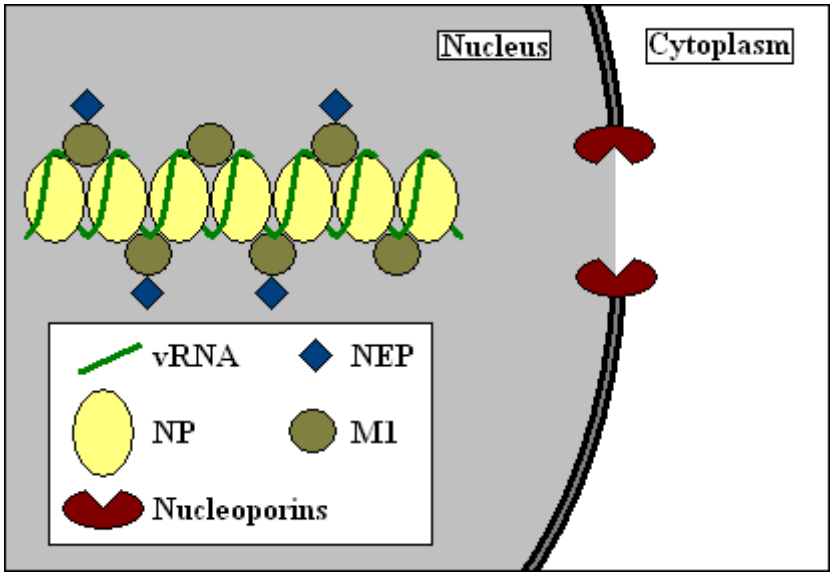

Figure 4: Nuclear export of native ribonucleoproteins. The M1 protein forms the link between NEP protein – interacting with cellular exportins – and the vRNPs. Adapted from O'Neill *et al.* (1995).

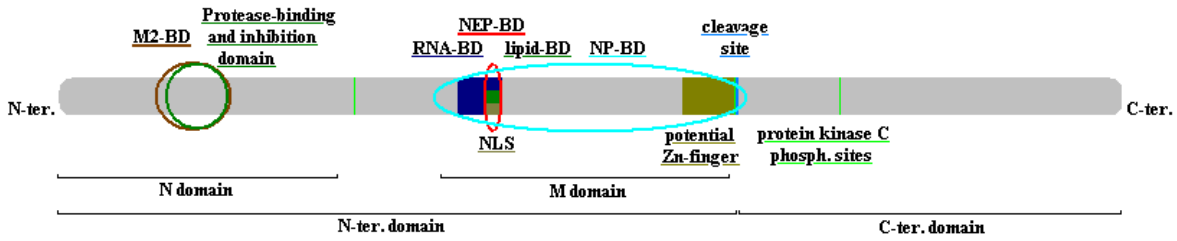

Figure 5: Functional domains of M1 protein. The M1 protein is 252 residue-long. Purified M1 is almost systematically cleaved at position 162, which defines an N-terminal domain and a C-terminal part (Sha & Luo, 1997). The N-terminal domain is further subdivided into a N domain and a M domain in the 3D-structure of the protein (Harris *et al.*, 2001). The M1 protein binds NEP (NEP-BD: 101-105), M2 (M2-BD: amino acids 22, 31 and 41), NP (88-165), and the cytoplasmic tail of HA and NA (undefined domains) (Ali *et al.*, 2000; Akarsu *et al.*, 2003; Baudin *et al.*, 2001; McCown & Pekosz, 2005; Noton *et al.*, 2007; Roberts *et al.*, 1998; Zebedee & Lamb, 1989). The 101-RKLKR-105 region also constitutes an NLS, the lipid-binding site (lipid-BD), and its residues are thought to be the most important of the 95-105 RNA-binding domain (RNA-BD) of the M1 protein (Artz *et al.*, 2001; Baudin *et al.*, 2001; Elster *et al.*, 1997; Hui *et al.*, 2003; Liu & Ye, 2002). A Zn-finger motif was described but its putative role in RNA-binding is still to be confirmed (potential Zn-finger: 148-162) (Wakefield & Brownlee, 1989). M1 contains three conserved protein kinase C phosphorylation sites (S70, S161 and T185) (Reinhardt & Wolff, 2000). Residues 25-40 of M1 are thought to inhibit the caspase-8 activation (protease-binding and inhibition domain) (Zhirnov *et al.*, 2002).

2.4.13. References

Akarsu H, Burmeister WP, Petosa C, *et al.* Crystal structure of the M1 protein-binding domain of the influenza A virus nuclear export protein (NEP/NS2). *Embo J* 2003; 22: 4646-4655.

Ali A, Avalos RT, Ponimaskin E, *et al.* Influenza virus assembly: effect of influenza virus glycoproteins on the membrane association of M1 protein. *J Virol* 2000; 74: 8709-8719.

Arzt S, Baudin F, Barge A, *et al.* Combined results from solution studies on intact influenza virus M1 protein and from a new crystal form of its N-terminal domain show that M1 is an elongated monomer. *Virology* 2001; 279: 439-446.

Arzt S, Petit I, Burmeister WP, *et al.* Structure of a knockout mutant of influenza virus M1 protein that has altered activities in membrane binding, oligomerisation and binding to NEP (NS2). *Virus Res* 2004; 99: 115-119.

Avalos RT, Yu Z, Nayak DP. Association of influenza virus NP and M1 proteins with cellular cytoskeletal elements in influenza virus-infected cells. *J Virol* 1997; 71: 2947-2958.

Balachandran S, Roberts PC, Kipperman T, *et al.* Alpha/beta interferons potentiate virus-induced apoptosis through activation of the FADD/Caspase-8 death signaling pathway. *J Virol* 2000; 74: 1513-1523.

Barman S, Ali A, Hui EK, *et al.* Transport of viral proteins to the apical membranes and interaction of matrix protein with glycoproteins in the assembly of influenza viruses. *Virus Res* 2001; 77: 61-69.

Baudin F, Petit I, Weissenhorn W, *et al. In vitro* dissection of the membrane and RNP binding activities of influenza virus M1 protein. *Virology* 2001; 281: 102-108.

Bucher DJ, Kharitonenkov IG, Zakomirdin JA, *et al.* Incorporation of influenza virus M-protein into liposomes. *J Virol* 1980; 36: 586-590.

Burleigh LM, Calder LJ, Skehel JJ, *et al.* Influenza a viruses with mutations in the m1 helix six domain display a wide variety of morphological phenotypes. *J Virol* 2005; 79: 1262-1270.

Chelsky D, Ralph R, Jonak G. Sequence requirements for synthetic peptide-mediated translocation to the nucleus. *Mol Cell Biol* 1989; 9: 2487-2492.

Elster C, Fourest E, Baudin F, *et al.* A small percentage of influenza virus M1 protein contains zinc but zinc does not influence *in vitro* M1-RNA interaction. *J Gen*

Virol 1994; 75 (Pt 1): 37-42.

Elster C, Larsen K, Gagnon J, *et al.* Influenza virus M1 protein binds to RNA through its nuclear localization signal. *J Gen Virol* 1997; 78 (Pt 7): 1589-1596.

Gao P, Watanabe S, Ito T, *et al.* Biological heterogeneity, including systemic replication in mice, of H5N1 influenza A virus isolates from humans in Hong Kong. *J Virol* 1999; 73: 3184-3189.

Garcia-Robles I, Akarsu H, Muller CW, *et al.* Interaction of influenza virus proteins with nucleosomes. *Virology* 2005; 332: 329-336.

Gomez-Puertas P, Albo C, Perez-Pastrana E, *et al.* Influenza virus matrix protein is the major driving force in virus budding. *J Virol* 2000; 74: 11538-11547.

Gregoriades A, Christie T, Markarian K. The membrane (M1) protein of influenza virus occurs in two forms and is a phosphoprotein. *J Virol* 1984; 49: 229-235.

Gregoriades A, Frangione B. Insertion of influenza M protein into the viral lipid bilayer and localization of site of insertion. *J Virol* 1981; 40: 323-328.

Gregoriades A, Guzman GG, Paoletti E. The phosphorylation of the integral membrane (M1) protein of influenza virus. *Virus Res* 1990; 16: 27-41.

Gregoriades A. Interaction of influenza M protein with viral lipid and phosphatidylcholine vesicles. *J Virol* 1980; 36: 470-479.

Harris A, Forouhar F, Qiu S, *et al.* The crystal structure of the influenza matrix protein M1 at neutral pH: M1-M1 protein interfaces can rotate in the oligomeric structures of M1. *Virology* 2001; 289: 34-44.

Hinshaw VS, Olsen CW, Dybdahl-Sissoko N, *et al.* Apoptosis: a mechanism of cell killing by influenza A and B viruses. *J Virol* 1994; 68: 3667-3673.

Hiromoto Y, Yamazaki Y, Fukushima T, *et al.* Evolutionary characterization of the six internal genes of H5N1 human influenza A virus. *J Gen Virol* 2000; 81: 1293-1303.

Hui EK, Ralston K, Judd AK, *et al.* Conserved cysteine and histidine residues in the putative zinc finger motif of the influenza A virus M1 protein are not critical for influenza virus replication. *J Gen Virol* 2003; 84: 3105-3113.

Hui EK, Smee DF, Wong MH, *et al.* Mutations in influenza virus M1 CCHH, the putative zinc finger motif, cause attenuation in mice and protect mice against lethal influenza virus infection. *J Virol* 2006; 80: 5697-5707.

Humphrey W, Dalke, A., Schulten, K. VMD - Visual Molecular Dynamics. *J. Molec. Graphics* 1996; 14: 33-38.

Jin H, Leser GP, Zhang J, *et al.* Influenza virus hemagglutinin and neuraminidase cytoplasmic tails control particle shape. *Embo J* 1997; 16: 1236-1247.

Katz JM, Lu X, Tumpey TM, *et al.* Molecular correlates of influenza A H5N1 virus pathogenesis in mice. *J Virol* 2000; 74: 10807-10810.

Kretzschmar E, Bui M, Rose JK. Membrane association of influenza virus matrix protein does not require specific hydrophobic domains or the viral glycoproteins. *Virology* 1996; 220: 37-45.

Lamb RA, Krug RM. *Orthomyxoviridae*: The viruses and their replication. In Fields Virology, Knipe DM, Howley PM, Martin MA, Griffin DE, Lamb RA (eds). Lippincott Williams & Wilkins: Boston, 2001; 1487-1531.

Liu C, Eichelberger MC, Compans RW, *et al.* Influenza type A virus neuraminidase does not play a role in viral entry, replication, assembly, or budding. *J Virol* 1995; 69: 1099-1106.

Liu T, Ye Z. Restriction of viral replication by mutation of the influenza virus matrix protein. *J Virol* 2002; 76: 13055-13061.

McCown MF, Pekosz A. The influenza A virus M2 cytoplasmic tail is required for infectious virus production and efficient genome packaging. *J Virol* 2005; 79: 3595-3605.

Nayak DP, Hui EK, Barman S. Assembly and budding of influenza virus. *Virus Res* 2004; 106: 147-165.

Nermut MV. Further investigation on the fine structure of influenza virus. *J Gen Virol* 1972; 17: 317-331.

Noton SL, Medcalf E, Fisher D, *et al.* Identification of the domains of the influenza A virus M1 matrix protein required for NP binding, oligomerization and incorporation into virions. *J Gen Virol* 2007; 88: 2280-2290.

O'Neill RE, Talon J, Palese P. The influenza virus NEP (NS2 protein) mediates the nuclear export of viral ribonucleoproteins. *Embo J* 1998; 17: 288-296.

Okada A, Miura T, Takeuchi H. Zinc- and pH-dependent conformational transition in a putative interdomain linker region of the influenza virus matrix protein M1. *Biochemistry* 2003; 42: 1978-1984.

Oxford JS, Hockley DJ. Orthomyxoviridae. In Perspective in Medical Virology: Animal Virus Structure., Nermut MV, Steven AC (eds). Elsevier: New York, 1987; 213-232.

Pattnaik AK, Brown DJ, Nayak DP. Formation of influenza virus particles lacking

hemagglutinin on the viral envelope. *J Virol* 1986; 60: 994-1001.

Reinhardt J, Wolff T. The influenza A virus M1 protein interacts with the cellular receptor of activated C kinase (RACK) 1 and can be phosphorylated by protein kinase C. *Vet Microbiol* 2000; 74: 87-100.

Roberts PC, Lamb RA, Compans RW. The M1 and M2 proteins of influenza A virus are important determinants in filamentous particle formation. *Virology* 1998; 240: 127-137.

Ruigrok RW, Barge A, Durrer P, *et al.* Membrane interaction of influenza virus M1 protein. *Virology* 2000; 267: 289-298.

Ruigrok RW, Calder LJ, Wharton SA. Electron microscopy of the influenza virus submembranal structure. *Virology* 1989; 173: 311-316.

Sha B, Luo M. Structure of a bifunctional membrane-RNA binding protein, influenza virus matrix protein M1. *Nat Struct Biol* 1997; 4: 239-244.

Shishkov AV, Bogacheva EN, Dolgov AA, *et al.* The *in situ* structural characterization of the influenza A virus matrix M1 protein within a virion. *Protein Pept Lett* 2009; 16: 1407-1413.

Shishkov AV, Goldanskii VI, Baratova LA, *et al.* The *in situ* spatial arrangement of the influenza A virus matrix protein M1 assessed by tritium bombardment. *Proc Natl Acad Sci U S A* 1999; 96: 7827-7830.

Smeenk CA, Brown EG. The influenza virus variant A/FM/1/47-MA possesses single amino acid replacements in the hemagglutinin, controlling virulence, and in the matrix protein, controlling virulence as well as growth. *J Virol* 1994; 68: 530-534.

Takizawa T, Matsukawa S, Higuchi Y, *et al.* Induction of programmed cell death (apoptosis) by influenza virus infection in tissue culture cells. *J Gen Virol* 1993; 74: 2347-2355.

Timofeeva TA, Klenk ND, Zhirnov OP. [Identification of the protease-binding domain in the N-terminal region of the influenza A virus matrix protein M1]. *Mol Biol (Mosk)* 2001; 35: 484-491.

Wakefield L, Brownlee GG. RNA-binding properties of influenza A virus matrix protein M1. *Nucleic Acids Res* 1989; 17: 8569-8580.

Ward AC, Castelli LA, Lucantoni AC, *et al.* Expression and analysis of the NS2 protein of influenza A virus. *Arch Virol* 1995; 140: 2067-2073.

Ward AC. Neurovirulence of influenza A virus. *J Neurovirol* 1996; 2: 139-151.

Ward AC. Specific changes in the M1 protein during adaptation of influenza virus to mouse. *Arch Virol* 1995; 140: 383-389.

Watanabe K, Fuse T, Asano I, *et al.* Identification of Hsc70 as an influenza virus matrix protein (M1) binding factor involved in the virus life cycle. *FEBS Lett* 2006; 580: 5785-5790.

Watanabe K, Handa H, Mizumoto K, *et al.* Mechanism for inhibition of influenza virus RNA polymerase activity by matrix protein. *J Virol* 1996; 70: 241-247.

Winter G, Fields S. Cloning of influenza cDNA into M13: the sequence of the RNA segment encoding the A/PR/8/34 matrix protein. *Nucleic Acids Res* 1980; 8: 1965-1974.

Wu CY, Jeng KS, Lai MM. The SUMOylation of Matrix Protein M1 Modulates the Assembly and Morphogenesis of Influenza A Virus. *J Virol* 2011; 85: 6618-6628.

Yasuda J, Nakada S, Kato A, *et al.* Molecular assembly of influenza virus: association of the NS2 protein with virion matrix. *Virology* 1993; 196: 249-255.

Ye Q, Krug RM, Tao YJ. The mechanism by which influenza A virus nucleoprotein forms oligomers and binds RNA. *Nature* 2006; 444: 1078-1082.

Ye Z, Liu T, Offringa DP, *et al.* Association of influenza virus matrix protein with ribonucleoproteins. *J Virol* 1999; 73: 7467-7473.

Ye Z, Robinson D, Wagner RR. Nucleus-targeting domain of the matrix protein (M1) of influenza virus. *J Virol* 1995; 69: 1964-1970.

Ye ZP, Baylor NW, Wagner RR. Transcription-inhibition and RNA-binding domains of influenza A virus matrix protein mapped with anti-idiotypic antibodies and synthetic peptides. *J Virol* 1989; 63: 3586-3594.

Ye ZP, Pal R, Fox JW, *et al.* Functional and antigenic domains of the matrix (M1) protein of influenza A virus. *J Virol* 1987; 61: 239-246.

Zebedee SL, Lamb RA. Growth restriction of influenza A virus by M2 protein antibody is genetically linked to the M1 protein. *Proc Natl Acad Sci U S A* 1989; 86: 1061-1065.

Zhang J, Lamb RA. Characterization of the membrane association of the influenza virus matrix protein in living cells. *Virology* 1996; 225: 255-266.

Zhang J, Li G, Liu X, Wang Z, *et al.* Influenza A virus M1 blocks the classical complement pathway through interacting with C1qA. *J Gen Virol* 2009; 90: 2751-2758.

Zhao H, Ekstrom M, Garoff H. The M1 and NP proteins of influenza A virus form homo- but not heterooligomeric complexes when coexpressed in BHK-21 cells. *J Gen Virol* 1998; 79 (Pt 10): 2435-2446.

Zhirnov OP, Klenk HD. Histones as a target for influenza virus matrix protein M1. *Virology* 1997; 235: 302-310.

Zhirnov OP, Ksenofontov AL, Klenk ND. [Influenza A virus M1 matrix protein is similar to protease inhibitors]. *Dokl Akad Nauk* 1999; 367: 690-693.

Zhirnov OP, Ksenofontov AL, Kuzmina SG, *et al*. Interaction of influenza A virus M1 matrix protein with caspases. *Biochemistry (Mosc)* 2002; 67: 534-539.

Zhirnov OP. Isolation of matrix protein M1 from influenza viruses by acid-dependent extraction with nonionic detergent. *Virology* 1992; 186: 324-330.

2.5. The nonstructural protein 1 and nuclear export protein

2.5.1. Non structural protein 1.

The non structural protein 1 (NS1) is a 237 amino acid-long protein found both in the nucleus (throughout the virus cycle) and the cytoplasm (late in the cycle) of influenza virus–infected cells, but not into virions, thus being non structural *stricto sensu* (Lamb & Krug, 2001). It essentially binds RNA and different cellular transcription factors. Nuclear NS1 plays two essential roles: inhibition of pre-mRNAs splicing and prevention of nuclear export of cellular poly(A)-containing mRNAs (Alonso-Caplen *et al.*, 1992; Fortes *et al.*, 1994; Lu *et al.*, 1994; Qian *et al.*, 1994; Qiu & Krug, 1994; Qiu *et al.*, 1995). Cytoplasmic NS1 associates with polysomes (Compans, 1973; Krug & Etkind, 1973; Krug & Soeiro, 1975), is implicated in the preferential translation of viral rather than cellular mRNAs, binds double-stranded RNA and prevents the activation of Protein Kinase R (PKR) and the subsequent interferon (IFN) response (de la Luna *et al.*, 1995; Enami *et al.*, 1994; Garfinke & Katze, 1993; Lu *et al.*, 1995). NS1 protein was shown to specifically enhance the initiation rate of translation of viral mRNAs (de la Luna *et al.*, 1995). As some strains with mutated NS1 show blunted expression of viral genes expressed late during the virus cycle, NS1 is also supposed to regulate their expression, which is compatible with its interference with cell translation and its enhancing of viral mRNAs translation (Koennecke *et al.*, 1981; Min *et al.*, 2007; Shimizu *et al.*, 1982). A variant of the A/PR/8/34 strain lacking the NS1 gene was shown to induce apoptosis more rapidly than the wild-type virus in MDCK (Madin-Darby Canine Kidney, ATCC CCL-34) cells, chicken fibroblasts and chicken embryos, but not in IFN-deficient Vero (African Green Monkey Kidney, ATCC CCL-81) cells (Zhirnov *et al.*, 2002). It is therefore also hypothesized that NS1 prevents apoptosis in an interferon-dependent way, probably through the aforementioned inhibition of PKR activation (Zhirnov *et al.*, 2002).

Mutational analysis combined with gel shift assays led to the identification of two functional domains, one permitting dimerization and binding of RNA (amino-terminal) and the other (carboxy-terminal) selectively blocking the poly(A)-mRNA nucleocytoplasmic translocation machinery (Qian *et al.*, 1994). Only dimerized NS1 binds RNA and blocks cellular mRNAs nuclear export (Chen *et al.*, 1999; Wang *et al.*, 1999).

Double mutation of residues 127 and 205 or single mutation of residue 209 were associated with enhanced virulence in mice (Pu *et al.*, 2010).

2.5.1.a. Structure and dimerization domain

Gel filtration chromatography results suggested that NS1 exists as a dimer both in the absence of an RNA target and when it is bound to a specific RNA target, U6 snRNA. Mutational analyses first indicated that the RNA-binding and dimerization domains were coincident (Nemeroff *et al.*, 1995). Dimerization was also demonstrated *in vivo* with yeast two-hybrid assays but, contrasting with *in vitro* results, deletion or mutations altering RNA-binding function did not automatically abolish NS1-NS1 interactions (Wang *et al.*, 1999). The dimer formation was shown to occur independently of the carboxy-terminal two-thirds (74-237 fragment) of the protein (Chien *et al.*, 1997; Liu *et al.*, 1997; Qian *et al.*, 1995). However, as addition of heterologous dimerization domains to the first 73 N-terminal residues of NS1 restores viral pathogenicity in wild-type mice, it is hypothesized that the carboxy-terminal two-thirds stabilize the dimers which maximizes interferon antagonism.

Nuclear Magnetic Resonance spectroscopy and X-ray crystallographic studies confirmed that the N-terminal (1-73) domain of the A/Udorn/72 NS1 protein is dimeric and showed that it forms six α-helices (three per monomer; Figure 1). For each monomer, helix 1 spans on residues 3 to 25, helix 2 on residues 30 to 50 and helix 3 on residues 54 to 69 (Chien *et al.*, 1997; Liu *et al.*, 1997). Two short turns connect the three helices and the two monomers are assembled in an anti-parallel orientation in the dimer (Chien *et al.*, 1997; Liu *et al.*, 1997). Helix 2 crosses helix 1 with an about 30° angle, while helix 3 is packed across the other two helices. The surface buried by the dimer interface is 1,477 $Å^2$ (Liu *et al.*, 1997). Within each monomer, and in addition to hydrophobic interactions between helix 1 and helix 2, salt bridges are present between R19 and D39 and between R46 and D12, and there is a hydrogen bond between W16 and L36 (Liu *et al.*, 1997). By alanine substitution experiments, five residues (D12, R19, D29, R35 and R46) were shown to be involved in the dimer formation by forming intermolecular hydrogen bonds and electrostatic interactions at the dimer interface (Chien *et al.*, 1997; Liu *et al.*, 1997; Wang *et al.*, 1999). There are hydrogen bonds between residues 26, 27 and 29 of first loop of one monomer with residues 4, 5, 7 and 8 of helix 1 of the other monomer, and between residue 35 of helix 2 of one monomer and

residue 12 of helix 1 of the other (Liu *et al.*, 1997). A structural network of H_20 molecules is present at the interface between residues 12 and 19 of helix 1 and residues 35 and 39 of helix 2. However, an intact helix 3 (residues 54-69) is required for the stabilization of the dimer, probably by hydrophobic interactions (Wang *et al.*, 1999).

This dimeric structure is able to bind RNA via one or more *α*-helices (Chien *et al.*, 1997; Liu *et al.*, 1997). RNA-binding domains of proteins classically present a *β*-sheet structure, but several *α*-helical RNA-binding domains have already been described, notably that of the HIV-1 (Human Immunodeficiency virus-1) Rev protein (Battiste *et al.*, 1996; Wang *et al.*, 1999). Although NS1 dimerization is a prerequisite for RNA binding, it is not sufficient. A specific set of residues critically affects the RNA binding activity of NS1-NS1 dimers (Wang *et al.*, 1999) (see further).

Further studies show that the H5N1 NS1 "effector domain" (residues 73-230) is made of seven *β*-strands and three *α*-helices (Bornholdt & Prasad, 2006) (Figure 2). This 73-230 C-terminal fragment is present as a dimer. The *β*-strands are present on residues: 88-91 (strand 1), 107-112 (strand 2), 115-120 (strand 3), 126-136 (strand 4), 142-151 (strand 5), 157-162 (strand 6), and 191-194 (strand 7). The *α*-helices span on residues 95-99, 171-188 and 195-205. Residues 73-78 and 206-230 are disordered. The first six *β*-strands form an antiparallel twisted *β*-sheet, while the last smaller one interacts with strand 4 in a parallel manner (Bornholdt & Prasad, 2006). The central 171-188 helix is surrounded by *β*-strands 2 to 7 (Bornholdt & Prasad, 2006) (Figure 2). This structure is stabilized by multiple hydrophobic interactions between the *α*-helix and the *β*-strands. For this C-terminal fragment, the dimer interface is formed by the first *β*-strand (88-91) of each monomer, which run antiparallely one to each other (Bornholdt & Prasad, 2006). The dimer thus consists in two antiparallel *β*-sheets, with the long *α*-helix of each monomer at each extremity of the dimer (Bornholdt & Prasad, 2006) (Figure 2).

The effector domain is thought to switch between several conformations putatively called 'helix-closed' and 'helix-open' conformations, which could allow the interaction with different cellular partners depending on the conformation during the infection cycle (Kerry *et al.*, 2011).

The C-terminal part of the NS1 effector domain and more specifically residue 196 is involved in the blockade of IRF3 activation and IFN*β* transcription (Kuo *et al.*, 2010). Since the NS1 mutant deficient for IRF3 inhibition still retain TRIM25 binding, this binding is probably not involved in IRF3 inhibition.

2.5.1.b. RNA-binding domain

Dimeric NS1 binds to dsRNA and to a specific stem-bulge in the spliceosomal U6 snRNA (and to U6atac snRNA) with similar dissociation constants and thus sequesters dsRNA and inhibits pre-mRNA splicing both *in vitro* and *in vivo* (Fortes *et al.*, 1994; Hatada & Fukuda, 1992; Lu *et al.*, 1994; Qiu & Krug, 1994; Qiu *et al.*, 1995; Wang & Krug, 1998). The NS1 RNA-binding function is exercised by the amino-terminal 1-73 third of the protein, provided this latter dimerizes (Chien *et al.*, 1997, Liu *et al.*, 1997; Qian *et al.*, 1995). Alanine substitution experiments showed that residues R38 and K41 (in helix 2) are essential to RNA-binding without being required for dimer formation, and that the side chains of R37 and R44, although not critically necessary, contribute to RNA-binding too (Wang *et al.*, 1999). Substitution of R38 or K41 by another basic residue such as lysine or arginine, respectively, does not affect the RNA-binding properties, thus emphasizing the need of a basic residue at these positions (Wang *et al.*, 1999). Further confirmation of the critical importance of these two residues is found in the fact that they are conserved among influenza A and B strains (Wang *et al.*, 1999). According to personal sequences alignments, both R38 and K41 are extremely conserved among influenza A strains. The R38K or K41R substitutions are observed in some strains, but these substitutions conserve the properties (basic residues) of the amino acids and are thus compatible with their role in RNA binding.

In the dimer conformation, helix 2 and helix 2' interface in an anti-parallel fashion, which generates an interacting domain where both R38 and K41 of each monomer are exposed (Figure 1). The distance between R38 and R38' is about 16.5 Å, which is very close to the distance between the anti-parallel phosphodiester backbones surrounding the minor groove in dsRNA, the arginine basic residues interacting with the negatively charged phosphate moieties (Wang *et al.*, 1999). K41 and K41' are thought either to directly bind RNA, or to improve/strengthen RNA-binding by residues R38 and 38' (Wang *et al.*, 1999).

By specific binding to dsRNA, the influenza NS1 protein was shown to suppress RNA interference mechanisms in plants and in *Drosophila* (Bucher *et al.*, 2004; Delgadillo *et al.*, 2004; Li *et al.*, 2004). It is tempting to suggest that those RNA silencing properties of NS1 could have appeared to protect the virus against such antiviral immunity inside the cell, but the possible existence of such cellular immunity has still to be confirmed (Li *et al.*, 2004). However, it was shown that NS1 protein was unable to suppress RNA

interference in HeLa cells (Kok & Jin, 2006). Further experiments are thus needed to enlighten this point.

NS1 was also shown to interact with vRNPs, especially with the nucleoprotein, via its RNA-binding domain and mutation of residues 38 and 41 of NS1 abolished the interaction, while RNA-binding only partially contributed to the NP-NS1 interaction (Robb *et al.*, 2011).

The NS1 protein interacts with heterogeneous nuclear ribonucleoprotein F (hnRNP-F) through its RNA-binding domain (residues 1-73), which regulates the viral transcription and the expression of host genes (Lee *et al.*, 2010).

2.5.1.c. Inhibition of Protein Kinase R activation

Until recently, the common hypothesis explaining the inhibition of the IFN-pathway activation was that NS1, by binding and masking dsRNA, prevented the activation of PKR (Garcia-Sastre, 2001). Studies by Li *et al.* (2006) showed that NS1 was able to bind PKR directly, which was shown to inhibit its activation (Li *et al.*, 2006; Min *et al.*, 2007). This binding was present even when a R38A mutant of NS1 was expressed instead of wild-type NS1, which demonstrates that the RNA-binding properties are not required for the inhibition of PKR activation (Li *et al.*, 2006). The 123-127 sequence of NS1 was proposed to be the PKR-binding site on NS1 protein, since the 123/124 and 126/127 alanine mutants were no more able to bind it (Min *et al.*, 2007). But it was not demonstrated whether these 123/124 and 126/127 alanine mutants were still able to dimerize. If those mutants are no more able to dimerize, nothing can prove that the 123-127 domain actually functions as the PKR-binding site. On the other hand, the fact that those two mutants are not able to bind PKR is not sufficient to conclude that the 123-127 sequence is the PKR-binding site since alanine substitution of these residues can disorganize the 3D-structure of the surrounding domains, which might contain the real PKR-binding site. Finally, studies with Vero-adapted influenza strains showed that mutants with shortened NS1 protein were able to grow with the same efficiency in Vero cells (type I IFN-deficient), but were less efficient in MDCK (Egorov *et al.*, 1998) (see further). Expression of a truncated NS1 protein consisting of residues 1-125 of wild-type NS1 rescued influenza strains with short NS1 protein when infecting MDCK cells or in IFN-stimulated Vero cells, showing that the 1-125 fragment was sufficient to inhibit the IFN-response activation and thus the PKR activation (Kittel *et al.*, 2004).

This last result partially disagrees with works of Min *et al.* (2007) since it tends to exclude the putative role of residues 126 and 127 in PKR-binding.
The A149V substitution was shown to render the NS1 protein unable to antagonize the interferon response in chicken embryo fibroblasts, suggesting that other residues are implicated than the sole 123-127 sequence (Li *et al.*, 2006). Thus, further investigations are required to delineate the PKR-binding site more precisely.

2.5.1.d. Viral mRNA synthesis regulating domain

During their experiments, Min and colleagues (2007) found an enhanced rate of viral protein synthesis as early as 0.75 h post-infection for the 123/124 alanine mutant, suggesting that the NS1 protein controls the temporal regulation of viral mRNA synthesis and that residues I123 and M124 of NS1 are involved in this function. This result is crucial because it partially elucidates what remained unanswered for more than twenty years, i.e. how the expression of the different influenza proteins is regulated during the infectious cycle. The NS1 protein was already suspected to be implicated in such a regulation but it was not confirmed yet (Falcon *et al.*, 2004; Marion *et al.*, 1997). Since this deregulation also occurs when infecting mouse PKR-/- cells with the 123/124 alanine mutant virus, this function is not dependent on the inhibition of PKR. The authors conclude to a probable interaction between NS1 and the viral polymerase, which remains to be confirmed. Residues I123 and M124 are exposed on a loop between two β-sheets and are thus potentially able to interact with the viral polymerase (Bornholdt & Prasad, 2006; Min *et al.*, 2007). However, as aforementioned, alanine substitution of residues 123 and 124 might disorganize the surrounding domains, which could be responsible for the observed phenotype without any role of these residues. Once more, it was not confirmed that the 123/124 alanine mutant NS1 protein is still able to dimerize. These questions are still to be answered for.

2.5.1.e. Domain coding for selective inhibition of cell mRNAs nuclear export

Dimeric NS1 protein inhibits the nucleocytoplasmic translocation of spliced mRNAs containing a poly(A) tail produced by the cellular cleavage/polyadenylation system (Alonso-Caplen *et al.*, 1992; Fortes *et al.*, 1994; Qian *et al.*, 1994; Qiu & Krug, 1994), thus leaving unaltered the nuclear export of poly(A) tail-containing viral mRNAs and

cellular mRNAs of which the 3'-end is produced by a specific set of factors (histones). This function is supported by the carboxyl half of NS1, provided a dimeric conformation is adopted. Conversely, an intact RNA-binding function by the amino-terminal third of the protein is dispensable (Chen & Krug, 2000). The inhibition of nuclear export was assigned to specific subdomains of the NS1 C-terminal two-thirds.

- *"Historical" Rev-like subdomain*

The blockade of cellular mRNAs nucleocytoplasmic translocation was first shown to be exercised by the carboxyl half of NS1, with a major role probably played by the 10-mer "FDRLETLILL" (amino acids 138 through 147) which is similar to the consensus sequence found in the effector domains of lentivirus Rev proteins (Qian *et al.*, 1994). By analogy with Rev, this NS1 domain was presumed to interact with host nuclear proteins involved in the nucleocytoplasmic RNA translocation machinery, an interaction that would thus block the nuclear export. Like the HIV Rev protein effector domain, the influenza virus NS1 Rev-like domain possesses two conserved leucine residues, at positions 7 and 9. However, although very suggesting at first sight, these similarities could be more cosmetic than really relevant in terms of biological function. For example, a recombinant HIV expressing a Rev protein with a loss of function mutation present a dominant negative phenotype (preventing the action of wild-type Rev protein), while a leucine to alanine substitution at position 7 of the RNA translocation blocking domain of NS1 led to a recessive negative phenotype (Qian *et al.*, 1994). Furthermore, a leucine to alanine change at position 7 or 9 renders NS1 equally dispersed in the whole cell throughout the virus cycle, while wild-type NS1 is nuclear at first, equally distributed after. By contrast, mutations in the effector domain of the Rev protein of the HIV-1 virus do not affect its nuclear localization (Greenspan *et al.*, 1988; Qian *et al.*, 1994). Another striking observation is that Rev facilitates nuclear export while NS1 inhibits it. Mutation of three residues of the NS1 subdomain (residues 6, 8 and 10) to mimic the sequence of the Rev effector domain without inducing major changes in the NS1 protein led to a loss of function of this NS1 effector domain but not to an enhanced nuclear export as expected (Qian *et al.*, 1994). Taken together, these sequence and function data suggest that both domains interact with the translocation machinery, but via distinct partner molecules (Qian *et al.*, 1994). L144 and 146 are much conserved, but L144 is more conserved than L146. L144 is replaced by isoleucine in many H3N2

strains and L146 is frequently replaced by serine (personal investigations). L146 is thus probably not essential. Recent experimental data led to the identification of two partner proteins for the NS1 protein.

- *Cleavage and polyadenylation specificity factor-binding subdomain*

Yeast two-hybrid assays and co-immunoprecipitation studies permitted the identification of an interaction between NS1 and the 30 kDa subunit of the cleavage and polyadenylation specificity factor (CPSF), a key component of the 3'-end processing machinery of pre-mRNAs (Barabino *et al.*, 1997; Keller *et al.*, 1991; Nemeroff *et al.*, 1998). Such NS1/CPSF interaction could explain, at least in part, the inhibition of the 3'-end cleavage and polyadenylation of cellular pre-mRNAs in influenza virus infected cells. The CPSF 30kDa subunit-binding site probably spans between residues 175 and 210 (Li *et al.*, 2001). A recombinant A/Udorn/72 virus, with an altered amino acid sequence around residue 186 (residues 184-188), displayed the following properties: (i) inability to bind the CPSF 30 kDA subunit, (ii) significant attenuation of virulence for GRE cells and (iii) dramatically enhanced production of cellular antiviral mRNAs as a result of the early interferon-independent activation of transcription (Noah *et al.*, 2003). The binding of CPSF by NS1 thus plays a major role in the inhibition of the processing of newly synthesized cellular mRNAs and notably the production of IFN-independent cellular antiviral mRNAs. This inhibition completes that afforded by the inhibition of PKR activation. Thus, the emerging paradigm is the following: nuclear and cytoplasmic NS1 oppose IFN-independent and IFN-dependent cellular antiviral responses by sequestering either the CPSF 30 kDa subunit or PKR, respectively (Krug *et al.*, 2003; Noah *et al.*, 2003). There remains that some IFNα and $-\beta$-induced mRNAs, such as the MxA mRNA in human cells, are still produced during influenza infection (Geiss *et al.*, 2002), suggesting that the inhibition of type I IFNs-dependent processes by NS1 is not complete (Krug *et al.*, 2003). It is suggested that a tuning of the CPSF-binding site availability occurs during infection, perhaps through the subcellular redistribution of NS1 upon activation of its nuclear export signal (NES, see after), thus causing a steep increase of the nuclear CPSF/NS1 ratio which should result in the restoration of CPSF-dependent mRNA processing activity (Krug *et al.*, 2003; Li *et al.*, 1998). CPSF is also involved in the splicing of cellular single-intron pre-mRNAs *in vivo* since they require the 3'-end processing of the pre-mRNA, which depends on CPSF. The NS1 protein,

which inhibits the 30 kDa subunit of CPSF, prevents the 3'-end processing of such pre-mRNAs and thus their subsequent splicing (Li *et al.*, 2001). In contrast, the inhibition of poly(A) binding protein II (see below) does not interfere with the single-intron splicing process (Li *et al.*, 2001).

Residues 184 to 188 ("GLEWN") were shown to be the most important for CPSF-binding by the NS1 protein (Noah *et al.*, 2003). On the crystal structure of the NS1 effector domain, it appears that these residues are at the base of the long eccentric *α*-helix (Bornholdt & Prasad, 2006) ("helix 2" on Figure 2). Each side of the dimer thus presents one CPSF-binding site, suggesting that the dimer is able to bind two CPSF molecules. Residues 184-188 are globally highly conserved, and W187 is invariable (personal results). L185 is frequently replaced by F in avian and swine strains, and exceptionally by I or P. A lysine at position 186 is typically found in all equine and canine influenza A strains available in GenBank instead of an E residue (but K186 is also present in some H5N2 avian strains). Our sequences alignments also show that a N188S substitution is infrequently observed, while a G184E substitution is present in some rare avian strains.

Glycine 184 was confirmed as critical for host interferon response control by the virus and subsequent virulence of PR8 influenza strain (Steidle *et al.*, 2010).

- *Poly(A)-binding protein II-binding subdomain*

In influenza virus–infected cells, 3' cleavage of some cellular pre-mRNAs still happens despite the NS1-associated inhibition of CPSF function. The cleavage is followed by the addition of short poly(A) tails catalyzed by the cellular poly(A) polymerase (PAP). However, subsequent processive elongation of these short poly(A) tails does not occur because NS1 also inhibits the postcleavage processive elongation of poly(A) chains mediated by poly(A)-binding protein II (PABII) and PAP. This results in the accumulation of cellular mRNAs with very short poly(A) tail (about ten A residues) and thus a reduced nucleocytoplasmic translocation (Chen *et al.*, 1999; Nemeroff *et al.*, 1998). PABII participates to the polyadenylation complex, with CPSF and PAP, it fixes on the short poly(A) stretch of 10-12 residues added by the PAP/CPSF pair after cleavage of the pre-mRNA, and by doing so permits the repetitive elongation of the short stretch to form a complete poly(A) tail (Bienroth *et al.*, 1993; Wahle, 1995). Binding of NS1 protein to PABII was demonstrated by yeast two-hybrid screening and

nonoverlapping regions of NS1 were found to be engaged in PABII and CPSF binding (Chen *et al.*, 1999). Moreover, PABII and the 30 kDa CPSF subunit are most likely to bind each other, independently on the presence of NS1. Binding of NS1 therefore generates a ternary complex which presumably alters the functional interaction of PABII with PAP, thus resulting in the cessation of poly(A) tract elongation (Chen *et al.*, 1999). PABII is essentially located in the nucleus but shuttles between nucleus and cytoplasm, which led to the hypothesis that PABII could be directly involved in the nuclear export of poly(A) tailed mRNAs by binding to the poly(A) tail when located in the nucleoplasm and freeing it when translocated in the cytoplasm (Chen& Krug, 2000). Therefore, blockade of cellular mRNAs nuclear export could also result from the known suppression of PABII shuttling by NS1.

In face of the plethoric blocking strategies opposed by influenza viruses to the traffic of cell mRNAs, it is still unclear how viral mRNAs are exported. These mRNAs are presumably also exported through the binding of one or more cellular protein(s) on their poly(A) tail. These proteins are not identified yet. Importantly, there are three different types of influenza mRNAs, with each being possibly exported by a specific mechanism (Chen & Krug, 2000). First, the six largest influenza genomic segments are transcribed into six colinear mRNAs, without introns. Second, there are the two intron-containing but unspliced mRNAs of the two smallest segments (M and NS) which encode the matrix 1 and the NS1 proteins. Finally, the third type consists of the two spliced mRNAs of the same two segments, encoding matrix 2 and NEP proteins. How these viral mRNAs are exported from the nucleus to the cytoplasm to be translated remains to be answered for (Chen & Krug, 2000).

Results gathered from deletion experiments are compatible with a PABII-binding subdomain extending between residues 223 and 237 (Li *et al.*, 2001).

2.5.1.f. Viral translation-enhancing domain

Co-immunoprecipitation assays revealed an interaction between NS1 and the eukaryotic initiation factor 4GI (eIF4GI), the largest subunit of the eIF4F cap-binding complex, implying a functional correlation between eIF4GI-binding by NS1 and enhancement of viral translation (Aragon *et al.*, 2000). Together with the RNA-binding properties of the NS1 protein, this new interaction suggests that NS1 recruits the eIF4GI subunit at the level of viral mRNAs and thus favors translation of viral over cellular proteins (Aragon

et al., 2000). As NS1 binds 5'-mRNA ends and poly(A) tail structures and because the poly(A) tail has been proposed to bind initiation factors for enhancing translation, an attractive hypothesis could be that NS1 causes a circularization of viral mRNAs that leads to the shunting of terminating ribosomes directly from the 3'-end of viral mRNAs to their 5'-end for a new translation. This would result in an exquisitely efficient cyclic translation process of influenza virus proteins (Aragon *et al.*, 2004; Gallie & Tanguay, 1994; Jacobson, 1996). The demonstration of an *in vivo* interaction between NS1 and the poly(A)-binding protein 1 (PABP1) agrees with this hypothesis (Burgui *et al.*, 2003) (see further).

Marion *et al.* (1997) were the first to show that the N-terminal 113 residues of NS1 were able to enhance the translation of influenza mRNAs, whereas the first 81 residues were not. Further studies by Aragon and colleagues (2000) enlightened the binding of eIF4GI on the first 113 N-terminal amino acids but not on the first 81. Thus, the viral translation enhancing-domain, or eIF4GI-binding site of NS1, most probably spans between residues 82 and 113. The precise residues involved in these functions have still to be determined.

2.5.1.g. Poly(A)-binding protein 1-binding site

Since NS1- and poly(A)-binding protein 1 (PABP1)-binding sites on eIF4GI are adjacent, the possibility that NS1 could displace PABP1 on eIF4GI had to be explored. Studies by Burgui *et al.* (2003) demonstrated that NS1 and PABP1 exploit adjacent but specific and nonexcluding binding sites and thus do not compete for eIF4GI binding. Moreover, both molecules bind to each other, suggesting the possible formation of complexes *in vivo*. The interaction of NS1 with both eIF4GI and PABP1 is thought to cooperatively enhance the translation of viral mRNAs (Burgui *et al.*, 2003). The PABP1-binding site on NS1 was located at residues 1 to 81 (Burgui *et al.*, 2003). It has to be emphasized here that PABP1 is strictly cytoplasmic and does not share any sequence homology with the nucleocytoplasmic PABII protein.

2.5.1.h. Caspase-1 inhibition

Infection of human macrophages by engineered mutant influenza viruses coding truncated variants of the NS1 protein results in a modification of pro-inflammatory

cytokines pattern (Stasakova *et al.*, 2005). By comparison with the wild-type A/PR/8/34 virus, a mutant virus encoding a NS1 protein shortened to its first 125 N-terminal residues (NS1|1-125|) caused a significantly enhanced production of IFN-*β*, interleukin 6 (IL6), Tumor Necrosis Factor *α* (TNF*α*) and CCL3 (MIP-1*α*), while levels of IL1*β* and IL18 remained low (Stasakova *et al.*, 2005). A second set of mutants (delNS1, lacking the NS1 gene, and NS1|del40-80|, lacking residues 40 to 80) caused an enhanced production of all cytokines measured (IL1*β* and IL18 included) accompanied by a rapid onset of apoptosis (Stasakova *et al.*, 2005). Interestingly, IL1*β* and IL18 are produced from the cleavage of pro-IL1*β* and pro-IL18 by caspase-1, a protease that is activated during the apoptosis process (Ghayur *et al.*, 1997). Since the activation of caspase-1 does not occur in human macrophages infected by either wild-type or by the NS1|1-125| influenza viruses, the first 125 amino-terminal residues are supposed to inhibit the caspase-1 activation. On the other hand, as the NS1|1-125| mutant activated the production of the aforementioned panel of cytokines, the C-terminal 126-237 domain of wild-type NS1 likely inhibits the production of these cytokines. The 1-125 fragment of NS1 is able to dimerize and to bind dsRNA as efficiently as the wild-type NS1 protein, and, as said previously, causes similar PKR binding and inhibition and thus similar prevention of IFN-*β* activation (Kittel *et al.*, 2004). This conclusion was confirmed by Donelan *et al.* (2003) who showed a critical role of residues of the second *α*-helix (residues 30 to 50) for the prevention of IFN-*α*/*β* secretion. The NS1|del40-80| mutant possesses an intact C-terminal two-thirds but is unable to dimerize which abolishes its RNA-binding activity and, probably, its PKR-binding activity. The inhibition of the production of the aforementioned set of cytokines thus simultaneously requires dimer formation, RNA-binding properties and an intact C-terminal domain (Stasakova *et al.*, 2005). Concerning the caspase-1 activation, the current view stands that it is prevented by keeping PKR inactivated. This hypothesis remains to be confirmed, at least by elucidating the precise mechanisms causing caspase-1 activation (Stasakova *et al.*, 2005).

2.5.1.i. Phosphatidylinositol 3-kinase-binding sites

The influenza virus was shown to activate the phosphatidylinositol 3-kinase (PI3K) Akt pathway, which favors its replication within the host cell (Ehrhardt *et al.*, 2006). An influenza virus with a mutant NS1 gene failed to present this activation, suggesting a

role of NS1 protein in the PI3K pathway activation (Ehrhardt *et al.*, 2006). It was hypothesized that NS1 protein was able to bind the p85*β* subunit of PI3K (Hale *et al.*, 2006; Shin *et al.*, 2007). This p85*β* subunit of PI3K contains two src Homology 2 (SH2) domains and one SH3 domain (Okkenhaug & Vanhaesebroeck, 2001; Shin *et al.*, 2007). Sequence analysis by Shin *et al.* (2007) showed that NS1 protein contains two proline-rich sequences at positions 164-167 and 213-216, with the consensus sequence "PXXP". Such sequences are typically found in SH3-binding proteins, especially those implicated in the PI3K signaling (Pawson, 1995; Shin *et al.*, 2007). This could permit NS1 protein to bind the p85*β* subunit of PI3K. In addition, NS1 presents an 89-93 "YXXXM" motif, very close to the p85*β* SH2-binding "YXXM" motif, and which also could be involved in the NS1-p85*β* interaction (Shin *et al.*, 2007; Songyang *et al.*, 1993). Co-immunoprecipitation experiments confirmed the NS1-p85*β* interaction (Shin *et al.*, 2007). Reverse genetics studies showed the importance of the two SH3-binding domains and the SH2-binding domain of NS1 in activating the PI3K pathway (Shin *et al.*, 2007). On the 3D-structure of NS1, the SH2-binding domain (89-93) is in *β*-strand 1, in the cleft of each monomer and the SH3-binding motif 1 (164-167) is located within the loop between *β*-strand 6 and the long *α*-helix, those two domains are thus exposed and available to interact with p85 ; the SH3-binding motif 2 (213-216) is in a disordered part of the NS1 protein structure, it can thus not be predicted if this domain is exposed or not (Bornholdt & Prasad, 2006; Shin *et al.*, 2007). Recent results tend to show that NS1 interacts with p85*β* in an SH2-independent manner (Hale *et al.*, 2008). The SH3-binding motif 2 corresponds to a perfect class II motif ("PxϕPx+", where x is any residue, ϕ a hydrophobic residue and [+] a positively charged residue) in many avian strains and in the 1918 Spanish flu NS1 strain, but is almost never present in human influenza isolates (Heikkinen *et al.*, 2008). It appears that such NS1 proteins possessing a perfect class II SH3-binding motif are able to bind the Crk/CrkL proteins, while other NS1 proteins are not (Heikkinen *et al.*, 2008). The SH3-binding motif 2 of such NS1 proteins was shown to interact with the SH3 domain of Crk/CrkL proteins. Besides, the PI3K activation was significantly increased when infecting cells with these avian strains or the 1918 Spanish flu strain, suggesting that the Crk/CrkL binding by NS1 could be responsible for this enhanced activation, which is consistent with the fact that physical and functional interactions are suspected between Crk/CrkL proteins and the PI3K pathway (Heikkinen *et al.*, 2008). A hypothesis is that Crk/CrkL could serve as a linker between NS1 and p85*β* and that the binding of p85*β* by NS1 protein would be sharply

enhanced by the direct binding of Crk/CrkL proteins by NS1 of avian strains (Heikkinen *et al.*, 2008).

2.5.1.j. Nuclear Localization Signals

NS1 protein is found in the cell nucleus during infection as well as in artificial expression systems, which suggests it encodes its own nuclear localization sequence (NLS) (Briedis *et al.*, 1981; Krug & Etkind, 1973; Lamb *et al.*, 1984; Smith *et al.*, 1987; Young *et al.*, 1983). Deletion and fusion proteins experiments showed that the NS1 protein encodes two distinct NLSs, a five-residue basic stretch (NLS1, 34-DRLRR-38) and a longer NLS2 extending between residues 203 to 237 (Greenspan *et al.*, 1983). The NLS1 is highly conserved among influenza A strains (more than the rest of the NS1 protein) and could be part of a larger nuclear localization domain (Greenspan *et al.*, 1983). The NLS2 contains a short basic stretch (216-PKQKRK-221) which could function as the effective NLS, but is much more variable than NLS1, with frequent substitutions by non basic amino acids (Q218 is the sole conserved residue), and is even absent in some naturally occurring strains and is thus most likely to be dispensable (Greenspan *et al.*, 1983) (personal investigations). Both NS1 NLSs are able to individually promote nuclear localization of the protein and are similar to basic NLSs of other known proteins (Simian Virus 40 T antigen and capsides polypeptides, polyomavirus T antigen, *Saccharomyces cerevisiae* ribosomal protein L3; reviewed in Greenspan *et al.* (1983)).

Intriguingly, a 79-173 NS1 fragment (thus without any NLS) located nuclearly, showing that the role played by the both NLSs might be dispensable (see further).

Alanine substitution of residues 69 and 77 is thought to alter the NS1 subcellular localization, resulting in lower replication efficiency (Li *et al.*, 2011).

2.5.1.k. Nuclear Export promoting and inhibiting signals

A truncated NS1 reduced to its 1-134 N-terminal fragment (thus containing NLS1) and expressed in transfected cells logically locates in the nucleus (Li *et al.*, 1998). But an amino-terminal 1-147 fragment accumulates in the cytoplasm of transfected cells. Moreover, nuclear localization is almost completely restored if the expressed NS1 fragment is slightly longer (1-161). Taken together, these results suggest that the 13-mer

135-147 displays a nuclear export signal (NES) and the 14-mer 148-161 contains an anti-NES signal (Li *et al.*, 1998). A series of bibliographic and experimental observations has confirmed this view. First, the putative NS1 NES displays the same spacing of hydrophobic residues (essentially leucine residues) than other well-known NESs (Fischer *et al.*, 195; Fridell *et al.*, 1996; Richards *et al.*, 1996; Wen *et al.*, 1995). Moreover, individually expressed GST (glutathion S-transferase) appears dispersed throughout the cell, with a slightly higher concentration in the nucleus; but when it is fused with the 135-147 stretch of NS1, it becomes almost totally cytoplasmic (Li *et al.*, 1998). Further mutation experiments showed the critical importance of both leucines 144 and 146 for the NES activity by opposition to I145 which can be replaced by a positive (arginine) residue without affecting the cytoplasmic localization (Li *et al.*, 1998). Addition of the next 14-mer (residues 148-161) caused a significant redistribution of the GST-fusion protein which became almost completely nuclear. A GST-fusion protein containing a larger NS1 fragment (79-173, thus devoid of any NLS) displayed the same localization (Li *et al.*, 1998). Conversely, replacement of the NS1 NES by the HIV-1 Rev NES within this 79-173 fragment led to a cytoplasmic localization, suggesting that the 148-161 14-mer NS1 sequence is unable to inhibit the Rev NES and is thus specific of the NS1 NES (Li *et al.*, 1998). Mutation experiments aimed at defining which residues are involved in the anti-NES function concluded that only the simultaneous alanine substitution of R148, E152 and E153 restored the cytoplasmic localization (Li *et al.*, 1998). Similar mutation experiments applied to the full-length NS1 protein essentially confirmed those results, showing in addition that the 148-161 motif is the only existing anti-NES sequence and that an "unmasked" NS1 NES always overcomes the two NLSs, thus rendering the protein cytoplasmic (Li *et al.*, 1998). Insertion of two alanine residues between the putative NES and adjacent anti-NES motifs suppressed the anti-NES activity. Conversely, insertion of 1 or 4 alanines did not cause any loss of function. Displacing the anti-NES motif one residue closer to the NES also abolished its inhibiting activity. Thus, the spacing between NES and anti-NES motifs is crucial for efficient inhibition (Li *et al.*, 1998). Comparison of subcellular localization of NS1 between infected and uninfected transfected cells revealed that whereas NS1 is present in large amounts in the nucleus and the cytoplasm during infection, it is only found in the nucleus after transfection (Li *et al.*, 1998). These observations led to the hypothesis that a still unknown viral protein probably binds to the anti-NES motif, thus causing the unmasking of NS1 NES, which in turn displaces

NS1 from nucleus to cytoplasm. Such an interaction was already demonstrated for other NES-containing proteins such as the adenovirus E4 34 kDa protein, the cellular PKI (protein kinase inhibitor) protein or the herpes simplex virus ICP27 protein (Li *et al.*, 1998). This NS1-interacting influenza virus protein has still to be identified.

The 135-147 NES is located in the loop between *β*-strands 4 and 5 and in the first half of *β*-strand 5 on the 3D-structure of NS1, and is thus exposed outwards (Bornholdt & Prasad, 2006).

Among the aforementioned residues, only L144, L146 and R148 are very conserved (but not completely), whereas positions 152 and 153 are highly variable between strains, and it is thus most likely that E152 and 153 do not play a critical role in the inhibition of the nuclear export of NS1 protein (personal results).

2.5.1.l. Non structural protein 1 "degeneration" in Vero cells

Vero cell-adapted influenza virus A strains are known to display a series of mutations in the NS1 gene that do not hamper their efficient growth (Egorov *et al.*, 1998). Furthermore, genetically engineered influenza virus mutants coding truncated NS1 proteins (containing the first 38, 80 or 124 N-terminal amino acids) are able to grow with an efficiency similar to that of wild-type strains in Vero cells (Egorov *et al.*, 1998). Conversely, these mutants and the Vero-adapted strains are less productive in MDCK cells or in mice lungs. In IFN*α*–treated Vero cells, among a panel of NS1 deletion mutants, only those with an intact RNA-binding site (and probably intact PKR-binding properties) were able to grow with the same efficiency as the wild-type virus (Kittel *et al.*, 2004). RNA- (or PKR-) binding deficient viruses were rescued when cells were first transfected with a plasmid expressing the 125 first residues of NS1 protein before infection. These observations result from the fact that Vero cells are unable to produce their own type 1 interferons (Desmyter *et al.*, 1968). As emphasized before, an essential role of NS1 consists in preventing the activation of PKR, the subsequent phosphorylation of eukaryotic translation initiation factor 2, and activation of interferons. In the absence of an interferon response, this NS1 function is unnecessary for guaranteeing viral growth, which results in a weakening of the selective pressure acting on NS1 domains involved in countermeasures against interferons.

2.5.1.m. Other poorly defined non structural protein 1 functions and interactors

Wolff and colleagues (1996 & 1998), using yeast two-hybrid interaction trap with confirmation by co-precipitation assays, demonstrated that NS1 interacts with two human proteins provisionally called NS1-I ("NS1-interactor") and NS1-BP ("NS1-binding protein"). NS1-I is a human homolog of the porcine 17*β*-estradiol dehydrogenase precursor protein and is thought to be posttranslationally processed from a 79.6 kDa to a 55 kDa protein. The NS1 domain involved in binding to the NS1-I protein is unknown but as highly divergent NS1 proteins from influenza A and B viruses all conserve the ability to bind it, this interaction is suspected to play a role in the viral replication cycle (Wolff *et al.,* 1996). The relevance of this interaction has still to be determined.

NS1-BP is a 70 kDa human protein colocalizing with the spliceosome assembly factor SC35, which suggests an association with the splicing apparatus (Wolff *et al.,* 1998). This colocalization disappears in influenza infected cells, suggesting a displacement through the binding of NS1 to the NS1-BP. This binding might, in part, explain how cellular pre-mRNAs splicing is inhibited by influenza virus. The interaction of NS1 with one of these factors does not exclude the interaction with other ones among the hundreds of cellular factors possibly involved in pre-mRNAs splicing (Green, 1991; Sharp, 1994; Wolff *et al.*, 1998) (see above).

Addition of type-1 IFNs to cultured cells typically results in the induction of a resistance state to subsequent inoculation of influenza virus A strains, but HPAI (highly pathogenic avian influenza) strains isolated from humans in Hong Kong in 1997 were less inhibited than expected. This resistance to type-1 IFNs was associated with a point mutation in the NS1 gene causing the D92E substitution (Seo *et al.,* 2002). Strains with this mutation also displayed enhanced virulence and virus yields in pigs. The mechanism underlying these observations has yet to be identified. In fact, a set of human HPAI strains revealed a spectrum of virulences which in turn was associated with a set of different mutations in the NS1, but unequivocal correlations are still elusive (Hiromoto *et al.,* 2000). Personal sequences alignments reveal that the amino acid at position 92 is frequently an aspartate residue, even in HPAI H5N1 influenza A strains. A glutamate or glutamine residue can be found in LPAI (low pathogenic) strains of different subtypes such as H6N1, H9N2, H3N2 or H1N1, suggesting that changing the residue at this position is not enough to render an influenza A strains highly

pathogenic.

In infected cells, NS1 is phosphorylated at one or two threonine residues, suggesting that phosphorylation could control the spectrum and/or amplitude of its biological activities (Privalsky & Penhoet, 1981). The biological role of such posttranslational modifications is still unexplored.

It was recently shown that the four C-terminal residues of avian influenza NS1 proteins constitute a PDZ ligand domain ("XS/TXV" type), enabling such NS1 proteins to bind about 30 known human PDZ-containing proteins (Jackson *et al.*, 2008). This ability is not present in the NS1 proteins from human influenza strains. Reverse genetics experiments demonstrated that this short domain was a virulence determinant for the 1918 Spanish influenza and H5N1 HPAI viruses (Jackson *et al.*, 2008). Currently circulating avian influenza virus bear a NS1 PDZ binding motif (PBM) with the consensus sequence "ESEV", while "RSKV" or "RSEV" is found in human strains. PDlim2 protein was found to be a cellular target of the PBM of HPAI H5N1 virus NS1 protein. The NS1 PBM of avian viruses was able to interact with the PDZ motif of PDlim2, NS1 from human viruses being not able of such a binding (Yu *et al.*, 2011). This observation clearly suggests the "ESEV" motif of avian NS1 as necessary for virulence in avian species.

Mutation F103L and M106I were shown to enhance viral replication and virulence in mice of both human and avian viruses (Dankar *et al.*, 2011).

Residues 144 to 188 of NS1 are necessary for the binding to p53 and the inhibition of p53-mediated transcriptional activity and apoptosis, but other still unidentified domains cooperate for full efficiency of this NS1 function (Wang *et al.*, 2010).

NS1 protein interacts with Hsp90 (heat shock protein 90) which binding leads to an increased interaction between Apaf-1 and cytochrome C, possibly facilitating caspases-3 and -9 activation and apoptosis (Zhang *et al.*, 2011).

2.5.1.n. Conclusion

The main roles of NS1 protein are to favor the production of viral mRNAs and proteins over cellular ones and to prevent the activation of the IFN response (and the apoptosis). These functions take place through the binding of NS1 to different transcription or translation factors, thus at both nuclear and cytoplasmic levels – which explains the presence of both NLS and NES sequences (Figures 3 and 4). The NS1 protein is thus

not required for the influenza replication cycle itself, but clearly appears as an essential factor of biofitness and virulence both *in vitro* and *in vivo*.

2.5.2. Nuclear Export protein.

The nuclear export protein, formerly non structural protein 2 (NS2), was renamed after 130-200 molecules were indeed identified within the virion where they bind to the M1 protein (Richardson & Akkina, 1991; Yasuda *et al.*, 1993). NEP is a 121 residue-long phosphoprotein coded by the spliced NS1 mRNA that mediates the nuclear export of native vRNPs by interacting with cellular exportins (Enami, 1997; Lamb *et al.*, 1980; Lamb & Lay, 1980). Spontaneous mutations within this protein were also associated with the production of defective interfering particles devoid of a PA (polymerase acidic protein) gene (RNA segment 3), suggesting a role of NEP protein in genomic RNA synthesis (Odagiri & Tobita, 1990). Such a regulatory role during virus-specific RNA synthesis was supported further by the finding that NEP downregulated vRNA, cRNA and mRNA synthesis in cells synthesizing the four influenza A virus core proteins – nucleoprotein (NP), polymerase basic proteins 1 and 2 (PB1 and PB2), and PA – and NEP from recombinant plasmids (Bullido *et al.*, 2001). It is most likely that, in those particular conditions, in the absence of many influenza proteins, NEP would promote the constant nuclear export of vRNPs, thus diminishing their expression (Bullido *et al.*, 2001).

Association between exacerbated virulence and some NEP amino acid substitutions among H5N1 isolates was made once, but not confirmed yet (Hiromoto *et al.*, 2000).

Proteolytic cleavage of NEP defines an N-terminal domain which mediates RanGTP-dependent binding to CRM1 (chromosome region maintenance 1 protein) and a C-terminal domain which binds to the viral matrix protein M1.

2.5.2.a. Matrix protein 1-binding domain

By a two-hybrid system assay, Ward *et al.* (1995) found that the C-terminal 90-252 M1 segment was able to bind the NEP protein. A subsequent filter-binding assay permitted the location of the binding partner domain within the 70 C-terminal residues of NEP (Ward *et al.*, 1995). As purification of the whole NEP protein systematically led to a set of fragments, crystallization of the proteolytically resistant C-terminal 54-121 fragment

obtained by limited digestion of recombinant NEP with elastase, trypsin or chymotrypsin was preferred. This latter bond the M1 protein as efficiently as the wild-type NEP, thus confirming first reported data (Akarsu *et al.*, 2003). This C-terminal NEP domain comprises two helices, C1 (residues 64-85) and C2 (residues 94-115), six helical turns each, connected by an interhelical turn (86-93), forming a helical hairpin (dimensions: 40 x 25 x 15 Å) (Figure 5). The two helices adopt an almost antiparallel orientation (they cross with a 14° angle), according to which they interface each other on their whole length. Interhelical contacts involve 12 hydrophobic and 4 polar residues (Akarsu *et al.*, 2003). Further stabilization of the hairpin is provided by (i) R84 which is hydrogen bonded to Q96, (ii) a bifurcated salt bridge of R77 with E74 and E110 and (iii) interaction between R66 guanidium moiety and carbonyl groups at the C-terminus of helix C2. The hairpin is amphipathic, combining a hydrophobic face and a hydrophilic face (which is essentially on C1). The hydrophilic face contains six glutamate residues near its centre and basic residues at both its ends. It also contains five hydrophobic residues, among which four (I97, M100, L103 and L107) form a continuous groove on the surface and one (W78) is exposed at the centre of the glutamate stretch.

As mutation of W78 dramatically abated M1-binding activity, it presumably constitutes a key component of the M1-binding site (Akarsu *et al.*, 2003). W78 is therefore likely to be engaged in the binding with the M1 NEP-binding site, i.e. its 101-105 NLS (Akarsu *et al.*, 2003), which resembles the crucial function played by tryptophan residues of nuclear import factor importin α for NLS recognition, by buttressing lysine residues of the NLS, rendering them able to interact with acidic residues of importin α (Akarsu *et al.*, 2003; Conti *et al.*, 1998; Conti & Kuriyan, 2000). Personal sequences alignments show that W78 is highly conserved among influenza A strains. Recent data point out the critical role played by residues 81-100 of NEP in M1 binding and nuclear export (Shimizu *et al.*, 2011).

2.5.2.b. Nuclear export signal

As the presence of M1 is required at the late times of viral replication for permitting nuclear export of vRNPs, a molecular interaction between M1 and the export machinery was originally suspected, but it was not confirmed by yeast two-hybrid assays (Martin & Helenius, 1991; O'Neill *et al.*, 1998; Whittaker *et al.*, 1996). In addition, none of the

proteic partners in the vRNPs (NP, PB1, PB2 and PA) was able to bind nucleoporins (O'Neill *et al.*, 1998). By contrast, NEP was shown to interact strongly with human Rab/hRIP1 and yeast yRIP1 proteins, two nucleoporins known to interact with HIV-1 Rev protein through their FG-repeat elements (Bogerd *et al.*, 1995; Fritz *et al.*, 1995; O'Neill *et al.*, 1998; Stutz *et al.*, 1995). A functional domain on the NEP with characteristics of a nuclear export signal (NES) was mapped: it is constituted of a leucine-rich stretch (spanning from residue 11 to residue 23), interacts with cellular nucleoporins, can functionally replace the effector domain of the HIV-1 Rev protein and mediates rapid nuclear export when cross-linked to a reporter protein (O'Neill *et al.*, 1998). Unlike the HIV-1 Rev protein however, NEP does not bind RNA, which suggests that binding to vRNPs requires at least one additional interactor. As the M1 protein binds both vRNPs and NEP and as it is the only component required for nuclear egress, it is very likely that it functions as an adaptor molecule (Bui *et al.*, 2000; Martin & Helenius, 1991; Neumann *et al.*, 2000; Whittaker *et al.*, 1996).

Direct interaction between NEP and hCRM1 (human chromosome region maintenance 1 protein, also called exportin 1) was demonstrated by yeast two-hybrid assays (Neumann *et al.*, 2000). As exportin 1 is a nuclear receptor for proteins displaying a leucine-rich NES containing 3 to 5 hydrophobic residues with a typical spacing (Fornerod *et al.*, 1997), the NEP NES was logically suspected to be engaged in the molecular interaction with CRM1. However, if alanine substitution of residues M14, M16, M19 and L21 of the NEP NES indeed led to mutant viruses unable to replicate and abolished the nuclear egress of ribonucleoproteins, it did not prevent the CRM1-binding, thus emphasizing a crucial role for NEP NES in viral replication and vRNPs egress but not in CRM1 binding (Iwatsuki-Horimoto *et al.*, 2004; Neumann *et al.*, 2000). Recently, the nuclear export of influenza vRNPs was shown to be mediated by the binding of CRM1/exportin 1 in a RanGTP-dependent manner (Elton *et al.*, 2001; Ma *et al.*, 2001; Watanabe *et al.*, 2001). In this new molecular context, the NEP NES is presumed to be essential for the formation of ternary NEP-CRM1-RanGTP complexes which interact with the nucleoporins for the export of vRNPs by the RanGTP nuclear export pathway (Akarsu *et al.*, 2003). The current "daisy chain" working hypothesis stands that one vRNP probably binds several M1 proteins and thus possibly several NEP proteins, themselves recruiting multiple CRM1/RanGTP pairs (Akarsu *et al.*, 2003; Baudin *et al.*, 2001) (Figure 6).

Among residues M14, M16, M19 and L21, the most conserved are M14 and M16. M19

can be found subtituted by R, L or V, while a glutamate or less frequently an aspartate residue can be found at position 21 (personal investigations). The high conservation degree of M14 and M16 is compatible with their proposed role in the nuclear export properties of the NEP protein.

Using MALDI (matrix assisted laser desorption ionization) technology, it was shown that full-length NEP protein adopts a globular conformation, very flexible, with a relatively rigid C-terminus and a mobile N-terminus (Lommer & Luo, 2002). Such plasticity might also be required for guaranteeing the correct assembly of the nuclear export complex, as for the HIV Rev protein (Lommer & Luo, 2002). This also suggests that regions surrounding the NES are also important for interaction with CRM1/RanGTP.

2.5.2.c. Dimerization domain

Structural studies showed that the NEP C-terminal (63-116) fragment is able to dimerize. Two hairpins (thus corresponding to two NEP C-terminal monomers) form an antiparallel four-helix bundle, with the four N- and C-termini on the same side of the dimer and with helix C1 of one monomer packed on helix C2 of the second monomer and inversely (Akarsu *et al.*, 2003) (Figure 5). The contact surface between monomers equals about 27% (1,268 Å) of the whole surface. The dimer is stabilized by interactions between 24 residues from each monomer. Among these interactions, the great majority is hydrophobic and forms a hydrophobic core at the centre of the four helix bundle, as observed in globular proteins (Akarsu *et al.*, 2003). In addition, the dimer structure is stabilized further by a hydrogen bond between E95 and the carbonyl moiety of V83 and a salt bridge between K72 and both E108 and E112. However, the full length NEP protein is systematically found as a monomer, presumably because the N-terminal fragment packs on and buries the hydrophobic face of the C-terminal fragment and thus prevents its dimerization (Akarsu *et al.*, 2003; Lommer & Luo, 2002). It is thus difficult to assess if these dimerization properties of the C-terminal part of NEP are relevant or not for full-length NEP protein.

2.5.2.d. Conclusion

NEP, formerly called "non structural protein 2", is actually present in the virion. It plays

a crucial role in the nucleo-cytoplasmic translocation of native viral ribonucleoproteins just before the budding process. This function is achieved by binding of NEP to M1, through its C-terminal half, and to cellular nucleoporins, via a nuclear export signal present within its N-terminal part (Figure 7). The C-terminal part of NEP is able to dimerize, but whether this property is needed for exercising the abovementioned functions is not known.

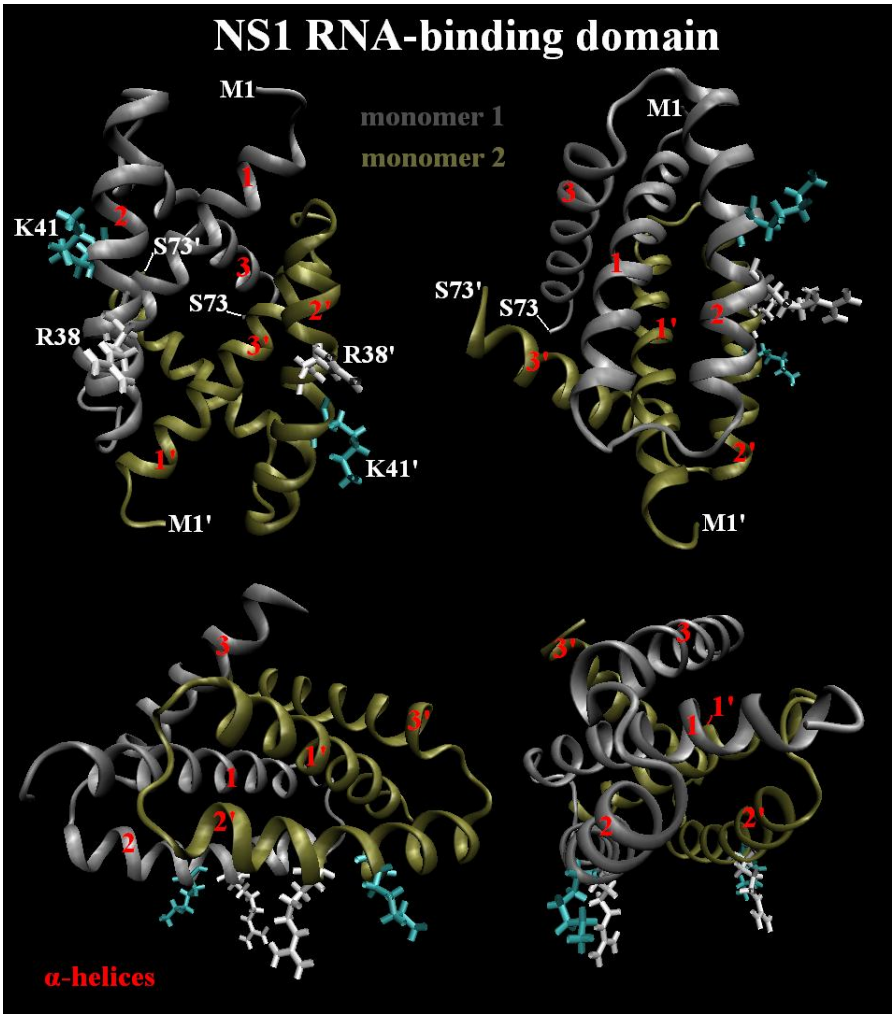

Figure 1: Structure of the NS1 RNA-binding domain and positioning of R38 and K41 on *α*-helix 2 of each monomer. The N-terminal NS1 1-73 fragment represented here is dimeric and is made of three *α*-helices per monomer. R38 and K41 of each monomer are exposed on the same side of the dimer and are thought to interact with RNA. Adapted from Chien *et al.* (1997) – pdb code 1NS1. Figure performed with VMD (Humphrey *et al.*, 1996).

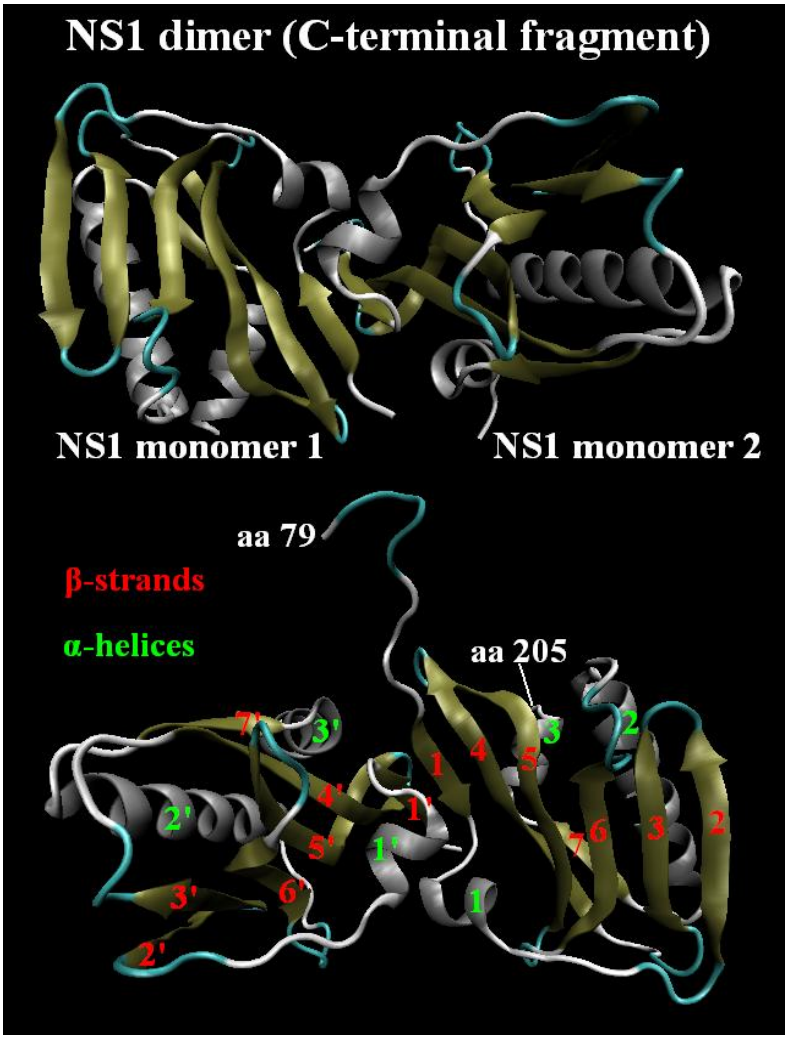

Figure 2: Structure of the NS1 dimer (C-terminal fragment: residues 79 to 205). Secondary structure elements (*α*-helices and *β*-strands) are represented, showing that this C-terminal part of NS1 is essentially composed of *β*-strands organized around a long *α*-helix, two other short *α*-helices being present, one after strand 1 and one at the C-terminal extremity. 3D-structure from Bornholdt & Prasad (2006) – pdb code: 2GX9. Figure performed with VMD (Humphrey *et al.*, 1996).

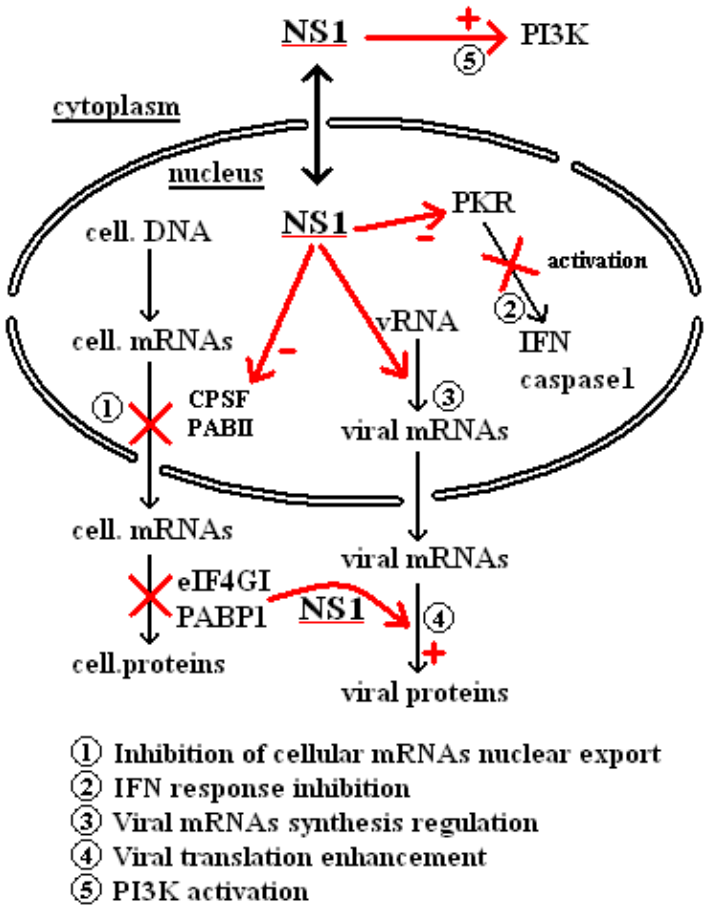

Figure 3: Schematic representation of the functions of the NS1 protein during the influenza virus replication cycle. NS1 is both nuclear and cytoplasmic. It inhibits the nuclear export of cellular poly(A)-tailed mRNAs by binding to the 30 kDa subunit of the cleavage and polyadenylation specificity factor (CPSF) and to poly(A)-binding protein II (PABII), which blocks the action of these two proteins (Chen & Krug, 2000; Noah *et al.*, 2003). It prevents the interferon (IFN) cascade activation and apoptosis induction by binding to and inhibiting Protein Kinase R (PKR) (Li *et al.*, 2006; Stasakova *et al.*, 2005). The NS1 protein was shown to regulate the expression of the different influenza genes during the replication cycle (Min *et al.*, 2007). It recruits the eukaryotic initiation factor 4GI (eIF4GI) and the poly(A)-binding protein 1 to specifically enhance the rate of translation of viral mRNAs (Aragon *et al.*, 2000; Burgui *et al.*, 2003). It was finally shown to activate the phosphatidylinositol 3-kinase (PI3K) Akt pathway, which is thought to favor the viral replication (Ehrhardt *et al.*, 2006).

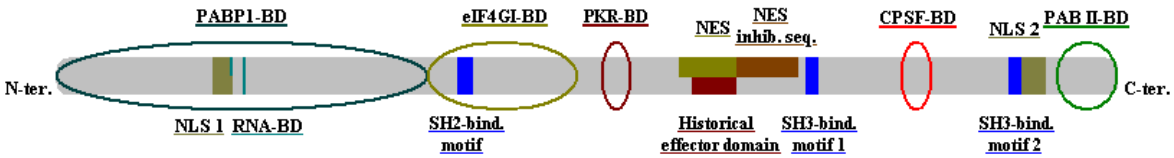

Figure 4: Functional domains of NS1 protein. NS1 is 237 residue-long. It binds different transcription or translation factors and poly(A)-binding proteins, which is in part responsible for its pro-viral and anti-interferon effects. Among these factors, NS1 binds the cleavage and polyadenylation specificity factor 30 kDa subunit (CPSF-BD: 184-188), the eukaryotic initiation factor 4GI (eIF4GI-BD: 82-113), the poly(A)-binding protein II (PABII-BD: 223-237), and the poly(A)-binding protein 1 (PABP1-BD: 1-81) (Burgui *et al.*, 2003; Li *et al.*, 2001; Marion *et al.*, 1997; Noah *et al.*, 2003). In addition, NS1 inhibits Protein Kinase R (putative PKR-BD: 123-127) and cellular caspase-1 (undefined domain – probably by inhibiting PKR), and it binds the p85*β* subunit of the phosphatidylinositol 3-kinase (p85-BDs: 89-93 [SH2-binding motif], 164-167 [SH3-binding motif 1] and 213-216 [SH3-binding motif 2]) (Min *et al.*, 2007; Shin *et al.*, 2007; Stasakova *et al.*, 2005). NS1 also presents a Rev-like effector domain (138-147) which was proposed to be involved in the inhibition of the nucleocytoplasmic translocation of cellular mRNAs (Qian *et al.*, 1994). The RNA-binding domain of NS1 protein was shown to be essentially constituted by residues R38 and K41 (Wang *et al.*, 1999). NS1 possesses two putative NLSs (NLS1: 34-38 and NLS2: 216-221) (Greenspan *et al.*, 1988) and a nuclear export signal (NES: 135-147), together with an anti-NES motif (148-161) (Li *et al.*, 1998).

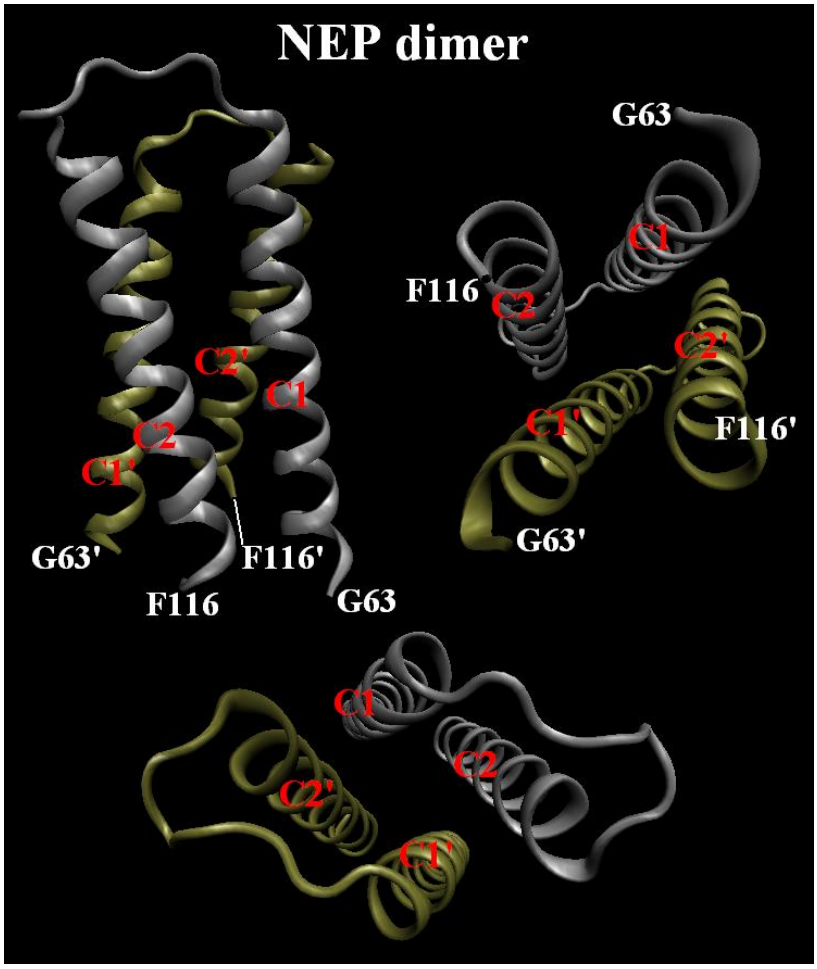

Figure 5: Structure of the NEP protein (63-116 fragment). A fragment corresponding to the C-terminal two-thirds of the NEP protein was shown to be able to dimerize. Each of these monomeric fragments presents two almost antiparallel α-helices (C1 and C2). Adapted from Akarsu *et al.* (2003) – pdb code: 1PD3. Figure performed with VMD (Humphrey *et al.*, 1996).

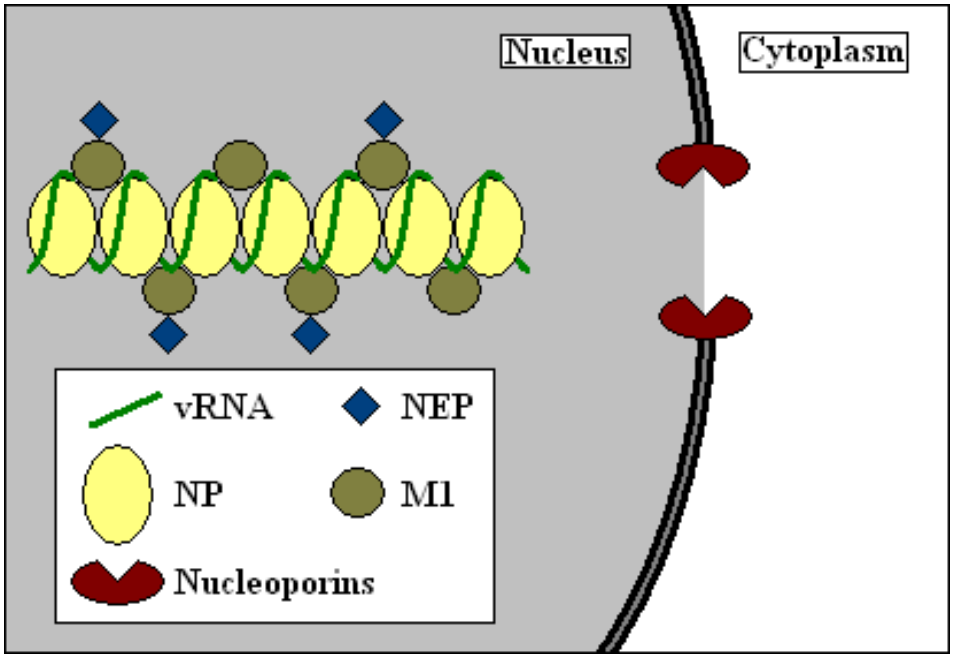

Figure 6: Nuclear export of native vRNPs. The NEP protein interacts with nucleoporins to promote nuclear export of viral ribonucleoproteins. The M1 protein is thought to constitute the link between NEP and vRNPs, and is thus required for this export. Adapted from (O'Neill *et al.*, 1998).

Figure 7: Functional domains of the NEP protein. NEP contains 121 residues. It is able to dimerize, the dimerization involving residues of the C-terminal half of the protein (63-116), which also constitutes the M1-binding site (Akarsu *et al.*, 2003; Ward *et al.*, 1995). It possesses a nuclear export signal, essential for its role in exporting new vRNPs out of the cell nucleus, which binds the cellular exportin 1 protein (NES/exportin1-BD: 11-23) (O'Neill *et al.*, 1998).

2.5.3. References

Akarsu H, Burmeister WP, Petosa C, *et al.* Crystal structure of the M1 protein-binding domain of the influenza A virus nuclear export protein (NEP/NS2). *Embo J* 2003; 22: 4646-4655.

Alonso-Caplen FV, Nemeroff ME, Qiu Y, *et al.* Nucleocytoplasmic transport: the influenza virus NS1 protein regulates the transport of spliced NS2 mRNA and its precursor NS1 mRNA. *Genes Dev* 1992; 6: 255-267.

Aragon T, de la Luna S, Novoa I, *et al.* Eukaryotic translation initiation factor 4GI is a cellular target for NS1 protein, a translational activator of influenza virus. *Mol Cell Biol* 2000; 20: 6259-6268.

Barabino SM, Hubner W, Jenny A, *et al.* The 30-kD subunit of mammalian cleavage and polyadenylation specificity factor and its yeast homolog are RNA-binding zinc finger proteins. *Genes Dev* 1997; 11: 1703-1716.

Battiste JL, Mao H, Rao NS, *et al.* Alpha helix-RNA major groove recognition in an HIV-1 rev peptide-RRE RNA complex. *Science* 1996; 273: 1547-1551.

Baudin F, Petit I, Weissenhorn W, *et al. In vitro* dissection of the membrane and RNP binding activities of influenza virus M1 protein. *Virology* 2001; 281: 102-108.

Bienroth S, Keller W, Wahle E. Assembly of a processive messenger RNA polyadenylation complex. *Embo J* 1993; 12: 585-594.

Bogerd HP, Fridell RA, Madore S, *et al.* Identification of a novel cellular cofactor for the Rev/Rex class of retroviral regulatory proteins. *Cell* 1995; 82: 485-494.

Bornholdt ZA, Prasad BV. X-ray structure of influenza virus NS1 effector domain. *Nat Struct Mol Biol* 2006; 13: 559-560.

Briedis DJ, Conti G, Munn EA, *et al.* Migration of influenza virus-specific polypeptides from cytoplasm to nucleus of infected cells. *Virology* 1981; 111: 154-164.

Bucher E, Hemmes H, de Haan P, *et al.* The influenza A virus NS1 protein binds small interfering RNAs and suppresses RNA silencing in plants. *J Gen Virol* 2004; 85: 983-991.

Bui M, Wills EG, Helenius A, *et al.* Role of the influenza virus M1 protein in nuclear export of viral ribonucleoproteins. *J Virol* 2000; 74: 1781-1786.

Bullido R, Gomez-Puertas P, Saiz MJ, *et al.* Influenza A virus NEP (NS2 protein) downregulates RNA synthesis of model template RNAs. *J Virol* 2001; 75: 4912-4917.

Burgui I, Aragon T, Ortin J, *et al.* PABP1 and eIF4GI associate with influenza virus NS1 protein in viral mRNA translation initiation complexes. *J Gen Virol* 2003; 84: 3263-3274.

Chen Z, Krug RM. Selective nuclear export of viral mRNAs in influenza-virus-infected cells. *Trends Microbiol* 2000; 8: 376-383.

Chen Z, Li Y, Krug RM. Influenza A virus NS1 protein targets poly(A)-binding protein II of the cellular 3'-end processing machinery. *Embo J* 1999; 18: 2273-2283.

Chien CY, Tejero R, Huang Y, *et al.* A novel RNA-binding motif in influenza A virus non-structural protein 1. *Nat Struct Biol* 1997; 4: 891-895.

Compans RW. Influenza virus proteins. II. Association with components of the cytoplasm. *Virology* 1973; 51: 56-70.

Conti E, Kuriyan J. Crystallographic analysis of the specific yet versatile recognition of distinct nuclear localization signals by karyopherin alpha. *Structure* 2000; 8: 329-338.

Conti E, Uy M, Leighton L, *et al.* Crystallographic analysis of the recognition of a nuclear localization signal by the nuclear import factor karyopherin alpha. *Cell* 1998; 94: 193-204.

Dankar SK, Wang S, Ping J, Forbes NE, *et al.* Influenza A virus NS1 gene mutations F103L and M106I increase replication and virulence. *Virol J* 2011; 8: 13.

de la Luna S, Fortes P, Beloso A, *et al.* Influenza virus NS1 protein enhances the rate of translation initiation of viral mRNAs. *J Virol* 1995; 69: 2427-2433.

Delgadillo MO, Saenz P, Salvador B, *et al.* Human influenza virus NS1 protein enhances viral pathogenicity and acts as an RNA silencing suppressor in plants. *J Gen Virol* 2004; 85: 993-999.

Desmyter J, Melnick JL, Rawls WE. Defectiveness of interferon production and of rubella virus interference in a line of African green monkey kidney cells (Vero). *J Virol* 1968; 2: 955–961.

Donelan NR, Basler CF, Garcia-Sastre A. A recombinant influenza A virus expressing an RNA-binding-defective NS1 protein induces high levels of beta interferon and is attenuated in mice. *J Virol* 2003; 77: 13257-13266.

Egorov A, Brandt S, Sereinig S, *et al.* Transfectant influenza A viruses with long deletions in the NS1 protein grow efficiently in Vero cells. *J Virol* 1998; 72: 6437-6441.

Ehrhardt C, Marjuki H, Wolff T, *et al.* Bivalent role of the phosphatidylinositol-3-kinase

(PI3K) during influenza virus infection and host cell defence. *Cell Microbiol* 2006; 8: 1336-1348.

Elton D, Simpson-Holley M, Archer K, *et al.* Interaction of the influenza virus nucleoprotein with the cellular CRM1-mediated nuclear export pathway. *J Virol* 2001; 75: 408-419.

Enami K, Sato TA, Nakada S, *et al.* Influenza virus NS1 protein stimulates translation of the M1 protein. *J Virol* 1994; 68: 1432-1437.

Enami M. [Structure and function of influenza virus NS1 and NS2 proteins]. *Nippon Rinsho* 1997; 55: 2605-2609.

Falcon AM, Marion RM, Zurcher T, *et al.* Defective RNA replication and late gene expression in temperature-sensitive influenza viruses expressing deleted forms of the NS1 protein. *J Virol* 2004; 78: 3880-3888.

Fischer U, Huber J, Boelens WC, *et al.* The HIV-1 Rev activation domain is a nuclear export signal that accesses an export pathway used by specific cellular RNAs. *Cell* 1995; 82: 475-483.

Fornerod M, Ohno M, Yoshida M, *et al.* CRM1 is an export receptor for leucine-rich nuclear export signals. *Cell* 1997; 90: 1051-1060.

Fortes P, Beloso A, Ortin J. Influenza virus NS1 protein inhibits pre-mRNA splicing and blocks mRNA nucleocytoplasmic transport. *Embo J* 1994; 13: 704-712.

Fridell RA, Fischer U, Luhrmann R, *et al.* Amphibian transcription factor IIIA proteins contain a sequence element functionally equivalent to the nuclear export signal of human immunodeficiency virus type 1 Rev. *Proc Natl Acad Sci U S A* 1996; 93: 2936-2940.

Fritz CC, Zapp ML, Green MR. A human nucleoporin-like protein that specifically interacts with HIV Rev. *Nature* 1995; 376: 530-533.

Gallie DR, Tanguay R. Poly(A) binds to initiation factors and increases cap-dependent translation *in vitro*. *J Biol Chem* 1994; 269: 17166-17173.

Garcia-Sastre A. Inhibition of interferon-mediated antiviral responses by influenza A viruses and other negative-strand RNA viruses. *Virology* 2001; 279: 375-384.

Garfinkel MS, Katze MG. Translational control by influenza virus. Selective translation is mediated by sequences within the viral mRNA 5'-untranslated region. *J Biol Chem* 1993; 268: 22223-22226.

Geiss GK, Salvatore M, Tumpey TM, *et al.* Cellular transcriptional profiling in influenza A virus-infected lung epithelial cells: the role of the nonstructural NS1

protein in the evasion of the host innate defense and its potential contribution to pandemic influenza. *Proc Natl Acad Sci U S A* 2002; 99: 10736-10741.

Ghayur T, Banerjee S, Hugunin M, *et al.* Caspase-1 processes IFN-gamma-inducing factor and regulates LPS-induced IFN-gamma production. *Nature* 1997; 386: 619-623.

Green MR. Biochemical mechanisms of constitutive and regulated pre-mRNA splicing. *Annu Rev Cell Biol* 1991; 7: 559-599.

Greenspan D, Palese P, Krystal M. Two nuclear location signals in the influenza virus NS1 nonstructural protein. *J Virol* 1988; 62: 3020-3026.

Hale BG, Batty IH, Downes CP, *et al.* Binding of influenza A virus NS1 protein to the inter-SH2 domain of p85 suggests a novel mechanism for phosphoinositide 3-kinase activation. *J Biol Chem* 2008; 283: 1372-1380.

Hale BG, Jackson D, Chen YH, *et al.* Influenza A virus NS1 protein binds p85beta and activates phosphatidylinositol-3-kinase signaling. *Proc Natl Acad Sci U S A* 2006; 103: 14194-14199.

Hatada E, Fukuda R. Binding of influenza A virus NS1 protein to dsRNA *in vitro. J Gen Virol* 1992; 73: 3325-3329.

Heikkinen LS, Kazlauskas A, Melen K, *et al.* Avian and 1918 Spanish influenza a virus NS1 proteins bind to Crk/CrkL Src homology 3 domains to activate host cell signaling. *J Biol Chem* 2008; 283: 5719-5727.

Hiromoto Y, Yamazaki Y, Fukushima T, *et al.* Evolutionary characterization of the six internal genes of H5N1 human influenza A virus. *J Gen Virol* 2000; 81: 1293-1303.

Humphrey W, Dalke, A., Schulten, K. VMD - Visual Molecular Dynamics. *J. Molec. Graphics* 1996; 14: 33-38.

Iwatsuki-Horimoto K, Horimoto T, Fujii Y, *et al.* Generation of influenza A virus NS2 (NEP) mutants with an altered nuclear export signal sequence. *J Virol* 2004; 78: 10149-10155.

Jackson D, Hossain MJ, Hickman D, *et al.* A new influenza virus virulence determinant: The NS1 protein four C-terminal residues modulate pathogenicity. *Proc Natl Acad Sci U S A* 2008; 105: 4381-4386.

Jacobson A. Poly(A) metabolism and translation: the closed loop model. In Translation control., Hershey JWB, Mathews, M.B., and Sonenberg, N. (eds). Cold Spring Harbor Laboratory Press, Plainview: New York, 1996; 451-480.

Keller W, Bienroth S, Lang KM, *et al.* Cleavage and polyadenylation factor CPF specifically interacts with the pre-mRNA 3' processing signal AAUAAA. *Embo J* 1991; 10: 4241-4249.

Kerry PS, Ayllon J, Taylor MA, *et al.* A transient homotypic interaction model for the influenza A virus NS1 protein effector domain. *Plos One* 2011; 6: e17946.

Kittel C, Sereinig S, Ferko B, *et al.* Rescue of influenza virus expressing GFP from the NS1 reading frame. *Virology* 2004; 324: 67-73.

Koennecke I, Boschek CB, Scholtissek C. Isolation and properties of a temperature-sensitive mutant (ts 412) of an influenza A virus recombinant with a ts lesion in the gene coding for the nonstructural protein. *Virology* 1981; 110: 16-25.

Kok KH, Jin DY. Influenza A virus NS1 protein does not suppress RNA interference in mammalian cells. *J Gen Virol* 2006; 87: 2639-2644.

Krug RM, Etkind PR. Cytoplasmic and nuclear virus-specific proteins in influenza virus-infected MDCK cells. *Virology* 1973; 56: 334-348.

Krug RM, Soeiro R. Studies on the intranuclear localization of influenza virus-specific proteins. *Virology* 1975; 64: 378-387.

Krug RM, Yuan W, Noah DL, *et al.* Intracellular warfare between human influenza viruses and human cells: the roles of the viral NS1 protein. *Virology* 2003; 309: 181-189.

Kuo RL, Zhao C, Malur M, *et al.* Influenza A virus strains that circulate in humans differ in the ability of their NS1 proteins to block the activation of IRF3 and interferon-β transcription. *Virology* 2010; 408: 146-158.

Lamb RA, Choppin PW, Chanock RM, *et al.* Mapping of the two overlapping genes for polypeptides NS1 and NS2 on RNA segment 8 of influenza virus genome. *Proc Natl Acad Sci U S A* 1980; 77: 1857-1861.

Lamb RA, Krug RM. *Orthomyxoviridae*: The viruses and their replication. In Fields Virology, Knipe DM, Howley PM, Martin MA, Griffin DE, Lamb RA (eds). Lippincott Williams & Wilkins: Boston, 2001; 1487-1531.

Lamb RA, Lai CJ. Expression of unspliced NS1 mRNA, spliced NS2 mRNA, and a spliced chimera mRNA from cloned influenza virus NS DNA in an SV40 vector. *Virology* 1984; 135: 139-147.

Lamb RA, Lai CJ. Sequence of interrupted and uninterrupted mRNAs and cloned DNA coding for the two overlapping nonstructural proteins of influenza virus. *Cell* 1980; 21: 475-485.

Lee JH, Kim SH, Pascua PN, *et al.* Direct interaction of cellular hnRNP-F and NS1 of influenza A virus accelerates viral replication by modulation of viral transcriptional activity and host gene expression. *Virology* 2010; 397: 89-99.

Li S, Min JY, Krug RM, *et al.* Binding of the influenza A virus NS1 protein to PKR mediates the inhibition of its activation by either PACT or double-stranded RNA. *Virology* 2006; 349: 13-21.

Li WX, Li H, Lu R, *et al.* Interferon antagonist proteins of influenza and vaccinia viruses are suppressors of RNA silencing. *Proc Natl Acad Sci U S A* 2004; 101: 1350-1355.

Li W, Noah JW, Noah DL. Alanine substitutions within a linker region of the influenza A virus NS1 protein alter NS1 subcellular localization and attenuate virus replication. *J Gen Virol* 2011 [Epub ahead of print].

Li Y, Chen ZY, Wang W, *et al.* The 3'-end-processing factor CPSF is required for the splicing of single-intron pre-mRNAs *in vivo*. *Rna* 2001; 7: 920-931.

Li Y, Yamakita Y, Krug RM. Regulation of a nuclear export signal by an adjacent inhibitory sequence: the effector domain of the influenza virus NS1 protein. *Proc Natl Acad Sci U S A* 1998; 95: 4864-4869.

Li Z, Jiang Y, Jiao P, *et al.* The NS1 gene contributes to the virulence of H5N1 avian influenza viruses. *J Virol* 2006; 80: 11115-11123.

Liu J, Lynch PA, Chien CY, *et al.* Crystal structure of the unique RNA-binding domain of the influenza virus NS1 protein. *Nat Struct Biol* 1997; 4: 896-899.

Lommer BS, Luo M. Structural plasticity in influenza virus protein NS2 (NEP). *J Biol Chem* 2002; 277: 7108-7117.

Lu Y, Qian XY, Krug RM. The influenza virus NS1 protein: a novel inhibitor of pre-mRNA splicing. *Genes Dev* 1994; 8: 1817-1828.

Lu Y, Wambach M, Katze MG, *et al.* Binding of the influenza virus NS1 protein to double-stranded RNA inhibits the activation of the protein kinase that phosphorylates the elF-2 translation initiation factor. *Virology* 1995; 214: 222-228.

Ma K, Roy AM, Whittaker GR. Nuclear export of influenza virus ribonucleoproteins: identification of an export intermediate at the nuclear periphery. *Virology* 2001; 282: 215-220.

Marion RM, Aragon T, Beloso A, *et al.* The N-terminal half of the influenza virus NS1 protein is sufficient for nuclear retention of mRNA and enhancement of viral

mRNA translation. *Nucleic Acids Res* 1997; 25: 4271-4277.

Martin K, Helenius A. Transport of incoming influenza virus nucleocapsids into the nucleus. *J Virol* 1991; 65: 232-244.

Min JY, Li S, Sen GC, *et al.* A site on the influenza A virus NS1 protein mediates both inhibition of PKR activation and temporal regulation of viral RNA synthesis. *Virology* 2007.

Nemeroff ME, Barabino SM, Li Y, *et al.* Influenza virus NS1 protein interacts with the cellular 30 kDa subunit of CPSF and inhibits 3'end formation of cellular pre-mRNAs. *Mol Cell* 1998; 1: 991-1000.

Nemeroff ME, Qian XY, Krug RM. The influenza virus NS1 protein forms multimers *in vitro* and *in vivo. Virology* 1995; 212: 422-428.

Neumann G, Hughes MT, Kawaoka Y. Influenza A virus NS2 protein mediates vRNP nuclear export through NES-independent interaction with hCRM1. *Embo J* 2000; 19: 6751-6758.

Noah DL, Twu KY, Krug RM. Cellular antiviral responses against influenza A virus are countered at the posttranscriptional level by the viral NS1A protein via its binding to a cellular protein required for the 3' end processing of cellular pre-mRNAS. *Virology* 2003; 307: 386-395.

O'Neill RE, Talon J, Palese P. The influenza virus NEP (NS2 protein) mediates the nuclear export of viral ribonucleoproteins. *Embo J* 1998; 17: 288-296.

Odagiri T, Tobita K. Mutation in NS2, a nonstructural protein of influenza A virus, extragenically causes aberrant replication and expression of the PA gene and leads to generation of defective interfering particles. *Proc Natl Acad Sci U S A* 1990; 87: 5988-5992.

Okkenhaug K, Vanhaesebroeck B. New responsibilities for the PI3K regulatory subunit p85 alpha. *Sci STKE* 2001; 2001: PE1.

Pawson T. Protein modules and signalling networks. *Nature* 1995; 373: 573-580.

Privalsky ML, Penhoet EE. The structure and synthesis of influenza virus phosphoproteins. *J Biol Chem* 1981; 256: 5368-5376.

Pu J, Wang J, Zhang Y, *et al.* Synergism of co-mutation of two amino acid residues in NS1 protein increases the pathogenicity of influenza virus in mice. *Virus Res* 2010; 151: 200-204.

Qian XY, Alonso-Caplen F, Krug RM. Two functional domains of the influenza virus NS1 protein are required for regulation of nuclear export of mRNA. *J Virol*

1994; 68: 2433-2441.

Qian XY, Chien CY, Lu Y, *et al.* An amino-terminal polypeptide fragment of the influenza virus NS1 protein possesses specific RNA-binding activity and largely helical backbone structure. *Rna* 1995; 1: 948-956.

Qiu Y, Krug RM. The influenza virus NS1 protein is a poly(A)-binding protein that inhibits nuclear export of mRNAs containing poly(A). *J Virol* 1994; 68: 2425-2432.

Qiu Y, Nemeroff M, Krug RM. The influenza virus NS1 protein binds to a specific region in human U6 snRNA and inhibits U6-U2 and U6-U4 snRNA interactions during splicing. *Rna* 1995; 1: 304-316.

Richards SA, Lounsbury KM, Carey KL, *et al.* A nuclear export signal is essential for the cytosolic localization of the Ran binding protein, RanBP1. *J Cell Biol* 1996; 134: 1157-1168.

Richardson JC, Akkina RK. NS2 protein of influenza virus is found in purified virus and phosphorylated in infected cells. *Arch Virol* 1991; 116: 69-80.

Robb NC, Chase G, Bier K, *et al.* The influenza A virus NS1 protein interacts with the nucleoprotein of viral ribonucleoprotein complexes. *J Virol* 2011; 85: 5228-5231.

Seo SH, Hoffmann E, Webster RG. Lethal H5N1 influenza viruses escape host anti-viral cytokine responses. *Nat Med* 2002; 8: 950-954.

Sharp PA. Split genes and RNA splicing. *Cell* 1994; 77: 805-815.

Shimizu K, Mullinix MG, Chanock RM, *et al.* Temperature-sensitive mutants of influenza A/Udorn/72 (H3N2) virus. I. Isolation of temperature-sensitive mutants some of which exhibit host-dependent temperature sensitivity. *Virology* 1982; 117: 38-44.

Shimizu T, Takizawa N, Watanabe K, *et al.* Crucial role of the influenza virus NS2 (NEP) C-terminal domain in M1 binding and nuclear export of vRNP. *FEBS Lett* 2011; 585: 41-46.

Shin YK, Liu Q, Tikoo SK, *et al.* Influenza A virus NS1 protein activates the phosphatidylinositol 3-kinase (PI3K)/Akt pathway by direct interaction with the p85 subunit of PI3K. *J Gen Virol* 2007; 88: 13-18.

Smith GL, Levin JZ, Palese P, *et al.* Synthesis and cellular location of the ten influenza polypeptides individually expressed by recombinant vaccinia viruses. *Virology* 1987; 160: 336-345.

Songyang Z, Shoelson SE, Chaudhuri M, *et al.* SH2 domains recognize specific phosphopeptide sequences. *Cell* 1993; 72: 767-778.

Stasakova J, Ferko B, Kittel C, *et al.* Influenza A mutant viruses with altered NS1 protein function provoke caspase-1 activation in primary human macrophages, resulting in fast apoptosis and release of high levels of interleukins 1beta and 18. *J Gen Virol* 2005; 86: 185-195.

Steidle S, Martínez-Sobrido L, Mordstein M, *et al.* Glycine 184 in nonstructural protein NS1 determines the virulence of influenza A virus strain PR8 without affecting the host interferon response. *J Virol* 2010; 84: 12761-12770.

Stutz F, Neville M, Rosbash M. Identification of a novel nuclear pore-associated protein as a functional target of the HIV-1 Rev protein in yeast. *Cell* 1995; 82: 495-506.

Wahle E. Poly(A) tail length control is caused by termination of processive synthesis. *J Biol Chem* 1995; 270: 2800-2808.

Wang W, Krug RM. U6atac snRNA, the highly divergent counterpart of U6 snRNA, is the specific target that mediates inhibition of AT-AC splicing by the influenza virus NS1 protein. *Rna* 1998; 4: 55-64.

Wang W, Riedel K, Lynch P, *et al.* RNA binding by the novel helical domain of the influenza virus NS1 protein requires its dimer structure and a small number of specific basic amino acids. *Rna* 1999; 5: 195-205.

Wang X, Basler CF, Williams BR, *et al.* Functional replacement of the carboxy-terminal two-thirds of the influenza A virus NS1 protein with short heterologous dimerization domains. *J Virol* 2002; 76: 12951-12962.

Wang X, Shen Y, Qiu Y, *et al.* The non-structural (NS1) protein of influenza A virus associates with p53 and inhibits p53-mediated transcriptional activity and apoptosis. *Biochem Biophys Res Commun* 2010; 395: 141-145.

Ward AC, Castelli LA, Lucantoni AC, *et al.* Expression and analysis of the NS2 protein of influenza A virus. *Arch Virol* 1995; 140: 2067-2073.

Watanabe K, Takizawa N, Katoh M, *et al.* Inhibition of nuclear export of ribonucleoprotein complexes of influenza virus by leptomycin B. *Virus Res* 2001; 77: 31-42.

Wen W, Meinkoth JL, Tsien RY, *et al.* Identification of a signal for rapid export of proteins from the nucleus. *Cell* 1995; 82: 463-473.

Whittaker G, Bui M, Helenius A. Nuclear trafficking of influenza virus ribonuleoproteins in heterokaryons. *J Virol* 1996; 70: 2743-2756.

Wolff T, O'Neill RE, Palese P. Interaction cloning of NS1-I, a human protein that binds to the nonstructural NS1 proteins of influenza A and B viruses. *J Virol* 1996; 70: 5363-5372.

Wolff T, O'Neill RE, Palese P. NS1-Binding protein (NS1-BP): a novel human protein that interacts with the influenza A virus nonstructural NS1 protein is relocalized in the nuclei of infected cells. *J Virol* 1998; 72: 7170-7180.

Yasuda J, Nakada S, Kato A, *et al.* Molecular assembly of influenza virus: association of the NS2 protein with virion matrix. *Virology* 1993; 196: 249-255.

Young JF, Desselberger U, Palese P, *et al.* Efficient expression of influenza virus NS1 nonstructural proteins in Escherichia coli. *Proc Natl Acad Sci U S A* 1983; 80: 6105-6109.

Yu J, Li X, Wang Y, Li B, *et al.* PDlim2 Selectively Interacts with the PDZ Binding Motif of Highly Pathogenic Avian H5N1 Influenza A Virus NS1. *PLoS One* 2011; 6: e19511.

Zhang C, Yang Y, Zhou X, *et al.* The NS1 protein of influenza a virus interacts with heat shock protein Hsp90 in human alveolar basal epithelial cells: implication for virus-induced apoptosis. *Virol J* 2011; 8: 181.

Zhirnov OP, Konakova TE, Wolff T, *et al.* NS1 protein of influenza A virus down-regulates apoptosis. *J Virol* 2002; 76: 1617-1625.

3. Les interactions Mx-influenza

3.1. Les protéines Mx dotées d'une fonction anti-influenza

Le spectre antiviral des protéines Mx est extrêmement variable, concernant une large gamme de virus à ARN et même certains virus à ADN (Haller et Kochs, 2011). D'une façon générale et assez logique, ce spectre est déterminé par la localisation subcellulaire de la protéine Mx. Ainsi, les protéines Mx nucléaires des rongeurs (Mx1 des souris *Mus musculus* et *Mus spretus*, et du rat *Rattus norvegicus*) ont un spectre antiviral étroit ne comportant que des virus ARN à réplication nucléaire de la famille des *Orthomyxoviridae* (Haller et Kochs, 2011). Les protéines Mx cytoplasmiques ont quant à elles un spectre souvent plus large, bien que très variable. Un effet inhibiteur de la protéine MxA humaine a été mis en évidence sur la réplication de virus des familles *Orthomyxoviridae, Bunyaviridae, Paramyxoviridae, Rhabdoviridae, Flaviviridae* (virus de la peste porcine classique) et même de virus à ADN comme le virus de la peste porcine africaine (*Asfarviridae*) (Haller et Kochs, 2002 ; Netherton *et al.*, 2009 ; Zhao *et al.*, 2011). De nouveaux virus sont ajoutés régulièrement à cette liste au fur et à mesure de leur étude. La protéine MxA humaine ne protège cependant pas contre l'infection par le virus *Dhori*, pourtant membre de la famille des *Orthomyxoviridae*, ni contre les *Picornaviridae*, tels que l'*EMCV* et le virus *Mengo*, ni contre les *Herpesviridae* comme l'*HSV* (Pavlovic *et al.*, 1990 ; Frese *et al.*, 1995).

Le spectre antiviral des autres protéines Mx cytoplasmiques semble beaucoup moins étendu, mais cela vient probablement aussi du fait qu'elles ont été nettement moins étudiées.

Une activité anti-influenza a été décrite pour les protéines Mx suivantes : MxA humaine, Mx1 des souris *Mus musculus* et *Mus spretus* et des rats *Rattus norvegicus* et *Sigmodon hispidus*, Mx1 et Mx2 porcines, Mx du poulet (résultat contesté) et, plus récemment décrite, la Mx1 bovine (Pavlovic *et al.*, 1992 ; Sandrock *et al.*, 2001 ; Ko *et al.*, 2002 ; Palm *et al.*, 2007 ; Sterz *et al.*, 2007 ; Vanlaere *et al.*, 2008 ; Morozumi *et al.*, 2009 ; Garigliany *et al.*, soumis).

3.2. Les mécanismes anti-influenza démontrés/suspectés

Malgré les nombreuses recherches à ce sujet, le mécanisme d'action des protéines Mx à

effet antiviral reste largement méconnu (Haller et Kochs, 2011). Il semble que les protéines Mx nucléaires, comme la protéine Mx1 murine, agissent à un stade plus précoce du cycle de réplication du virus influenza A que les protéines cytoplasmiques, comme la protéine Mx1 humaine (Pavlovic *et al.*, 1992). La protéine Mx1 murine inhiberait la transcription primaire (au minimum 50 fois moins de transcrits primaires), alors que la protéine MxA humaine agirait à un niveau ultérieur. Cette donnée n'est toutefois pas cohérente avec les observations faites avec la protéine Mx1 porcine, qui semble quant à elle affecter le cycle viral beaucoup plus tôt, en inhibant le trafic centripète des ribonucléoprotéines virales entrantes (Palm *et al.*, 2010). Il reste possible que les protéines Mx agissent à différents niveaux, ce qui permettrait de rendre compte des variations observées entre protéines quant au spectre antiviral et à la puissance de cet effet antiviral.

La protéine Mx1 bovine étant cytoplasmique, c'est surtout à cette catégorie de protéines Mx que nous nous intéresserons.

L'association de la protéine MxA, archétype des Mx cytoplasmiques, avec des composants viraux tels que la nucléocapside des virus *Thogoto* et *La Crosse* fut démontrée par des expériences de cosédimentation et d'immuno-marquage (Kochs et Haller, 1999 ; Kochs *et al.*, 2002). Une expérience portant sur la protéine MxA humaine a permis la co-immunoprécipitation de cette protéine avec la nucléoprotéine du virus influenza, mais uniquement après *cross-linking* (Turan *et al.*, 2004). De par la structure en cercle des oligomères de protéine MxA, il a été proposé que ces oligomères puissent entourer et séquestrer les nucléocapsides virales et produire ainsi un effet antiviral (Haller et Kochs, 2011). Cette hypothèse est corroborée par le fait que l'introduction de mutations au niveau des sites d'auto-assemblage de la protéine MxA ou de la boucle désorganisée L4 mène à une perte totale d'activité anti-influenza de la protéine (Haller *et al.*, 2010). Enfin, cette hypothèse est compatible avec un effet de la protéine MxA humaine à différents stades du cycle viral (ribonucléoprotéines entrantes, puis ribonucléoprotéines natives plus tard dans le cycle).

Néanmoins, cette hypothèse d'un mécanisme d'interaction spécifique Mx-nucléoprotéine virale suppose que la protéine MxA humaine soit capable de fixer la nucléoprotéine de tous les virus influenza, mais aussi d'une foule d'autres virus à ARN voire à ADN, issus de nombreuses familles différentes, et ce malgré la grande variation de séquences protéiques pour chaque virus. Cela semble difficile à défendre, d'autant qu'une interaction MxA-nucléoprotéine du virus influenza n'a pu être montrée que dans une

seule étude et que pour une seule souche virale uniquement (Turan *et al.*, 2004). Ce résultat n'a pu être obtenu qu'avec l'utilisation d'un agent de *cross-linking*, sans lequel aucun signal n'a pu être mis en évidence, suggérant une interaction faible, peu en faveur d'un phénomène aussi puissant que l'inhibition de la réplication virale induite par les protéines Mx. Enfin, ce type d'interaction n'a jamais pu être démontré pour aucune autre protéine Mx à activité anti-influenza et nos expériences de co-immunoprécipitation avec la protéine Mx1 bovine et un virus influenza H1N1 n'ont jamais permis d'identifier une interaction entre la protéine Mx et la nucléoprotéine virale, avec ou sans utilisation d'agent de *cross-linking* (Turan *et al.*, 2004 ; Garigliany *et al.*, soumis).

Il semble dès lors plus plausible d'envisager un effet des protéines Mx à activité antivirale sur des fonctions cellulaires communément employées par des virus de différentes familles pour leur réplication, comme suggéré antérieurement (Mibayashi *et al.*, 2002). En faveur de cette dernière hypothèse, on peut ajouter que les protéines Mx dépourvues d'activité antivirale, comme la protéine MxB humaine, sont exprimées de façon constitutive et semblent posséder des fonctions précises, notamment dans le cycle cellulaire (King *et al.*, 2004). La protéine MxA humaine, en dehors de toute infection virale, affecte l'expression des gènes cellulaires et favorise l'apoptose (Mibayashi *et al.*, 2002). Les protéines Mx à activité antivirale, exprimées uniquement de façon inductible, pourraient par exemple avoir un effet inhibiteur compétitif sur les fonctions de protéines cellulaires proches, comme les dynamines par exemple. Des travaux récents ont par ailleurs permis de mettre en évidence un effet inhibiteur de la protéine Mx1 bovine sur la cascade NF-κB, dont l'activation est un prérequis indispensable au cours du cycle réplicatif du virus influenza A (Cornet *et al.*, soumis ; Nimmerjahn *et al.*, 2004). L'inhibition de la voie d'activation de NF-κB pourrait ainsi rendre compte de l'effet inhibiteur de cette protéine sur le virus influenza A.

Quoi qu'il en soit, certaines données récentes ont permis d'approcher et même d'identifier la protéine virale qui semble être la cible, directe ou indirecte, des protéines Mx cytoplasmiques, la nucléoprotéine (Dittmann *et al.*, 2008 ; Zimmermann *et al.*, 2011). Dans un système de mini-réplicon comportant des vecteurs d'expression des trois sous-unités de la polymérase virale, de la nucléoprotéine, d'un gène rapporteur « influenza-spécifique », et de la protéine MxA humaine, il a pu être montré que les différences de sensibilité entre souches de virus influenza A à l'effet inhibiteur de la protéine MxA humaine coségrégeait avec la nucléoprotéine (Dittmann *et al.*, 2008 ;

Zimmermann *et al.*, 2011). La protéine PB2, une des trois sous-unités de la polymérase virale, avait été proposée dans un premier temps car sa surexpression a permis de partiellement titrer l'effet Mx, mais il est probable que cette surexpression ait mené à une surexpression de nucléoprotéine, elle-même responsable de la plus grande résistance à la Mx (Huang *et al.*, 1992 ; Stranden *et al.*, 1993 ; Haller *et al.*, 2010). Aucun domaine ou résidu précis de la nucléoprotéine n'a été proposé comme cible de la protéine MxA humaine et aucun mécanisme moléculaire précis n'a pu être confirmé à ce jour.

Partie II : Contributions personnelles

4. Création d'un jeu de lignées de souris transgéniques exprimant la protéine Mx1 bovine

4.1. Résumé

Les protéines Mx sont des GTPases de haut poids moléculaire, interféron-dépendantes, de la famille des dynamines. Ces protéines ont suscité un intérêt scientifique particulier de par le fait que certaines d'entre-elles présentent une activité antivirale contre certains virus à ARN pathogènes, tels que des membres de la famille des *Orthomyxoviridae*, des *Bunyaviridae* ou des *Rhabdoviridae*. Parmi les différentes protéines Mx étudiées à ce jour, nous avons récemment démontré *in vitro* l'activité antirabique exceptionnelle de l'isoforme 1 de la protéine Mx bovine (boMx1).

Ce résultat nous a poussés à développer un modèle *in vivo* approprié, nous permettant de confirmer ces observations et de tester des stratégies de thérapie génique. En utilisant comme transgène un BAC complet, nous avons généré des lignées de souris transgéniques exprimant les protéines Mx1 et Mx2 bovines sous la dépendance de leurs séquences promotrices naturelles et des éléments régulateurs à courte et longue distance correspondants. Les protéines Mx1 et Mx2 bovines ainsi produites sont assemblées correctement, comme en témoignent les résultats des séquençages d'ARN messagers et des *Western blotting* réalisés. Après stimulation au poly-I/C, l'expression de la protéine Mx1 bovine a été évaluée dans différents organes par immunohistochimie et les lignées de souris transgéniques ont ensuite été classées en lignées à haut ou bas niveau d'expression sur base d'une mesure des concentrations tissulaires en protéine Mx1 bovine par ELISA.

Des cellules *Madin-Darby Bovine Kidney*, des cellules bovines des cornets nasaux et des cellules issues des lignées de souris à haut niveau d'expression présentaient, après stimulation au poly-I/C, des concentrations similaires en protéine Mx1 bovine, suggérant une expression proche des valeurs physiologiques dans les lignées de souris. De plus, l'introduction du gène Mx1 bovin a rendu les souris résistantes, tant en termes de morbidité que de mortalité, à l'infection par le virus de la stomatite vésiculeuse et, d'autre part, des fibroblastes embryonnaires obtenus à partir des lignées de souris à haut niveau d'expression de la protéine Mx1 bovine se sont montrés beaucoup moins permissifs à l'infection par le virus. Les résultats présentés ici démontrent que le système Mx de *Bos taurus* est un puissant agent anti-VSV *in vivo* et suggèrent que les

lignées de souris transgéniques décrites ici constituent un intéressant modèle d'étude *in vivo* des différentes fonctions antivirales – connues et à découvrir – des protéines Mx bovines.

4.2. Garigliany *et al.*, Modulating mouse innate immunity to RNA viruses by expressing the *Bos taurus* Mx system. Transgenic Research 18: 719-732 (2009)

Transgenic Res (2009) 18:719–732
DOI 10.1007/s11248-009-9268-x

ORIGINAL PAPER

Modulating mouse innate immunity to RNA viruses by expressing the *Bos taurus* Mx system

M.-M. Garigliany · K. Cloquette · M. Leroy · A. Decreux · N. Goris · K. De Clercq · D. Desmecht

Received: 17 February 2009 / Accepted: 2 April 2009 / Published online: 23 April 2009
© Springer Science+Business Media B.V. 2009

Abstract Mx proteins are interferon-induced members of the dynamin superfamily of large guanosine triphosphatases. These proteins have attracted much attention because some display antiviral activity against pathogenic RNA viruses, such as members of the orthomyxoviridae, bunyaviridae, and rhabdoviridae families. Among the diverse mammalian Mx proteins examined so far, we have recently demonstrated in vitro that the *Bos taurus* isoform 1 (boMx1) is endowed with exceptional anti-rabies-virus activity. This finding has prompted us to seek an appropriate in vivo model for confirming and evaluating gene therapy strategies. Using a BAC transgene, we have generated transgenic mouse lines expressing the antiviral boMx1 protein and boMx2 proteins under the control of their natural promoter and short- and long-range regulatory elements. Expressed boMx1 and boMx2 are correctly assembled, as deduced from mRNA sequencing and western blotting. Poly-I/C-subordinated expression of boMx1 was detected in various organs by immunohistochemistry, and transgenic lines were readily classified as high- or low-expression lines on the basis of tissue boMx1 concentrations measured by ELISA. Poly-I/C-induced Madin-Darby bovine kidney cells, bovine turbinate cells, and cultured cells from high-expression line of transgenic mice were found to contain about the same concentration of boMx1, suggesting that this protein is produced at near-physiological levels. Furthermore, insertion of the bovine Mx system rendered transgenic mice resistant to vesicular-stomatitis-virus-associated morbidity and mortality, and embryonic fibroblasts derived from high-expression transgenic mice were far less permissive to the virus. These results demonstrate that the *Bos taurus* Mx system is a powerful anti-VSV agent in vivo and suggest that the transgenic mouse lines generated here constitute a good model for studying in vivo the various antiviral functions—known and yet to be discovered—exerted by bovine Mx proteins, with priority emphasis on the antirabic function of boMx1.

Keywords Innate resistance · Virus · VSV · Host–pathogen

M.-M. Garigliany and K. Cloquette have contributed equally to the study.

M.-M. Garigliany · K. Cloquette · M. Leroy · A. Decreux · D. Desmecht (✉)
Department of Pathology, Faculty of Veterinary Medicine, University of Liège, FMV Sart-Tilman B43, 4000 Liège, Belgium
e-mail: Daniel.desmecht@ulg.ac.be

N. Goris · K. De Clercq
Veterinary Agrochemical Center, Groeselenberg 99, 1180 Brussels, Belgium

Introduction

Living organisms are constantly mobilizing numerous and powerful defense mechanisms in order to resist pathogenic agents. A method of choice for identifying

the molecular actors of these defense mechanisms is to detect and analyze variant organisms in which the defenses are altered. Although many variants have been clearly identified in plants (Fraser 1990) and mammals (Green 1989), notably by us (Faisca et al. 2005; Bui Tran Anh et al. 2006), only a few genes and their associated proteins have been characterized to date. One of the best-studied virus-disease susceptibility variants studied is the A2G mouse strain, with its exceptional resistance to the influenza virus. This innate resistance, discovered by Lindenmann (1962), concerns orthomyxoviruses specifically. It protects A2G mice effectively against high virus doses whatever the inoculation route and is inherited as a single autosomal dominant trait (reviewed in Haller 1981). It has now emerged that this resistance is caused by a single gene, named *Mx1*, whose transcription is induced by type-I interferons, themselves being induced by viral infection. The gene codes for a single GTPase, the Mx1 protein (reviewed in Haller et al. 2007). The Mx1-dependent susceptibility of most laboratory mouse lines is due to a structural modification of the *Mx1* gene, either a point substitution creating a premature stop codon or a deletion of exons 9–11. This leads to synthesis of a C-terminally-truncated Mx1 protein (Staeheli et al. 1988). Since this discovery it has emerged that all vertebrates possess between two and three interferon-inducible *Mx-like* genes and that vertebrate Mx proteins, while targeting RNA viruses as a rule, have different antiviral spectra. From these observations has stemmed the hypothesis that each Mx protein might inhibit a set of viruses specifically pathogenic towards the species in which it evolved. One might thus assume that within the pool of Mx isoforms available in nature, there exist diverse antiviral proteins likely to reveal as yet unknown antiviral mechanisms and thus to promote the development of new antiviral drugs. Alternatively, Mx-encoding polynucleotides might be exploitable in gene therapy.

Previously we looked closely at the Mx proteins of the bovine species and we validated a cell culture system for evaluating the antiviral spectrum of the Mx1 protein (boMx1) in vitro (Gérardin et al. 2004; Baise et al. 2004; Leroy et al. 2005). This work revealed an antiviral activity directed against the vesicular stomatitis virus (VSV). In another in vitro study, we recently showed that the boMx1 protein can also very strongly repress two different rabies virus strains, although the antirabic activity of the prototype Mx protein (human MxA [huMxA]) is negligible (Leroy et al. 2006). As rabies is an incurable and inexorably fatal disease in humans, causing some 70,000 deaths annually (http://www.who.int/), the unique antirabic activity of boMx1 has quite understandably raised hopes of developing at last a first curative, rather than merely supportive, therapeutic strategy. Yet a prerequisite to such a project is the demonstration that the antirabic resistance conferred by boMx1 in vitro can be reproduced in vivo. The aim of the present work was to create and characterize transgenic mouse lines equipped with the bovine Mx system. As the three previous attempts to produce a transgenic animal expressing an exogenous Mx protein resulted in multiple problems of expression (Arnheiter et al. 1996), we have chosen to use a transgene of a totally different nature, which has enabled us to produce mouse lines endowed with a bovine Mx operon mimicking very closely the way the native system functions. These lines should be useful for examining in vivo the various antiviral functions—known and yet to be discovered—of bovine Mx proteins, with priority emphasis on the antirabic function of boMx1.

Materials and methods

Characterization of the bacterial artificial chromosome transgene

A single bacterial artificial chromosome (BAC) clone (305L8) unequivocally containing the whole *Bos taurus Mx1* gene (*boMx1*) was identified by screening the RPCI-42 BAC library made from Holstein bull white blood cell DNA (bacpac.chori.org). As DNA probes, we used 5′ (nt 281–315) and 3′ (nt 1,837–1,871) fragments of the *boMx1* gene (U88329) radioactively labeled with [^{32}P]dCTP. Following expansion, small amounts of clone 305L8 DNA were isolated by alkaline lysis, and preparative BAC DNA isolation was carried out with the Nucleobond AX kit (Macherey-Nagel). By *NotI* restriction digestion and pulse-field gel electrophoresis, we estimated the size of the genomic insert to be about 220 kb (data not shown). The DNA sequences of the genomic insert extremities were determined with the Universal Genome Walker™ kit (BD Bioscience Clontech). Pools of adaptor-ligated genomic DNA

fragments of the BAC were constructed by digesting BAC DNA with a set of restriction enzymes. The two fragments containing the vector-insert interfaces were PCR amplified with the help of adaptor- and pBACe3.6-specific primers (Frengen et al. 1999), the latter two corresponding to the regions directly flanking the insert (the T7 and Sp6 promoters). Nucleotide sequencing of the PCR bands revealed the BAC end sequences, which could be anchored on the *Bos taurus* genome sequence (www.ensembl.org). The BAC genomic insert was found to extend over 211,270 bp and to include the complete *boMx2* (AF355147) and *boMx1* (AF047692) genes and the truncated coding sequence of the androgen-regulated serine protease *boTMPRSS2* (BC133425). Further comparison of the BAC sequence with the human genome sequence revealed the putative presence of the bovine homologue of *FAM3B* (NM_058186).

Generation of transgenic mice carrying *BAC305L8*

The $Mx1^{-/-}$ allelic status of FVB/J mice at the *Mx1* locus was first demonstrated by combining in silico comparisons of available SNP data from a series of strains (http://www.informatics.jax.org/), PCR amplification of the intron 10 to exon 11 junction and PCR-RFLV analysis of exon 14 using *Hha*I as described (Jin et al. 1998; Vanlaere et al. 2008). The purified BAC DNA was dissolved in microinjection buffer (10 mM Tris–HCl [pH 7.5], 0.1 mM EDTA, 30 μM spermine, 70 μM spermidine, 100 mM NaCl) at a concentration of about 2–4 ng/μl and microinjected into the pronuclei of FVB/J blastocysts. These were subsequently implanted in pseudo-pregnant recipients. Screening for integration of the *BAC305L8* transgene in the resulting offspring and testing for further germ line transmission (after crossing of selected animals with wild-type FVB/J) were done by DNA genotyping following PCR with *Bos taurus*-specific *Mx1* primers (Table 1). About 11 of 350 offspring contained at least one copy of the transgene, of which nine proved to transmit it to the next generation. Hemi- and homozygous transgenic mice were obtained through further breeding. F6 animals were analyzed for expression and functional studies of the inserted bovine *Mx* genes. Construction of these mice was authorized by the University Bioethics Committee, and anesthesia/euthanasia procedures were consistent with the recommendations of the American Veterinary Medical Association. All mice were housed in a temperature-controlled room (22°C) with 12 h light/12 h dark cycling and fed Purina or Altromin chow.

Generation of embryonic fibroblasts carrying *BAC305L8*

Primary mouse embryonic fibroblasts (MEF) from wild-type and transgenic mice were harvested from 14-day-post-coitum embryos. First the head, liver, and intestine were dissected and the remaining fetal tissues were minced and rinsed in PBS. Fetal homogenates were then treated with trypsin (0.25% in Dulbecco's PBS), incubated for 30 min at 37°C, and subsequently dissociated in medium. After removal of perceptible tissue clumps, the remaining cells were plated out in a 25-cm^2 flask containing DMEM supplemented with 10% heat-inactivated FCS, 1% (v/v) penicillin-streptomycin, and 0.5% amphotericin B. After a 4 h incubation, nonadherent cells were eliminated by gentle mixing, directly followed by medium replacement. Primary cultures reached confluence after ~60 h and were split 1:2 for freezing in liquid nitrogen (passage 1 MEFs) or for plating out in 175-cm^2 flasks. For semi-continuous culturing, MEF cultures were split 1:4 approximately every 4 days.

Analysis of *boMx* mRNA levels

Mx transcript levels were compared in wild-type and transgenic mice, after a standardized stimulation (poly-I/C, 15 μg/kg ip for 24 h). Amounts of boMx-protein-encoding mRNAs were normalized with respect to the amount of endogenous reference mRNA (encoding glyceraldehyde-3-phosphate dehydrogenase, GAPDH).

Production of cDNA samples

Brain, lung, and spleen tissues (50–100 mg) were taken from wild-type and transgenic 7- to 8-week-old female poly-I/C-stimulated mice (five specimens of each line tested). Each tissue sample was individually homogenized (Qiagen's TissueLyser, 30 Hz for 5 min) in TRIzol (Invitrogen) for preparation of total mRNA. Each homogenate was treated with TURBO DNase

Table 1 Primers used in genotype (PCR) and expression (real time PCR) analyses

Target	Amplified fragment length (bp)	Primer sequences
Genotyping		
boMx1-upstream	1,100	Fwd: 5′-CATTCTCTTGATTGGGGAGCTTTA-3′
		Rev: 5′-GCTTCAAAATTCACATTATGCTCA-3′
boMx1-downstream	150	Fwd: 5′-CCGTAGTCTCTGCTGTCTCT-3′
		Rev: 5′-ACCCTTCTACAGTGCTGTGT-3′
boMx2-upstream	883	Fwd: 5′-AATTTGCCCACAAGTCAGG-3′
		Rev: 5′-AGACTCGAGAGCCACGTTTATCAGGAAGC-3′
boMx2-downstream	824	Fwd: 5′-TTGGTTGGTACTGACCACTG-3′
		Rev: 5′-AACTGGATTTAAGCCACAGC-3′
moMST	350	Fwd: 5′-AGTGGAAGAAATTCTCTCTTCACTC-3′
		Rev: 5′-GTAGCTCACCTCACCCTGCATGTT-3′
moMx1[IN10/EX11]	290	Fwd: 5′-GTGACCTTTGAACCTGCTTCCT-3′
		Rev: 5′-GCAGACTCTTCCAGGGCTTTGA-3′
moMx1[EX3/IN3/EX4]	1,100	Fwd: 5′-GTATTGACCTCATCGACACCCT-3′
		Rev: 5′-GGGCATCTGGTAACAATACCTA-3′
moMx1[EX14]	334	Fwd: 5′-CCGTTGCTCATCTCCGACTGT-3′
		Rev: 5′-CACCTTCCTCTGCCCCTACCT-3′
mRNA expression analysis		
moGAPDH	156	Fwd: 5′-TGGCAAAGTGGAGATTGTTGCC-3′
		Rev: 5′-AAGATGGTGATGGGCTTCCCG-3′
boMx1	202	Fwd: 5′-GGGAATGAAGACGAGTGGAA-3′
		Rev: 5′-TGCCAGGAAGGTCTATCAGG-3′
boMx2	201	Fwd: 5′-CAGAAGGCCATGGAAATTGT-3′
		Rev: 5′-CACGCCGTAAATCTGGTCTT-3′

Bo Bovine, *mo* mouse, *MST* myostatin, *GAPDH* glyceraldehyde-3-phosphate dehydrogenase, *IN* intron, *EX* exon

(Ambion) for 30 min at 37°C. Next, line-and organ-specific total RNA extracts were produced by pooling the five individual extracts. After purification the purity and concentration of each extract were determined spectrophotometrically (the OD260/280 and OD260/230, respectively, were in the range 1.9 → 2.0 and 1.8 → 2.2, NanoDrop-1000/Isogen), and mRNA integrity was checked by agarose gel electrophoresis. An aliquot of each line- and organ-specific total RNA extract (2 μg RNA) was then reverse-transcribed at 50°C for 60 min in the presence of 50 μg 18-mer oligonucleotide primers (Table 1) and Superscript III reverse transcriptase (Invitrogen).

Production of DNA calibrators

To estimate the number of copies of each target cDNA in each sample, it was necessary to generate calibrators containing known target copy numbers. To this end, each target sequence was amplified by RT-PCR (see primers in Table 1), purified (Nucleospin Extract II, Macherey-Nagel), and cloned into the pCRII vector (Invitrogen). Then stock solutions of known concentration were generated for each target, the number of copies (per ml) being calculated by dividing the plasmid concentration (μg/μl) by the mass of the plasmid (μg). For this calculation the plasmid concentration was determined by spectrometry (OD at 260 nm) and the plasmid mass was calculated by multiplying the length of the plasmid (vector length [bp] + insert length [bp]) by the mass of a nucleotide ($1.096\ 10^{-15}$ [μg]). For each target, a standard curve for quantitative PCR was constructed on the basis of six dilutions of the appropriate stock solution, corresponding to 5×10^1, 5×10^2, 5×10^3, 5×10^4, 5×10^5, and 7.5×10^5 copies. For

comparisons between lines and organs, the number of *Mx* transcripts was normalized with respect to the corresponding number of *GAPDH* transcripts.

Real-time PCR

The primer pairs used to detect fragments of the *boMx1* and *boMx2* transgene transcripts and of the mouse *GAPDH* transcript are listed in Table 1. The PCR mixture consisted of 100 ng/µl template DNA (1 µl), 70 nM primers (0.7 µl of each), and 12.5 µl ABsolute™ Blue QPCR SYBR Green ROX Mix (ABgene) in a final volume of 25 µl. The mixture was placed in an ABI PRISM® 7900HT thermocycler and amplification was carried out under the following conditions: initial denaturation at 95°C for 15 min, followed by 40 cycles of denaturation at 95°C for 15 s and annealing-extension at 58°C for 30 s, and then a final extension at 72°C for 30 s. Amplification of all transcripts was performed in triplicate, and three independent sessions were carried out with each RNA extract. The melting curve of each amplicon was monitored by means of a swing back to 50°C, followed by a stepwise rise in temperature up to 95°C. Melting curve analysis always revealed the presence of a single product. To check for false positives, RT-free and no-template controls were run for each template and primer pair.

Analysis of boMx1 protein levels

Production of antisera targeting Bos taurus Mx proteins

A 1,974-bp fragment of the *boMx1* gene (NM_173940.2) was PCR amplified from template DNA extracted from IFNα-induced (1,000 U/ml recombinant IFNα A/D for 24 h, Sigma) Madin-Darby bovine kidney cells (MDBK, ATCC # CCL-22) as previously described (Baise et al. 2004). The forward primer was 5′-ggg**ggatcc**gatggttcattctgacttgggtatcg-3′, and the reverse primer was 5′-ccc**aagctt**gcccgggaacttgg ccagc-3′, with the boldface type indicating the *BamHI* and *HindIII* restriction sites chosen for cloning in the vector pET-28b[+] (Novagen). A PCR fragment of the expected size was then generated and cloned. The presence and integrity of the recombinant *boMx1*-pET28b plasmid were confirmed in the kanamycin-resistant transformants by restriction endonuclease digestion and by sequencing of the *boMx1* cDNA. The recombinant plasmid was used to transform competent *E. coli* Rosetta DE3 pLysS cells (Novagen), which were induced with 1 mM isopropylthio-ß-D-galactoside for 2 h and then harvested by centrifugation (1,000 g for 10 min at 4°C). The pellets were stored at −80°C. Total protein extraction and purification under denaturing conditions were done with and as recommended for the ProBond Purification system (Invitrogen). Elution fractions showing a measurable absorbance at 280 nm and a band at ~80 kDa on western blots (corresponding to recombinant boMx1) were pooled, supplemented with 0.5% Triton-X100, and dialyzed stepwise against successive dilutions of PBS-urea (6–0.5 M). The concentration of recombinant boMx1 in the resulting stock solution was determined with the BCA Protein Assay Kit (Pierce Biotechnology), and a rabbit antiserum was obtained from two rabbits injected four times ip with boluses containing 200 µg boMx1. A second antiserum was raised in FVB/J mice by six consecutive ip injections with 100 µl boluses containing spleen extracts from poly-I/C-induced (15 µg/g body weight 24 h before spleen extraction) transgenic mice.

Extraction

For each mouse line and each tissue sampled (brain, heart, kidney, liver, lung, and spleen) the frozen (−80°C) organs from five poly-I/C-exposed (15 µg/g body weight 24 h before sacrifice) 8-week-old animals were pooled and pulverized with pestle and mortar in a liquid nitrogen bath. About 500 mg crude frozen homogenate of each organ was resuspended in 600 µl extraction buffer (LLB, Eurogentec), vortexed for 2 min, and kept on ice. Samples were then sonicated (three pulses of 30 s each with 30-s intervals on ice) and centrifuged at 11,000*g* for 10 min at 4°C. The supernatants were stored at −80°C in protein-repellant-coated tubes (Protein LoBind Eppendorf Tubes®) and total protein content was measured with the BCA Protein Assay kit.

Immunoblot analysis

Aliquots of resulting supernatants corresponding to 50 (spleen), 70 (lung), or 250 µg (brain) total protein were loaded onto 10% SDS–PAGE gels and electrophoresed.

After electrotransfer onto nitrocellulose membranes, the blots were blocked for 30 min with Tris-buffered saline containing 0.1% Tween and 10% bovine serum albumin and incubated for 1 h at room temperature with the mouse antiserum (dilution 1:1000). Immune complexes were revealed with HRP-conjugated pig anti-rabbit IgG F(ab′)2 fragments (dilution 1:1000, Dakocytomation), and peroxidase detection with the CN/DAB Substrate Kit (Pierce Biotechnology). Densitometry was performed with the Fluor S Multiimager CCD camera system and Quantity One software (Bio-Rad).

ELISA

A non-competitive indirect sandwich enzyme-linked immunosorbent assay (ELISA) was developed, using rabbit antiserum for capture, mouse antiserum followed by HRP-conjugated polyclonal rabbit-anti-mouse-Ig (#P0260, Dakocytomation) for detection, and finally TMB conversion as the read-out parameter for enzyme activity (Enhanced K-Blue, Neogen). First, 96-well Microlon 600 plates (Greiner, #655081) were coated overnight at 4°C with 100 µl rabbit antiserum diluted 1:1000 in carbonate buffer (100 mM, pH 9.5). They were then blocked for 1 h at 37°C with 250 µl casein solution (1% in PBS). For boMx1 content determinations, the wells were first incubated for 1 h at 37°C with 100 µl calibrator (see below) or with organ extract diluted in PBS, then incubated for 1 h at 37°C with 100 µl mouse antiserum diluted 1:1000 in PBS-0.5% casein. For detection of immune complexes, the wells were incubated for 1 h at 37°C with 100 µl rabbit anti-mouse-Ig diluted 1:1000 in PBS-0.5% casein, then incubated at room temperature for 20 min with 100 µl TMB in substrate buffer with H_2O_2, according to the manufacturer's recommendations. Development was stopped by adding 100 µl of 1 M HCl and the plates were read at 450 nm. The OD was determined with respect to a subtractive reference (an extract of the corresponding organ from stimulated wild-type FVB/J mice). Calibrators were derived from a stock of recombinant boMx1 titrating 100 µg/ml. The highest calibrating concentration used was 375 ng/ml, and this solution was subjected to a 9-step serial dilution in PBS. The concentrations of the resulting calibrating samples were as follows: 375, 250, 200, 150, 100, 80, 60, 40, 20, and 10 ng/ml. New calibrators were generated from the stock for each session of tissue boMx1 content measurements. They provided an absolute correlation of signal vs. concentration (ng boMx1 per µg soluble protein). Successive dilutions of primordial protein extracts from each organ were first assayed in order to determine the range of concentrations yielding the highest signal. Spleen, lung, and brain protein extracts were diluted so as to incorporate respectively ~5, ~50, and ~300 µg total protein per well.

Immunohistochemistry

Tissue sampling was performed according to a standard protocol. After fixation in 4% neutral-buffered ice-cold paraformaldehyde and embedding in paraffin, tissue sections were stained for boMx1 detection by an indirect immunohistological method using the rabbit antiserum followed by an HRP-conjugated goat-anti-rabbit immunoglobulins secondary antibody. Peroxidase was revealed with 3-amino-9-ethyl-carbazole, resulting in a bright red precipitate. Tissues were counterstained with Mayer's hematoxylin and embedded in glycerol–gelatin. Rabbit pre-immunization serum, omission sections, and mock-exposed MDBK cell cytospins were used as negative controls and IFNα-exposed MDBK cell cytospins were used as positive controls. The following tissues were examined: lung, heart, intestine, liver, spleen, kidney, cerebrum, cerebellum, and brain stem.

Functional analysis of boMx proteins

Modulation of mouse innate immunity against RNA viruses by the transgene products was probed by examining whether the biological cycle of the vesicular stomatitis virus (VSV), a rhabdovirus, is altered in transgenic MEFs or mice. A stock and appropriate dilutions of VSV serotype Indiana were prepared from the supernatant of virus-infected BHK-21 cells. Two independent in vitro experiments were first conducted, in which viral suspensions were incorporated (300 µl/well, 24-well plates) for 1 h at a multiplicity of infection of 0.1, 1, or 10 into near-confluent (80%) cultures of noninduced or induced (50 µg/ml poly-I/C for 24 h) MEF lines derived from wild-type (WT), transgenic low-expression, and transgenic high-expression FVB/J mice. After a 1 h

adsorption period, excess inoculum was removed by washing with PBS, and the cultures were re-incubated for 24 h at 37°C in fresh DMEM. The culture supernatants were then sampled for virus titration. For in vivo studies, sets of 15 WT, 10 ML-555, and 15 ML-549 FVB/J mice were inoculated with the virus by slowly instilling 50 µl of the viral suspension (i.e., $\sim 10^7$ cell culture infective dose 50% [$CCID_{50}$]) into the nostrils under anesthesia (30/5 mg kg^{-1} xylazine/ketamine ip). In all sets, body weight and survival were monitored for 14 days. Subsets of 5 WT and 5 ML-549 mice were euthanized on day 4 after inoculation. Their lungs and brains were removed and homogenized with a TissueLyser for subsequent virus titration. Viral titers from supernatants and organ suspensions were first determined in duplicate on Vero cells. They were expressed in $CCID_{50}$ units at 48 h after inoculation as previously described (Baise et al. 2004). Relative quantification of the viral load was also done by real-time PCR. Total RNA was extracted with the help of commercially available NucleoSpin silica-based spin-columns according to the manufacturer's instructions (Macherey-Nagel). In a separate reverse transcription (RT) step, 2 µg extracted RNA was added to 1× Multiscribe RT Buffer (TaqMan® Reverse Transcription Reagents, Applied Biosystems) supplemented with 25 pmol random hexamer primers (Applied Biosystems), 5 nmol dNTP's, 55 nmol $MgCl_2$, 4 IU RNase inhibitor; and 12.5 IU Multiscribe reverse transcriptase (Applied Biosystems) in a total volume of 10 µl. RT conditions were as follows: 10 min at 25°C, followed by 30 min at 48°C and 5 min at 95°C. For the subsequent real-time PCR, 5 µl template cDNA was added to 12.5 µl of 2× SYBR Green PCR Master Mix (Applied Biosystems) supplemented with 5 pmol forward and reverse primers in a total volume of 25 µl (for primer sequences, refer to Núñez et al. 1998). The mixture was placed in an ABI 7900HT thermocycler for 10 min at 95°C, then the targeted VSV-specific cDNA segment was amplified by means of a program consisting of 40 cycles of 15 s at 95°C and 60 s at 60°C. The melting curve of the resulting amplicon was monitored by means of a swing back to 50°C for 15 s, followed by a stepwise rise in temperature up to 95°C. A VSV-positive sample and a negative water sample were included as internal controls in both the RT and the PCR step. All samples were analyzed in duplicate reactions.

Statistical analysis

All data are reported as means ± SD. Differences between mean values were tested for statistical significance by the two-tailed Student's *t* test, survival curves were subjected to Kaplan-Meier analysis, and the significance threshold was set at $P < 0.05$.

Results

Development of transgenic mouse lines with a functional *BAC305L8* insert

SNP data available between positions 976 686 42 and 976 845 14 on chromosome 16 (*Mx1* gene) do not reveal variation between the FVB/J line on the one hand, BALB/c, C57BL/6, DBA/2, and C3H/HeN lines on the other. Moreover, the genomic stretch overlapping intron 10 and exon 11 was retrieved by PCR from BALB/c-A2G mice but never from BALB/c, FVB/J and ML-549 lines (Fig. 1A). PCR-RFLV analysis of exon 14 revealed the presence of an *Hha*I restriction site in all strains tested, which refuted the hypothesis of a CBA/J-like $Mx1^{-/-}$ allele in FVB/J (Fig. 1B). Collectively, these results show that the FVB/J line carries the Mx1-negative allele common to the vast majority of inbred lines. About 11 mice born through oviduct transfer of microinjected oocytes were transgenic. Nine of these transmitted the transgene to their offspring, as revealed by PCR analysis, but two of the nine lines became rapidly extinct because of very low reproduction rates. Next, a more detailed analysis by standard PCR enabled us to amplify from the DNA of the seven remaining lines specific segments corresponding to the 5′ and 3′ ends of the *boMx1* and *boMx2* genes. This suggests that at least one intact copy of each bovine *Mx* gene was inserted in each line (Fig. 1).

Maximum levels of *boMx1* and *boMx2* mRNAs were measured in lung tissues from poly-I/C-injected mice by reverse transcription followed by real-time PCR. They were normalized against GAPDH mRNA. This analysis demonstrated efficient transcription of the inserted *boMx1* and *boMx2* genes in the lungs in all lines except ML-555, where *boMx2* mRNA was never detected (Fig. 1). The transgenic lines were readily classified as high-expression (ML-549, ML-556), medium-expression (ML-310, ML-375), or

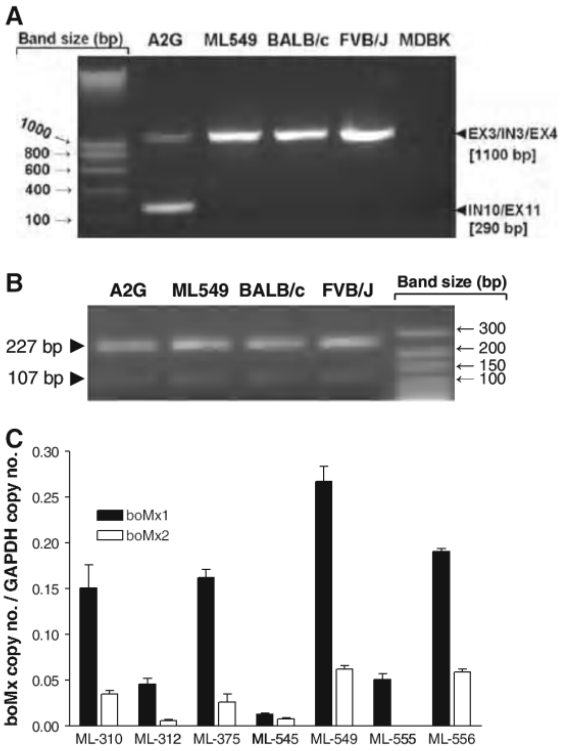

Fig. 1 **A** and **B** Genotyping of the *moMx1* locus in mice with known (BALB/c-A2G, BALB/c) and unknown (FVB/J and ML-549) allelic status. The BALB/c-A2G congenic line was generously provided by Drs O. Haller and P. Staeheli. **A** FVB/J and ML-549 mice carry the BALB/c-like $moMx^{-/-}$ allele. Targeted genomic segment consists in the junction between intron 10 and exon 11 which are deleted in most of inbred mouse strains but not in A2G (Staeheli et al. 1988). Primers are listed in Table 1. **B** The $moMx1^{+/+}$ allele of BALB/c-A2G mice and $Mx1^{-/-}$ alleles of BALB/c, FVB/J and ML-549 carry the *Hha*I restriction site in exon 14 (two *bands*), which suggests that the $moMx^{-/-}$ allele of FVB/J is that of BALB/c rather than that of CBA/J (Staeheli et al. 1988). Primers are listed in Table 1. **C** Detection and quantitation by real-time PCR of *boMx1* and *boMx2* transcripts in lung extracts from transgenic mice. Induction was carried out with poly-I*/C* for 24 h before sampling. Using a set of lungs from specific pathogen-free noninduced mice, the positive/negative cut-off threshold was set at a Ct value of 28. *GAPDH* transcript copy number was used for normalization. See text for key

low-expression lines (ML-312, ML-545 & ML-555), according to the amount of transcripts produced. In silico translation of the boMx polynucleotide sequences retrieved by RT-PCR from poly-I/C-induced transgenic mice yielded the expected amino acid sequences.

Western blot (immunoblot) analysis of lung (Fig. 2B), spleen, and brain (data not shown) extracts showed that *boMx1* mRNA was duly translated in all three tissues. A semi-quantitative densitometric analysis of three blots, obtained from the lungs of three mice, yielded the same classification by expression level as determined by real-time RT-PCR: ML-549 ≈ ML-556 > ML-310 ≈ ML-375 > ML-312 ≈ ML-545 ≈ ML-555 (Fig. 2B). Immunohistochemical analysis of brain, heart, lung, intestine, kidney, liver, and spleen tissues confirmed these results and further revealed inter- and intra-organ differences in expression (Fig. 3). In all mice of all transgenic lines but one (ML-545, whose tissues displayed no staining), boMx1-specific staining was more intense in the kidneys and intestines than in the other organs. In the brain and liver, it was more intense in some cell types (Kupffer cells) or structures (the choroid plexus); in the lungs, staining was more intense in the epithelium of the alveoli than in the epithelium of the bronchioles. We used an ELISA to measure the concentration of boMx1 protein in various organs of five poly-I/C pretreated mice of each line. For line ML-545, whatever the animal or the organ, the results were the same as for the organs of wild-type mice. Among the six boMx1-producing lines, no clear expression pattern emerged, although the dominant trend was for the concentration to be about 15 times as high in the spleen as in the lungs and about five times as high in the lungs as in the brain (Fig. 2C). In the lungs, four lines displayed concentrations of 200–300 and the other two about 100 ng per mg soluble protein. On the basis of concentrations in the brain, three pairs were identifiable: ML-549 and ML-556 with about 50, ML-310 and ML-375 with 15-25, and ML-312 and ML-375 with about 5 ng per mg soluble protein. With regard to spleen concentrations, there emerged two high-expression (~5 μg/mg soluble protein), two low-expression, and two no-expression lines. Among the latter is line ML-310, with high boMx1 levels in the lungs and none in the spleen. Upon maximum stimulation by poly-I/C, fifth-passage embryonic fibroblasts from ML-549 and ML-555 mice expressed about 1.4 and 0.2 μg boMx1 per mg of soluble protein. Our stably transfected Vero cell line, which shows a high degree of VSV resistance (Baise et al. 2004), contains about 1 μg/mg, and the bovine BT and MDBK cell lines produce ~1 and ~0.6 μg/mg, respectively (Fig. 2D). For comparison we also conducted a large-scale screening of the boMx1 content of bovine spleens collected at a local

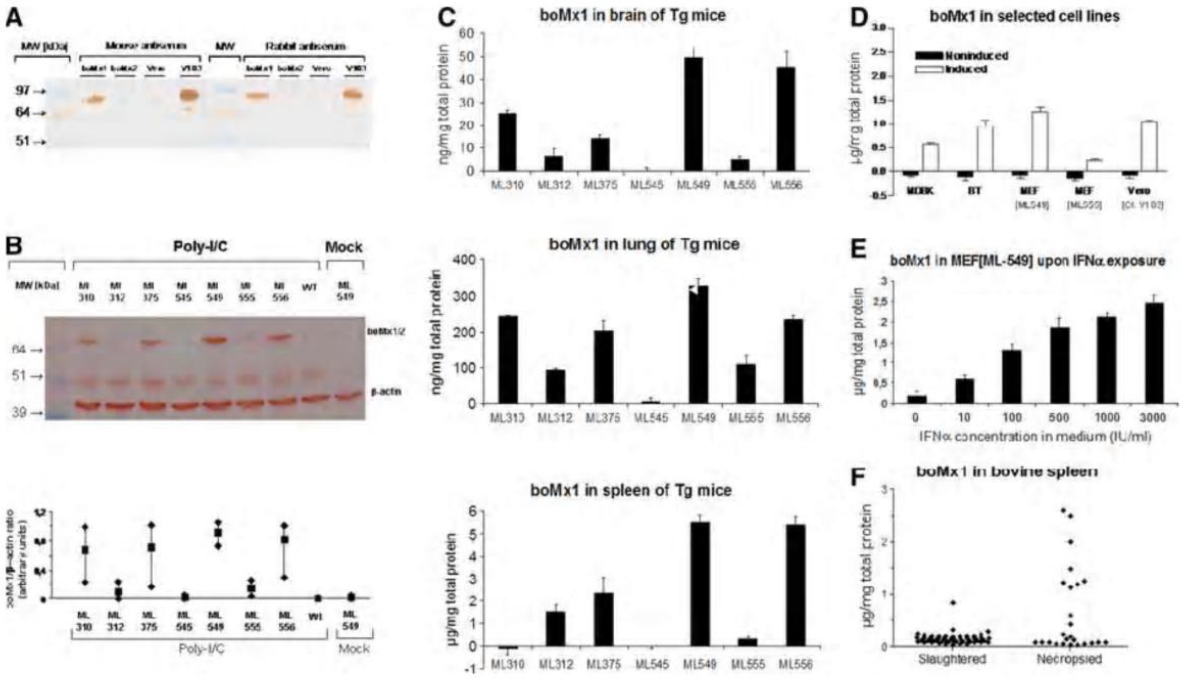

Fig. 2 Patterns of boMx1 expression among transgenic lines and comparison with the boMx1 content of bovine cells/tissues. **A** Mouse and rabbit antisera tag boMx1, but not boMx2. Vero cells were transiently transfected with cDNA constructs encoding boMx1, or boMx2. Vero cells and vero cells stably transfected with cDNA conditionally expressing the bovine *Mx1* gene are included (clone #V103, see Baise et al. 2004). About 24 h after transfection/stimulation, bovine Mx proteins were detected after 10% polyacrylamide SDS–PAGE of cell extracts and western blotting with rabbit (*left*) or mouse (*right*) antiserum. Transient expression of boMx2 had been duly detected by real time PCR. **B** Bovine Mx proteins are readily detectable in lung extracts from poly-I/C-pretreated transgenic mice, but not in extracts from either mock- or poly-I/C-pretreated ML-549 and wild-type mice, respectively. About 24 h after pretreatment, boMx1 protein and β-actin were detected in pooled lung protein extracts by 10% polyacrylamide SDS–PAGE and western blotting with mouse anti-boMx1 antiserum and an anti-actin mAb (*top*). Molecular weight markers are shown on the *left*. Densitometric semi-quantitation of the boMx1-associated bands was performed and the results reported are mean (squares) and extreme (lozenges) values retrieved from three independent immunoblots (*bottom*). **C** BoMx1 content determinations in brain, lung, and spleen from transgenic mice reveal line-specific expression patterns. BoMx1 values were determined in triplicate by ELISA on pooled ($n = 5$) protein extracts retrieved from organs taken from 8-week-old female mice that had been injected with poly-I/C 24 h earlier. See text for ELISA specifications. Values are means ± SD. **D** Spontaneous or forced boMx1 expression in bovine cells yields concentrations of the same order of magnitude as measured in transgenic mouse and Vero cells. Control and induced boMx1 expression in bovine cell lines (MDBK and BT), mouse embryonic fibroblasts (MEF) derived from transgenic lines ML-549 and ML-555, and in the Vero cell clone #V103. Values are means ± SD of triplicate ELISA determinations. Induction was done by adding poly-I/C (50 µg/ml) to the cell culture broth 24 h before harvest. **E** boMx1 expression is induced by exposure to IFNα and its level of expression is subordinated to IFNα concentration in the medium. Mouse embryonic fibroblasts from the ML-549 line were seeded in 24-well plates and IFNα was incorporated when the monolayers reached confluence and the reaction was stopped 24 h after. Values are means ± SD of duplicate ELISA determinations from protein extracts of each of three wells treated separately. **F** Spontaneous boMx1 expression in bovine spleens collected at a local slaughterhouse ($n = 80$) and at the Faculty necropsy clinic ($n = 25$). *Postmortem* spleen boMx1 concentrations amounted between 0.5 and 3 µg/mg among the ten virus-positive cases detected in the cohort of necropsied animals, thus being of the same order of magnitude as measured in transgenic mouse spleens

slaughterhouse and at the Faculty necropsy clinic. This revealed spontaneous (thus submaximal) concentrations of ~0.15 µg/mg soluble protein among slaughtered animals and among necropsied animals in which no viruses were detected, whereas boMx1 concentrations amounted between 0.5 and 3 µg/mg among the ten virus-positive cases. In summary, we have produced transgenic mice that lack endogenous antiviral Mx proteins (their genetic background is that of the FVB/J strain) but that conditionally express the bovine *Mx1* and *Mx2* genes, in various organs and under the control of their natural promoter,

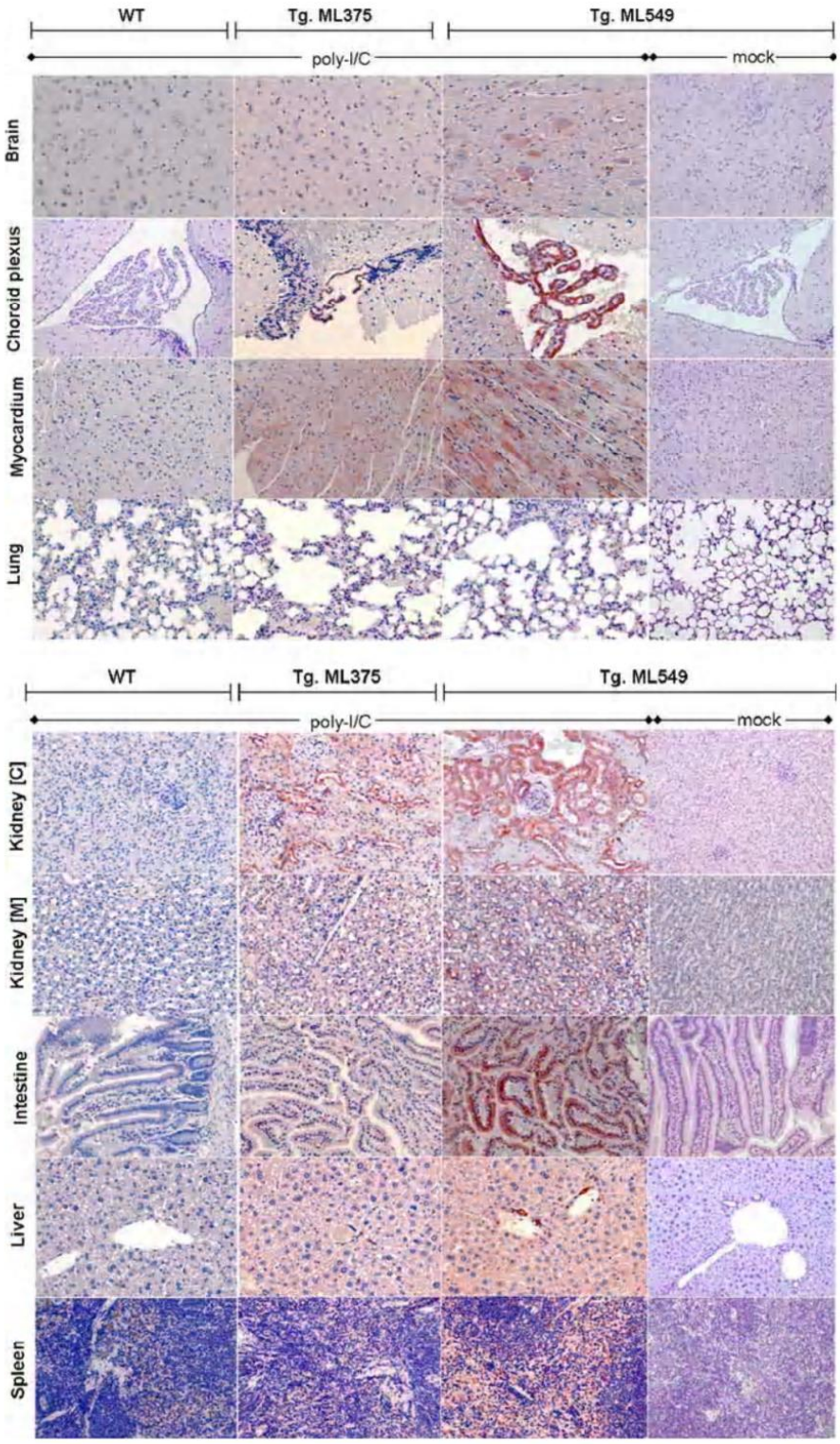
WT
Tg. ML375
Tg. ML549
poly-I/C
mock
Brain
Choroid plexus
Myocardium
Lung
WT
Tg. ML375
Tg. ML549
poly-I/C
mock
Kidney [C]
Kidney [M]
Intestine
Liver
Spleen

◀ **Fig. 3** Immunohistochemical BoMx1 detection in tissues from transgenic mice reveals widespread expression along with line- and organ-specific patterns. Overall staining is always more intense in kidney and intestine than elsewhere. Intra-organ staining differences are also obvious. Staining is much more intense, for instance, in the choroid plexuses or in the Kupffer cells of the liver, and in the type II pneumocytes of the lungs than in the surrounding tissues. About 24 h before euthanasia/sampling, both wild-type and transgenic mice were induced by injection of either poly-I/C (15 µg/g body weight, ip) or saline

up to protein concentrations comparable to those measured in bovine cells and tissues.

Transgenic mice expressing the intact *Bos taurus* Mx genes are protected against lethal VSV infection

Using weight loss as a measure of morbidity, we then examined whether the bovine Mx genes could protect transgenic mice against lethal VSV infection. We observed that at $\sim 10^7$ $CCID_{50}$ of the virus, transgenic $boMx^{+/-}$ ML-549 mice did not experience any significant weight loss, whereas transgenic $boMx^{+/-}$ ML-555 and wild-type mice lost significant body weight after inoculation (Fig. 4A). Follow-up of survival among these mice revealed highly significant differences between ML-549 mice, on the one hand, and ML-555 and wild-type mice on the other (Kaplan-Meier analysis, $P < 0.01$); all ML-549 mice survived whereas the mortality rate was 100 and 70% among the two other lines, respectively (Fig. 4B). In summary, mice expressing both bovine Mx1 and Mx2 were protected against the high mortality and morbidity caused by the VSV virus. To test hypothesis that this boMx1/2-induced reduction in clinical severity was associated with repression of the virus itself, we quantified VSV viral loads by qPCR and conventional titration. The 4 days post-VSV infection, VSV genomic

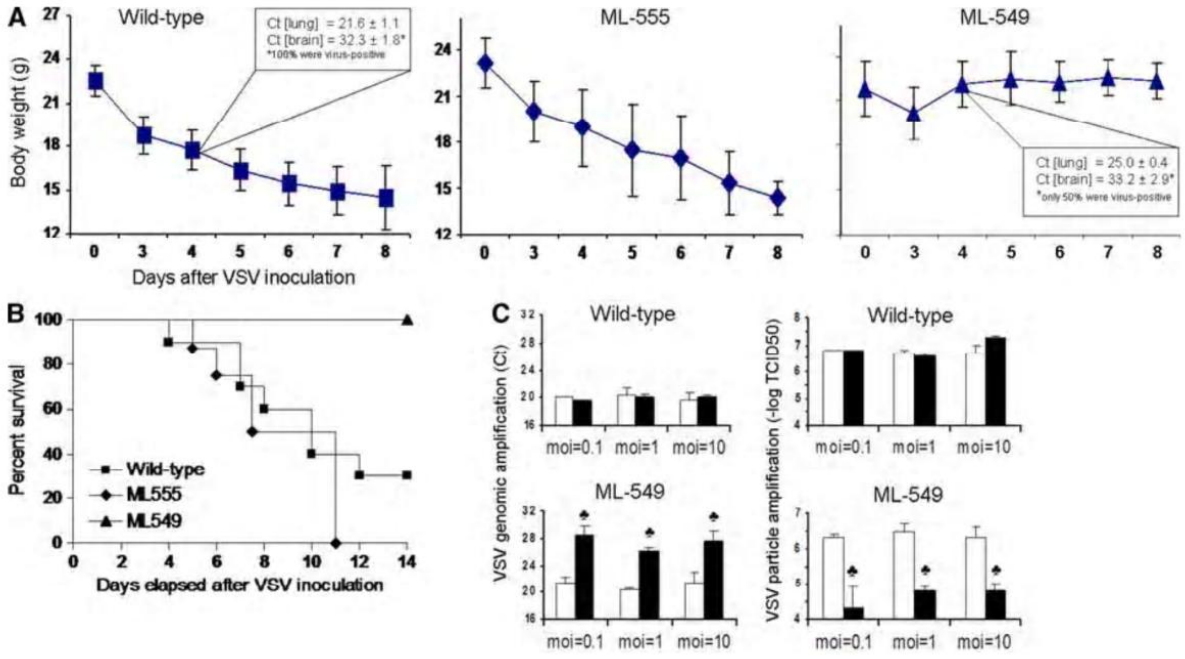

Fig. 4 Vesicular stomatitis virus (*VSV*, strain Indiana) is not lethal to high-expression $boMx^{+/-}$ (ML-549) mice at a dose lethal to both low-expression $boMx^{+/-}$ (ML-555) and zero-expression $boMx^{-/-}$ (wild-type) mice. **A** Body weight change (mean ± SD) and **B** survival of mice ($n = 10$ per group) inoculated with $\sim 10^7$ $CCID_{50}$. Inset: cycle thresholds (means ± SD) recorded for VSV genomic amplification in lung and brain homogenates from $boMx^{-/-}$ (wild-type) and $boMx^{+/-}$ (ML-549) mice 4 days after inoculation. **C** Effect of transgenic expression of the *Bos Taurus* Mx system on VSV genomic (*left*) and particle (*right*) amplification in embryonic fibroblasts derived from wild-type and transgenic (ML-549) mice, as measured on supernatants collected 24 h after virus incorporation. Values are means ± SD of two independent experiments. *White* and *black boxes* refer, respectively to mock- and IFNα-exposed cells. *Black clovers* point to results significantly different from those obtained with the corresponding mock-exposed cells ($P < 0.01$). m.o.i., multiplicity of infection

loads were significantly higher in the lungs of wild-type mice than in ML-549 mice, as judged from the increased cycle threshold in samples from the latter (Fig. 4A, inset). The brain is another target organ for VSV following intranasal infection (Chesler and Reiss 2002). On day 4 post infection, the VSV genome was retrieved from 100% of the wild-type but only 50% of the ML-549 mice, and a comparison of the qPCR-positive samples revealed a lower level in ML-549 mice. We also measured replication of VSV in the lung and brain tissues of the mice 4 days after inoculation. The virus titers found in the brains of all mice were below the limit of detection of our assay at this time point. The virus was detected in the lungs of all wild-type mice (4.17 ± 0.65 [-1]log$TCID_{50}$), but never in the lungs of the transgenic mice. Overall, expression of the bovine *Mx* genes in mice was thus crucial to reducing the viral load in lungs after VSV infection. About 24 h after infection of embryonic fibroblast monolayers with VSV, both the genome copy number and the infectious particle load were again dramatically lower in ML-549 than in wild-type-derived cells (Fig. 4C).

Discussion

We have created transgenic mouse lines in which the genomic fragment encoding the bovine antiviral Mx system is inserted and is transmitted from one generation to the next. As the genetic background of these lines is that of strain FVB/J, carrying defective Mx genes that no longer code for a functional endogeneous Mx protein (Fig. 1A, B), these transgenic lines constitute an ideal experimental model for testing the antiviral activities of bovine Mx proteins in vivo. The FAM3B gene included in the BAC encodes a 235-amino-acid cytokine with a secretion signal peptide. As this cytokine is expressed specifically in the islets of Langerhans of the pancreas and the testes (Zhu et al. 2002), its presence, if any, is unlikely to generate any artefact when the antiviral function of the bovine Mx proteins is examined.

Several attempts of this type have been made in the past to examine the antiviral function of the mouse Mx1 protein (Arnheiter et al. 1990; Kolb et al. 1992; Müller et al. 1992) or the human MxA protein (Pavlovic et al. 1995) in vivo. These previous attempts have always consisted in inserting a small artificial construct bearing a mouse promoter (that of Mx1, 3-hydroxy-3-methylglutaryl coenzyme A reductase, or albumin), a human promoter (that of metallothioneine IIA), or a viral promoter (the SV40 early enhancer/promoter) upstream from the *moMx1* or *huMxA* cDNA. Many expression problems appeared: absence of transcription (Pavlovic et al. 1995), absence of mRNA translation (Müller et al. 1992), gradual extinction (Kolb et al. 1992), mosaicism (Arnheiter et al. 1990; Kolb et al. 1992), or loss of inducibility of expression (Arnheiter et al. 1990). To avoid these problems we opted for a large transgene ($\sim$210 kb) because we could legitimately expect it to contain both genes in their entirety, including the short-range (UTRs, introns) and long-range *cis*-regulatory elements required for correct spatio-temporal expression. The second advantage of the use of a BAC is that BACs are expected to be more resistant to position effects than smaller transgenes (Giraldo and Montoliu 2001; Gong et al. 2003). Overall, we have confirmed the advantages linked to a larger transgene size, since we have detected inducible production of the boMx proteins in all organs of $\sim$90% (8/9) of the lines showing germinal insertion, whereas expression of the huMxA protein was previously demonstrated in only $\sim$13% (2/15) of the transgenic lines obtained (Pavlovic et al. 1995). The transgenic lines produced here differ slightly between each other as regards the regulation of both transcription and translation. Firstly, the levels of mRNA measured after standardized induction and the ratio of *boMx1* to *boMx2* transcripts were found to vary from line to line. For example, the *boMx2* transcript appears to be totally absent from ML-555 (Fig. 1B). On the other hand, a look at transcript levels in relation to the corresponding protein concentrations suggests that the rate of conversion from transcripts to protein also varies from line to line. Furthermore, we have found expression to vary considerably from organ to organ (spleen > lung > brain), with a clear variation of the spatial expression pattern according to the line. Expression differences between lines thus appear to be slighter in the lungs and greater in the spleen, as illustrated by the spectacular case of line ML-310, which shows high expression in the lungs and zero expression in the spleen. These differences probably reflect different numbers of insertions and/or random excision of certain BAC fragments in the course of purification and pronuclear microinjection. The absence of *boMx2* transcripts in line ML-555 suggests insertion of a

single, truncated BAC. It is likewise plausible that the other differences stem from excision of certain remote *cis*-regulatory elements. Similarly, the fact that the two high-expression lines share a common spatial expression pattern may reflect insertion of several BACs, complete or truncated, ensuring the presence of at least one copy of all the regulatory elements present in nature.

As the objective was to validate the use of these transgenic mice in characterizing the functions of the two bovine Mx proteins in vivo, it was important to examine whether the protein concentrations obtained are biologically pertinent or not. Our comparison of maximum expression levels measured after poly-I/C induction in bovine and transgenic-mouse-derived cell lines shows that the amount of boMx1 accumulated over a 24 h period in response to poly-I/C was practically the same in bovine MDBK and BT cells, in embryonic fibroblasts from the high-expression line ML-549, and in cells of clone Vero #V103, where the antiviral functions of the boMx1 protein were previously studied (Baise et al. 2004; Leroy et al. 2005, 2006): roughly between 0.6 and 1.4 µg/mg soluble protein (Fig. 2D). The level recorded in embryonic fibroblasts of the low-expression line ML-555 reached about a third/quarter of the level recorded in MDBK and BT bovine cells, respectively. These results indicate that insertion of the chosen BAC transgene has enabled us to generate two high-expression lines that both faithfully reproduce the conditional expression pattern typical of the species from which the transgene derived and produce similar quantities of boMx1. We have additionally compared the levels of boMx1 reached in the spleens of a cohort of bovines in response to a viral disease with the concentrations generated artificially in response to poly-I/C in the spleens of transgenic mice (Fig. 2D). Again the concentrations arising spontaneously in the spleens of infected bovines was of the same order of magnitude as the maximal concentrations measured in the spleens of transgenic mice. This confirms that the Mx system introduced into the transgenic mice functionally mimics the Mx system present in the species of origin, *Bos taurus*.

We further show that a high degree of resistance to VSV can be conferred to mice by germinal transformation. This resistance should reflect both the effective antiviral action of the protein(s) concerned and its/their inducibility by the virus itself. We conclude that the boMx1 protein, the boMx2 protein, or both and their regulatory machinery constitute a genetic substrate capable of transforming an inexorably fatal infection into a benign and transient one (Fig. 4A, B). This confirms in vivo the anti-VSV activities detected in vitro, here in embryonic fibroblasts from line ML-549 (Fig. 4C) and previously in Vero cells for boMx1 (Baise et al. 2004) and in NIH-3T3 cells for boMx2 (Babiker et al. 2007). As the viral disease is not attenuated at all in line ML-555 despite production of boMx1, one might hypothesize that the protection conferred in vivo requires the simultaneous presence of both boMx1 and boMx2. Alternatively, the protection conferred in vivo might be dose-dependent, since an ~3-fold-lower level of boMx1 is observed in the lungs and an ~10-fold-lower level in the brain in line ML-555 (Fig. 3C). A third possibility is that the time required for the antiviral protein to accumulate to an effective level is crucial. This timing is likely to depend on the presence or absence of as yet unidentified regulatory elements that line ML-555 might lack.

In conclusion, we have generated transgenic mice expressing the complete bovine antiviral Mx system under the control of its close and remote natural regulatory elements. The various transgenic lines produced differ as regards their spatio-temporal *Mx* expression patterns, which suggests that predictable breaks in the BAC used for pronuclear injection may have caused amputation of certain remote elements in certain lines. We have further shown that two of these lines display boMx1 protein levels quite similar to those observed in bovine tissues, and that transgenesis has conferred to these lines a high degree of resistance to VSV amplification and VSV-associated disease. These transgenic lines constitute good models for identifying new regulatory elements and for studying in vivo the various known and as yet undiscovered antiviral activities of the bovine Mx proteins, with priority emphasis on the exceptional antirabic function of boMx1 recently detected in vitro.

Acknowledgments The authors thank Dr. Fabien Ectors for his enthusiasm and exceptional skill at performing the 350 pronuclear microinjections and implanting transformed blastocysts into pseudo-pregnant mouse recipients. Many thanks are also due to Anne Cornet for genotyping the *Mx1* locus of the different mouse lines.

References

Arnheiter H, Skuntz S, Noteborn M et al (1990) Transgenic mice with intracellular immunity to influenza virus. Cell 62:51–61

Arnheiter H, Frese M, Kambadur R et al (1996) Mx transgenic mice: animal models of health. Curr Top Microbiol Immunol 206:119–147

Babiker H, Nakatsu Y, Yamada K et al (2007) Bovine and water buffalo Mx2 genes: polymorphism and antiviral activity. Immunogenetics 59:59–67. doi:10.1007/s00251-006-0167-5

Baise E, Pire G, Leroy M et al (2004) Conditional expression of type I interferon-induced bovine Mx1 GTPase in a stable transgenic vero cell line interferes with replication of vesicular stomatitis virus. J Interferon Cytokine Res 24:513–521

Bui Tran Anh D, Faisca P, Desmecht D (2006) Differential resistance/susceptibility patterns to pneumovirus infection among inbred mouse strains. Am J Physiol Lung Cell Mol Physiol 291:L426–L435. doi:10.1152/ajplung.00483.2005

Chesler D, Reiss C (2002) IL-12, while beneficial, is not essential for the host response to VSV encephalitis. J Neuroimmunol 131:92–97. doi:10.1016/S0165-5728(02)00257-6

Faisca P, Bui Tran Anh D, Desmecht D (2005) Sendai virus-induced alterations in lung structure/function correlate with viral loads and reveal a wide resistance/susceptibility spectrum among mouse strains. Am J Physiol Lung Cell Mol Physiol 289:L777–L787. doi:10.1152/ajplung.00240.2005

Fraser R (1990) The genetics of resistance to plant viruses. Annu Rev Phytopathol 28:179–200. doi:10.1146/annurev.py.28.090190.001143

Frengen E, Weichenhan D, Zhao B et al (1999) A modular, positive selection bacterial artificial chromosome vector with multiple cloning sites. Genomics 58:250–253. doi:10.1006/geno.1998.5693

Gérardin JA, Baise EA, Pire GA et al (2004) Genomic structure, organisation, and promoter analysis of the bovine (Bos taurus) Mx1 gene. Gene 326:67–75. doi:10.1016/j.gene.2003.10.006

Giraldo P, Montoliu L (2001) Size matters: use of YACs, BACs and PACs in transgenic animals. Transgenic Res 10:83–103. doi:10.1023/A:1008918913249

Gong S, Zheng C, Doughty ML et al (2003) A gene expression atlas of the central nervous system based on bacterial artificial chromosomes. Nature 425:917–925. doi:10.1038/nature02033

Green M (1989) Catalog of mutant genes and polymorphic loci. In: Green M (ed) Genetic variants and strains of the laboratory mouse, 2nd edn. Oxford University Press, London/New York, pp 12–403

Haller O (1981) Inborn resistance of mice to orthomyxoviruses. Curr Top Microbiol Immunol 92:25–52

Haller O, Stertz S, Kochs G (2007) The Mx GTPase family of interferon-induced antiviral proteins. Microbes Infect 9:1636–1643. doi:10.1016/j.micinf.2007.09.010

Jin HK, Yamashita T, Ochiae K et al (1998) Characterization and expression of the *Mx1* gene in wild mouse species. Biochem Genet 36:311–322. doi:10.1023/A:1018741312058

Kolb E, Laine E, Strehler D et al (1992) Resistance to influenza virus infection of Mx transgenic mice expressing Mx protein under the control of two constitutive promoters. J Virol 66:1709–1716

Leroy M, Baise E, Pire G et al (2005) Resistance of paramyxoviridae to type I interferon-induced Bos taurus Mx1 dynamin. J Interferon Cytokine Res 25:192–201. doi:10.1089/jir.2005.25.192

Leroy M, Pire G, Baise E et al (2006) Expression of the interferon-alpha/beta-inducible bovine Mx1 dynamin interferes with replication of rabies virus. Neurobiol Dis 21:515–521. doi:10.1016/j.nbd.2005.08.015

Lindenmann J (1962) Resistance of mice to mouse-adapted influenza A virus. Virology 16:203–204. doi:10.1016/0042-6822(62)90297-0

Müller M, Brenig B, Winnacker E et al (1992) Transgenic pigs carrying cDNA copies encoding the murine Mx1 protein which confers resistance to influenza virus infection. Gene 16:263–270. doi:10.1016/0378-1119(92)90130-H

Núñez J, Blanco E, Hernández T et al (1998) RT-PCR assay for the differential diagnosis of vesicular viral diseases of swine. J Virol Methods 72:227–235. doi:10.1016/S0166-0934(98)00032-9

Pavlovic J, Arzet H, Hefti H et al (1995) Enhanced virus resistance of transgenic mice expressing the human MxA protein. J Virol 69:4506–4510

Staeheli P, Grob R, Meier E et al (1988) Influenza virus-susceptible mice carry Mx genes with a large deletion or a nonsense mutation. Mol Cell Biol 8:4518–4523

Vanlaere I, Vanderrijst A, Guénet JL et al (2008) Mx1 causes resistance against influenza A viruses in the *Mus spretus*-derived inbred mouse strain SPRET/Ei. Cytokine 42:62–70. doi:10.1016/j.cyto.2008.01.013

Zhu Y, Xu G, Patel A et al (2002) Cloning, expression and initial characterization of a novel cytokine like gene family. Genomics 80:144–150. doi:10.1006/geno.2002.6816

5. Etablissement de modèles d'infection de la souris par un virus influenza A

5.1. Résumé

Selon l'Organisation Mondiale de la Santé, le virus influenza infecte chaque année entre 5 et 15 % de la population mondiale, résultant en 2 à 3 millions de cas sévères et environ 500.000 décès. La récente pandémie de 2009 à virus H1N1 et la persistance de souches hautement pathogènes de virus H5N1 dans les populations aviaires domestiques en Asie notamment suscitent des questions quant au risque de voir se renouveler une pandémie aussi tragique que celle de 1918.

Si les symptômes classiques d'une infection par le virus influenza A chez l'homme consistent principalement en un syndrome fébrile et une atteinte respiratoire supérieure, les cas sévères sont quant à eux associés au développement d'un syndrome de détresse respiratoire aigu (ARDS) ou à la survenue d'une surinfection bactérienne. Les mortalités associées au virus influenza, épidémique ou pandémique, sont liées à l'une ou l'autre de ces conditions.

La létalité très importante liée au virus H1N1 de 1918 et aux souches de virus H5N1 hautement pathogènes rend la compréhension des mécanismes physiopathologiques liés à ces infections essentielle pour pouvoir envisager des traitements plus adaptés. Ainsi, si les infections bactériennes secondaires peuvent être contrôlées dans la plupart de cas par l'usage d'antibiotiques, l'amélioration de la prévention et du traitement de l'ARDS associé au virus influenza A est une priorité pour diminuer le taux de mortalité à l'infection par ce virus. La connaissance des mécanismes impliqués dans le développement de cet ARDS apparait donc cruciale.

Si l'on s'en réfère à la littérature, les lésions histopathologiques décrites en cas d'ARDS mortel associé au virus influenza A ont toutes traits à des « dommages alvéolaires diffus » et la pathogénie de ces lésions apparait comme identique quelle que soit la souche virale impliquée.

Dans cette étude, nous étudions en détail l'ARDS induit en modèle murin par des doses identiques de deux souches de virus influenza A rendues extrêmement virulentes par adaptation à la souris. Bien que toutes deux létales à 100%, avec développement de dommages alvéolaires diffus et des titres viraux pulmonaires comparables, les infections par chacune de ces deux souches virales étaient associées à une cinétique et à des

lésions histopathologiques radicalement différentes, démontrant le caractère souche-spécifique de la pathogénie associée au développement d'un ARDS. Ainsi, une meilleure compréhension des mécanismes spécifiques sous-jacents permettrait d'adapter de manière beaucoup plus efficace les traitements au pathotype viral impliqué.

5.2. Garigliany *et al.*, Influenza A strain-dependent pathogenesis in fatal H1N1 and H5N1 subtype infections of mice. Emerging Infectious Diseases 16: 595-603 (2010)

Influenza A Strain-Dependent Pathogenesis in Fatal H1N1 and H5N1 Subtype Infections of Mice

Mutien-Marie Garigliany, Adélite Habyarimana, Bénédicte Lambrecht, Els Van de Paar, Anne Cornet, Thierry van den Berg, and Daniel Desmecht

To determine if fatal infections caused by different highly virulent influenza A viruses share the same pathogenesis, we compared 2 different influenza A virus subtypes, H1N1 and H5N1. The subtypes, which had shown no pathogenicity in laboratory mice, were forced to evolve by serial passaging. Although both adapted viruses evoked diffuse alveolar damage and showed a similar 50% mouse lethal dose and the same peak lung concentration, each had a distinct pathologic signature and caused a different course of acute respiratory distress syndrome. In the absence of any virus labeling, a histologist could readily distinguish infections caused by these 2 viruses. The different histologic features described in this study here refute the hypothesis of a single, universal cytokine storm underlying all fatal influenza diseases. Research is thus crucially needed to identify sets of virulence markers and to examine whether treatment should be tailored to the influenza virus pathotype.

According to the World Health Organization, influenza annually infects 5%–15% of the global population, causing 3–5 million cases of severe illness and ≈500,000 reported deaths. The persistence of influenza A virus (H5N1) in poultry populations over the past 6 years and the ability of those viruses to cause fatal infections in humans, along with the recent pandemic (H1N1) 2009 outbreaks, have raised fears of a renewed catastrophic influenza outbreak comparable to that of 1918, which caused death in 0.2%–8% of those infected in various countries and ≈50 million deaths worldwide (*1*). Standard influenza symptoms include fever, cough, headache, sore throat, and dehydration, with some reports of diarrhea, vomiting, and bleeding from the mouth or throat. In benign cases, not all of these symptoms are exhibited. In severe cases, additional signs typical of either secondary bacterial pneumonia or acute respiratory distress syndrome (ARDS) occur. Notably, these 2 manifestations are those that cause death in patients with influenza, whether seasonal or pandemic or caused by the 1918 subtype H1N1 strain or by recent subtype H5N1 strains.

The catastrophic lethality of the 1918 pandemic makes it paramount that we understand the disease pathogenesis of both severe forms of influenza. Because most secondary bacterial pneumonias can be controlled with antimicrobial agents, prevention and treatment of influenza-associated ARDS are the major medical challenges that must be addressed to reduce the influenza-related death rate. This requires more knowledge about the pathogenesis of ARDS. Alterations in human and mouse lungs have been described for fatal virus infections with pandemic virus strains (subtypes H1N1, H2N2, and H3N2 strains of 1918, 1957, and 1968, respectively) or subtype H5N1 strains. They are all characterized by similar lung dysfunctions and lesions (*2*,*3*). The lung becomes flooded as its alveolocapillary membranes leak, and the alveoli fill with body fluids. Consequently, the exchange of carbon dioxide and oxygen is reduced, and fatal acute lung failure ensues. The histologic findings depend on the stage of the disease. Edema, epithelial necrosis, fibrin, and hyaline membranes are found during the early exudative phase, and fibroblast and type II cell hyperplasia are found during the proliferative phase. This array of morphologic alterations is known as diffuse

Author affiliations: University of Liège, Liège, Belgium (M.-M. Garigliany, E. Van de Paar, A. Cornet, D. Desmecht); and Veterinary Agrochemical Center, Brussels, Belgium (A. Habyarimana, B. Lambrecht, T. van den Berg).

DOI: 10.3201/eid1604.091061

alveolar damage. Moreover, mice infected with the 1918 influenza virus or with a recent subtype H5N1 human isolate also show considerable similarities in overall lung cellularity, composition of lung immune cell subpopulation, and cellular immune temporal dynamics (*4*). On the basis of these mostly retrospective studies, the pathogenesis of influenza-associated ARDS is widely viewed as being the same whatever the infecting strain.

In this study, we closely monitored ARDS in mice, caused by inoculation of identical doses of 2 different influenza strains rendered highly pathogenic toward mice by adaptation. The 2 strains elicited dramatically different disease courses and histopathologic signatures, although both strains caused death in 100% of those infected, evoked the expected diffuse alveolar damage, and led to comparable virus titers in the lungs. The pathogenesis underlying influenza-associated fatal ARDS thus depended on the infecting strain.

Materials and Methods

Animals

Eight-week-old female FVB/J mice weighing 20–25 g were obtained from Charles River Laboratories (L'Arbresle, France). Challenge studies were conducted under BioSafety Level 3 laboratory conditions and in facilities accredited by the Belgian Council for Laboratory Animal Science, under the guidance of the Institutional Animal Care and Use Committees of the Veterinary Agrochemical Research Center and University of Liège. The mice were housed in microisolator cages ventilated under negative pressure with HEPA-filtered air. The light/dark cycle was 12/12 h, and the animals were allowed free access to food and water. Before each inoculation or euthanasia procedure, the animals were anesthetized by intraperitoneal injection of a mixture of ketamine (50 mg/kg) and xylazine (30 mg/kg).

Viruses

Two influenza A virus strain subtypes that had low pathogenicity for laboratory mice were used in this study: a clade 1 avian influenza virus (H5N1) (A/crested_eagle/Belgium/1/2004), and a porcine influenza virus (H1N1) (A/swine/Iowa/4/76). Both viruses were first propagated in the allantoic cavity of 10-day-old embryonating hen eggs and then adapted to the mice by lung-to-lung passaging. At each passage, a set of mice were inoculated intranasally with 50 μL of either allantoic fluid or lung homogenate containing influenza A virus. At 5 days postinoculation (dpi), the mice were killed humanely by an overdose of pentobarbital, followed by exsanguination. The lungs were combined and homogenized in phosphate-buffered saline (PBS)–penicillin-streptomycin, the homogenates were centrifuged at 3,000 g for 10 min, and the supernatant was used for the next passage. The process was stopped when the mice showed a substantial loss of bodyweight on 4 dpi. This occurred after 5 (H5N1) or 31 (H1N1) passages. Lung homogenates from the last passage were homogenized and divided into aliquots for direct use in pathotyping studies, and their titers were determined by standard plaque (subtype H1N1) or median tissue culture infective dose assays (H5N1). Serial dilutions of each adapted virus stock were then injected into FVB/J mice, and the 50% mouse lethal dose (MLD_{50}) was calculated according to the method of Reed and Muench (*5*).

Pathotyping Studies

For assessment of virus-induced pathogenicity, 2 series of mice were inoculated intranasally with 10 MLD_{50} of virus by instillation of 50 μL of diluted stock. Mice were monitored daily for changes in bodyweight to assess virus-induced illness. At selected intervals, 5 (virus titration or histopathology) or 10 (virus titration + dry/wet weight ratio) mice were given an overdose of sodium pentobarbital and exsanguinated by cutting the brachial artery. Lungs and pieces of heart, liver, spleen, pancreas, kidney, brain, and adipose tissue from 5 mice were fixed in 4% neutral-buffered, ice-cold paraformaldehyde, routinely processed, and embedded in paraffin for histopathologic evaluation. Five-micrometer sections were stained with hematoxylin and eosin (HE) or periodic acid–Schiff (PAS) for lesion detection. For virus detection, sections were stained by a streptavidin-biotin complex immunoperoxidase method. An in-house immunoglobulin (Ig) G–purified polyclonal rabbit antiserum raised against recombinant influenza virus nucleoprotein was used as the source of primary antibodies, and horseradish peroxidase (HRP)–conjugated anti–rabbit IgGs (Dako, Glostrup, Denmark) were used as secondary antibodies. Peroxidase was indicated by the bright red precipitate produced in the presence of 3-amino-9-ethyl-carbazole, and sections were counterstained with Mayer hematoxylin. For virus titrations, lungs from 5 mice were weighed, homogenized in 1 mL PBS, and clarified. The supernatants were used for virus titration by plaque or median tissue culture infectious dose assays. Because the appearance of a biphasic expiratory pattern has been shown to announce death within ≈24 h (*6*), this qualitative sign was chosen, for humane reasons, as the endpoint of the experimental disease. On this endpoint day, lungs from 5 mice were sampled and weighed, and homogenates thereof were desiccated for dry weight determination.

Results

Clinical, Gross Pathologic, and Virologic Observations

The influenza A virus strains (subtypes H1N1 and H5N1) used in this study were isolated, respectively, from

a diseased pig in the United States in 1976 and from a crested eagle smuggled from Thailand in 2003 (*7*). Both were nonpathogenic for FVB/J mice (MLD_{50} >10^6 PFU/50% tissue culture infective dose [$TCID_{50}$]). After adaptation, the strains showed a similar pathogenic outcome in FVB/J mice, i.e., close MLD_{50} values: 3.2 PFUs for the subtype H1N1 strain and 6.4 $TCID_{50}$ for the subtype H5N1 strain. These results allowed a relevant comparison of their respective pathologic signatures. Overall, virus-associated illness, bodyweight loss, and gross lesions caused by inoculation of 10 MLD_{50} were similar for both viruses, except that body condition and respiratory function deteriorated far more rapidly after subtype H5N1 inoculation, the endpoint being reached on 4 dpi for subtype H5N1–induced disease and 8 dpi for subtype H1N1–induced disease. The pathologic processes caused no symptoms for the first 2 (H5N1) or 3 (H1N1) days and then gave rise to general signs such as gradually slower, less frequent, and more erratic spontaneous displacements and a ruffled coat. By 3 dpi (H5N1) or 5 dpi (H1N1), all mice became lethargic and abruptly showed clinical signs of respiratory disease, including respiratory distress, labored breathing, and forced expiration. Mice inoculated with subtype H5N1 lost 10% of their bodyweight during the last 48 hours before the endpoint day. In mice that were inoculated with subtype H1N1, weight loss was acute and biphasic: a 10% loss occurred between virus inoculation and the appearance of respiratory symptoms, and an additional 20% was lost during ARDS (Figure 1). Autopsies performed on the endpoint day of subtype H1N1 disease consistently showed dark, purplish, bulky, noncrepitant, liverlike lungs, findings compatible with a diagnosis of massive pulmonary congestion and consolidation. In subtype H5N1–inoculated mice, the lungs at endpoint were bulky, noncrepitant, and diffusely pinkish gray, which suggests a diagnosis of congestion with massive pulmonary edema. Mice inoculated with either virus had a lung wet weight at endpoint approximately double that of controls, but this weight gain was achieved during the last ≈24 hours in mice inoculated with subtype H5N1, whereas mice inoculated with subtype H1N1 showed a progressive lung weight increase over 96 hours, from 4 dpi to the endpoint day (Figure 2). At the endpoint, the dry/wet weight ratio of the lungs was ≈22% lower for subtype H5N1-infected mice (17.6% ± 1.1%) than for subtype H1N1-infected mice (21.4% ± 1.4%). No obvious gross lesions were observed in the heart, liver, spleen, kidney, brain, or perivisceral fat. The lung virus loads measured on 2, 4, 6, and 8 dpi are shown in Figure 3. The time required to reach the peak virus titer was the same for both virus strains. Death occurred at the peak lung virus concentration for subtype H5N1, but subtype H1N1–associated disease did not become fatal until 4 days after this peak, when virus clearance was already substantial (Figure 3).

Histopathologic Observations

An exhaustive list of the histopathologic lesions caused by the 2 viruses is given in the online Appendix Table (www.cdc.gov/EID/content/16/4/595-appT.htm). Some changes in lung morphology were identical for both viruses. First, a clear topographic extension of the lesions was perceptible between the first and the last day of infection, with centrifugal spreading from the terminal bronchioles or the alveoli adjacent to the airways. Qualitatively, all alterations characterizing the exudative phase of the histopathologic condition termed diffuse alveolar damage were identifiable, with intense congestion of the alveolar

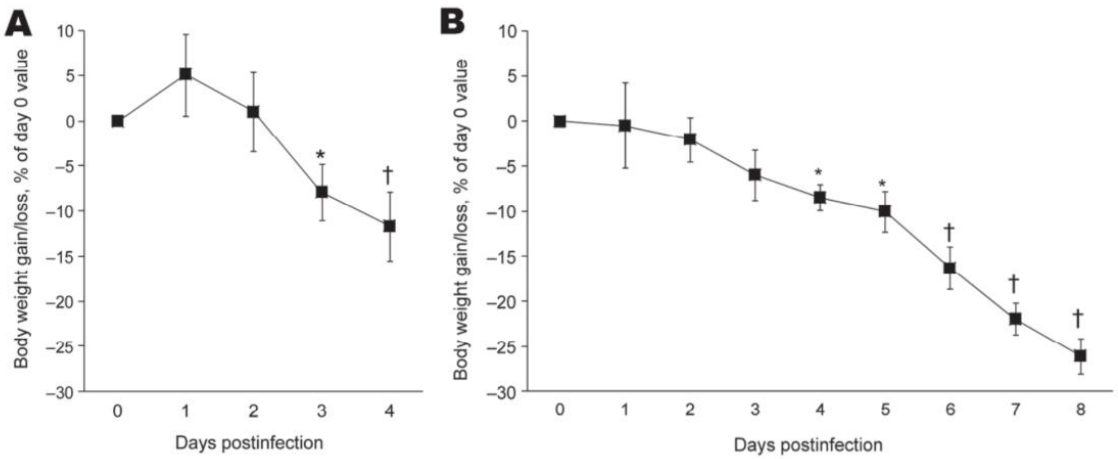

Figure 1. Effect of influenza A virus subtype H5N1 (A) and H1N1 (B) strains on bodyweight gain or loss after intranasal inoculation of 10× the 50% mouse lethal dose on day 0. Relative values are given, as calculated with respect to preinoculation control values (mean ± SD). For each virus strain, means significantly different from baseline are indicated (Student *t* test for paired values). *p<0.05; †p<0.01.

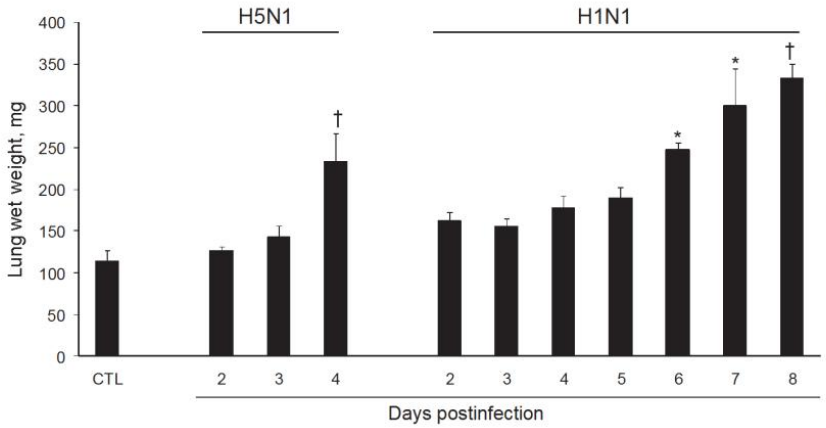

Figure 2. Effect of influenza A virus subtype H5N1 and H1N1 strains on lung weight after intranasal inoculation of 10× the 50% mouse lethal dose on day 0. Absolute values are given as means ± SD for 5 mice at each time point. For each virus strain, means significantly different from those of control (CTL) lungs are indicated (nonparametric Mann-Whitney test). *p<0.05; †p<0.01.

capillaries, marginated intracapillary neutrophils, necrosis of the alveolar epithelium, interstitial and alveolar edema, hyaline membranes, and invasion of the alveoli by (mostly) mononucleate cells. On the other hand, we did not observe cuboidalization of the alveoli (hyperplasia of type II pneumocytes) or hyperplasia or squamous metaplasia of the airway epithelia. These results indicate extremely rapid disease progression, nearly complete elimination of type II pneumocytes, or both. Despite these similarities, when sections of lung tissue samples taken on the last day from infected mice were pooled by subtype, an examiner unaware of which infection he was looking could easily distinguish one from the other (Figures 4, 5). The criteria for attributing lung lesions to the subtype H1N1 strain were the following: 1) earlier and much more extensive degeneration, necrosis, and desquamation of the airway epithelium; 2) a much higher cell density of the peribronchial, peribronchiolar, interstitial, and intra-alveolar infiltrates; 3) the presence of dense cuffs of mononucleate cells around the arterioles; 4) far less extensive alveolar edemas; and 5) the rarity of alveolar hemorrhages. The lesions caused by the subtype H5N1 strain were distinguishable by the late and mild regressive alterations of the airway epithelium, the extent of alveolar edema, the low cell density of the inflammatory infiltrates, the high number of alveolar hemorrhage foci, and the unusual appearance of the pulmonary arterioles (which seemed to have been dissected from the surrounding tissues because of the magnitude of the perivascular edema).

On the other hand, no arteriole showed any cuff of infiltrated mononucleate cells. Some blood-vessel walls also showed hemorrhage inside the muscle layer. No other organ examined was found to carry any histopathologic lesions except, notably, the liver in subtype H5N1–infected mice (Figure 5). These livers displayed multifocal necrosis, with necrotic foci consisting of aggregates of hypereosinophilic, pyknotic, and caryorhectic hepatocytes, admixed with a few neutrophils and lymphocytes. Such foci were

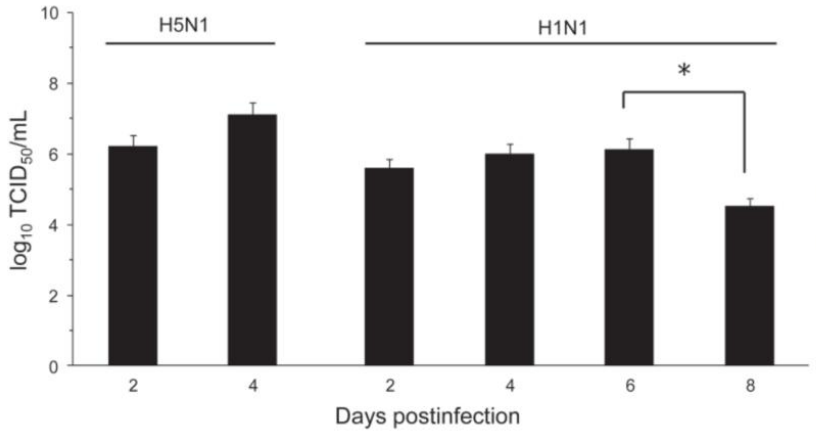

Figure 3. Effect of influenza A virus subtype strains H5N1 and H1N1 on lung virus titers 2–8 days after intranasal inoculation of 10× the 50% mouse lethal dose on day 0. Titers are expressed as the $\log_{10}$ median tissue culture infectious dose ($TCID_{50}$) units per milliliter of lung homogenate. Significantly different titers are indicated (nonparametric Mann-Whitney test). Error bars indicate SD calculated from individual virus titers. *p <0.05.

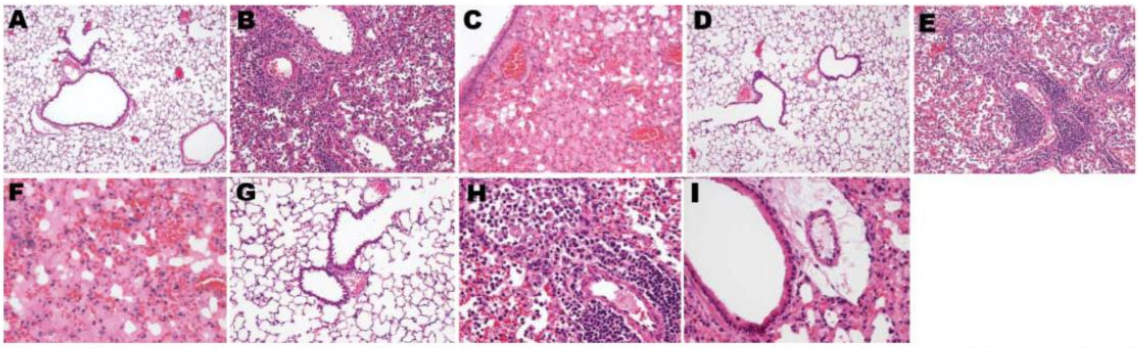

Figure 4. Photomicrographs of the lung sections of influenza A virus (H1N1)– and (H5N1)–infected mice at endpoint (hematoxylin and eosin stain). Dramatically different histopathologic signatures are observed, with either a mostly cellular reaction (H1N1) or a mostly humoral reaction (H5N1). Panels A, D, and G: 3 views of vehicle-infected lungs (original magnification ×100). Panels B and E, subtype H1N1: Dense granulocytic and lymphocytic cell infiltrates in the interstitium and around vessels and airways with focally denuded lamina propria due to epithelial necrosis and desquamation (original magnification ×100). Panel C, subtype H5N1: Airway epithelium is intact; note the striking difference in the number of infiltrated inflammatory cells between subtypes H1N1- and H5N1-infected lungs. Dramatic congestion of the vessels is visible, with extensive interstitial and alveolar edema (original magnification ×100). Panel F, subtype H5N1: Alveoli are completely filled with edema and hemorrhages; cellular infiltrates are conspicuously absent (original magnification ×200). Panel H, subtype H1N1: An airway with a totally denuded lamina propria is shown (top, left), with its lumen filled with granulocytic and lymphocytic exsudate (original magnification ×200). A prominent periarteriolar lymphocytic cuff is visible (bottom right). Panel I, subtype H5N1: Moderate inflammatory cell infiltrate, with no cuffing of any airway or vessel; an airway with a still intact epithelium is shown, located just beside a vessel with dramatic peripheral edema (original magnification ×200).

also seen in the spleen in some animals. Strikingly, numerous PAS-positive islets were detected throughout the livers of subtype H5N1–infected animals, each overlapping with a necrotic focus. Patterns of centrolobular, hydropic, granular (2 dpi), centrolobular (3 dpi), and panlobular (4 dpi) microvesicular fatty degeneration were also observed in the livers of all subtype H5N1-infected animals. Interstitial hemorrhages were seen in the renal medulla.

Detection of Viruses in Tissues

The results of immunohistochemical tests were homogeneous for mice infected with the same strain. Overall, they showed that the subtype H1N1 strain swarmed centrifugally from the bronchioles throughout the lungs over 4–5 days, but remained strictly confined to the lungs. The subtype H5N1 virus, in contrast, conquered the whole lung over 24–48 hours; infected some bronchioles only later; and spread to the liver, pancreas, kidneys, spleen, brain, and perivisceral fat.

Topologic Distribution of Subtype H1N1 Antigens over Time

The virus was first detectable in the epithelium of the bronchi and bronchioles on 3 dpi. By 5 dpi, the stain was more conspicuous and appeared also in the alveolar epithelium of the areas adjacent to the airways. By 7 dpi, the virus was detectable in the epithelia of almost all bronchi and bronchioles and in the alveolar epithelium in extensive areas of the lungs. In the alveolar structures, staining showed the virus in type I and type II pneumocytes and in alveolar macrophages (Figure 6, panels A, C, and E). Nonrespiratory organs sampled on 3, 5, or 7 dpi remained strictly virus negative.

Topologic Distribution of Subtype H5N1 Antigens over Time

The virus was detectable from 2 dpi in some type II pneumocytes in peribronchiolar alveoli, some interstitial/alveolar macrophages, and some endothelial cells in the vicinity of the positive alveoli. In contrast, no nonrespiratory organ examined showed any virus-positive cells. By 3 dpi, staining of the airway epithelium was still discrete and limited, whereas the alveolar epithelium showed more pronounced staining, diffusely distributed throughout the lung. In the liver, multiple nests of positive hepatocytes were detectable, corresponding exactly with the above-mentioned necrotic PAS-positive foci. A few renal tubular epithelial cells were also positive. On 4 dpi, the alveolar epithelium was still diffusely stained, but more intensely than on 3 dpi. For the first time, staining of the bronchiolar epithelium was also visible, but not all bronchioles—far from all, in fact—showed this staining. Type II pneumocytes and alveolar macrophages were more often positive than type I pneumocytes (Figure 6, panels B, D, and F). The appearance of the kidneys and liver was the same as on 3 dpi, with more conspicuous staining. Additionally, virus-

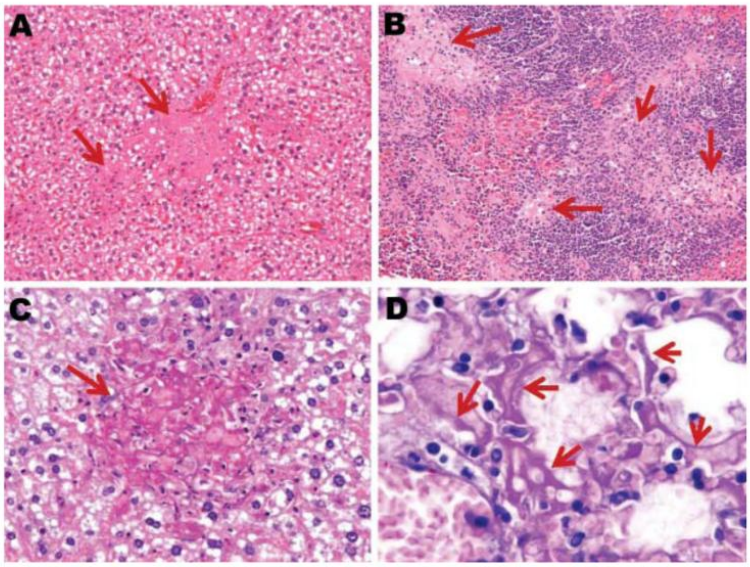

Figure 5. Photomicrographs of liver, spleen, and lung sections from influenza virus A (H5N1)–infected mice at endpoint. Necrotic foci (arrows) scattered throughout the liver (A) (original magnification ×200) and spleen (B) (original magnification ×100) from subtype H5N1–infected mice (hematoxylin and eosin stain); these foci are absent from subtype H1N1–infected mouse livers. C) Necrotic foci in the liver stain periodic acid–Schiff (PAS)–positive (arrow), which suggests focal accumulation of glycogen (original magnification ×400). D) Numerous alveolar walls lined with PAS-stained hyaline membranes (arrows), suggestive of necrosis and desquamation of pneumocytes (original magnification ×1,000).

positive glial cells, splenic macrophages, cardiomyocytes, islets of Langerhans cells, and peritoneal adipocytes were also detected (Figure 7).

Discussion

Two influenza A viruses of different subtypes, derived from different species and showing no pathogenicity toward mice, were forced to evolve by serial passaging in mouse lungs. The 2 adapted viruses obtained showed practically identical virulence levels, with similar MLD_{50} values. On the basis of this criterion, they appear to be more virulent than most other viruses used to date in murine models (*4*,*8*–*16*). Their virulence is of the same order of magnitude as those of the A/Vietnam/1203/2004 (H5N1) and A/Vietnam/1204/2004 (H5N1) viruses, whose respective MLD_{50}s are 0.7 and 2.1 PFUs (*17*). In both cases, inoculation of 10 MLD_{50} causes biphasic weight loss, culminating in death with a loss of ≈10% (H5N1) or ≈25% (H1N1) bodyweight. Viral amplification is maximal for both viruses on 4 dpi, roughly corresponding to the typical inoculation-to-peak lag of natural murine respiratory viruses (*6*,*18*). On the other hand, the 2 viruses adapted in the lungs showed replication kinetics that differed substantially from what is observed with natural viruses, with a quasi-plateau from 2 to 5/6 dpi instead of the classical Gaussian profile. Notably, this peculiar amplification kinetics profile has been described previously for mice infected with mouse-adapted forms of the A/Puerto Rico/8/34 (H1N1) virus (*19*), the A/South Carolina/1/18 (H1N1) virus (*4*), and several human subtype H5N1 strains showing high or low pathogenicity (*4*,*14*). These reports suggest that this profile is typical of influenza virus amplification by the murine respiratory system.

A final common feature of infection with the 2 virus subtypes was diffuse alveolar damage, which dominates both histopathologic profiles; these results corroborate the pathologic data found in the literature. Seasonal human influenza epidemics typically consist of a transient tracheobronchitis caused by preferential attachment of the virus to the laryngeal, tracheal, and bronchial epithelia. In contrast, those influenza viruses which are highly pathogenic toward humans, from the pandemic viruses of 1918 (H1N1), 1957 (H2N2), and 1968 (H3N2) to the subtype H5N1 strains isolated from humans since 2003, additionally colonize the bronchiolar and alveolar epithelia, preferentially or not, and cause diffuse alveolar damage as an additional primary lesion (*20*–*23*). The same lesion has been found in experimental animals injected with a recent subtype H5N1 strain (*14*,*24*–*26*).

Although both viruses share the same pathogenicity, replication kinetics, and concentration peak, and although they both evoke diffuse alveolar damage by the endpoint day, they differ dramatically in terms of the ARDS course and pathologic signature. Flagrant differences make it easy to distinguish infections by the 2 subtypes. In subtype H1N1 infection, the disease becomes fatal at a point when the pulmonary edema is much less intense and leaves a histopathologic picture characterized by much more dense inflammatory cell infiltrates, generating cuffs around the bronchioles and blood vessels. Second, subtype H1N1 colonizes the epithelia of both the upper and lower airways, without any obvious preference, whereas subtype H5N1

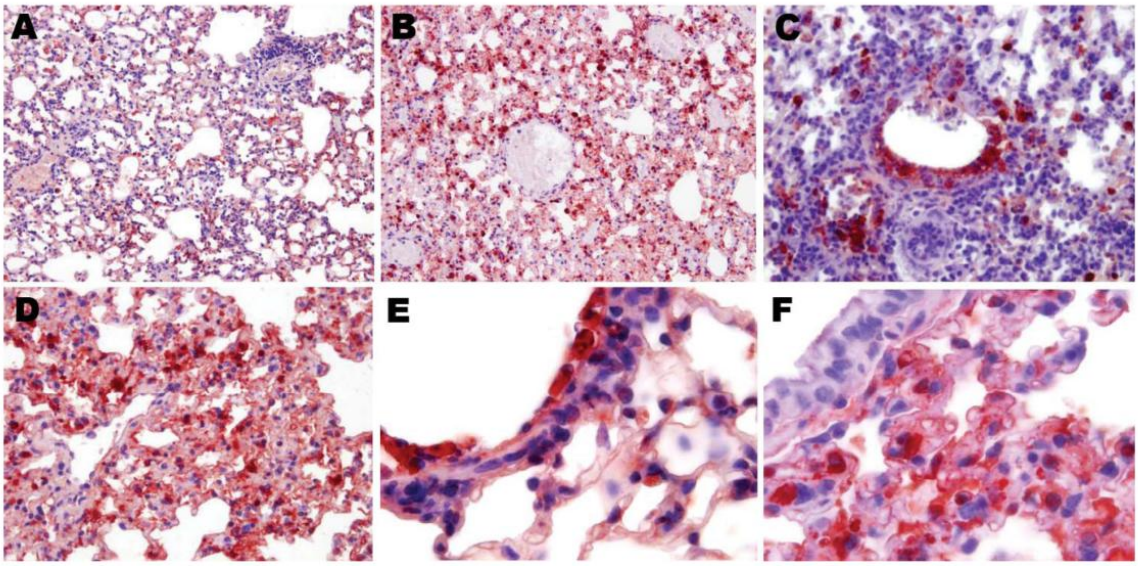

Figure 6. Topologic distribution of influenza antigens in the lungs of mice infected with influenza virus A subtype H1N1 and H5N1 strains at endpoint (antinucleoprotein immunohistochemical staining). A) Subtype H1N1 and B) subtype H5N1, both showing diffusely distributed positive staining of numerous pneumocytes and alveolar macrophages (original magnification ×100). C) Subtype H1N1, showing antigens massively present in the remaining non-desquamated airway epithelial cells (original magnification ×400); viral amplification in type I and type II pneumocytes is far more intense and widespread 4 days after inoculation of the subtype H5N1 virus (D) than 7 days after inoculation of the subtype H1N1 virus (original magnification ×400). E) Desquamated, necrotic, and intensely virus-positive airway epithelial cells in a terminal bronchiole and adjacent alveoli of a mouse infected with subtype H1N1, compared with F) uninfected, intact airway epithelial cells in a terminal bronchiole and adjacent alveoli of a mouse infected with subtype H5N1, illustrating the different pneumotropism of the 2 viruses (original magnification ×1,000). Conversely, the density of virus-positive cells in the lung/alveoli is higher after inoculation of the subtype H5N1 strain (Mayer hematoxylin counterstain).

remains confined essentially to the alveoli and terminal bronchioles. Within the alveoli, unlike the subtype H1N1 strain, the subtype H5N1 strain shows a preferential tropism for type II pneumocytes and alveolar macrophages. Lastly, whereas subtype H1N1 remains strictly confined to the respiratory system, subtype H5N1 spreads to other organs. These differences demonstrate unambiguously that the 2 highly virulent influenza A viruses studied here cause 2 different forms of ARDS. This finding suggests that the physiopathologic data obtained when studying 1 virulent strain should not be extrapolated automatically to other strains. The observed differences also suggest that diverse constellations of critical mutations in the viral genome might lead to the same fatal result.

This work addresses the question of possible differences between 2 fatal diseases caused by influenza A viruses, although some previous evidence that pointed in the same direction has already been reported. For example, the pandemic human strains of 1918, 1957, and 1968, on the one hand, and the recent subtype H5N1 strains, on the other, show different tropisms: panepithelial for the former strains (*20*,*27*,*28*) and limited to the bronchiolar and alveolar epithelia for the latter strains, a result compatible with our own observations on mouse-adapted viruses. Likewise, a panepithelial tropism has been observed for the A/South Carolina/1/18 (H1N1) virus in mice (*29*), whereas a preference for the bronchioles and alveoli has been noted for recent subtype H5N1 strains that have been injected into macaques, mice, ferrets, and cats (*14*,*25*,*30*–*37*). In addition, the observed strict confinement of our subtype H1N1 strain to the respiratory system confirms previously reported data that refute the existence of polysystemic dissemination of non-H5 viruses that are lethal to humans or laboratory animals (*20*,*27*,*29*,*38*). Conversely, our observation that the subtype H5N1 strain spreads beyond the respiratory system confirms similar observations of both humans (*22*,*22*,*39*) and laboratory animals (*14*,*24*,*25*,*30*–*34*).

Although other subtype H5N1 and subtype H1N1 viruses infect other susceptible hosts, they may not show trends similar to those observed here. These results, when integrated with the diverse pieces of evidence reported elsewhere, suggest that fatal infections caused by different highly virulent influenza A viruses do not necessarily share the same pathogenesis. To be convinced, one has only to

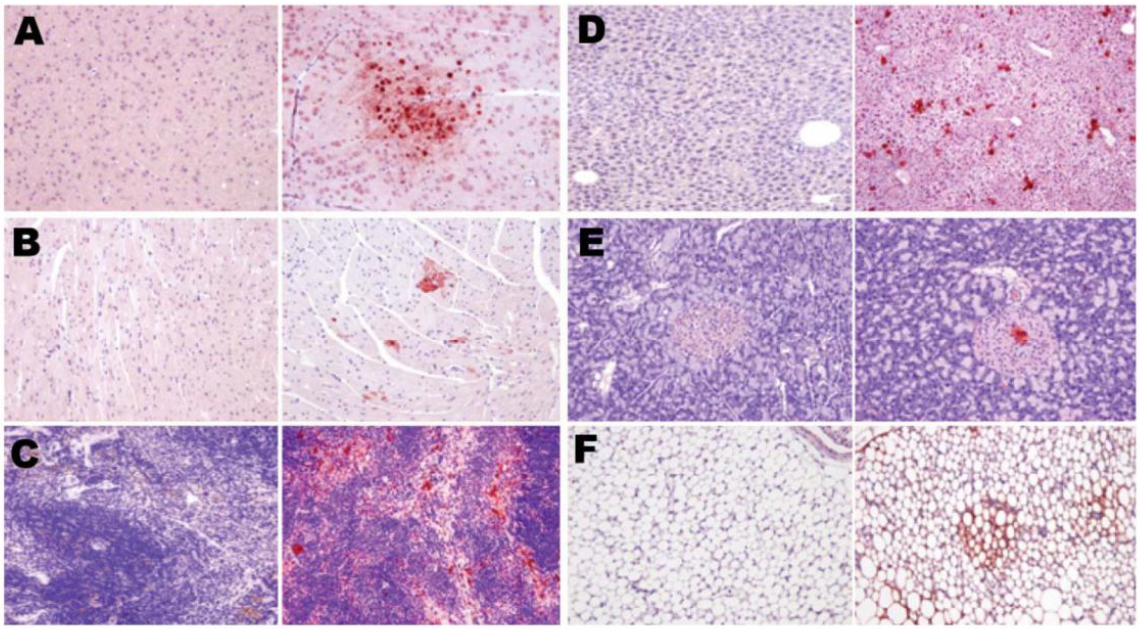

Figure 7. Topologic distribution of antigens in mice infected with influenza A virus subtype H1N1 at day 7 postinfection (left columns) and subtype H5N1 at day 4 postinfection (right columns) in various nonrespiratory organs. A) Glial cells (mostly oligodendrocytes); B) cardiomyocytes; C) spleen macrophages; D) hepatocytes; E) islets of Langerhans cells in the pancreas; and F) adipocytes. Bright virus-positive staining can be seen in subtype H5N1–infected mice (antinucleoprotein immunohistochemical staining), while absence of any staining can be seen in subtype H1N1–infected mice (Mayer hematoxylin counterstain). Original magnification ×100.

note the ease of distinguishing, in the absence of any virus labeling, the histopathologic sections typical of the 2 strains used here (Figure 4). These different histopathologic signatures and different pathogeneses probably reflect the presence of specific sets of virulence markers that will have to be decrypted to anticipate the emergence of a pandemic. In this respect, sequence analysis of both strains will lead to insight on specific residues that are relevant for the adaptation and virulence of an influenza strain in a new host.

Furthermore, the differences between these 2 strains suggest that >1 universal cytokine storm underlies fatal influenza diseases. Thus, it might be advantageous to tailor the therapeutic approach to the influenza virus pathotype.

Acknowledgments

We thank Michaël Sarlet and François Cornet for logistical and technical support.

This work was supported by the Interuniversity Attraction Poles, phase VI, project P6/14 (GPCRS, to A.C.) and by the European Union–funded European Animal Disease Genomics Network of Excellence.

Dr Garigliany is a research fellow of the Fonds National de la Recherche Scientifique, Brussels, Belgium. His research interests include influenza virus biology and host–virus interactions.

References

1. Murray CJ, Lopez AD, Chin B, Feehan D, Hill KH. Estimation of potential global pandemic influenza mortality on the basis of vital registry data from the 1918–20 pandemic: a quantitative analysis. Lancet. 2006;368:2211–8. DOI: 10.1016/S0140-6736(06)69895-4
2. Korteweg C, Gu J. Pathology, molecular biology, and pathogenesis of avian influenza A (H5N1) infection in humans. Am J Pathol. 2008;172:1155–70. DOI: 10.2353/ajpath.2008.070791
3. Kuiken T, Taubenberger JK. Pathology of human influenza revisited. Vaccine. 2008;26:D59–66. DOI: 10.1016/j.vaccine.2008.07.025
4. Perrone LA, Plowden JK, Garcia-Sastre A, Katz JM, Tumpey TM. H5N1 and 1918 pandemic influenza virus infection results in early and excessive infiltration of macrophages and neutrophils in the lungs of mice. PLoS Pathog. 2008;4:e1000115. DOI: 10.1371/journal.ppat.1000115
5. Reed LJ, Muench HA. A simple method of estimating fifty per cent endpoints. Am J Hyg. 1938;27:493–7.
6. Anh BD, Faisca P, Desmecht DJ. Differential resistance/susceptibility patterns to pneumovirus infection among inbred mouse strains. Am J Physiol Lung Cell Mol Physiol. 2006;291:L426–35. DOI: 10.1152/ajplung.00483.2005
7. Van Borm S, Thomas I, Hanquet G, Lambrecht B, Boschmans M, Dupont G, et al. Highly pathogenic H5N1 influenza virus in smuggled Thai eagles, Belgium. Emerg Infect Dis. 2005;11:702–5.
8. Brown EG, Liu H, Kit LC, Baird S, Nesrallah M. Pattern of mutation in the genome of influenza A virus on adaptation to increased virulence in the mouse lung: identification of functional themes. Proc Natl Acad Sci U S A. 2001;98:6883–8. DOI: 10.1073/pnas.111165798
9. Evseenko VA, Bukin EK, Zaykovskaya AV, Sharshov KA, Ternovoi VA, Ignatyev GM, et al. Experimental infection of H5N1 HPAI in

BALB/c mice. Virol J. 2007;4:77–82. DOI: 10.1186/1743-422X-4-77
10. Isobe H, Alt F, Bona CA, Schulman J. Intact antiinfluenza virus immune response in targeted kappa-deficient mice. Viral Immunol. 1994;7:25–30. DOI: 10.1089/vim.1994.7.25
11. Kawaoka Y. Equine H7N7 influenza A viruses are highly pathogenic in mice without adaptation: potential use as an animal model. J Virol. 1991;65:3891–4.
12. Lipatov AS, Andreansky S, Webby RJ, Hulse DJ, Rehg JE, Krauss S, et al. Pathogenesis of Hong Kong H5N1 influenza virus NS gene reassortants in mice: the role of cytokines and B- and T-cell responses. J Gen Virol. 2005;86:1121–30. DOI: 10.1099/vir.0.80663-0
13. Lu X, Tumpey TM, Morken T, Zaki SR, Cox NJ, Katz JM. A mouse model for the evaluation of pathogenesis and immunity to influenza A (H5N1) viruses isolated from humans. J Virol. 1999;73:5903–11.
14. Maines TR, Lu XH, Erb SM, Edwards L, Guarner J, Greer PW, et al. Avian influenza (H5N1) viruses isolated from humans in Asia in 2004 exhibit increased virulence in mammals. J Virol. 2005;79:11788–800. DOI: 10.1128/JVI.79.18.11788-11800.2005
15. Tumpey TM, García-Sastre A, Taubenberger JK, Palese P, Swayne DE, Basler CF. Pathogenicity and immunogenicity of influenza viruses with genes from the 1918 pandemic virus. Proc Natl Acad Sci U S A. 2004;101:3166–71. DOI: 10.1073/pnas.0308391100
16. Tumpey TM, Basler CF, Aguilar PV, Zeng H, Solórzano A, Swayne DE, et al. Characterization of the reconstructed 1918 Spanish influenza pandemic virus. Science. 2005;310:77–80. DOI: 10.1126/science.1119392
17. Hatta M, Hatta Y, Kim JH, Watanabe S, Shinya K, Nguyen T, et al. Growth of H5N1 influenza A viruses in the upper respiratory tracts of mice. PLoS Pathog. 2007;3:1374–9. DOI: 10.1371/journal.ppat.0030133
18. Faisca P, Anh DB, Desmecht DJ. Sendai virus-induced alterations in lung structure/function correlate with viral loads and reveal a wide resistance/susceptibility spectrum among mouse strains. Am J Physiol Lung Cell Mol Physiol. 2005;289:L777–87. DOI: 10.1152/ajplung.00240.2005
19. Hennet T, Ziltener HJ, Frei K, Peterhans E. A kinetic study of immune mediators in the lungs of mice infected with influenza A virus. J Immunol. 1992;149:932–9.
20. Winternitz MC, Wason IM, McNamara FP. The pathology of influenza. New Haven (CT): Yale University Press; 1920. p. 20–45.
21. To KF, Chan PK, Chan KF, Lee WK, Lam WY, Wong KF, et al. Pathology of fatal human infection associated with avian influenza A H5N1 virus. J Med Virol. 2001;63:242–6. DOI: 10.1002/1096-9071(200103)63:3<242::AID-JMV1007>3.0.CO;2-N
22. Gu J, Xie Z, Gao Z, Liu J, Korteweg C, Ye J, et al. H5N1 infection of the respiratory tract and beyond: a molecular pathology study. Lancet. 2007;370:1137–45. DOI: 10.1016/S0140-6736(07)61515-3
23. van Riel D, Munster VJ, de Wit E, Rimmelzwaan GF, Fouchier RA, Osterhaus AD, et al. Human and avian influenza viruses target different cells in the lower respiratory tract of humans and other mammals. Am J Pathol. 2007;171:1215–23. DOI: 10.2353/ajpath.2007.070248
24. Maines TR, Chen LM, Matsuoka Y, Chen H, Rowe T, Ortin J, et al. Lack of transmission of H5N1 avian-human reassortant influenza viruses in a ferret model. Proc Natl Acad Sci U S A. 2006;103:12121–6. DOI: 10.1073/pnas.0605134103
25. Nishimura H, Itamura S, Iwasaki T, Kurata T, Tashiro M. Characterization of human influenza A (H5N1) virus infection in mice: neuro-, pneumo- and adipotropic infection. J Gen Virol. 2000;81:2503–10.
26. Salomon R, Franks J, Govorkova EA, Ilyushina NA, Yen HL, Hulse-Post DJ, et al. The polymerase complex genes contribute to the high virulence of the human H5N1 influenza virus isolate A/Vietnam/1203/04. J Exp Med. 2006;203:689–97. DOI: 10.1084/jem.20051938
27. Opie EL, Blake FG, Small JC, Rivers TM. Respiratory disease. London (UK): H. Kimpton;1921. p. 402–20.
28. Herfs JF, Mulder J. Broad aspects of the pathology and pathogenesis of human influenza. Am Rev Respir Dis. 1961;83:84–97.
29. Kash JC, Tumpey TM, Proll SC, Carter V, Perwitasari O, Thomas MJ, et al. Genomic analysis of increased host immune and cell death responses induced by 1918 influenza virus. Nature. 2006;443:578–81.
30. Rimmelzwaan GF, van Riel D, Baars M, Bestebroer TM, van Amerongen G, Fouchier RA, et al. Influenza A virus (H5N1) infection in cats causes systemic disease with potential novel routes of virus spread within and between hosts. Am J Pathol. 2006;168:176–83. DOI: 10.2353/ajpath.2006.050466
31. Govorkova EA, Rehg JE, Krauss S, Yen HL, Guan Y, Peiris M, et al. Lethality to ferrets of H5N1 influenza viruses isolated from humans and poultry in 2004. J Virol. 2005;79:2191–8. DOI: 10.1128/JVI.79.4.2191-2198.2005
32. Zitzow LA, Rowe T, Morken T, Shieh WJ, Zaki S, Katz JM. Pathogenesis of avian influenza A (H5N1) viruses in ferrets. J Virol. 2002;76:4420–9. DOI: 10.1128/JVI.76.9.4420-4429.2002
33. Yen HL, Lipatov AS, Ilyushina NA, Govorkova EA, Franks J, Yilmaz N, et al. Inefficient transmission of H5N1 influenza viruses in a ferret contact model. J Virol. 2007;81:6890–8. DOI: 10.1128/JVI.00170-07
34. Rimmelzwaan GF, Kuiken T, van Amerongen G, Bestebroer TM, Fouchier RA, Osterhaus AD. Pathogenesis of influenza A (H5N1) virus infection in a primate model. J Virol. 2001;75:6687–91. DOI: 10.1128/JVI.75.14.6687-6691.2001
35. Xu T, Qiao J, Zhao L, Wang G, He G, Li K, et al. Acute respiratory distress syndrome induced by avian influenza A (H5N1) virus in mice. Am J Respir Crit Care Med. 2006;174:1011–7. DOI: 10.1164/rccm.200511-1751OC
36. Katz JM, Lu X, Frace AM, Morken T, Zaki SR, Tumpey TM. Pathogenesis of and immunity to avian influenza A H5 viruses. Biomed Pharmacother. 2000;54:178–87. DOI: 10.1016/S0753-3322(00)89024-1
37. Kuiken T, Rimmelzwaan GF, Van Amerongen G, Osterhaus AD. Pathology of human influenza A (H5N1) virus infection in cynomolgus macaques (*Macaca fascicularis*). Vet Pathol. 2003;40:304–10. DOI: 10.1354/vp.40-3-304
38. Lowen AC, Mubareka S, Tumpey TM, García-Sastre A, Palese P. The guinea pig as a transmission model for human influenza viruses. Proc Natl Acad Sci U S A. 2006;103:9988–92. DOI: 10.1073/pnas.0604157103
39. de Jong MD, Simmons CP, Thanh TT, Hien VM, Smith GJ, Chau TN, et al. Fatal outcome of human influenza A (H5N1) is associated with high viral load and hypercytokinemia. Nat Med. 2006;12:1203–7. DOI: 10.1038/nm1477

Address for correspondence: Daniel Desmecht, University of Liège, Department of Pathology, Faculty of Veterinary Medicine, Sart Tilman B43, Liège 4000, Belgium; email: daniel.desmecht@ulg.ac.be

All material published in Emerging Infectious Diseases is in the public domain and may be used and reprinted without special permission; proper citation, however, is required.

Use of trade names is for identification only and does not imply endorsement by the Public Health Service or by the U.S. Department of Health and Human Services.

6. La Mx1 bovine, un effecteur inné doté d'une activité anti-influenza sans précédent

6.1. Résumé

Les interférons de type I (α & β) constituent un mécanisme inné de défense intracellulaire contre les virus à la fois puissant et universel. Parmi les nombreux effecteurs de la cascade associée aux interférons de type I, les protéines Mx de plusieurs espèces sont largement connues comme de puissants inhibiteurs de la réplication du virus influenza A *in vitro*. Cet effet identifié *in vitro* ne se traduit néanmoins pas forcément par une résistance accrue des espèces permissives *in vivo*, comme le démontre la grande sensibilité de l'homme ou du porc à l'infection par le virus influenza A.

Nous démontrons ici que la protéine Mx1 bovine confère une protection contre l'infection par le virus influenza A plus puissante que tous les effecteurs de la réponse immune innée décrits à ce jour. Des expériences *in vitro* dûment contrôlées nous ont permis de mettre en évidence une supériorité très importante de la protéine Mx1 bovine comme inhibiteur de la réplication du virus influenza A par rapport aux protéines Mx1 murine et MxA humaine, archétypes des protéines Mx à activité anti-influenza. De plus, grâce à des modèles de souris congéniques ou transgéniques largement caractérisés, nous avons pu montrer que la protéine Mx1 bovine rend les souris testées complètement résistantes dans des expériences d'infection par des virus H1N1 et H5N1 hautement pathogènes pour la souris, alors que la protéine Mx1 murine, la plus puissante protéine Mx anti-influenza *in vivo* décrite jusqu'ici, ne confère qu'une protection partielle. A n'en point douter, les résultats présentés ici constitueront le point de départ de nouvelles recherches visant à identifier les mécanismes sous-jacents à cette activité anti-influenza exceptionnelle, ouvrant la voie au développement de nouvelles thérapeutiques antivirales.

7. Vers l'identification du partenaire viral : isolement et caractérisation de souches virales capables d'esquiver la protéine Mx1 bovine

7.1. Résumé

Le virus influenza est responsable d'épidémies annuelles dans la population humaine, et a été à l'origine de plusieurs pandémies associées à de nombreuses mortalités. Les protéines Mx, dont la première fut identifiée en 1962 par Jean Lindenmann, sont des GTPases de haut poids moléculaire de la famille des dynamines. Elles sont dépendantes de l'expression d'interférons de types I et III et la protéine Mx1 de certaines espèces (souris, rat, porc, poulet, bovin et homme) présente un effet inhibiteur significatif sur la réplication du virus influenza A. Parmi celles-ci, la protéine Mx1 bovine a été décrite comme l'effecteur de la réponse innée présentant la plus puissante activité inhibitrice du virus influenza A. Peu de choses sont connues quant au mécanisme d'action des protéines Mx, qu'elles soient nucléaires (Mx1 des rongeurs) ou cytoplasmiques (Mx1 bovine, Mx1 porcine, MxA humaine). Les protéines Mx nucléaires semblent inhiber une étape précoce du cycle de réplication du virus influenza A, probablement la transcription primaire. Quant aux protéines Mx cytoplasmiques étudiées, elles semblent agir lors d'une étape postérieure (MxA humaine) ou antérieure (Mx1 porcine) à la transcription primaire et il est tout à fait possible qu'elles agissent à plusieurs niveaux. Des expériences utilisant un système de mini-réplicon ont mis en évidence le rôle déterminant de la nucléoprotéine pour expliquer les différences de sensibilité entre souches virales à l'effet antiviral de la protéine MxA humaine. Des données cristallographiques récentes tendent à montrer que la protéine MxA humaine forme des structures oligomériques circulaires, qui pourraient entourer et complexer les nucléocapsides virales. Mais une interaction nucléoprotéine du virus influenza – MxA humaine n'a été montrée que dans une seule étude, malgré le nombre impressionnant de publications scientifiques adressant le mécanisme d'action de la protéine MxA humaine, pour une seule souche virale, et avec recours à un agent de *cross-linking*, aucune interaction n'ayant mis être mise en évidence sans cet agent. Il apparaît peu probable qu'une interaction aussi faible puisse rendre compte d'une activité inhibitrice aussi importante que celle présentée par la protéine Mx1 bovine. Par ailleurs, il est difficile d'imaginer que des interactions virus-spécifiques puissent expliquer l'effet inhibiteur de la protéine MxA humaine sur de très nombreux virus à ARN et même à ADN, de

familles très diverses. Un effet inhibiteur des protéines Mx sur une fonction cellulaire communément employée par ces virus parait beaucoup plus plausible.

Pour tenter de résoudre cette question, nous avons choisi d'aborder le problème d'une autre manière, selon le procédé ayant permis la découverte du mode d'action de la drogue antivirale amantadine (inhibiteur de la protéine M2). C'est en effet suite à la découverte des mutations au sein de la protéine M2, un canal à proton actif principalement dans le compartiment endosomal lors de l'entrée du virus dans la cellule-cible, qui rendaient certaines souches résistantes à l'amantadine, que le mécanisme d'action de cette molécule a été compris. De même, nous avons entrepris l'isolement des variants viraux résistants à l'effet antiviral de la protéine Mx1 bovine et leur caractérisation phénotypique et génétique. Nous avons ainsi pu identifier quatre mutations candidates, réparties sur trois segments génomiques différents, comme potentiellement responsables de l'acquisition du phénotype de résistance à l'effet inhibiteur de la protéine Mx1 bovine *in vitro*. Des expériences de complémentation et de *reverse genetics* ont conclu au caractère suffisant de la substitution I100T au sein de la nucléoprotéine du virus influenza A H1N1 utilisé pour conférer le phénotype de Mx-résistance. Cette substitution confère une résistance complète et est stable après plusieurs passages sans pression Mx ou dans un contexte de co-infection. Elle rend par ailleurs le virus résistant à d'autres Mx, tant cytoplasmiques (protéines MxA humaine et Mx1 porcine) que nucléaire (protéine Mx1 murine). Aucune interaction entre la protéine Mx1 bovine et la nucléoprotéine présentant ou non la substitution en question n'a pu être mise en évidence, avec ou sans utilisation d'agent de *cross-linking*, selon le protocole employé par Turan et collègues (2004) pour la protéine MxA humaine.

Par ailleurs, la protéine Mx1 bovine possède un effet inhibiteur marqué sur l'activation de la voie NF-κB et il est aujourd'hui admis que l'activation de cette voie est un prérequis nécessaire au cycle de réplication du virus influenza A. Il apparaît donc comme possible que la supériorité de la protéine Mx1 bovine par rapport à d'autres protéines Mx à effet anti-influenza lui vienne de cette activité particulière. De façon très intéressante, la nucléoprotéine possédant la substitution I100T, rendant le virus Mx-résistant, induit une activation de la voie NF-κB significativement plus faible que la nucléoprotéine parentale, qu'elle soit exprimée seule ou dans le cadre du cycle réplicatif viral, suggérant une moindre dépendance de la souche virale Mx-résistante envers une activation de la voie NF-κB comme un des mécanismes d'acquisition de cette Mx-résistance. Néanmoins, un agent inhibiteur de la voie NF-κB (BAY 11-7082) semble

sans effet sur l'expression des protéines virales, tant pour le virus parental que pour le virus Mx-résistant. Il reste par ailleurs que la position 100 de la nucléoprotéine est hôte-spécifique, ce qui suggère qu'elle intervient dans l'interaction de la nucléoprotéine avec un facteur cellulaire. Une telle substitution d'une isoleucine en une thréonine en position 109 de la nucléoprotéine, soit dans l'environnement proche du résidu 100, a été reliée à une efficacité de transcription supérieure du génome viral dans l'encéphale du poulet. Il apparait logique que cet hypothétique facteur cellulaire puisse être impliqué et dans le cycle de réplication du virus influenza et dans l'activation de la voie NF-κB. Les recherches en cours visent à identifier ce ou ces facteur(s) et à déterminer si le lien entre nucléoprotéine, Mx et ce facteur est direct ou indirect.

8. Vers l'identification du partenaire Mx : réfutation du modèle « GED-nécessaire-et-suffisant »

8.1. Résumé

Les interferons de type I (IFN-α/β) constituent un mécanisme de défense innée intracellulaire à la fois puissant et universel. Parmi les effecteurs antiviraux induits par ces interférons, les protéines Mx de certaines espèces apparaissent comme des éléments clés de la défense contre les virus influenza A. Les données de la littérature disponibles à ce jour suggèrent que pour être efficace contre la réplication du virus influenza, une protéine Mx doit posséder un domaine de liaison au GTP, des bases structurelles permettant la multimérisation et un domaine effecteur GTPase spécifique (GED). La protéine MxA humaine et la protéine Mx1 bovine rencontrent toutes les deux ces critères, mais la protéine bovine est plus active contre les virus influenza. Nous étudions ici l'activité anti-influenza exercée par deux chimères des protéines Mx bovine et humaine. Nous démontrons que la substitution du domaine GED de la protéine MxA humaine par le domaine bovin ne change pas son activité antivirale. Par contre, introduire le domaine GED humain dans la protéine Mx1 bovine donne une protéine chimérique beaucoup plus efficace que la protéine MxA humaine.

Nous en concluons, et en contradiction avec l'hypothèse actuellement en vogue dans la littérature, que le domaine GED seul ne détermine pas la puissance antivirale des protéines Mx. Nos résultats suggèrent que d'autres domaines de la protéine Mx, toujours non définis et localisés côté N-terminal par rapport au GED, puissent interagir avec des composants viraux ou cellulaires, menant à une altération du cycle de réplication virale. Identifier, dans la partie N-terminale de la protéine Mx1 bovine, le(s) motif(s) responsable(s) de sa plus grande puissance antivirale pourrait contribuer au développement de nouvelles molécules anti-influenza.

Partie III : Discussion générale & Perspectives

Le virus influenza représente un pathogène majeur, tant en médecine humaine qu'en médecine vétérinaire. S'il est associé, selon l'Organisation Mondiale de la Santé, à la mortalité de 250.000 à 500.000 personnes dans le cadre des épidémies annuelles qui touchent entre 5 et 15% de la population mondiale, il fut par ailleurs responsable d'épisodes de mortalité à grande échelle lors de différentes pandémies au cours de l'histoire (Morens *et al.*, 2010). Les agents antiviraux disponibles, adamantanes et inhibiteurs de la neuraminidase, font l'objet d'un taux de résistance de plus en plus important, notamment parmi les souches de virus influenza A épidémiques (Thorlund *et al.*, 2011). Ces résistances, l'efficacité relative de ces traitements (ils inhibent le virus mais ne modifient pas la réponse de l'hôte, qui est critique en termes de survie) et le fait qu'ils sont le plus souvent administrés trop tard dans le cours de la maladie, rendent la mise à disposition de nouvelles thérapeutiques absolument essentielle, d'autant que la disponibilité de vaccins efficaces s'avérerait très insuffisante pour faire face à une pandémie sévère.

Les protéines Mx, effecteurs de la réponse innée sous dépendance d'interférons de type I et III, sont, pour certaines d'entre elles, de puissants inhibiteurs de la réplication du virus influenza A, et confèrent une résistance très importante à l'infection par ce virus *in vivo* (Holzinger *et al.*, 2007 ; Haller *et al.*, 2010). Elles représentent donc une voie de recherche prometteuse pour la mise au point de nouvelles thérapeutiques plus efficaces en termes de taux de survie après infection par le virus influenza A chez l'homme.

Partant d'une expérience préliminaire mettant à jour une activité inhibitrice de la protéine Mx1 bovine sur ce virus et dans l'optique d'une contribution significative à la compréhension du mécanisme d'action de l'effet antiviral des protéines Mx, il s'est avéré nécessaire de créer et de valider des outils permettant l'étude de l'effet de la protéine Mx1 bovine sur la réplication virale *in vivo*, des modèles d'expression *in vitro* ayant déjà été produits et validés antérieurement (Baise *et al.*, 2004 ; Leroy *et al.*, 2006). Pour ce faire, un BAC complet, comportant les séquences génomiques des protéines Mx1 et Mx2 bovines, ainsi que leurs séquences promotrices et éléments régulateurs, a été injecté dans le *pronucleus* mâle d'oocytes de souris de souche FVB/J, avant réimplantation de ces oocytes chez des souris receveuses (Garigliany *et al.*, 2009). La souche FVB/J présente des gènes Mx défectifs, ce qui évite l'interférence avec la Mx murine dans les études sur l'activité antivirale des protéines Mx bovines introduites par transgenèse. Plusieurs tentatives similaires ont visé à introduire un gène Mx *in vivo*, que ce soit la protéine Mx1 murine ou la protéine MxA humaine (Arnheiter *et al.* 1990 ;

Kolb *et al.* 1992 ; Müller *et al.* 1992 ; Pavlovic *et al.* 1995). Toutes ces expériences ont eu recours à une construction artificielle de petite taille, portant un promoteur de souris (celui du gène de la protéine Mx1 murine, de la 3-hydroxy-3-methylglutaryl coenzyme A reductase ou de l'albumine), un promoteur humain (celui de la métallothionéine) ou un promoteur viral (celui du SV40), devant le cDNA codant pour la protéine Mx1 murine ou la protéine MxA humaine. Plusieurs problèmes ont été observés : absence d'expression (Pavlovic *et al.*, 1995), absence de traduction de l'ARNm (Müller *et al.*, 1992), extinction graduelle (Kolb *et al.*, 1992), mosaïcisme (Arnheiter *et al.*, 1990 ; Kolb *et al.*, 1992) ou perte de l'inductibilité de l'expression (Arnheiter *et al.*, 1990). Nous avons dès lors choisi d'utiliser un transgène de grande taille (environ 210 kb), soit un BAC complet, pour être sûr d'introduire le gène d'intérêt et toutes ses séquences régulatrices dans leur entièreté. Il a par ailleurs été démontré que les BACs sont moins sensibles aux effets de position que les transgènes de petite taille, ce qui laissait augurer une meilleure expression (Giraldo et Montoliu, 2001 ; Gong *et al.*, 2003). Les résultats d'expression des transgènes ont confirmé nos attentes, tant pour les niveaux d'expression globaux qu'au vu du pourcentage de lignées sélectionnées qui exprimaient correctement les transgènes et quant à l'inductibilité de l'expression. Neuf lignées de souris transgéniques ont ainsi été obtenues, dont deux n'ont pas transmis le transgène à leur progéniture et ont dû être éliminées. Après sélection, les lignées restantes ont été dûment caractérisées quant à leur niveau d'expression en protéines Mx1 et Mx2 bovines, et classées en lignées à haut ou faible niveau d'expression. L'expression des protéines Mx dans ce modèle est inductible, sous la dépendance du promoteur naturel, c'est-à-dire en cas de stimulation par les interférons de type I et III, et correspond aux valeurs physiologiques observées en cellules bovines (Garigliany *et al.*, 2009). Un choix judicieux des lignées utilisées a ainsi permis de tester l'effet de l'expression de la protéine Mx1 bovine sur la résistance à l'inoculation de doses létales de virus de la stomatite vésiculeuse. Une résistance très importante des souris transgéniques produisant des quantités physiologiques de protéine Mx1 bovine a été observée au cours de ces expériences, en comparaison avec les souris FVB/J contrôles (Garigliany *et al.*, 2009).

La seconde étape consistait en la mise au point de modèles d'infection par le virus influenza *in vivo* chez la souris. Pour ce faire, deux souches de virus influenza A, A/swine/Iowa/4/76 (H1N1) et A/crested_eagle/Belgium/1/04 (H5N1), non pathogènes pour la souris, ont été adaptées par passages multiples jusqu'à l'obtention d'un

phénotype hautement virulent (Garigliany *et al.*, 2010). Une caractérisation complète des signes cliniques et des lésions induites au cours d'une infection de souris de souche FVB/J par des doses létales identiques de ces deux souches virales a été réalisée (Garigliany *et al.*, 2010). En dépit d'une létalité similaire, de titres viraux pulmonaires très proches et du développement d'un syndrome de détresse respiratoire aigu (ARDS) après infection par chacune des deux souches comparées, avec induction de dommages alvéolaires diffus, des différences très marquées en termes de cinétique d'infection et de lésions histopathologiques induites ont été observées. Ainsi, si le virus H5N1 mène à une mort rapide (moins de quatre jours) par œdème pulmonaire aigu et en l'absence quasi complète d'inflammation, le virus H1N1 induit quant à lui une pneumonie sévère avec remplissage progressif des alvéoles pulmonaires par des cellules inflammatoires, pour finalement mener à une insuffisance respiratoire mortelle huit jours après l'infection (Garigliany *et al.*, 2010). Par ailleurs, la souche H5N1 présentait un pneumotropisme marqué, avec invasion systémique (foie, rate, rein, pancréas, encéphale, etc.), alors que le virus H1N1 ciblait prioritairement les voies respiratoires, avant de s'étendre au parenchyme pulmonaire, sans jamais quitter le système respiratoire. Ces deux modèles vont permettre de tester l'efficacité des protéines Mx1 bovines et Mx1 murine, *in vivo*, sur des virus très différents l'un de l'autre, mais à létalité identique (100%).

Les modèles d'expression *in vitro* et *in vivo* dûment validés, il était alors possible d'entreprendre la caractérisation complète de l'effet de la protéine Mx1 bovine sur la réplication du virus influenza A. Cette étude a permis de montrer la supériorité de l'effet inhibiteur de la protéine Mx1 bovine sur la réplication des souches de virus influenza A testées par rapport aux autres protéines Mx à activité anti-influenza, tant *in vivo* que *in vitro*, avec un effet protecteur complet tant sur le plan de la morbidité que de la mortalité (Garigliany *et al.*, soumis). Les expériences d'infection par le virus H5N1, mortelles pour les souris porteuses du gène Mx1 murin, archétype des protéines Mx anti-influenza *in vivo* (Salomon *et al.*, 2007 ; Tumpey *et al.*, 2007), au plus haut titre viral utilisé, étaient à peine associées à quleques signes cliniques modérés, sans aucune mortalité, pour les souris porteuses du gène Mx1 bovin et exprimant cette protéine à des taux physiologiques (Garigliany *et al.*, soumis). De plus, aucun signe clinique néfaste n'a été associé au cours de nos expériences à l'expression d'une protéine Mx *in vivo*. Ces observations démontrent tout l'intérêt que présente la protéine Mx1 bovine dans une optique thérapeutique.

Comprendre le mode d'action de la protéine Mx1 bovine, au vu de la protection clinique qu'elle offre contre les virus influenza de type A, ouvrira la voie à de nouvelles thérapeutiques visant à réduire le taux de mortalité associé à ces virus. De nombreuses équipes se sont attelées à l'étude des mécanismes impliqués dans l'effet antiviral des protéines Mx, mais les connaissances actuelles à ce sujet restent très limitées (Haller *et al.*, 2010). Il n'est toujours pas établi si les protéines Mx agissent via un mode virus-spécifique ou via l'inhibition d'une fonction cellulaire nécessaire à l'accomplissement du cycle viral. Des mécanismes spécifiques ont notamment été proposés pour le virus Thogoto, un virus de la famille des *Orthomyxoviridae*, proche du virus influenza, pour lequel une interaction entre la protéine MxA humaine et la nucléocapside virale a été identifiée lors d'une expérience de cosédimentation (Kochs et Haller, 1999). Ce serait la séquestration des nucléocapsides du virus Thogoto par la protéine MxA humaine qui expliquerait l'effet antiviral observé. Une interaction similaire a été identifiée entre la protéine MxA humaine et la nucléoprotéine d'une souche de virus influenza A, mais l'interaction restait faible et nécessitait le recours à un agent de *cross-linking* pour être mise en évidence, et rien ne prouve qu'elle soit directe (Turan *et al.*, 2004). Qui plus est, jamais aucune autre équipe n'a mis en évidence ce type d'interaction, ni pour la protéine MxA ni pour toute autre protéine Mx.

Devant ces attentes, nous avons imaginé mettre en œuvre une stratégie différente, bien que déjà éprouvée par le passé, pour apporter de nouveaux éléments de réponse. Le mode d'action de la drogue antivirale amantadine a en effet été découvert en mettant le doigt sur le rôle central joué par des substitutions au sein de la séquence de la protéine M2 dans l'acquisition d'une résistance à l'amantadine par une souche de virus influenza A (Hay *et al.*, 1985). Cette protéine M2 étant un canal à proton qui joue notamment un rôle essentiel pour permettre l'acidification interne du virion et la libération des ribonucléoprotéines virales lors du passage dans le compartiment endosomal à l'entrée du virus dans la cellule, il est apparu que l'amantadine bloquait le fonctionnement de ce canal (Hay *et al.*, 1985). De la même manière, nous avons entrepris la sélection *in vitro* de souches de virus influenza A résistantes à l'effet antiviral de la protéine Mx1 bovine, tâche délicate vu le puissant effet antiviral de cette protéine. Pour valider notre méthode, nous avons, dans un premier temps, sélectionné des variants amantadine-résistants de notre souche virale (A/swine/Iowa/4/76 [H1N1]) en culture cellulaire (cellules Vero). L'acquisition de la résistance fut confirmée par l'apparition d'une substitution dans la protéine M2 (V27A) connue comme conférant une résistance à l'amantadine (Holsinger

et al., 1994 ; Betakova *et al.*, 2005). Sur cette base, nous avons entrepris un processus de sélection comparable en utilisant des cellules Vero V103 exprimant la protéine Mx1 bovine de façon inductible. Après deux premiers échecs dus à un avortement de l'infection, la troisième vague de sélection a permis d'obtenir un stock de virus phénotypiquement résistant à l'effet de la protéine Mx1 bovine *in vitro*, après 15 passages sous pression Mx (Garigliany *et al.*, soumis). Cinq clones viraux ont été isolés par *plaque purification*. Ils ont été testés par screening en cytométrie en flux, ce qui a confirmé leur résistance, totale, à l'effet inhibiteur de la protéine Mx1 bovine par rapport au virus parental. Le même résultat fut obtenu quel que soit le type cellulaire (Vero ou HEK293) ou le type de transfection (stable ou transitoire) utilisé. Une mesure des titres viraux dans le surnageant de culture cellulaire confirme également ces observations, puisque le virus résistant se comporte comme le virus parental sans pression Mx, alors que ce dernier est fortement affecté par l'expression de la protéine Mx. Pour vérifier si l'acquisition de cette résistance s'est faite aux dépens de la biofitness du virus, la cinétique de réplication a été étudiée *in vitro* et a montré que les souches résistantes se comportent ici aussi, avec ou sans pression Mx, comme le virus parental sans pression Mx, ce même virus parental étant très atténué en cas d'expression de la protéine Mx1 bovine (Garigliany *et al.*, soumis).

D'autre part, le phénotype de Mx-résistance est stable puisqu'il se maintient même après dix passages sans pression Mx et il persiste après dix passages en cas de co-infection entre une souche résistante et la souche parentale, toujours sans pression Mx. Tous ces résultats montrent que la biofitness du virus est parfaitement conservée malgré l'acquisition du phénotype de résistance complète à l'effet Mx (Garigliany *et al.*, soumis).

Autre fait intéressant, le variant résistant a été exposé à l'effet inhibiteur d'autres protéines Mx cytoplasmiques (huMxA et poMx1) et nucléaire (moMx1) *in vitro* et s'est révélé résistant à ces trois protéines également. Les virus résistants doivent donc échapper à un mécanisme inhibiteur commun à ces quatre protéines Mx.

Si la protéine MxA a été proposée comme étant capable de se lier à la nucléoprotéine du virus influenza A, bien que de manière faible, une première hypothèse serait que la protéine Mx1 bovine, qui inhibe le virus de façon beaucoup plus puissante, se fixe à la nucléoprotéine avec d'autant plus d'affinité (Turan *et al.*, 2004). En immunofluorescence sur cellules infectées, les co-marquages Mx – NP ne montrent pas de colocalisation, à l'exception notable de certains granules péri-nucléaires (Garigliany *et al.*, soumis). Nous

avons donc reproduit l'expérience de co-immunoprécipitation réalisée par Turan et collègues (2004), mais avec notre Mx (boMx1) et notre NP. Aucune co-précipitation, même faible, malgré l'utilisation d'un agent de *cross-linking* et la multiplication des épreuves (infection virale ou incubation directe Mx – NP recombinante), n'a pu être mise en évidence (Garigliany *et al.*, soumis). Les hypothèses les plus récentes basées sur la structure oligomérique de la protéine MxA suggèrent que des anneaux de protéine MxA entourent et séquestrent les nucléocapsides virales, voire induisent leur destruction prématurée (Haller *et al.*, 2010), mais, au vu de l'absence d'interaction boMx1-NP, et compte tenu de la puissance de l'effet inhibiteur de la protéine Mx1 bovine, cette hypothèse paraît très peu probable pour expliquer un mode d'action universel des protéines Mx cytoplasmiques. De plus, au vu du large spectre antiviral de ces protéines, une action inhibitrice sur une fonction cellulaire communément employée par des virus de différentes familles au cours de leur cycle de réplication paraît beaucoup plus plausible qu'une multitude d'interactions spécifiques différentes, d'autant que, si les protéines Mx à activité antivirale, inductibles, ne semblent pas avoir de fonction cellulaire précise, les protéines Mx sans activité antivirale, comme la protéine MxB humaine, sont exprimées de façon constitutive et semblent exercer des fonctions cellulaires essentielles, notamment au niveau de l'import nucléaire et de la régulation du cycle cellulaire (King *et al.*, 2004). Une hypothèse qui se tient serait que les protéines Mx à activité antivirale puissent interférer avec les fonctions d'autres protéines cellulaires, et ainsi, indirectement, empêcher l'accomplissement du cycle viral.

L'analyse génétique des variants viraux Mx-résistants a permis l'identification de quatre mutations candidates, deux dans l'hémagglutinine, une dans la nucléoprotéine et une dans la neuraminidase. Des expériences de complémentation ont montré que l'expression de la nucléoprotéine portant la substitution découverte chez les variants résistants (I100T) était suffisante pour conférer un phénotype Mx-résistant au virus parental (Garigliany *et al.*, soumis). Dans les mêmes conditions, l'expression de la nucléoprotéine parentale n'apporte qu'un petit gain (mais y compris en l'absence de Mx), alors que l'hémagglutinine ou la neuraminidase des souches Mx-résistantes n'apportent aucune modification (Garigliany *et al.*, soumis). L'introduction de la substitution I100T dans la nucléoprotéine du virus parental est également suffisante pour conférer le phénotype de Mx-résistance observé chez les variants obtenus par sélection, sans modification de la biofitness. De plus, une seconde campagne de sélection de variants Mx-résistants a conduit à l'identification de la même substitution au sein de la

nucléoprotéine virale (I100T). Parmi les trois autres substitutions, seule la substitution N173D dans l'hémagglutinine était également présente. Les autres substitutions acquises parallèlement dans l'hémagglutinine et la neuraminidase ne semblent donc jouer aucun rôle, ni direct, ni compensatoire, et paraissent purement fortuites (Garigliany *et al.*, soumis). Le résidu 173 de l'hémagglutinine est situé à proximité immédiate du site de liaison au récepteur et il est probable que cette substitution affecte la spécificité de l'hémagglutinine quant au type d'acide sialique lié préférentiellement, en réponse aux multiples passages sur cellules Vero. Elle n'affecte en tout cas pas la sensibilité à l'effet Mx.

Ces résultats concordent avec les données de la littérature. En effet, il a été montré qu'une surexpression de la NP, et dans une moindre mesure de la protéine PB2, permettait de titrer partiellement l'effet Mx (Turan *et al.*, 2004). De plus, la nucléoprotéine explique les différences de sensibilité à l'effet de la protéine MxA humaine entre souches de virus influenza A (Dittmann *et al.*, 2008 ; Zimmermann *et al.*, 2011). La nucléoprotéine est donc bien l'élément viral essentiel dans le mécanisme d'action des protéines Mx anti-influenza.

Si une interaction directe Mx – NP n'a pu être détectée dans nos expériences, vu l'importance de l'effet antiviral de la protéine Mx1 bovine sur la réplication du virus influenza et la capacité de la simple substitution I100T de la NP à annihiler cet effet, il faut chercher dans les fonctions connues de la nucléoprotéine à quel niveau la Mx peut agir. Le résidu 100 de la NP se situe au sein d'un vaste domaine de liaison à la protéine PB2, mal défini. C'est un résidu fortement exposé de la nucléoprotéine, tant dans sa structure monomérique que dans sa structure oligomérique et donc, probablement, des ribonucléoprotéines (Ye *et al.*, 2006 ; Coloma *et al.*, 2009). C'est, de plus, un marqueur d'adaptation à l'hôte, puisque R ou K sont présents à cette position chez les souches aviaires, V chez les souches porcines et I ou V pour les souches humaines (Pan *et al.*, 2009 ; Varich *et al.*, 2011 ; observations personnelles). Il est donc extrêmement probable que ce résidu soit impliqué dans la liaison de la NP avec un facteur cellulaire hôte-spécifique. Si ce facteur n'est pas une Mx, ce pourrait être une protéine cellulaire cytoplasmique et nucléaire qui interagit physiquement avec la nucléoprotéine virale et sur laquelle les protéines Mx à activité anti-influenza seraient capables d'agir, avec même éventuellement une compétition Mx – NP pour la liaison à ce facteur. Cette hypothèse expliquerait la proximité Mx – NP observée au niveau de granules péri-nucléaires et la possibilité de « titrer » l'effet Mx en surexprimant la NP. Autre fait

marquant, aucune souche de virus influenza A n'a jamais présenté de thréonine en position 100, rendant nos souches de virus Mx-résistants absolument uniques. Cela suggère une adaptation nécessaire du virus, peut-être en augmentant l'affinité de la NP pour le facteur cellulaire pour lequel la Mx entre en compétition. Ce partenaire reste à identifier. Des résultats récents sur l'adaptation du virus influenza A à l'encéphale de poulet montrent qu'une même substitution isoleucine → thréonine, mais en position 109, soit dans l'environnement proche du résidu 100, permet l'adaptation en augmentant fortement l'efficacité de transcription du génome viral dans l'encéphale de poulet (Tada *et al.*, 2011). D'autre part, l'ARN hélicase UAP56, connue pour son rôle de « chaperon » dans la liaison de la nucléoprotéine aux ARNs viraux (Kawaguchi *et al.*, 2011), a été proposée comme cible de la huMxA pour expliquer l'effet antiviral de celle-ci (Wisskirchen *et al.*, 2011). Diminuer l'expression de UAP56 par ARN interférence mène à une baisse de l'export nucléaire des ARNm viraux et donc de l'expression des protéines virales, mais l'ARNm de la nucléoprotéine, protéine dont l'expression dans nos expériences est fortement affectée par les Mx, semble peu sensible à l'inhibition de UAP56, suggérant que l'export nucléaire de cet ARN se fait via une autre voie (Read et Digard, 2010). UAP56 n'apparaît donc pas comme la cible qui explique tous les effets inhibiteurs des protéines Mx sur la réplication du virus influenza A.

Une autre observation intéressante découle de l'effet inhibiteur de la protéine Mx1 bovine sur l'activation de la voie NF-κB, et ce indépendamment de toute infection virale (Cornet *et al.*, soumis). Cette fonction de la protéine Mx1 bovine pourrait expliquer la différence d'efficacité entre la protéine Mx1 bovine et les autres protéines Mx cytoplasmiques en termes d'inhibition de la réplication du virus influenza A. Il est en effet connu que le virus influenza dépend d'une activation de la voie NF-κB au cours de son cycle de réplication virale (Nimmerjahn *et al.*, 2004). De plus, il a été démontré au sein du laboratoire qu'une protéine boMx1 rendue incapable d'inhiber la voie NF-κB par substitution de 6 acides aminés était également incapable d'inhiber la réplication du virus influenza A (Cornet *et al.*, soumis). Ce qui est particulièrement interpellant, dans ce contexte, est le comportement présenté par les variants Mx-résistants sélectionnés dans cette étude au niveau de l'activation de la voie NF-κB. En effet, tant les variants Mx-résistants que le virus parental contenant la substitution I100T induisent une activation de la voie NF-κB beaucoup plus faible que celle induite par le virus parental *wild-type* (Garigliany *et al.*, soumis). Ce comportement est identique lorsque la seule

nucléoprotéine, avec ou sans la substitution I100T, est exprimée. Le virus devenu Mx-résistant stimule beaucoup moins la voie NF-κB et pourrait donc être nettement moins dépendant d'une activation de celle-ci pour accomplir son cycle de réplication.

Au terme de ce travail, certains éclaircissements ont été apportés, parallèlement aux études réalisées par d'autres équipes sur d'autres Mx, quant au rôle prépondérant de la nucléoprotéine virale. Nous sommes d'une part les premiers à identifier le rôle crucial du résidu 100 de cette protéine dans le mécanisme d'action des protéines Mx. Nous sommes d'autre part également les premiers à avoir isolé un virus Mx-résistant, qui plus est à plusieurs Mx, cytoplasmiques et nucléaire. Par ailleurs, nous avons écarté l'hypothèse d'une interaction directe Mx – NP pour expliquer le mode d'action des protéines Mx et abouti à la conclusion que les protéines Mx devaient inhiber une fonction cellulaire utilisée par le virus au cours de son cycle réplicatif. Nous suggérons que cette inhibition puisse être compétitive. De plus, de par l'activité particulière de la protéine Mx1 bovine sur la voie NF-κB, nous avons mis à jour le fait que les variants boMx1-résistants de notre souche virale stimulaient beaucoup moins la voie NF-κB, ce qui explique peut-être en partie leur résistance.

Il reste néanmoins plusieurs points à élucider. D'une part, quel(s) facteur(s) cellulaire(s) pourrai(en)t être complexé(s) ou régulé(s) par les protéines Mx1 bovine, MxA humaine, Mx1 porcine et Mx1 murine, de sorte que l'introduction de la substitution I100T dans la nucléoprotéine virale puisse restaurer la fonction de ce facteur ou augmenter l'affinité de la nucléoprotéine pour ce facteur et rendre ainsi le virus résistant à l'effet inhibiteur de ces quatre protéines ? Il s'agit à présent de se focaliser sur les interactomes des protéines Mx et de la nucléoprotéine du virus influenza A. Une autre hypothèse serait que cette mutation permette à la NP d'interagir avec une autre protéine cellulaire, autorisant le virus à utiliser une voie alternative. D'autre part, si le facteur en question existe et est identifié, comment expliquer les différences d'efficacité entre les protéines Mx ? Et comment expliquer leur différence de spectre antiviral ? Ces différences pourraient venir de l'affinité de chaque protéine Mx pour ce facteur et/ou de l'existence de fonctions supplémentaires, comme cela semble être le cas pour la protéine boMx1 et la voie NF-κB. Au sujet de cette voie NF-κB, il est essentiel de vérifier l'hypothèse selon laquelle la substitution I100T rendrait le virus moins dépendant de l'activation de cette voie, et l'impact que cela pourrait avoir sur la biofitness du virus *in vivo*. Par

ailleurs, l'effet potentiel des protéines Mx sur d'autres voies de signalisation intracellulaire reste à explorer. Enfin, il apparait essentiel de contrôler si l'introduction de la substitution en position 100 de la nucléoprotéine d'autres souches virales leur confère également une Mx-résistance *in vitro*, de voir si la résistance est également transposable *in vivo* et d'examiner la possibilité que d'autres substitutions puissent conférer un même phénotype de résistance. Quelles que soient les réponses à ces questions, l'identification du mécanisme d'action précis de la protéine Mx1 bovine laisse augurer une nouvelle génération d'agents antiviraux à large spectre visant non pas à inhiber la réplication virale de façon directe, mais à le faire de façon indirecte et beaucoup plus puissante, avec des résultats cliniques impressionnants comme ceux observés avec les souris congéniques ou transgéniques porteuses d'un gène Mx actif.

Partie IV : Bibliographie

Accola MA, Huang B, Al Masri A, *et al.* The antiviral dynamin family member, MxA, tubulates lipids and localizes to the smooth endoplasmic reticulum. *J Biol Chem* 2002 ; 277: 21829-21835.

Aebi M, Fäh J, Hurt N, *et al.* cDNA structures and regulation of two interferon-induced human Mx proteins. *Mol Cell Biol* 1989 ; 9: 5062-5072.

Arnheiter H, Skuntz S, Noteborn M, *et al.* Transgenic mice with intracellular immunity to influenza virus. *Cell* 1990 ; 62: 51-61.

Babiker HA, Nakatsu Y, Yamada K, *et al.* Bovine and water buffalo Mx2 genes: polymorphism and antiviral activity. *Immunogenetics* 2007 ; 59: 59-67.

Baise E, Pire G, Leroy M, *et al.* Conditional expression of type I interferon-induced bovine Mx1 GTPase in a stable transgenic vero cell line interferes with replication of vesicular stomatitis virus. *J Interferon Cytokine Res* 2004 ; 24: 513-521.

Betakova T, Ciampor F, Hay AJ. Influence of residue 44 on the activity of the M2 proton channel of influenza A virus. *J Gen Virol* 2005 ; 86: 181-184.

Carr JF, Hinshaw JE. Dynamin assembles into spirals under physiological salt conditions upon the addition of GDP and gamma-phosphate analogues. *J Biol Chem* 1997 ; 272: 28030-28035.

Coloma R, Valpuesta JM, Arranz R, *et al.* The structure of a biologically active influenza virus ribonucleoprotein complex. *PLoS Pathog* 2009 ; 5: e1000491.

Cornet A, Garigliany M., Desmecht D. Antiviral *Bos taurus* Mx1 protein inhibit TRAF2- and TRAF6-mediated nuclear factor-kappaB signaling. Submitted.

De Zoysa M, Kang HS, Song YB, *et al.* First report of invertebrate Mx: cloning, characterization and expression analysis of Mx cDNA in disk abalone (Haliotis discus discus). *Fish Shellfish Immunol* 2007 ; 23: 86-96.

Dittmann J, Stertz S, Grimm D, *et al.* Influenza A virus strains differ in sensitivity to the antiviral action of Mx-GTPase. *J Virol* 2008 ; 82: 3624-3631.

Dreiding P, Staeheli P, Haller O. Interferon-induced protein Mx accumulates in nuclei of mouse cells expressing resistance to influenza viruses. *Virology* 1985 ; 140: 192-196.

Ellinwood NM, Berryere TG, Fournier BP, *et al.* MX1 maps to cattle chromosome 1. *Anim Genet* 1999 ; 30: 164-165.

Ellinwood NM, McCue JM, Gordy PW, *et al.* Cloning and characterization of cDNAs

for a bovine (*Bos taurus*) Mx protein. *J Interferon Cytokine Res* 1998 ; 18: 745-755.

Flohr F, Schneider-Schaulies S, Haller O, *et al.* The central interactive region of human MxA GTPase is involved in GTPase activation and interaction with viral target structures. *FEBS Lett* 1999 ; 463: 24-28.

Frese M, Kochs G, Meier-Dieter U, *et al.* Human MxA protein inhibits tick-borne Thogoto virus but not Dhori virus. *J Virol* 1995 ; 69: 3904-3909.

Gao S, von der Malsburg A, Paeschke S, *et al.* Structural basis of oligomerization in the stalk region of dynamin-like MxA. *Nature* 2010 ; 465: 502-506.

Garigliany MM, Cloquette K, Leroy M, *et al.* Modulating mouse innate immunity to RNA viruses by expressing the *Bos taurus* Mx system. *Transgenic Res* 2009 ; 18: 719-732.

Garigliany MM, Habyarimana A, Lambrecht B, *et al.* Influenza A strain-dependent pathogenesis in fatal H1N1 and H5N1 subtype infections of mice. *Emerg Infect Dis* 2010 ; 16: 595-603.

Garigliany MM, Van de Paar E, Cornet A, *et al.* A new mammalian innate effector with unprecedented anti-influenza activity. Submitted.

Gérardin JA, Baise EA, Pire GA, *et al.* Genomic structure, organisation, and promoter analysis of the bovine (*Bos taurus*) Mx1 gene. *Gene* 2004 ; 326:67-75.

Giraldo P, Montoliu L. Size matters: use of YACs, BACs and PACs in transgenic animals. *Transgenic Res* 2001 ; 10: 83-103.

Goetschy JF, Zeller H, Content J, *et al.* Regulation of the interferon-inducible IFI-78K gene, the human equivalent of the murine Mx gene, by interferons, double-stranded RNA, certain cytokines, and viruses. *J Virol* 1989 ; 63: 2616-2622

Gong S, Zheng C, Doughty ML *et al.* A gene expression atlas of the central nervous system based on bacterial artificial chromosomes. *Nature* 2003 ; 425: 917–925.

Haller O, Frese M, Kochs G. Mx proteins: mediators of innate resistance to RNA viruses. *Rev Sci Tech* 1998 ; 17: 220-230

Haller O, Gao S, von der Malsburg A, *et al.* Dynamin-like MxA GTPase: structural insights into oligomerization and implications for antiviral activity. *J Biol Chem* 2010 ; 285: 28419-28424.

Haller O, Kochs G. Human MxA protein: an interferon-induced dynamin-like GTPase with broad antiviral activity. *J Interferon Cytokine Res* 2011 ; 31: 79-87.

Haller O, Kochs G. Interferon-induced Mx proteins: dynamin-like GTPases with

antiviral activity. *Traffic* 2002 ; 3: 710-717.

Hay AJ, Wolstenholme AJ, Skehel JJ, *et al.* The molecular basis of the specific anti-influenza action of amantadine. *EMBO J* 1985 ; 4: 3021-3024.

Holsinger LJ, Nichani D, Pinto LH, *et al.* Influenza A virus M2 ion channel protein: a structure-function analysis. *J Virol* 1994 ; 68: 1551-1563.

Holzinger D, Jorns C, Stertz S, *et al.* Induction of MxA gene expression by influenza A virus requires type I or type III interferon signaling. *J Virol* 2007 ; 81: 7776-7785.

Horisberger MA, Gunst MC. Interferon-induced proteins: identification of Mx proteins in various mammalian species. *Virology* 1991 ; 180: 185-190.

Horisberger MA, Hochkeppel HK. An interferon-induced mouse protein involved in the mechanism of resistance to influenza viruses. Its purification to homogeneity and characterization by polyclonal antibodies. *J Biol Chem* 1985 ; 260: 1730-1733.

Horisberger MA, McMaster GK, Zeller H, *et al.* Cloning and sequence analyses of cDNAs for interferon- and virus-induced human Mx proteins reveal that they contain putative guanine nucleotide-binding sites: functional study of the corresponding gene promoter. *J Virol* 1990 ; 64: 1171-1181.

Huang T, Pavlovic J, Staeheli P, *et al.* Overexpression of the influenza virus polymerase can titrate out inhibition by the murine Mx1 protein. *J Virol* 1992 ; 66: 4154-4160.

Janzen C, Kochs G, Haller O. A monomeric GTPase-negative MxA mutant with antiviral activity. *J Virol* 2000 ; 74: 8202-8206.

Johannes L, Kambadur R, Lee-Hellmich H, *et al.* Antiviral determinants of rat Mx GTPases map to the carboxy-terminal half. *J Virol* 1997 ; 71: 9792-9795.

King MC, Raposo G, Lemmon MA.Inhibition of nuclear import and cell-cycle progression by mutated forms of the dynamin-like GTPase MxB. *Proc Natl Acad Sci U S A* 2004 ; 101: 8957-8962.

Ko JH, Jin HK, Asano A, *et al.* Polymorphisms and the differential antiviral activity of the chicken Mx gene. *Genome Res* 2002 ; 12: 595-601.

Kochs G, Haener M, Aebi U, *et al.* Self-assembly of human MxA GTPase into highly ordered dynamin-like oligomers. *J Biol Chem* 2002 ; 277: 14172-14176.

Kochs G, Haller O. Interferon-induced human MxA GTPase blocks nuclear import of Thogoto virus nucleocapsids. *Proc Natl Acad Sci U S A* 1999 ; 96: 2082-2086.

Kochs G, Janzen C, Hohenberg H, *et al.* Antivirally active MxA protein sequesters La Crosse virus nucleocapsid protein into perinuclear complexes. *Proc Natl Acad Sci U S A* 2002 ; 99: 3153-3158.

Kojima T, Oshima K, Watanabe H, *et al.* The bovine Mx1 gene: characterization of the gene structure, alternative splicing, and promoter region. *Biochem Genet* 2003 ; 41: 375-390.

Kolb E, Laine E, Strehler D, *et al.* Resistance to influenza virus infection of Mx transgenic mice expressing Mx protein under the control of two constitutive promoters. *J Virol* 1992 ; 66: 1709-1716.

Leroy M, Baise E, Pire G, *et al.* Resistance of paramyxoviridae to type I interferon-induced *Bos taurus* Mx1 dynamin. *J Interferon Cytokine Res* 2005 ; 25: 192-201.

Leroy M, Pire G, Baise E, *et al.* Expression of the interferon-alpha/beta-inducible bovine Mx1 dynamin interferes with replication of rabies virus. *Neurobiol Dis* 2006 ; 21: 515-521.

Melén K, Julkunen I. Mutational analysis of murine Mx1 protein: GTP binding core domain is essential for anti-influenza A activity. *Virology* 1994 ; 205: 269-279.

Melén K, Ronni T, Broni B, *et al.* Interferon-induced Mx proteins form oligomers and contain a putative leucine zipper. *J Biol Chem* 1992 ; 267: 25898-25907.

Mibayashi M, Nakad K, Nagata K. Promoted cell death of cells expressing human MxA by influenza virus infection. *Microbiol Immunol* 2002 ; 46: 29-36.

Morens DM, Taubenberger JK, Folkers GK, *et al.* Pandemic influenza's 500th anniversary. *Clin Infect Dis* 2010 ; 51: 1442-1444.

Morozumi T, Naito T, Lan PD, *et al.* Molecular cloning and characterization of porcine Mx2 gene. *Mol Immunol* 2009 ; 46: 858-865.

Muller M, Brenig B, Winnacker E *et al.* Transgenic pigs carrying cDNA copies encoding the murine Mx1 protein which confers resistance to influenza virus infection. *Gene* 1992 ; 16: 263–270.

Mushinski JF, Nguyen P, Stevens LM, *et al.* Inhibition of tumor cell motility by the interferon-inducible GTPase MxA. *J Biol Chem* 2009 ; 284: 15206-15214.

Nakatsu Y, Yamada K, Ueda J, *et al.* Genetic polymorphisms and antiviral activity in the bovine MX1 gene. *Anim Genet* 2004 ; 35: 182-187.

Nakayama M, Nagata K, Kato A, *et al.* Interferon-inducible mouse Mx1 protein that confers resistance to influenza virus is GTPase. *J Biol Chem* 1991 ; 266: 21404-21408.

Nakayama M, Yazaki K, Kusano A, *et al.* Structure of mouse Mx1 protein. Molecular assembly and GTP-dependent conformational change. *J Biol Chem* 1993 ; 268: 15033-15038

Netherton CL, Simpson J, Haller O, *et al.* Inhibition of a large double-stranded DNA virus by MxA protein. *J Virol* 2009 ; 83: 2310-2320.

Nimmerjahn F, Dudziak D, Dirmeier U, *et al.* Active NF-kappaB signalling is a prerequisite for influenza virus infection. *J Gen Virol* 2004 ; 85: 2347-2356.

Palm M, Garigliany MM, Cornet F, *et al.* Interferon-induced Sus scrofa Mx1 blocks endocytic traffic of incoming influenza A virus particles. *Vet Res* 2010 ; 41:29.

Palm M, Leroy M, Thomas A, *et al.* Differential anti-influenza activity among allelic variants at the Sus scrofa Mx1 locus. *J Interferon Cytokine Res* 2007 ; 27: 147-155.

Pan C, Cheung B, Tan S, *et al.* Genomic signature and mutation trend analysis of pandemic (H1N1) 2009 influenza A virus. *PLoS One* 2010 ; 5: e9549.

Pavlovic J, Arzet HA, Hefti HP, *et al.* Enhanced virus resistance of transgenic mice expressing the human MxA protein. *J Virol* 1995 ; 69: 4506-4510.

Pavlovic J, Haller O, Staeheli P. Human and mouse Mx proteins inhibit different steps of the influenza virus multiplication cycle. *J Virol* 1992 ; 66: 2564-2569.

Pavlovic J, Zürcher T, Haller O, *et al.* Resistance to influenza virus and vesicular stomatitis virus conferred by expression of human MxA protein. *J Virol* 1990 ; 64: 3370-3375.

Pitossi F, Blank A, Schröder A, *et al.* A functional GTP-binding motif is necessary for antiviral activity of Mx proteins. *J Virol* 1993 ; 67: 6726-6732.

Read EK, Digard P. Individual influenza A virus mRNAs show differential dependence on cellular NXF1/TAP for their nuclear export. *J Gen Virol* 2010 ; 91: 1290-1301.

Rothman JH, Raymond CK, Gilbert T, *et al.* A putative GTP binding protein homologous to interferon-inducible Mx proteins performs an essential function in yeast protein sorting. *Cell* 1990 ; 61: 1063-1074.

Salomon R, Staeheli P, Kochs G, *et al.* Mx1 gene protects mice against the highly lethal human H5N1 influenza virus. *Cell Cycle* 2007 ; 6: 2417-2421.

Sandrock M, Frese M, Haller O, *et al.* Interferon-induced rat Mx proteins confer resistance to Rift Valley fever virus and other arthropod-borne viruses. *J Interferon Cytokine Res* 2001 ; 21: 663-668.

Schwemmle M, Richter MF, Herrmann C, *et al.* Unexpected structural requirements for GTPase activity of the interferon-induced MxA protein. *J Biol Chem* 1995 ; 270: 13518-13523.

Staeheli P, Horisberger MA, Haller O. Mx-dependent resistance to influenza viruses is induced by mouse interferons alpha and beta but not gamma. *Virology* 1984 ; 132: 456-461.

Staeheli, P., O. Haller, W. Boll, *et al.*. Mx protein: constitutive expression in 3T3 cells transformed with cloned Mx cDNA confers selective resistance to influenza virus. *Cell* 1986 ; 44: 147-158.

Stertz S, Dittmann J, Blanco JC, *et al.* The antiviral potential of interferon-induced cotton rat Mx proteins against orthomyxovirus (influenza), rhabdovirus, and bunyavirus. *J Interferon Cytokine Res* 2007 ; 27: 847-855.

Stranden AM, Staeheli P, Pavlovic J. Function of the mouse Mx1 protein is inhibited by overexpression of the PB2 protein of influenza virus. *Virology* 1993 ; 197: 642-651.

Tada T, Suzuki K, Sakurai Y, *et al.* Emergence of Avian Influenza Viruses with Enhanced Transcription Activity by Single Amino Acid Substitution in Nucleoprotein During Replication in Chicken Brains. *J Virol* 2011 Epub ahead of print].

Thorlund K, Awad T, Boivin G, *et al.* Systematic review of influenza resistance to the neuraminidase inhibitors. *BMC Infect Dis* 2011 ; 11: 134.

Tumpey TM, Szretter KJ, Van Hoeven N, *et al.* The Mx1 gene protects mice against the pandemic 1918 and highly lethal human H5N1 influenza viruses. *J Virol* 2007 ; 81: 10818-10821.

Turan K, Mibayashi M, Sugiyama K, *et al.* Nuclear MxA proteins form a complex with influenza virus NP and inhibit the transcription of the engineered influenza virus genome. *Nucleic Acids Res* 2004 ; 32: 643-652.

Vanlaere I, Vanderrijst A, Guénet JL, *et al.* Mx1 causes resistance against influenza A viruses in the Mus spretus-derived inbred mouse strain SPRET/Ei. *Cytokine* 2008 ; 42: 62-70.

Varich NL, Sadykova GK, Prilipov AG, *et al.* Antibody-binding epitope differences in the nucleoprotein of avian and mammalian influenza A viruses. *Viral Immunol* 2011 ; 24:101-107.

Wisskirchen C, Ludersdorfer TH, Mueller DA, *et al.* The interferon induced antiviral

protein MxA interacts with the cellular RNA Helicases UAP56 and URH49. *J Biol Chem* 2011 [Epub ahead of print].

Yamada K, Nakatsu Y, Onogi A, *et al.* Specific intracellular localization and antiviral property of genetic and splicing variants in bovine Mx1. *Viral Immunol* 2009 ; 22: 389-395.

Ye Q, Krug RM, Tao YJ. The mechanism by which influenza A virus nucleoprotein forms oligomers and binds RNA. *Nature* 2006 ; 444: 1078-1082.

Zhao Y, Pang D, Wang T, *et al.* Human MxA protein inhibits the replication of classical swine fever virus. *Virus Res* 2011 ; 156: 151-155.

Zimmermann P, Mänz B, Haller O, *et al.* The viral nucleoprotein determines Mx sensitivity of influenza A viruses. *J Virol* 2011 [Epub ahead of print].

Zürcher T, Pavlovic J, Staeheli P. Mechanism of human MxA protein action: variants with changed antiviral properties. *EMBO J* 1992 ; 11: 1657-1661.